An essential role of IRF4 in translating TCR affinity-mediated activation and CD8+ effector T cell fate decisions

Dissertation
zur Erlangung des akademischen Grades
doctor rerum naturalium
(Dr. rer. nat.)

im Fach Biologie

eingereicht an der
Lebenswissenschaftlichen Fakultät
der Humboldt-Universität zu Berlin

von
M.Sc. Anett Hartung

Präsident der Humboldt-Universität zu Berlin
Prof. Dr. Jan-Hendrik Olbertz

Dekan der Lebenswissenschaftlichen Fakultät
Prof. Dr. Richard Lucius

Tag der mündlichen Prüfung
02.06.2016

Promotionsausschuss:

Vorsitzender:	Prof. Dr. Kai Matuschewski
Gutachter:	Prof. Dr. Andreas Thiel
Gutachter:	Prof. Dr. med. Hans-Dieter Volk
Gutachter:	Prof. Dr. Alf Hamann

Berlin 2016

Contents

List of Figures

List of Tables

Abstract

CD8+ T lymphocytes play a crucial role in controlling bacterial infections, as they promote pathogen clearance. Recent studies emphasize that besides antigen (ag) dose and inflammatory cytokine milieu, the T cell receptor (TCR) stimulation contributes to the programming of the CD8+ T cell response. This strongly suggests that the initiation of a distinct developmental program, the final magnitude, and the duration of clonal expansion, as well as the timing of the onset of T cell contraction, are determined by the TCR signaling strength. It is well known that weak TCR stimulation results in a diminished magnitude of expansion and accelerates the onset of contraction, as it favors the development of memory cells at the expense of effector cells. The interferon regulatory factor 4 (IRF4) is a transcription factor (TF), which is upregulated in CD8+ T cells following TCR ligand interaction. Furthermore, the modulation of its expression level is highly dependent on the TCR signaling strength, which initiated activation. The IRF4 expression profile is tightly regulated, as it translates the TCR signaling strength of the activating signal and transmits it into a proper transcriptional and developmental program.

Results of the present study show that IRF4-deficient CD8+ T cells become initially activated and proliferate after strong TCR engagement. Nonetheless, in contrast to their wild type (WT) counterparts, they display drastically impaired cytokine production and decreased cytotoxic activity, as well as an altered differentiation pattern. This study provide unique evidence that the absence of IRF4 expression in CD8+ T cells leads to a hasted termination of clonal expansion and a premature contraction, which was initiated by the FAS - mediated cell death pathway. Furthermore, IRF4-deficient CD8+ T cells exposed phosphatidylserine on their cell surface and showed increased complement pathway activation, both facilitate their recognition and uptake by phagocytes. The findings of this study strongly indicate that IRF4 deficiency drives a molecular differentiation program that give rise to an early memory formation and results in a premature onset of effector CD8+ T cell contraction, which is characterized by a lower final magnitude of proliferation and a drastically diminished frequency of ag-specifc CD8+ T cells already early after infection. IRF4 deficiency mimics weak TCR engagement and in turn transmits every TCR signal, independent of its actually affinity and duration, into a developmental program, which initiates a cell fate very similar to the fate of low affinity TCR activated WT CD8+ T cells.

Taken together, present results demonstrate that similar to the fate of low affinity TCR activated WT CD8+ T cells, IRF4-deficient CD8+ T cells were prone to die early during immune response, as they were more susceptible to cell death and phagocytosis. This study extend previous knowledge of the central role of the IRF4 playing an essential TF for the differentiation and functionality of ag-specific effector CD8+ T cells after primary infection. Moreover, these results additionally show that IRF4 is a key regulator of the CD8+ T cell response, as it furthermore drastically influences the magnitude and kinetic of the effector response and dictates the onset of CD8+ T cell contraction via the activation of several death and phagocytosis inducing pathways.

Zusammenfassung

CD8+ T Lymphozyten spielen eine sehr wichtige Rolle bei der Bekämpfung bakterieller Infektionen, da sie die Beseitigung von Pathogenen vermitteln. Aktuelle Studien betonen, dass neben der Antigendosis und dem inflammatorischen Zytokinmilieu, auch die Stimulation durch den T Zell-Rezeptor (TZR) einen entscheidenden Einfluss auf die Programmierung der CD8+ T Zellenantwort hat. Das deutet stark darauf hin, dass die Initialisierung eines bestimmten transkriptionellen Programms, die finale Größe der klonalen Expansion und das Einleiten der Kontraktionsphase durch die Stärke des TZR-Signales bestimmt werden. Es ist bekannt, dass eine schwache TZR-Stimulation zu einer verminderten Expansion führt und eine frühzeitige Kontraktionsphase vermittelt, da diese eine Entwicklung von Gedächtniszellen auf den Kosten der Effektorzellen favorisiert. Die Expression des Interferon Regulatorischen Faktors 4 (IRF4) wird nach TZR-Ligand-Interaktion in CD8+ T Zellen hochreguliert. Des weiteren ist das Expressionslevel von IRF4 stark von der Signalstärke der TZR-Aktivierung abhängig. Die Kinetik der IRF4 Expression übersetzt die Stärke des aktivierenden TZR-Signales und sorgt für die Umsetzung in ein entsprechendes transkriptionelles und differentielles Programm.

In dieser Arbeit konnte gezeigt werden, dass IRF4-defiziente CD8+ T Zellen nach Stimulation mit einem starken TZR-Signal zwar zu Beginn aktiviert werden und eine klonale Expansion initiiert wird, aber nichtsdestotrotz im Vergleich zu normalen CD8+ T Zellen eine stark verminderte Zytokinexpression und zytotoxische Aktivität zeigten, sowie ein verändertes Differenzierungsmuster aufwiesen. Es konnte zudem erstmals gezeigt werden, dass die Defizienz von IRF4 in CD8+ T Zellen zu einem verfrühten Abbruch der klonalen Expansion führt und zu einem vorzeitigen Beginn der Kontraktionsphase, die durch den FAS-vermittelten Tod-induzierenden Signalweg initiiert wird. Des weiteren präsentieren IRF4-defiziente CD8+ T Zellen vermehrt Phosphatidylserine an deren Oberfläche und weisen eine erhöhte Aktivierung des Komplementsignalweges auf, dies vermittelt deren Erkennung und Aufnahme durch Phagozyten. Diese Ergebnisse weisen stark darauf hin, dass die fehlende Expression von IRF4 in CD8+ T Zellen ein molekulares Differenzierungsprogramm initiiert, welches zu einer Verkürzung der Expansionsphase führt und eine verfrühte Kontraktionsphase der Effektorzellen auslöst. Dies wiederum ist durch eine verminderte Proliferation und einer drastisch reduzierten Anzahl von antigen-spezifischen CD8+ T Zellen nach Infektion charakterisiert.

Zusammenfassend deuten die Ergebnisse dieser Arbeit stark darauf hin, dass durch die fehlende Expression von IRF4 in CD8+ T Zellen, jedes Signal als ein schwaches TZR-Signal übermittelt wird, unabhängig von der tatsächlichen Stärke des aktivierenden Signals. Das lässt wiederum darauf schließen, dass IRF4-defiziente CD8+ T Zellen einem Schicksal unterliegen, dass dem von normalen CD8+ T Zellen, welche mit einem schwachen TZR-Signal aktiviert wurden, sehr ähnelt. Beide CD8+ T Zell-Populationen sind gegenüber Zelltod und Phagozytose anfälliger im Vergleich zu stark TZR-aktivierten normalen CD8+ T Zellen. Diese Arbeit erweitert schon bekanntes Wissen, da die erstmals hier gezeigten Ergebnisse darauf schließen lassen, dass IRF4 als Schlüsselreg-

ulator der CD8+ T Lymphozyten vermittelten Immunantwort nach einer Infektion agiert. Seine Expression beeinflusst zusätzlich drastisch die Stärke und Kinetik der Effektor-CD8+ T Zellanwort und diktiert den Beginn der Kontraktionsphase indem es zu einer Aktivierung verschiedener Tod und Phagozytose induzierenden Signalwege führt.

Acknowledgement.

First of all, I would like to thank my mentor Prof. Dr. Andreas Thiel for giving me the opportunity to work in his research group. Additionally, I would like to thank the reviewers for taking the time to referee my dissertation. My deepest appreciation goes to Dr. Regina Stark for her supervision. I am extremely grateful for her helpful comments, valuable suggestions and guidance through all the experimental work.

I want to give my special thanks to Kerstin Hoffmann for answering my questions, for synergistic help, mental support and becoming a very good friend. Furthermore, I would like to thank all the members of the AG Thiel for the enjoyable company, cooperation, the excellent technical assistance, and for the fruitful discussions. For cell sorting, flow cytometry maintenance, and trouble shooting, I would like to acknowledge Dr. Désirée Kunkel and her group members Dr. Sarah Meier and Antje Malluck.

Most of all, I would like to thank my family and my friends, especially my husband and my parents, for all assistance and patience through my entire studies. Without you, many things would not have been possible. Thank you for giving me a helping hand whenever I asked for it, thanks for your love and never-ending encouragement.

Abbreviations

ActA actin-assembly-inducing protein

ag antigen

AICD activation-induced cell death

APCs antigen presenting cells

APL altered peptide ligand

BHI brain heart infusion

BSA bovine serum albumin

BM bone marrow

BrefA brefeldin A

BrdU bromdeoxyuridine

C degree celsius

CD cluster of differentiation

CFSE carboxyfluorescein succinimidyl ester

CFDA-SE carboxyfluorescein diacetate succinimidyl ester

CFU colony forming unit

CTL cytotoxic T lymphocyte

C-terminal carboxy-terminal

DMSO dimethyl sulfoxide

DCs dendritic cells

dH_2O demineralized water

DAPI 4', 6-diamidino-2-phenylindole

DN double-negative

DP double- positive

DNA deoxyribonucleic acid

DBD DNA binding domain

°C degree

dsDNA double stranded DNA

d day(s)

dH2O demineralized water

EDTA ethylenediaminetetraacetic acid

EOMES eomesodermin

i.v. intravenous

FCS fetal calf serum

FSC forward scatter

FSC-A forward scatter area

FSC-H forward scatter height

FACS fluorescence-activated cell sorting

g gram

GO Gene Ontology

xg times gravity

IAD IRF-associated domain

Iono ionomycin

IL interleukin

IFN interferon

IRF interferon regulatory factor

IRF4 interferon regulatory factor 4

IRSE interferon stimulatory response element

IFNγ interferonγ

i.p. intraperitoneal

i.v. intravenous

KO knock out

LCMV lymphocytic choriomeningitis virus

LD Red live-dead red fluorescent reactive dye

Ll liver

l liter

LM *Listeria Monocytogenes*

LM-OVA *Listeria Monocytogenes* expressing Ovalbumin

LLO listeriolysin

LN lymph node

MACS magnetic-activated cell sorting

MFI mean fluorescence intensity

mg milligram

MHC major histocompability complex

µl microliter

µm micrometer

µg microgram

min minutes

ml milliliter

nm nanometer

MPEC memory-precursor effector cells

NK natural killer cells

N-terminal amino-terminal

OVA Ovalbumin

OD_{600nm} optical density at 600 nm

PBS phosphate buffered saline

PE phycoerythrin

% percent

pH potential hydrogen

p.i. post infection

PI propidium iodide

PMA phorbol 12-myristate 13-acetate

RNA ribonucleic acid

RNAse ribonuclease

RPMI Rosewell Park Memorial Institute (medium)

P/S penicillin/streptomycin

PS phosphatidylserine

RT room temperature (defined as 25°C)

SEM standard error of the mean

SI SIINFEKL

SLEC short-lived effector cells

SP spleen

SSC side scatter

SSC-A side scatter area

SSC-H side scatter height

Tbet T-box transcription factor, T-box21

TCM central-memory T cells

TCR T cell receptor

TEM effector-memory T cells

TF transcription factor

TP time point

TNF tumor necrosis factor

TH CD4+ T cell subset

THY thymus

U unit

WT wild type

Part I

Introduction

Humans are exposed to a diverse range of bacteria, viruses, fungi, and parasites. If these microorganisms enter the body, they need to be detected and eliminated. The central task of the immune system is the protection of the body against all invading pathogens. The immune system itself can be divided into the adaptive and innate immune system, which both utilize different recognition components, mechanisms and cells, complementing one another.

The adaptive immune system provides specific recognition of invading microorganisms and their components, and additionally, immunological memory for life time. This immune response is mediated by B and T cells with pathogen-specific adapter proteins in the late phase of infection. The two major types of T lymphocytes are CD8+ cytotoxic T cells and CD4+ helper T cells. Here, this study focuses on the adaptive immune response mediated by CD8+ T lymphocytes after *Listeria monocytogenes* infection in mice. Thereby, investigate the role of the transcription factor IRF4 on effector CD8+ T cell differentiation and functionality. Additionally, its impact on the magnitude and duration of the expansion and the onset of T cell contraction.

Chapter 1

CD8+ T cells

CD8+ T lymphocytes are very important mediators of the immune defense against intracellular pathogens like viruses and bacteria. This cytotoxic T cell population expresses the dimeric co-receptor CD8, which is composed of two CD8α, forming a homodimer or made of one CD8α and one CD8β chain. CD8+ T cells recognize pathogenic peptides presented by major histocompability complex (MHC) class I molecules on antigen

presenting cells (APCs) [3]. Their major function is the killing of infected cells, the production of cytokines and chemokines to activate other immune cells, and to initiate anti-infectious mechanisms.

1.1 CD8+ T cell development

Lymphoid progenitors arise in the bone marrow and migrate via the blood into the thymus where they undergo several differentiation stages, as they respond to signals in their micro-environment (Figure 1.1). Early committed T cells lack the expression of the T cell receptor (TCR), they are not CD4+ nor CD8+ and termed therefore as double-negative (DN) thymocytes. Double-negative thymocytes can be further subdivided into four stages of differentiation. With ongoing differentiation processes, they express a pre-TCR, which is composed of the non-rearranging pre-TCRα and TCRβ chain. A transition from the DN to the double-positive (DP) stage occurs, leading to a substantial cell proliferation of the CD4+ CD8+ thymocytes and a replacement of the pre-TCR with a complete TCR$\alpha\beta$ [243]. The rearrangement of the somatic deoxyribonucleic acid (DNA) and random chain pairing of the two chains of the TCR lead to an individual TCR locus in each T cell, ensuring their diversity [202]. The TCR$\alpha\beta$ expressing DP thymocytes have to undergo selective processes to generate a receptor repertoire, to reduce the risk of autoreactivity and to keep cells alive [67]. The DP thymocytes interact with cortical epithelial cells in the thymus that express high density MHC class I and class II molecules associated with self-peptides. The interaction between the TCR with these self-peptide MHC ligands decides on the cell fate of the thymocytes, as too strong signaling will result in apoptosis. When the interaction between the TCRs and the presented self-peptides is too weak, the cells do not get intracellular signals. Those signals are required to sustain viability and leading to cell death by neglect. Only a small fraction of cells with an intermediate level of TCR signaling will be positively selected and will undergo maturation [197]. Mature thymocytes expressing TCRs that bind to self-peptide MHC class I complexes become CD8+ T lymphocytes, whereas those that bind to self-peptides presented on MHC class II molecules become CD4+ T cells [62]. Both matured T cell subsets leave the thymus and travel to peripheral lymphoid organs awaiting an encounter with antigen (ag).

T lymphocytes express different TCRs, which are specific against certain foreign molecules. The TCR consists of multiple chains but it lacks an intracellular domain. Therefore, the TCR is associated with CD3, which contains an intracellular signaling domain [45]. The TCR and the CD3 subunit form a complex to assist the transmission of the signal into the T cell. Thus, leading to activation induced proliferation and differentiation [120]. The TCR/CD3 complex is made up of diverse chains. In detail, one α and β or γ and δ chain, which are additional joined with two ϵ, two ζ and another δ and γ chain.

1.2 CD8+ T cell activation and expansion

CD8+ T lymphocytes are very important mediators of the adaptive immunity against certain viral and bacterial pathogens, as they contribute to resistance against intra-

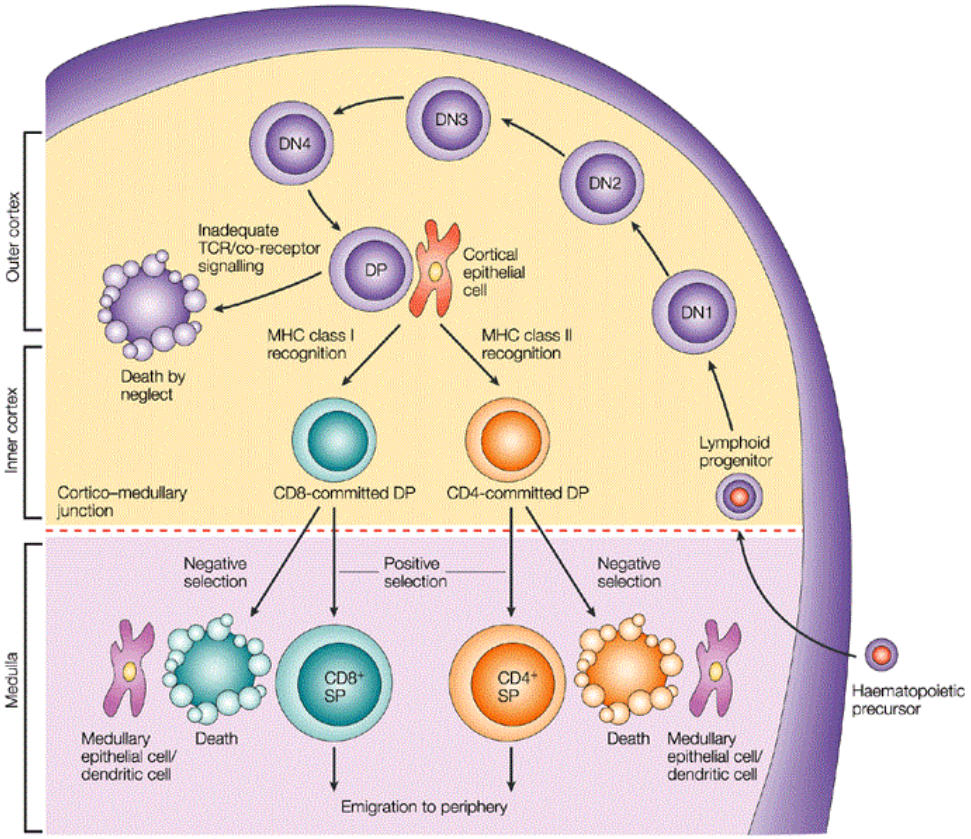

Figure 1.1: **T lymphocyte development.** Lymphoid progenitors arise in the bone marrow and travel into the thymus where they undergo several differentiation stages. Early committed T cells lack the expression of the T cell receptor (TCR), they are double-negative (DN) thymocytes and express with ongoing differentiation a pre-TCR. A transition from the DN to the double-positive (DP) stage occurs, leading to a substantial cell proliferation and development of TCR$\alpha\beta$ surface expression. All thymocytes have to successfully undergo TCR gene re-arrangements, positive and negative selection processes. Only a small fraction of lymphocytes will undergo maturation. Mature thymocytes that express TCRs that bind to self-peptide MHC class I complexes become CD8+ T lymphocytes, whereas those that bind to self-peptides presented on MHC class II molecules become CD4+ T cells. Both matured T cell subsets leave the thymus and become peripheral naïve T lymphocytes. Figure is adopted from Germain [63].

cellular infections [24, 254]. Small pathogen-derived peptides are presented to CD8+ T lymphocytes on the surface of professional APCs by MHC class I molecules. The ligation of the peptide-MHC (pMHC) with the TCR lead to the priming and activation of naïve CD8+ T cells [66, 174]. The strength of the TCR determines the choice of the transcriptional and differential program, which is initiated. The TCR signaling strength is dependent on the magnitude and the duration of the signal, as well as on the number of TCR molecules on the T cell surface [123, 187]. Moreover, the amount of peptide MHC class I complexes, the TCR affinity and avidity influence the development, differentiation, and the formation of effector and memory CD8+ T cells [112, 264]. Recent publications have demonstrated that the recruitment of low and high affinity clones lead to a broad TCR diversity of effector and memory cells [12, 41]. However, it has been shown that strong TCR engagement or prolonged exposure to antigen resulted in enhanced generation of effector cells [89, 235]. In contrast, although even very weak TCR ligand interactions are sufficient do induce initial proliferation and effector cell formation, they preferentially trigger memory cell differentiation [54].

Nevertheless, an efficient priming and activation of T lymphocytes requires 3 signals. Besides the ag-specific stimulation of the TCR via pathogenic peptides presented on MHC class I molecules on professional APCs, two other signals are needed [151]. Signal 2 is presented by the engagement of co-stimulatory molecules, which can be provided by the interaction of distinct surface molecules expressed by an APC with its respective receptor on the T cell surface. Such co-stimulatory interactions occur for example between the B7 ligands (CD80 and CD86) on dendritic cells (DCs) with the CD28 receptor on CD8+ T cells, and lead to the generation of Interleukin 2 (IL2) [147]. Reduced co-signals lead to a lower magnitude of the CD8+ T cells response. Furthermore, as third signal, the availability of cytokines like interferon (IFN), IL2 and IL12 play additionally a major role for the tight regulation of the acquisition of cytotoxic functions [36, 204]. They also include IL1 and IL6, which have been shown to be required at different stages of T cell differentiation and to have distinct effects on the responsiveness to IL2 [194]. Different pro- and anti-inflammatory cytokines work in opposition to promote terminal effector or memory precursor formation [100]. It has been shown that in the absence of specific cytokine signals the T cells fail to develop a full effector function, survive poorly, and do not form a proper memory population [37].

1.3 Acquisition of cytotoxic functions by CD8+ T cells

Different effector mechanisms are initiated after priming of naïve CD8+ T cells to combat an infection (Figure 1.2). One effector mechanism is the cytolysis of infected cells via the pore-forming molecule perforin [102]. The membrane-bound perforin on cytotoxic CD8+ T lymphocytes (CTLs) polymerizes and forms pores, which result in an influx of small molecules, such as Ca^{2+} or induces osmotic stress, leading to colloid osmotic lysis [244]. Efficient lysis by perforin is dependent on the contribution of granule enzymes, both secreted by exocytosis and together inducing apoptosis of the target cell [231]. There exist various types of granzymes, such as granzyme A and B, stored within the granular matrix of CTL lysosomes [53]. CD8+ T cells release cytotoxic granzymes in the direction of the target cells, aligned along the immune synapse to avoid non-specific

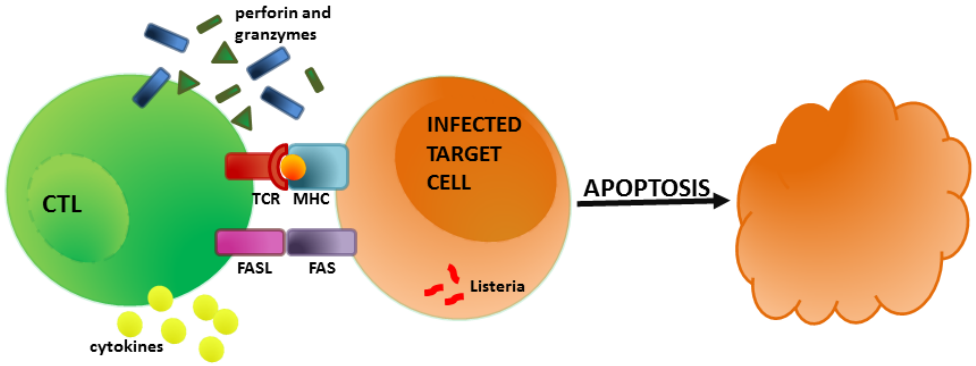

Figure 1.2: **Cytotoxic CD8+ T cells acquire various effector functions.** Cytotoxic effector CD8+ T cells become activated, as they recognize pathogen-derived peptides bound to MHC class I molecules. They express the pore-forming molecule perforin and granzymes to lyse infected target cells via cell-induced apoptosis. Furthermore, CTLs upregulation of FASL (CD95L) molecule, which can lead to activation of the caspase cascade, thereby initiating programmed cell death by aggregation of FAS (CD95) on the target cells. Additionally, CTLs express different cytokines, like IL2 and TNF, to recruit and activate other cells of the immune system, such as macrophages. Modified figure from Trapani and Smyth [231] is shown.

damage of surrounding cells. Pores formed by perforin into the membrane of the target cell allow the cytotoxic granzymes to enter infected cells. These serine proteases cleave proteins inside the target cell, thereby shutting down the production of bacterial or viral proteins [11]. Additional, granzymes induce fragmentation and degradation of DNA at the internucleosomal level, resulting in apoptosis of target cells [79]. Although granzymes and perforin mostly involved synergistically in cytolysis, granzymes are also capable of crossing the plasma membrane and entering the target cells in the absence of perforin [207].

Another killing feature of cytotoxic CD8+ T cells is mediated via the upregulation of FASL (CD95L). This molecule can lead to an activation of the caspase cascade, thereby initiating programmed cell death by aggregation of FAS (CD95) on the target cells [208]. The FAS-FASL interaction results in typical apoptosis of the target cells where cytoplasmic proteases are involved in the induction of programmed cell death [180].

Additionally, following ag-specific stimulation, CD8+ T lymphocytes produce several cytokines and chemokines to orchestrate to full wingspread of the immune response. Effector CD8+ T cells produce IFNγ and tumor necrosis factor (TNF) to recruit other cells of the immune system like macrophages to the site of infection and inflammation, and additionally increases their anti-microbicidal activity [75].

1.4 Differentiation of CD8+ T cells

Naive CD8+ T lymphocytes circulate between the blood and secondary lymphoid organs where they encounter their cognate antigen. The homing of immune cells to secondary lymphoid organs is possible due to the expression of a defined set of homing receptors, such as CD62L (L-selectin) and chemokine receptors like CCR7 (CC-chemokine rezeptor 7). Effector T cells show decreased expression of lymph node homing receptors, allowing them to circulate and home to non-lymphoid tissues, as they have to migrate to the side of inflamation and infection.

During the early phase of infection, CD8+ T cells upregulate activation markers, like CD44 and CD11α (integrinα) but downregulate the naïve marker CD127 (interleukin-7Rα) [203]. CD8+ T cells differentiate into short-lived effector cells (SLEC) and memory-precursor effector cells (MPEC). Both CTL subsets can be distinguished according to their surface marker expression of KLRG1 (killer cell lectin-like receptor G1) and CD127. SLEC express high levels of KLRG1 and low levels of CD127 [97]. Cells of this cell subset are not able to establish memory after clearance of infection, as these cells undergo contraction. In contrast, MPEC express low levels of KLRG1 and high levels of CD127, CD27, and Bcl-2 (B cell lymphoma 2) [97, 101, 200]. MPEC have the ability to survive and form long-term persistent memory. However, CD8+ T cells expressing nor CD127 neither KLRG1 are termed to be early effector cells (EEC), which are meant to become SLEC or MPEC. Cells expressing both markers at the same time are termed to be double-positive effector cells (DPEC) and can be detected after infection [169]. Besides that, another method to distinguish between effector and memory CD8+ T cells is based on expression of CD27, KLRG1 and CD127 [217].

Environmental factors, such as cytokines like IL2 [253], IFNγ [251], type I IFN (IFNα and IFNβ) [38, 116], and IL12 [111, 257] promote the generation of effector cells and longevity, as well as the function of memory CD8+ T cells. IFNγ not only contributes to the pathogen clearance through its activation of antimicrobial mechanisms, it also plays a role in T cell homeostasis and might participate in the selection of the memory pool by increasing the expression of self-MHC complexes [7]. IL2 promotes effects on lymphocyte cell survival and proliferation. Furthermore, IL2 can directly regulate the cytotoxicity of CD8+ T cells via direct impact on the perforin and granzyme gene expression during primary activation of CD8+ T cells upon activation [94]. Like IL2, also IL15 utilizes the common gamma (γc) and IL-2Rβ chain, has been shown to have co-stimulatory features and to be crucial for maintaining CD8+ T cell homeostasis and basal proliferation [64, 68, 133]. Additionally, IL4, IL7, IL9, and IL21 cytokines use also the γc subunit for signaling playing a role in the survival and proliferation of thymocytes [221, 238]. Taken together, all these different cytokines participate in the immune response to intracellular bacteria and there are more or less capable to promote anti-pathogenic resistance, are associated with phagocyte influx or support activation and proliferation.

CD122, the IL-2Rβ chain, is a part of the IL-15R complex and is highly expressed by memory CD8+ T cells. In the absence of CD4+ T cell help, CD8+ T cells express lower CD122 and show declined numbers, as well reduced functionality. It has been shown that the transcription factor (TF) T-box transcription factor, T-box21 (Tbet) and eomesodermin (EOMES) are linked to the CD122 expression, a receptor that confers

cellular responsiveness to IL15.

Different regulators, like T-bet and EOMES among others, were shown to be essential key mediators for the cell fate decisions of CD8+ T cells [91, 97, 181]. Both transcription factors, Tbet and EOMES control IFNγ expression and the generation of cytokine producing CD8+ T cells, which additionally have acquired cytolytic functionality. They have a partially redundant activity. Furthermore, Blimp-1 (B lymphocyte activator protein 1) and Bcl-6 (B cell lymphoma 6) play a role for the balance between effector and memory cell formation [88, 103].

Memory CD8+ T cells can be further divided into two subsets dependent on their distinct phenotypic and functinal properties, as there is a cellular heterogeneity within the pool of memory T cells. Based on the categorization made by Sallusto and colleagues [199], memory CD8+ T cells can be divided into T_{EM} and T_{CM}. T_{CM} reside in secondary lymphoid organs, as they highly express CD62L but do not express immediately lytic functions. In contrast, T_{EM} are mainly located in non-lymphoid tissues. They do not express CD62L but they display certain effector functions and cytotoxic functionality.

Several potential models exists to explain how the heterogeneous pool of memory cells arise during the cause of infection [100]. Nevertheless, there are several controverse publications claiming different models to be true. It is well possible that multiple pathways lead to the generation of a memory T cell pool where cells having distinct genotype, potential, and functions.

1.5 Expansion, contraction, and memory phase

Upon initial antigen encounter, naive CD8+ T cells pass 3 different phases, namely expansion, contraction, and memory phase, which is illustrated in Figure 1.3. CD8+ T cells bearing TCRs specific for several pathogen-derived antigens leave the naïve stage and undergo clonal expansion, thereby increasing in numbers and differentiating into effector cells gaining a variety of effector functions [25]. The naïve CD8+ T lymphocyte repertoire is comprised of small numbers of precursors ranging from 10 to 10.000 cells, which are specific for a single antigen [15]. Therefore, if a naïve CD8+ T cell becomes activated, it must undergo a massive proliferative expansion to reach a sufficient number of effector cells. Clonal expansion requires a high energy supply, which is achieved due to an alteration of the metabolic program, characterized by a switch to aerobic glycolysis and higher rates of biosynthesis [140].

The goal of the clonal expansion of ag-specific CD8+ T cells is to combat the invading pathogen efficiently via their cytotoxic capacities, and to contribute to its clearance. After the peak of proliferation concluding the expansion phase, most of the cells die by apoptosis in a contraction phase, which often correlates with the clearance of acute infection. CD8+ T cells then decline in numbers in all tissues to a memory level, where just a small heterogeneous population be maintained at 5-10 % of the initial numbers and persisting for life [93]. The size of the memory population resulting due to the contraction phase is substantially bigger than the naïve precursor pool. Different memory CD8+ T cell subsets arise from the contraction phase having different tissue homing, self-renewal, and effector recall potentials. In case of reinfection, upon second antigen

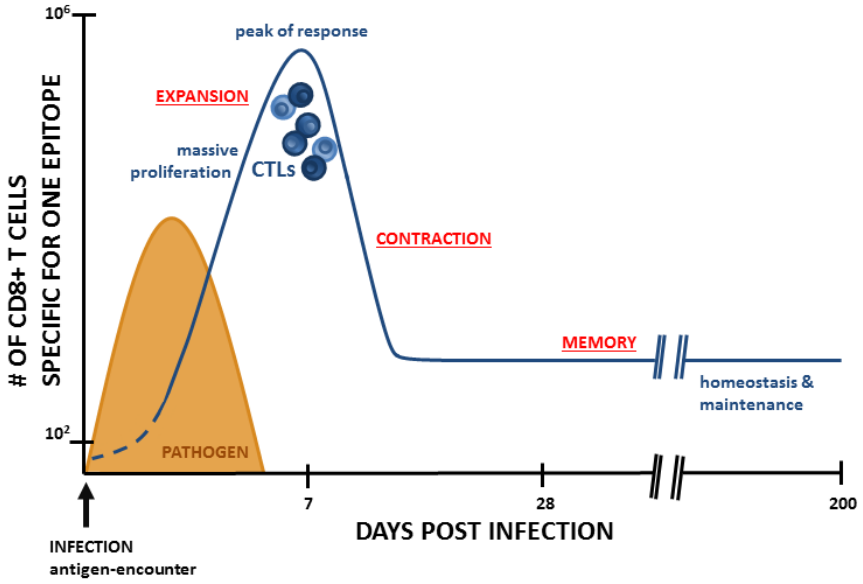

Figure 1.3: **Graphic illustration of the CD8+ T cell development during acute infection.** Naïve CD8+ T cells undergo massive proliferation after encounter their cognate antigen and differentiate into cytotoxic CD8+ T lymphocytes (CTLs). CTLs acquire cytolytic effector functions, which contribute to pathogen clearance. After the peak of response, CTL decline in numbers during the contraction phase due to apoptosis to a memory level leading to long-live protection. Modified figure from Williams and Bevan [252] is shown.

encounter, memory CD8+ T cells mobilize very rapid their effector functions [125] and are less dependent on co-stimulatory signals, which are required for priming of naive ag-specific T cells [89].

There are different mediators and signaling pathways that maintain the memory pool, such mediators like antigen persistence [89, 157] and the activation of the TCR via MHC or the influence of various cytokines [228]. The cytokine milieu additionally shapes CD8+ T cell responses, as these environmental factors influence the clonal expansion, effector function acquisition, contraction phase, and memory formation. IL2 stimulation of CD8+ T cells during their priming phase is critical for CD8+ T cell memory formation.

1.6 Different molecules, receptors, and death pathways mediate contraction

T cell contraction is mediated via intrinsic and extrinsic pathways of apoptosis, including caspase-dependent and -independent death programs, which initiate morphological, biochemical, transcriptional, and metabolic changes [58]. CD8+ T cells cannot evade apoptotic pathways if an engagement of death receptors and eat-me signals, cytokine

derivation or inhibition of cytokine signaling occurs [43, 118, 144]. The intrinsic pathway is mediated by the mitochondria and is tightly regulated via members of the Bcl-2 superfamily [39]. The inflammatory environment [97], as well as the engagement of death receptors due to the expression pattern of pro- and anti-apoptotic molecules can trigger apoptosis.

The balance between different molecules dictates whether effector T cells survive and expand, or go into contraction as consequence of initiated apoptotic pathways. It is challenging to detect apoptosis of cells, as rapid clearance of dying cells by phagocytes takes place [8] and as it is difficult to define the exact moment in which contraction begins. T cell proliferation and cell death might occur simultaneously till one gain the upper hand. Dying cells are quickly recognized and removed by phagocytes, like macrophages, which can be either neighboring cells or cells especially recruited to the sites where increased cell death occurs. Furthermore, the location of T cell contraction, whether T cells preferentially die in lymphoid organs or in infected tissue, might vary based on the infection model [148, 247].

Several inhibitory molecules have been linked to an impaired T cell function or an exhausted T cell phenotype [250]. Some belong to the B7 family (CTLA4, PD-1) [28], immunoglobulin family (Tim3, CD160, LAG3) or CD2/SLAM family (2B4) [26].

The death receptor-mediated pathway is triggered by certain mediators, which regulate apoptosis and lead to the activation of caspases, if the interplay of pro- and anti-apoptotic molecules is in imbalance. Recent publications provided evidence that at the onset of contraction, effector CD8+ T cells express lower levels of anti-apoptotic proteins like Bcl-2 [126] but increase their co-expression of pro-apoptotic molecules like CD160, PD-1, 2B4, CTLA4, BIM, and LAG3, all being associated with functional impairment and disease progression [170, 171].

During the early stage of apoptosis, dying cells release find-me signals or exposure eat-me signals on their surfaces (Figure 1.4), which facilitate their recognition by receptors expressed on professional phagocytes, such as macrophages, monocytes, dendritic cells, and neutrophils [182, 191, 192]. Viable cells actively expose don't eat-me signals, which deliver a negative engulfment signal to prevent their recognition and uptake by phagocytes [50]. Don't eat-me signals, such as CD46 [51], CD47 [59], and CD31 [20] are not longer expressed which further favor the uptake of those cells.

Additionally, apoptotic cells secret soluble factors acting as chemoattractant, which in turn recruit monocytes and macrophages migrating to their proximity and lead to phagocytic activation and cell clearance [193]. Just to mention some signaling molecules, phosphatidylserine (PS) exposure on the outer surface of the cell membrane can be detected by phagocytosing cells, removing all cells targeted with this early apoptotic surface marker [145]. The regulated release of triphosphate nucleotides like ATP and UTP [49] or shingosine 1-phosphate (S1P) [249], lipid lysophosphatidylcholine (LPC), and the fractalkine CX3CL1 [232], or ICAM-3 [70] from early apoptotic cells attract macrophages towards cells undergoing apoptosis and lead to cell clearance. Furthermore, some molecules like fractalkine are shown to induce the production of bridging molecules like milk fat globule EGF factor 8 (MFG-E8) and thereby upregulate the engulfment machinery components and facilitates recognition [152]. PS binds with high affinity to the bridging molecule MFG-E8 on activated macrophages, which in turn promotes the clearance of the apoptotic cell, as it enables the recognition by engulfment receptors [72].

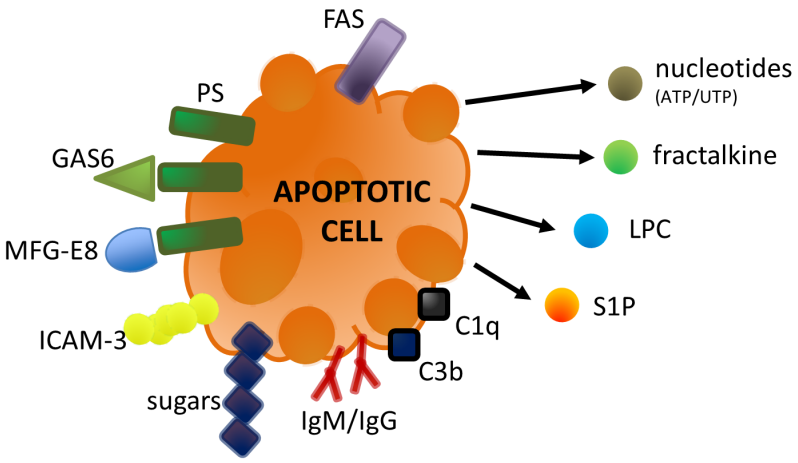

Figure 1.4: **Release of find-me signals and exposure of eat-me signals on the apoptotic cell surface.** Cells prone to death release several find-me signals, such as nucleotides, lysophatidylcholine (LPC), shingosine 1-phosphate (S1P), and fractalkine. Additionally, as apoptotic cells undergo programmed cell death they expose a variety of eat-me signals on their surface, such as phosphstidylserine (PS), complement activating molecules C1q and C3, altered sugars and ICAM-3, among others. Molecules like GAS6 and MFG-E8 bridge the interaction between eat-me signals on target cells and the phagocytic receptors on phagocytes. Modified and merged figure from Ravichandran [193] and Hochreiter-Hufford and Ravichandran [82] is shown.

Another bridging molecule is Gas6, which also binds to PS and mediates the recognition of the apoptotic cells by receptors on phagocytes [132].

Furthermore, antibodies and other mediators such as IgM, IgG, and SAP can act as bridging molecules to induce apoptotic pathways or to facilitate binding of complement components, like IgM facilitates C1q binding. Thus, leading to the activation of the classical component pathway [172]. Taken together, the presentation of eat me signals on the cell surface of an early apoptotic cell attract phagocytic cells, followed by a rapidly engulfment, leading to digestion in phagocytic lysosomes, and cell death.

Extrinsic apoptotic pathways can be initiated by membrane bound receptors. Death receptors like FAS (also known as CD95), TNFa receptor 1 (TNFR1) and TRAIL (CD262/DR5) induce extrinsic apoptosis by binding to their respective ligand. TRAIL death receptor expressed on T cells renders cells susceptible to caspase-8-mediated apoptosis. During the contraction phase, CD8+ T cells can express both FAS and FASL molecules [237]. Via the interaction of FAS-FASL [161], CD8+ T cells can kill each other to eliminate effector cells at the end of an immune response, when the immune system combated the invading pathogens. Therefore, the FAS-FASL pathway offers an additional lytic ability of CTL to control T cell proliferation by the initiation of apoptosis-induced cell death (AICD). The surface molecule FAS (CD95 or APO-1) consists of an intracellular death domain, which initiates signaling to death after ligand binding [92], either lead directly to caspase-mediated death by the activation of the

procaspase cascade or direct cells to necrosis [81, 240].

The complement system is composed of over 30 soluble and membrane bound proteins generated primarily in second lymphoid tissue and the liver, which than circulate in the blood and mediate distinct biochemical pathways involved in innate and adaptive immune responses [30]. It includes additionally several pathway components, receptors as well as certain regulators. The complement system can be activated by three different pathways (Figure 1.5), namely the lectin, the classical, and the alternative pathway [156].

The activation of the lectin complement pathway through mannose-binding lectin (MBL)- associated serine protease (MAPS) mediates mainly pathogen removal, as MBL can recognize carbohydrates on microbial surfaces. Furthermore, it is able to interact with nucleic acids and phospholipids, among others [223]. It has been shown that MBL clusters in dying cell surfaces to trigger phagocytosis [219].

The major molecule of the classical pathway is the C1 component, which is composed of C1q and the proteases C1r and C1s [57]. The protease C1s cleaves the C4 component into C4a and C4b followed by the C4b deposition on the microbe or cell surface where it triggers opsonization and leading further to the cleavage of C2 into Cs2 and C2b. This pathway generates a common C3 convertase known as C4b2a [245]. The C3 component also serves as central molecule for the alternative complement pathway being spontaneous activated by hydrolysis of the internal C3 thioester bond [179]. Its cleavage result in the C3 convertase complex C3bBb creating an efficient cycle of C3 cleavage and convertade assembly [74].

The activation of the C3 molecule is a shared step in all three pathways, which leads to a terminal pathway with the generation of C3 and C5 convertase enzyme complexes. Those complexes cleave C3 and C5 into the opsonins C3b and C5b and additional generate anaphylatoxins, namely C3a and C5a [196]. These very potent chemoattractants and inflammatory mediators play a crucial role in the complement cascade. In detail, C3 convertase promotes the further cleavage of C3 into C3a and C3b. C3b remains bound on the cell surface of the microorganism or the target cell forming a complex namely C4b2a3b generated by the classical or lectin pathway or C3bBb3b complex when the generation occurred via the alternative pathway. Nevertheless, both complexes are known as C5 convertase, which promotes the cleavage of C5 into C5b and C5a [114]. C5b participates in the assembly of the MAC while the generated anaphylatoxins C3a and C5a are released and signal through their cognate G-protein-couples receptors [52]. The generation of these key anaphylatoxin molecules after the activation of the complex cascade initiates chemotaxis of phagocytic cells and induces strong pro-inflammatory signaling [210]. The deposition of the C5b molecule induces assembly of the other complement proteins C6, C7, C8 and C9. This terminal pathway leads to the formation of the lytic membrane attack complex initiating target lysis [155].

The main functions of the complement system are diverse. First, it promotes opsonization and phagocytosis through the release of C3b and C5b peptides leading to direct cell lysis. Second, the clearance of invaded microorganisms and deletion of apoptotic cells through assembly of the membrane-attack complex (MAC) by C5-C9, and third to trigger inflammation through fragments of the complement cascade such as C3a, C4a, and C5a.

Furthermore, the generation of chemotactic and inflammatory peptides promote phagocytosis through their interaction with several complement receptors coupled to G-proteins

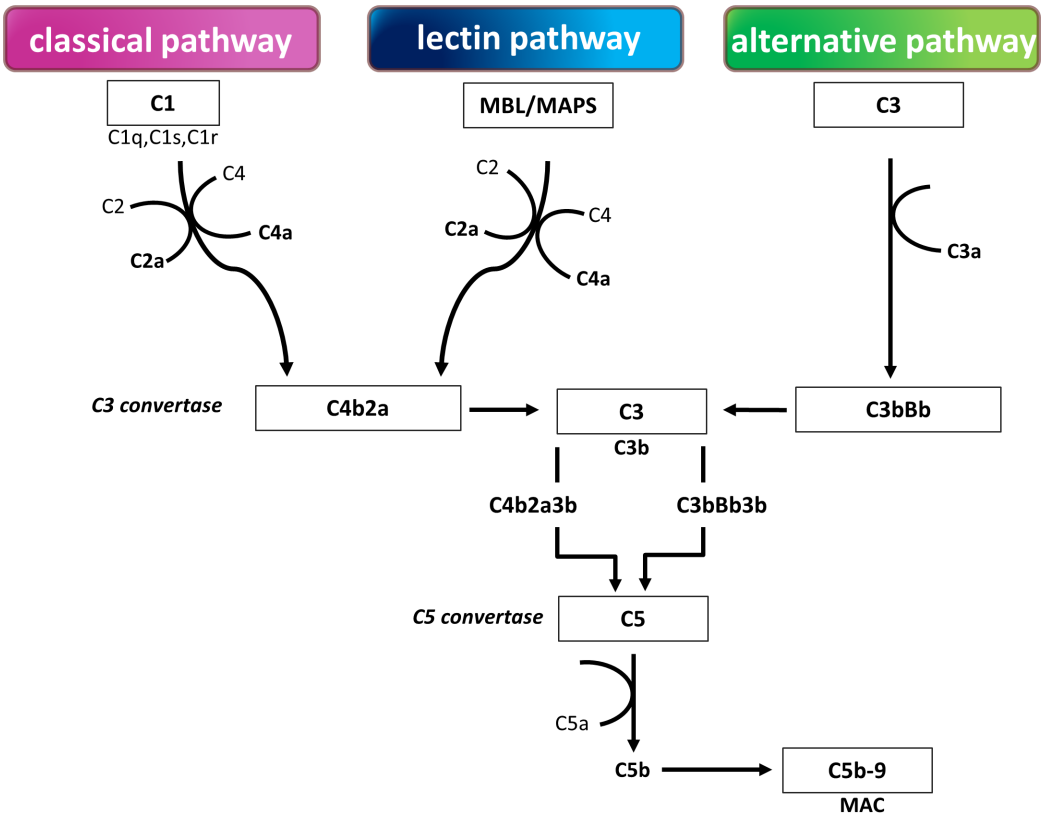

Figure 1.5: **The complement cascade.** Activation of the complement cascade can be induced via (1) the lectin pathway initiated via mannose-binding lectin (MBL) to carbohydrates on target surfaces, (2) via the classical pathway initiated by the C1 component, and (3) by the alternative pathway by hydrolysis of internal C3. All three pathways leading to the activation of C3 and C5 convertases and to the formation of anaphylatoxin C3a and C5a. Additional, to the generation of C3b and C5b serving as opsonins. The C5b deposition induces the assembly of the other complex proteins C6-C9, leading to the formation of the lytic membrane attack complex (MAC) initiating target lysis. Modified figure from Józsi [98] and Murray et al. [160].

mostly present on macrophages, namely CR1 (CD35), CR2 (CD21), C3a receptor (C3aR), and C5a receptor (C5aR, also called CD88) having distinct but synergistic functions [134, 198, 236, 255]. For example, CD88 (also known as C5aR1) is expressed on myeloid, endothelial and epithelial cells. C5ar1 binds the activated complement anaphylatoxin C5a and triggers chemotaxis of phagocytosing cells and the release of pro-inflammatory mediators. There are many regulators being involved in those complex processes, such as CD46 being a co-factor for serum factor I inactivating C3b and C4b components, CD55 (also known as DAF) leading to dissociation of C3 convertase, CD59 inhibiting the MAC formation or Serpin G1 inhibiting the C1 component of the classical pathway. Viable cells express several complement regulators to inhibit the deposition of the complement components such as C3 and C4, and the activation of the complement cascade.

Chapter 2

Listeria monocytogenes

In 1926, the gram-positive bacteria *Listeria Monocytogenes* (*LM*) was first described in animals by Murrey and colleagues [159]. Three years later in 1929, the foodborne pathogen was also described in humans [168]. This ubiquitous organism can be found in diverse environments, such as soil but it also contaminates water, food products, and colonizes humans and animals. After ingestion of Listeria contaminated food, this bacteria is able to cross several barriers inflicting gastroenteritis via passing the intestinal barrier and thereby invade the intestinal epithelium. It also crosses the blood-brain barrier causing meningitis and encephalitis [71], as well as abortion in pregnant woman [128].

2.1 Pathogenesis

Listeria monocytogenes is a gram-positive, facultative intracellular rod-shaped bacterium that is widely used as model system to investigate cell-mediated immunity against intracellular pathogens [108]. The pathogenesis of this intracellular bacterium is based on various virulence factors (Figure 2.1).

Following intravenous (i.v.) injection into mice, *LM* accumulates rapidly in the spleen and liver, which serves as sites of infection and bacterial replication. The bacteria is then phagocytosed by macrophages and neutrophils in these organs. Most of the bacteria are destroyed but some can escape from the phagosome into the cytoplasm of the infected cell, thereby escaping the arm of the complement and their detection by neutralizing antibodies [71]. This process is highly dependent on the secreted virulence factor listeriolysin (LLO), a pore-forming toxin, which lyses the phagosomal mem-

brane [60, 186], and two phospholipase C enzymes (PlcA and PlcB) [212].

Additionally, several other virulence factors of *LM* are expressed, which are instrumental in invasion and intracellular replication of the bacterium. Bacterial surface proteins such as internalin A and B enable the entry into non-phagocytic cells, such as hepatocytes, epithelial and endothelial cells [18, 129]. Once in the cytoplasm, the bacteria multiplies and initiate movement, as *LM* can polymerizes host-derived F-actin to spread from cell to cell without leaving the intracellular space [34].

The bacterium starts its lifecycle again, once internalized by neighboring cells. The escape from autophagy and its actin-based mobility within the cytosol is mediated by the virulence factor actin-assembly-inducing protein (ActA) [211]. Both, LLO and ActA play a critical role for the survival of *LM* in phagocytic cells, the dissemination within tissue and the pathogenicity. The importance of many virulence factors has been shown by the demonstration that mutant strains having a single or a combinatorial defect in these factors, compared to wild type stain, are avirulent or attenuated in their capability to induce systemic infection [69, 263].

2.2 Murine listeriosis model

Listeria monocytogenes infections in animal models have become a useful tool to investigate host-pathogen interaction, cell-mediated immune responses, mechanisms of bacterial clearance, and the subsequent acquisition of life-long protective immunity. The murine model of systemic listeriosis, via an intravenous inoculation of *LM* into mice, represents an adequate model system to investigate the pathophysiology of a complex intracellular bacterial infection and to study the host defense mechanisms against intracellular pathogens. Oral inoculation of *LM* into mice, which would be closer to the natural root of infection through the gastrointestinal tract in humans, is not efficient as only small numbers of *LM* cross the mouse intestinal barrier due to a mutation of the murine E-cadherin [46]. The intravenous infection of mice provides a suitable infection model resulting in a systemic listeriosis.

Some advantages, beside many others, are the possibility to generate *LM* with attenuated pathology as this bacterium can easily genetically manipulated. Other advantages are the alteration of the infection duration with antibiotic treatment and the knowledge of T cell specific epitopes. Early studies of CD8+ T cell responses were hampered by the lack of knowledge of specific CD8+ T cell epitopes. But nowadays, many different CD8+ T cell specific natural and constructed epitopes are known, which are presented either on H-2K^{d} or H-2K^{b} restricted MHC class I molecules, making it possible to analyze CD8+ T cell-mediated immune responses in mice from BALB/c or C57BL/6J background, respectively [23, 233].

The first MHC class I restricted bacterial pathogen-derived epitopes recognized by CD8+ T cells were the listeriolysin derived epitope LLO$_{91\text{-}99}$ [177], and the hydrolase p60 derived epitope p60$_{217\text{-}255}$ [175] in Balb/c mice. This study has focused on the MHC class I restricted CD8+ T cell response of mice with BL/6J background. Since natural Listeria derived epitopes are mainly for H-2K^{d} mice, a recombinant *Listeria monocytogenes* stains expressing Ovalbumin (OVA) or altered peptide ligands (APL) to enable the detection of CD8+ T cells recognizing H-2K^{b}- class I restricted determinant

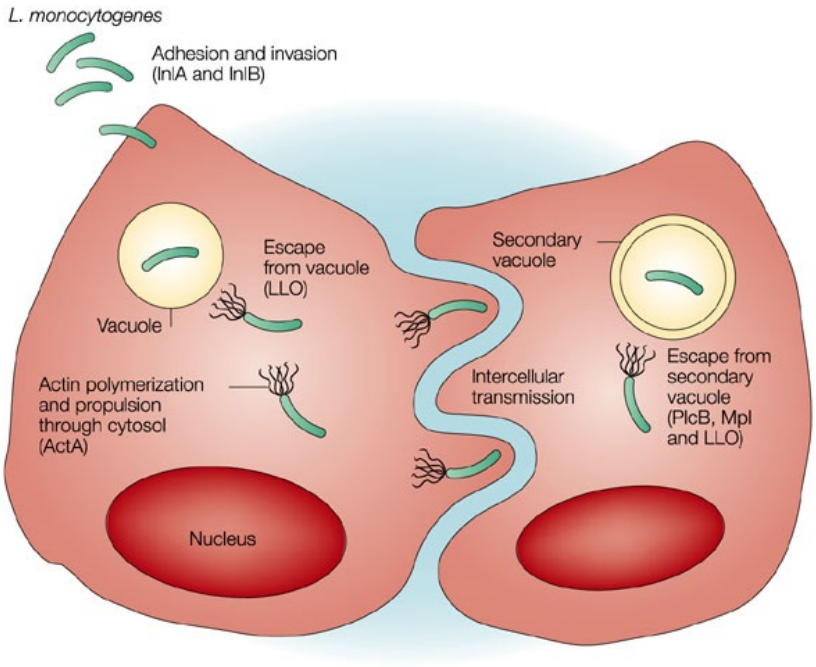

Figure 2.1: **The pathogeneses of the intracellular bacterium *Listeria monocytogenes* (LM) is dependent on various virulence factors.** Listeria express bacterial surface proteins such as internalin A and B, which enable the entry into non-phagocytic cells such as hepatocytes, epithelial and endothelial cells. The secreted pore-forming toxin listeriolysin (LLO) lyses the phagosomal membrane and two phospholipase C enzymes (PlcA and PlcB) enable the bacterium to escape from the autophagy. The actin-based mobility within the cytosol is mediated by the virulence factor actin-assembly-inducing protein (ActA). Therefore, LM is capable of spreading from cell to cell without leaving the intracellular space. Figure is adopted from Pamer [176].

derived from OVA, such as SIINFEKL (SI) or SIYNFEKL (Y3) and SIITFEKL (T4) were used in this study, respectively. Additionally H-2K^b- peptide tetramer staining was used to examine the generation, differentiation and memory formation of OVA-specific CD8+ T cells after systemic Listeria infection in H-2K^b mice.

2.3 Cell-mediated immune response against Listeria

A large variety of cytokines and a wide range of cell types are involved in the immune response against *Listeria monocytogenes* (LM). Although, LM has evolved clever ways to manipulate the host cell to its advantage and to escape different protective mechanisms by the host cell via remarkable adaptation. Its presence within the cytosol can be recognized by the immune system and induces a potent cell-mediated immune response. The host response against LM is a complex interplay between innate and adaptive immune elements. Several cytokines like IFNγ, IL2 and TNFα play a major role for a proper immune response together with the cooperation of various cell types including neutrophils, natural killer cells (NK), macrophages, and cytotoxic CD8+ and helper CD4+ T lymphocytes [108].

The bacterium penetrates the epithelial cell membrane and disseminates in the blood stream through the whole body and into the organs. During the early phase of infection, T cell independent mechanisms cause remarkable reduction of bacterial numbers. Nevertheless, these mechanisms can not completely eliminate the pathogens. In the liver and spleen, two of the main target organs of the bacteria, the pathogen is rapidly internalized by splenic and hepatic macrophages. During the initial stage of infection, IFNγ and TNFα secreting cells like NK and neutrophils play a crucial role in controlling bacterial growth, especially in liver [32, 47]. The rapidly triggered innate immune response is essential for the survival of the host [234]. As in liver, also in spleen, neutrophils together with macrophages rapidly accumulate as first line defense of the host [33]. Furthermore, at the cell surface also toll-like receptors have been implicated in the recognition of LM as they transmit signals to activate innate immune defenses [224].

After cellular invasion, bacteria escape from the double-membrane-bound vacuole, gain access, and multiplies intracellular within the cytosol of the host cell. Therefore, foreign peptides secreted by the bacterium are mostly processed by the endogenous MHC class I antigen processing pathway (Figure 2.2) and presented to CD8+ cytotoxic T lymphocytes [178]. Due to this process, CD4+ T cells play a minor role for the protective immunity [124] and CD8+ T cells are the most effective mediators of anti-listerial immunity. Nevertheless, class II-restricted CD4+ T cells promote help for CD8+ T cells, among others, produce IL2 and IFNγ.

However, activated CD8+ T cells are involved in the primary response to Listeria, as they produce a broad range of cytokines upon antigen encounter. CD8+ T cell responses to LM reach peak frequencies after approximately 7 days after intravenous infection. They are especially important for the protective immune response to secondary LM infections as the protection is dependent on IFNγ production by CD8+ T cells. Secreted cytokines, like IFNγ and TNFα, also produced by other cells, are very important for the resistance of mice to this pathogen [22, 77]. Additionally, a pore-forming perforin exclusively produced by cytotoxic CD8+ T cells, play thereby the major role in the T cell

mediated resistance to LM together with the FAS-dependent cytolysis of the infected cells. Once in the cytoplasm, the bacterium multiplies and polymerizes host-derived F-actin, thereby initiating movement from cell to cell without leaving the intracellular milieu. This is the reason why it has been shown that neither antibodies nor B cells participate in the immunity against Listeria. Mainly, CD8+ T cells promote anti-listerial resistance in naive mice and mediate clearance of this bacteria.

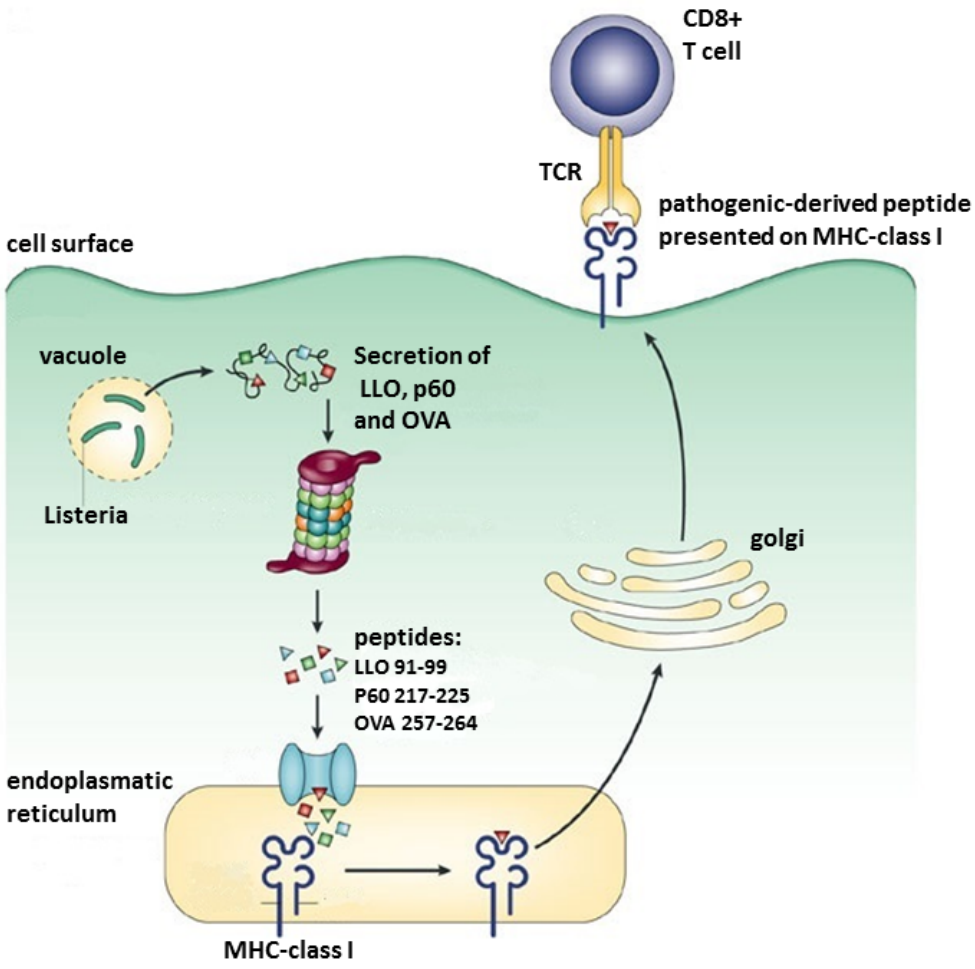

Figure 2.2: **Pathogenic peptides secreted by *Listeria monocytogenes* are mostly processed by the MHC class I antigen processing pathway.** After cellular invasion, Listeria bacteria escape from the double-membrane-bound vacuole and gain access to the cytosol of the host cell. Therefore, foreign peptides secreted by the bacterium are mostly processed by the endogenous MHC class I antigen processing pathway. Pathogenic-derived peptides are then presented on MHC class I molecules to CD8+ T cells. Modified figure from Pamer [176].

Chapter 3

Interferon regulatory factor 4

The interferon regulatory factor 4 (IRF4) is a member of the interferon regulatory factor (IRF) family comprising several transcription factors, first described as downstream regulators of interferon signaling. Unlike other family members, IRF4 is not induced by interferon, but rather by antigen receptor engagement. IRF4 is a critical transcriptional regulator for the development and functionality of the immune system, as its expression is mainly restricted to several lymphoid and myeloid cell types. It can act either as activator or repressor on its target genes, dependent on its interaction partner.

3.1 IRF4 is a member of the IRF family

The IRF family consists of 9 members (IRF1-IRF9) in mammals, sharing homologue sequences but have distinct functions in several cell types. IRFs were first described as downstream regulators of interferon signaling but nowadays it has been shown that they are also involved in cytokine signaling, cell growth regulation and homeostasis, and they control the differentiation and functionality of different immune cells [226]. Furthermore, IRFs are key mediators against anti-viral responses.

The first members of this family, IRF1 and IRF2, were found to bind to enhancer elements in the promoter region of genes that encode for IFN [73, 154]. Because both IRF family members bound to a common DNA motif namely IRF enhancer [227]. Later, similar sequences were also detected in the promoters of genes that are regulated by IFNs, this motif was then defined as interferon stimulatory response element (IRSE) [40].

Additional family members show sequence homology and all share a DNA binding domain (DBD), which is localized in the first 115 amino acids of the amino-terminal region. It contains a helix-turn-helix motif, consisting of 5 tryptophan residues that are each separated by 10-18 amino acids [73]. This motif recognizes a 5'-GAAA-3' core sequence and mediates IRF binding to the ISRE. Furthermore, all IRF family members, except IRF6, contain a carboxy (C)-terminal IRF-associated domain (IAD), enabling heterodimerization between family members [150] and mediating heterodimeric interactions with other transcription factors.

3.2 IRF4 and its structural features

The IRF4 is one member of the IRF family of transcription factors. It was first investigated by distinct research groups with different contexts and has therefore several names. IRF4 is also called Pip as it is a PU.1 interaction partner [19, 48, 185], and LSIRF as it is characterized as a lymphocyte specific IRF [146]. IRF4 was additionally named

Figure 3.1: **Domain structure of the transcription factor IRF4.** IRF4 is composed of a N-terminal DNA-binding domain (DBD; blue), which consists of five conserved tryptophan (W) residues that are each separated by 8-18 amino acids. The IRF-association domain (IAD type 1; green) facilitates hetero-dimerization with other family members or co-regulators. The repressor domain (orange) alters the function from activation to suppression and vice versa of the IRF4 molecule dependent on its interaction partners. A nuclear localization signal (red) enables IRF4 to not only reside in the cytoplasma, it can translocate in the nucleus where it exerts its function through regulation of its transcriptional target genes. Modified figure from Lohoff and Mak [137].

interferon consensus sequence-binding (ICSAT) protein in adult T cell leukemia [260] and MUM1 because of its role in oncogenesis of multiple myeloma [90]. Its expression is restricted to cells of the adaptive immune system, like macrophages [143], T and B cells [153]. In T cells, its expression can be initiated via TCR stimulation.

IRF4 is similar to IRF8, as they are highly homologous proteins, which can interact with each other exercising transcriptional regulatory functions [209]. Both, IRF4 and IRF8, unlike other family members, they do not activate the transcription of Type I interferon genes or positively regulate interferon-induced gene expression, as they have a weak affinity to the 5'-GAAA-3' motif of the ISREs.

The IRF4 protein is composed of a single polypeptide chain [185] with a N-terminal DBD and a C-terminal regulatory domain, composed of a nuclear-localization signal, a C-terminal IAD type 1, and a repressor domain [127], shown in Figure 3.1.

The DBD of the IRF4 enables its binding on the DNA at the ISRE. Its DNA binding specificity depends on its cell lineage-specific co-regulators. Many of this co-regulators have been identified depending on the cellular context, such as PU.1 [185], BATF [135, 158], STAT3 [122], NFAT [195], and PGC-1a [117], among others. In CD8+ T lymphocytes, IRF4 binds to its co-regulator BATF and both form a complex binding to a composite DNA element called AICE (AP-1-IRF composite element) in their target genes [65].

Due to its IAD, IRF4 can form homodimers or heterodimers with IRF8 or other family members. Furthermore, IRF4 can also form heterodimers with members of the Ets family [105] or activator protein 1 (AP-1) family [65] of transcription factors. The repressor domain facilitates an alteration of the function of an IRF molecule in the presence of particular binding partners. Depending on its interacting partner, IRF4 serves as suppressor or activator. The nuclear-localization signal enables IRF4 to not only reside in the cytoplasma, it additional can translocate in the nucleus. It exerts its

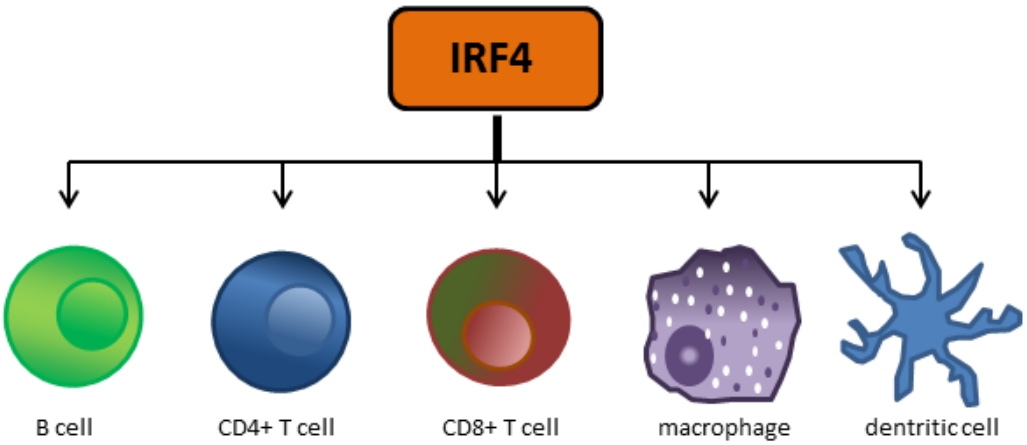

Figure 3.2: **IRF4 has pivotal functions in several immune cells.** IRF4 plays a wide variety of roles for the formation, differentiation, and function in different cells of the immune system, like dendritic cells (DCs), macrophages, B cells, and T lymphocytes.

function through regulation of its transcriptional target genes.

3.3 IRF4 has pivotal functions in different immune cells

IRF4 plays a wide variety of roles for the formation, differentiation and function in different cells of the immune system, as shown in Figure 3.2. IRF4 is required for a proper formation of germinal centers and plasma cell differentiation to produce high titers of ag-specific antibodies [113, 206]. It is together with BLIMP-1 (B lymphocyte-induced maturation protein 1) the master regulator of class-switch recombination [5]. This TF promotes M2 polarization of macrophages [201], acts as negative regulator of TLR (toll-like receptor) signaling, as it negatively regulates the production of pro-inflammatory cytokines [164]. IRF4 has been shown to be essential for different dentritic cell (DC) subsets [225], especially for the development of CD8- CD11b+ DCs [200, 222]. It has critical functions within the T cell compartment, as IRF4 is essential for T cell differentiation and functionality [138]. IRF4 is important for the development of various CD4+ T cell subsets like Th1, Th2 [230], Th9 [215], Th17 [21, 87], follicular Th cells [17, 167], and regulatory T cells [35, 173]. IRF4 has additionally pivotal roles for the expansion and differentiation of effector CD8+ T lymphocytes [27, 86, 142, 153, 163, 262].

Chapter 4

Aim of the study

Interferon regulatory factor 4 is one of the key transcription factors, which have been shown to be very fundamental for the development and functionality of several immune cells, such as B cells, dendritic cells, macrophages, and several CD4+ T lymphocyte subsets [21, 113, 139, 201, 216, 222, 225, 267]. However, it has remained an open question whether IRF4 expression additionally plays an essential role for the differentiation and functionality of CD8+ effector T cells.

Hence, this current work aimed to investigate in detail the influence of IRF4 on the CD8+ T lymphocyte response regarding activation, differentiation, and formation of a functional anti-pathogenic effector CD8+ T cell population. Therefore, in this study a new transgenic mouse model was used, where the IRF4 gene is exclusively excised in mature peripheral CD8+ T cells, other cell types being not affected. To investigate the role of IRF4 expression for the CD8+ T cell fate decision upon primary infection, mainly the murine listeriosis model was used as infection system to study CD8+ T cell responses.

Additionally and most important, this present study further wanted to examine in detail whether IRF4 influences the initiation, kinetic, and magnitude of the clonal CD8+ T cell expansion upon primary infection and its impact on the initiation of T cell contraction and fate decision.

Part II

Material and Methods

Chapter 5

Materials

5.1 Consumables

MATERIAL	COMPANY
cell culture plates (48-, 24-well flat bottom, 96- well round bottom)	Greiner/Costar
1 ml cuvettes (PMMA)	Carl Roth
reaction tubes (0.5, 1.5 and 2 ml)	Eppendorf
conical FALCON tubes (15 ml, 50 ml)	Corning Life Sciences
cell strainer (40 µm, 70 µm)	BD Bioscience
sterile cell trics filter (30 µm)	Partec
syringes and needles of different sizes	BD Bioscience
FACS tubes (5 ml) with/without lid	BD Bioscience
FACS tubes (5 ml) with filter (40 µm) lid	BD Bioscience
MACS LS-separation columns	Miltenyi Biotec
cell culture dish for agar plates	Becton Dickinson

Table 5.1: Consumables

5.2 Laboratory equipment

LABORATORY EQUIPPMENT	COMPANY
Aria II cell sorter	BD Bioscience
flow cytometer LSR II	BD Bioscience
Casy® cell counter	Innovartis
incubator innova co-170	NewNew Brunswick Scientific
pipettes	Eppendorf
Nanodrop ND-1000 spectrophotometer	Thermo Scientific
water bath	GFL
vacuum pump	Vacuubrand
ice machine	scotsman
Vortexer Genie2	Scientific Industries
flow cytometer MACS Quant	Miltenyi Biotec
Herasafe lamina flow	Thermo Scientific
autoclave (Serie EC)	Webco
incubator	New Brunswick Scientific
Allegra X-15R centrifuge	Beckman Coulter
Allegra X-22 centrifuge	Beckman Coulter
centrifuge 5810R	Eppendorf
photometer (UV-3100PC)	VWR
midiMACS magnet	Miltenyi Biotec
QuadroMACS TM Seperator Magnet	Miltenyi Biotec
Magnetic MultiStand	Miltenyi Biotec

Table 5.2: Laboratory equipment.

5.3 Chemicals and reagents

CHEMICALS/REAGENTS	COMPANY
ACK lysing buffer	Gibco
bovine serum albumin (BSA)	PAA
brefeldin A	Sigma Aldrich
brain heart infusion (BHI)	Oxoid
brain heart infusion agar (BHI-agar)	Oxoid
CD8α MicroBeads, mouse	Miltenyi Biotech
CD90.1 MicroBeads, mouse	Miltenyi Biotech
dimethyl sulfoxide (DMSO)	Sigma Aldrich
erythrocyte lysis buffer	Qiagen
ethanol, absolute	Roth
Easycoll	Biochrom
fetal calf serum (FCS)	Lonza
gelantine veronal buffer	Sigma Aldrich
ionomycin (Iono)	Sigma Aldrich
isoflurane	Abbott
isopropanol (2-Propanol)	Roth
penicillin/ streptomycin (P/S)	Biochrom
phorbol 12-myristate 13-actetate (PMA)	Sigma Aldrich
phosphate buffered saline (PBS)	Gibco
RPMI 1640 + GlutaMAX™-I (Roswell Park Memorial Institute Medium)	Gibco
β-Mercaptoethanol	Gibco
Tween-20	Sigma Aldrich
ovalbumin (OVA) derived peptides SIINFEKL (N4) SIYNFEKL (Y3) SIITFEKL (T4)	IBA Lifescience

Table 5.3: Chemicals and reagents.

5.4 Media, buffer and solutions

5.4.1 Media

Rosewell Park Memorial Institute (medium) (RPMI)

RPMI was purchased from Gibco in 500 ml bottles. RPMI 1640 with GlutaMAX™-I was supplemented with heat inactivated fetal calf serum (FCS) (10 %), β-ME (50 µM final) and a mixed solution (P/S) of penicillin (100 U/ml final) and streptomycin (100 µg/ml final). Media were stored at 4 °C and pre-warmed in a 37 °C water bath before usage.

Brain heart infusion (BHI)

For the solid BHI media, 9.25 g of the Oxoid brain heart infusion (CM1135) was dissolved in 250 ml dH_2O and autoclaved (20 min at 121 °C). The BHI media was stored at 4 °C until usage.

brain heart infusion (BHI)-Agar

Brain heart infusion agar (Oxoid, #CM1136) was made by solving 23.5 g of brain heart infusion agar in 500 g dH_2O. The media was autoclaved (20 min at 121 °C) and after cooling down to 40-50 °C, 2 ml streptomycin (stock 50 mg/ml in dH_2O, final 200 µg/ml) and 75 µl chloramphenicol (stock 50 mg/ml in ethanol, final 7.5 µg/ml) was added if needed. Under sterile conditions, 12 ml of the liquid BHI media was poured into cell plates. After the agar cooled down and solidified, the plates were sterile packaged and stored at 4 °C until usage.

5.4.2 Buffer and solutions

FCS

Fetal calf serum (FCS) was purchased from Lonza and long-term stored at -20 °C. Before usage, thawed serum was heat inactivated at 56 °C for 30 minutes and aliquoted as needed. Aliquots were additionally stored at -20 °C and re-warmed in a 37 °C water bath before usage.

PBS

Phosphate buffered saline was purchased from Gibco. The 10X phosphate buffered saline (PBS) solution was diluted with dH_2O and the pH value was adjusted to 7.2 and autoclaved. **PBS/BSA** was made by adding 0.2 % bovine serum albumin (BSA) (PAA) into the PBS solution. All buffers were stored at 4 °C and used ice-cold for cell preparation.

dH_2O

Demineralized water was made in house via TKA GenPore.

GVB

Gelantine veronal buffer (GVB) was purchased from Sigma Aldrich containing $CaCl_2$ and $MgCl_2$, to study all three pathways of the complement cascade.

5.5 Antibodies

All antibodies, which were used in these experiments for immunofluorescence staining, are listed in Table 5.4. For optimal staining, all antibodies were titrated before usage. Antibodies bound to different fluorochromes were used to stain for cell linage markers, cytokines, differentiation status, and transcription factors of murine cells. For surface staining and intracellular staining, cells were incubated in 100 µl total antibody mixture, composed of several antibodies being coupled to different fluorochromes.

ANTIGEN	MANUFACTURER	CLONE
C1q	Cedarlane	RmC7H8
C3	Cedarlane	RmC11H9
C4	Cedarlane	RmC16D2
CD3	Biolegend	145-2C11
CD3	Miltenyi	17A2
CD4	eBioscience	RM4-5
CD4	Miltenyi	GK1.1
CD8	Biolegend	53-6.7
CD8	Miltenyi	53-6.7
CD11a	Biolegend	2D7/M17I4
CD11b	Biolegend	M1/70
CD11c	Biolegend	N418
CD19	Miltenyi	6D5
CD25	Biolegend	PC62
CD44	Biolegend	IM7
CD45.1	Biolegend	A20
CD45.2	Biolegend	104
CD45R (B220)	Biolegend	RA3-6B2
CD62L	Biolegend	MEL-14
CD69	Biolegend	H1.2F3
CD90.1	Biolegend	OX-7
CD90.2	Biolegend	30-H12
CD90.2	Miltenyi	30-H12
CD95 (FAS)	BD Bioscience	Jo2
CD107a	Biolegend	1D4B
CD127	Biolegend	A7R34
CD152 (CTLA4)	Biolegend	UC10-4B9
CD160	Biolegend	7H1
CD178 (FASL)	Biolegend	MFL3
CD233 (LAG3)	eBiosciences	eBioC9B7W
CD244 (2B4)	eBiosciences	eBio244F4
CD279 (PD-1)	Biolegend	RMP1-30
CD366 (Tim3)	Biolegend	RMT3-23
Annexin V	Biolegend	
BrdU	Biolegend	Bu20a
EOMES	eBiosciences	Dan11mag
FAS	BD	Jo2
F4/80	Biolegend	BM8
granzym B	Biolegend	GB11
IFNg	eBiosciences	XMG1.2
IL2	Biolegend	JES6-5H4
IRF4	eBiosciences	3E4
Ki-67	BD Biosciences	B56
KLRG-1	eBiosciences	2F1
Ly6C	Biolegend	HK1.4
Ly6G	Biolegend	1A8
Tbet	Biolegend	4B10
TNFα	Biolegend	MP6-XT22

Table 5.4: Fluorochrome conjugated antibodies used for FACS.

5.6 Tetramer staining

To identify, enrich or analyze antigen-specific CD8+ T cells by flow cytometry fluorescent tetramers of MHC I peptide complexes were used in this study. In detail, MHC class I H-2K^b tetramers loaded with the Ovalbumin peptide SIINFEKL, containing the Strep-tag® affinity tag and coupled to Strep-Tactin PE or APC, were used to label SIINFEKL-specific CD8+ T cells after LM-OVA infection. All reagents are listed in Table 5.3. CD8+ T cells of interest, which are specific for the SIINFEKL peptide expressed by LM-OVA, were labeled based on their binding specificity of their cell surface receptors for these particular MHC-peptide complexes and could be analyzed without altering the qualitative and quantitative parameters of the cells due to restimulation or other *in vitro* manipulation.

REAGENT	MANUFUCTURER
Strep-Tactin PE	IBA Lifescience (Cat#6-5000-005)
Strep-Tactin APC	IBA Lifescience (Cat#6-5010-005)
MHC class I H-2K^b tetramers with SIINFEKL (Ovalbumin peptide)	IBA Lifescience (Cat#6-7015-005)

Table 5.5: Reagents for tetramer staining.

5.7 Kits

BD Fixation and Permeabilization Kit

REAGENT	MANUFACTURER
BD FACS Lysing solution (10X solution)	BD Biosciences (Cat#349202)
BD FACS Perm solution 2 (10X solution)	BD Biosciences (Cat#347692)

Table 5.6: Fixation and permeabilization buffers (intracellular staining)

BD CytoFix/CytoPerm Kit

REAGENT	MANUFACTURER
BD CytoFix/CytoPerm solution	BD Biosciences (Cat#512090KZ)
BD Perm/Wash Buffer (10X solution)	BD Biosciences (Cat#5122091KZ)

Table 5.7: Fixation and permeabilization buffers (BrdU staining).

Dead cell apoptosis Kit

REAGENT	MANUFACTURER
Annexin V PE antibody	Biolegend (cat#640908)
Annexin V-Binding-Buffer	Biolegend (cat#422201)
cell staining buffer	Biolegend (cat#420201)

Table 5.8: Reagents of the dead cell apoptosis kit.

5.8 Stimulation of CD8+ T cells

Murine cells were stimulated either polyclonal with aCD3/aCD28 in culture or with PMA/Iono for restimulation of *ex vivo* CD8+ T cells. All reagents, which were used for short and long-term stimulation, are listed in the Table 5.9 below.

REAGENT	MANUFACTURER	CONCENTRATION
Brefeldin A	Sigma Aldrich	5 mg/ml in 70 % ethanol usage: 10 µg/ml
PMA	Sigma Aldrich	1 mg/ml in ethanol usage: 10 ng/ml final
Ionomycin	Sigma Aldrich	1 mg/ml in DMSO usage: 2 µg/ml
Ovalbumin peptide SIINFEKL (N4) SIYNFEKL (Y3) SIITFEKL (T4)	IBA Lifescience	5 mg/ml usage: 5 µg/ml final
aCD3 antibody	BD Bioscience clone 17A2	3 µg/ml
aCD28 antibody	BD Bioscience clone 37.51	1 µg/ml

Table 5.9: Reagents for short and long-term stimulation of murine cells.

5.9 Live-dead discrimination

Different viability dyes were used to discriminate between live and dead cells in flow cytometry analysis. All specific dyes are listed in the Table 5.10 and further details are described below.

REAGNET	MANUFACTURER
DAPI	
PI	
Annexin V	Biolegend
LD-Red	Invitrogen

Table 5.10: Live-dead discrimination reagents.

DAPI

4', 6-diamidino-2-phenylindole (DAPI) is a blue fluorescent nucleic acid dye used for the identification of cell cycle and in this study to distinguish between viable and dead cells, as DAPI specifically stains nucleic double stranded DNA (dsDNA) in dead cells, which leads to an increased fluorescence with approximately 20-fold.

PI

Fluorescent staining with propidium iodide (PI) was used to evaluate cell viability in flow cytometry, as it stoichiometrically binds to nucleic acids. The cell membrane integrity excludes PI from staining viable and apoptotic cells. Additionally, PI was used as counterstaining in multicolor fluorescent assays together with anti-Annexin V antibody staining, which is specific for cellular structures to distinguish between viable cells or cells that are early or late in the apoptosis process. In this apoptosis assay, PI detects phosphatidylserine (PS) on the cytoplasmic surface of the cell membrane and membrane integrity.

Annexin V

In viable cells, PS is predominantly located along the cytosolic side of the plasma membrane. The cell membrane integrity excludes viability dyes such as PI in healthy cells or at early stages of apoptosis. Therefore, cells displaying only Annexin V staining are in the early stage of apoptosis, where the PS loses its asymmetric distribution and translocates to the extracellular membrane, where it is detectable with fluorochrome coupled Annexin V antibody. In the late stages of apoptosis, cells are stained with both, Annexin V antibody and PI, as Annexin V can bind to the accessible PS because an uptake of PI into the cell occurs.

LD-Red

Live-Dead Red Fluorescent Reactive Dye (LD-Red) was used to label dead cells before fixation. The reactivity of this fixable viability dye is restricted to the cell-surface amines. In viable cells, the dye can exclusively bind to extracellular amines resulting in a less intensive fluorescence. If cells having compromised membranes, the dye reacts with the free amines both inta- and extra-cellular, yielding intense fluorescent staining typically greater than 50-fold. This procedure makes it possible to distinguish between viable and dead cells also after fixation and permeabilization of the cells to enable intracellular staining for cytokines and transcription factors as described in Section 6.7.2.

5.10 Proliferation dyes

Depending on the experimental setup, different reagents were used to monitor cell proliferation. All reagents are listed in Table 5.11 and further details are described below.

PROLIFERATION DYE	COMPANY	STOCK	FINAL CONC.
BrdU	Sigma Aldrich	1 mM in PBS	1 µM/ml
CFDA-SE	Molecular Probes	5 mM in DMSO	10 µm in PBS
Cell Proliferation Dye eFluor® 450	eBioscience	10 mM in DMSO	20 µM in PBS

Table 5.11: Proliferation dyes.

Bromdeoxyuridine

bromdeoxyuridine (BrdU) is an analog of the nucleoside thymidine, which is permanently incorporated into replicating DNA of dividing cells during DNA synthesis. It allows the identification of cells that were dividing during the period of BrdU exposure. For *in vivo* administration, 1 mg/ml BrdU was given in drinking sugar water from day 5 till day 8 after infection. A combination of BrdU with phenotypic markers allowed to determine between proliferated and non-proliferated cells during the period of BrdU administration. The cellular incorporation of BrdU was detected by anti-BrdU specific antibodies following membrane permeabilization by flow cytometry.

Carboxyfluorescein succinimidyl ester

carboxyfluorescein diacetate succinimidyl ester (CFDA-SE) incorporate stably within the cells via covalently binding to free amines. This permeable cell permanent dye is converted into carboxyfluorescein succinimidyl ester (CFSE), which is a fluorescein-based tracer for long-term cell labeling, both *in vivo* and *in vitro*. It is used to monitor cell proliferation, as progressive halving of CFSE fluorescence intensity within daughter cells occurs following each cell division.

Cell Proliferation Dye eFluor® 450 staining

The Cell Proliferation Dye eFluor® 450 (eBioscience, cat#65-0842) is used to monitor cell proliferation over the long-term. This fluorescent dye binds to amines on the surface and inside the cell and, as the cell divides, the dye is distributed equally between the daughter cells and thereby successive halving the fluorescent dye with each cell division.

5.11 Cytokines

Recombinant murine cytokines, listed in Table 5.12 were used for culturing of murine cells. Of interest, IL2 was used in different concentrations dependent on the experimental setup. A final IL2 concentration of 10 ng/ml equals 50 U.

CYTOKINE	MANUFACTURER	ORIGIN	STOCK	FINAL
IL2	Miltenyi Biotech	rec. murine	10 µg/ml	10 ng/ml
IL7	Miltenyi Biotech	rec. murine	10 µg/ml	10 ng/ml
IL12	Miltenyi Biotech	rec. murine	10 µg/ml	10 ng/ml
IL15	Miltenyi Biotech	rec. murine	10 µg/ml	10 ng/ml

Table 5.12: Cytokines used for cell culture experiments.

5.12 Listeria infection

For infection experiments, recombinant strains of *Listeria monocytogenes* expressing different peptide ligands of ovalbumin were used to analyze CD8+ T cell responses after bacterial infection. If not indicated otherwise, the recombinant Listeria strain N4 (LM-OVA or LM-OVA N4) was used. Bacteria belonging to this strain express the native but high TCR affinity OVA ligand $SIINFEKL_{257\text{-}264}$(N4). Other recombinant bacteria strains, which were used in this study, express altered peptide ligands (APL), which differ in their stimulatory potency to activate OT1 cells, as they differ in their TCR affinity/avidity. In this study, a recombinant Listeria expressing OVA protein containing the epitopes SIYNFEKL (Y3) or SIITFEKL (T4) were used. All recombinant *Listeria monocytogenes* strains were kindly provided by Dietmar Zehn [264]. For both, primary and secondary infection, independent of the Listeria strain which was used, mice were infected with Listeria through the tail vein (i.v.) with 2000 CFU LM-OVA in 200 µl PBS.

5.13 Mouse strains

C57BL/6J and CD45.1 congenic wild type mice and **OT1** mice (on C57BL/6 background) were purchased from the Jackson Laboratory or Charles River Laboratories. OT1 transgenic mice have MHC class I-restricted, ovalbumin-specific, CD8+ T cells [110]. Those cells have a transgenic T cell receptor (TCR), which expresses the Vα2 and Vβ5 variable regions of the TCR [78]. OT1 cells can recognize ovalbumin residues 257-264 (SIINFEKL), as well as altered peptide ligands with lower affinity, in the context of $H\text{-}2K^b$. **IRF4flox** mice were kindly provided by Ulf Klein [113]. Ulf Klein and collogues generated a transgenic mouse strain carrying a lox-P-flanked IRF4 allele. They additionally placed a gene encoding for enhanced green fluorescent protein (eGFP) in an opposite orientation upstream of the IRF4 promoter region, leading to its expression in IRF4-deficient cells after CRE-mediated recombination.

The transgenic mice **E8Icre** (on C57BL/6 background) were kindly provided by Ichiro Taniuchi. Those mice express CRE recombinase driven by a combination of the core E8I enhancer and the CD8α promoter [141].

IRF4flox.E8Icre mice (in this study termed as $IRF4KO^{CD8}$ mice) with CD8+ T cells lacking the transcription factor IRF4 were generated by crossing. Therefore, IRF4flox (heterocygote) conditional mice with loxP-flanked IRF4 alleles were crossed with E8Icre transgenic mice, thereby initiating IRF4 deletion in the thymus in all CD8α expressing T cells. E8Icre is specifically expressed in CD8α+CD8β+ αβ T cells and CD8αα+

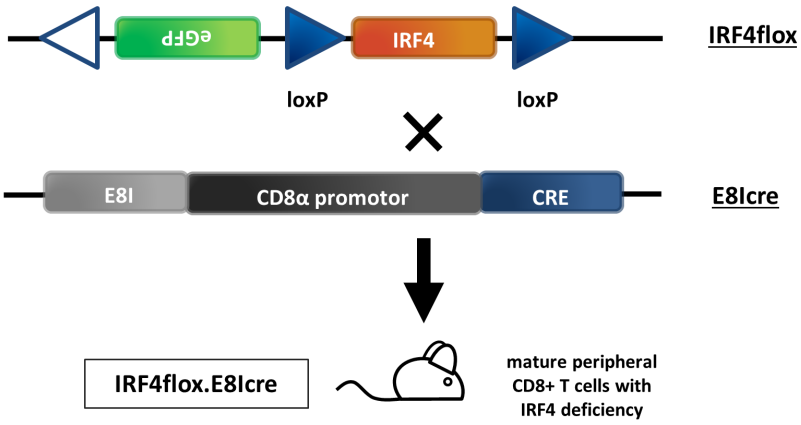

Figure 5.1: **Generation of the conditional knockout mouse strain IRF4flox.E8Icre.** In these transgenic mice, only the mature peripheral CD8+ T lymphpcytes lack the expression of the transcription factor IRF4.

CD8β- αβ T cells and therefore IRF4flox.E8Icre mice lack IRF4 expression in peripheral CD8+ T cells but not in other cells (Figure 5.1).

The **OT1.IRF4flox.E8Icre** mice (in this study termed as OT1.IRF4KO^{CD8}) are TCR transgenic mice, which have IRF4-deficient CD8+ T cells with a specific TCR recognizing ovalbumin derived epitopes, such as SIINFEKL (SI), were obtained by cross-breeding of OT1 mice with IRF4flox.E8Icre mice.

All mice were bred and maintained in the research institute for Experimental Medicine (FEM) at the Charité-Universitätsmedizin Berlin. All animal experiments were approved by the LAGeSo-Berlin (Landesamt für Gesundheit und Soziales) and were performed in accordance with the German law for animal protection. All mice were used between 6-12 weeks of age and sex-matched control mice were used for *in vivo* and *in vitro* experiments.

Chapter 6

Methods

6.1 Isolation and preparation of murine cells

All organs were dissected from sacrificed mice, which were anesthetized with Isoflurane before cervical dislocation. After disinfection of the fur, all desired organs and both hind legs were explanted and stored in appropriate containers with PBS on ice or at 4 °C until further processing.

6.1.1 Extraction from spleen, lymph node and thymus

Single-cell suspension of either spleen (SP), thymus (THY) or lymph node (LN) were obtained by meshing the organs through a 70 µm cell strainer using a syringe plunger. After a centrifugation step (500xg, 5 min), the supernatant was aspirated and the cell pellet was resuspended in 1 ml ACK buffer (Gibco) and incubated for 3 minutes at room temperature (RT) to lyse erythrocytes. After stopping the erythrocyte lysis reaction by adding PBS/BSA, the cell preparation was finalized by an additional washing step with PBS/BSA. Cell suspensions were stored at 4 °C until further usage.

6.1.2 Extraction from liver

In brief, murine livers (LI) (without gall bladder) were meshed through a 70 µm cell strainer using a syringe plunger to generate a single cell suspension in PBS. After centrifugation (500xg, 5 min), the cell pellet was resuspended in 5 ml of 40 % Easycoll (Biochrom) diluted in RPMI and layered on 5 ml 70 % Easycoll solution. A gradient centrifugation (580xg, 20 min, acceleration 5, deceleration 0) without brake was performed. After removing carefully the uppermost layer containing mostly hepatocytes, the thin interface with the lymphocytes was harvested carefully and transferred into a new tube. After washing the cells twice with PBS/BSA (500xg, 5 min), the erythrocytes were removed by a lysis reaction. Therefore, the cell pellet was resuspended in 1 ml ACK buffer (Gibco) and after incubation of 3 minutes at RT, an additional washing step with PBS/BSA was performed to stop the lysis reaction. Cell suspensions were stored at 4 °C until further usage.

6.1.3 Extraction from bone marrow

After sacrificing mice, the bones of the hind extremities (tibia and femur) were collected by removing all muscles and tissue. Bones were kept in PBS till the preparation procedure continued and stored at 4 °C or on ice. Using a syringe, the bone marrow (BM) was flushed out of the bone and a single cell suspension was generated by passing the

suspension through a 70 µm cell strainer using the plunger of a syringe. To remove any erythrocytes, the cell pellet was resuspended in 0.5 ml ACK buffer (Gibco) and after incubation of 3 minutes at RT, an additional wash step with PBS/BSA was performed to stop the erythrocyte lysis reaction. Cell suspensions were stored at 4 °C until further usage.

6.1.4 Extraction from blood

After warming the mouse prior with an infrared lamp, blood was drawn from the tail vein and collected into a MiniCollect Tube K3EDTA (Greiner Bio-one). Erythrocytes were lysed via erythrocyte lysing buffer from Qiagen for 10 minutes at RT. Lysis reaction was stopped by adding PBS/BSA. After centrifugation (500xg, 5 min), the cell pellet was washed another time with PBS/BSA and stored at 4 °C until further usage.

6.2 Enrichment of cells via magnetic beads

Manual cell separation with the column-based method of magnetic labelling was used to enrich or purify CD8+ T cells from heterogeneous cell suspensions made of murine secondary lymphoid organs. The basic principle of the magnetic-activated cell sorting (MACS) cell separation technology (Miltenyi Biotech) is a magnetic-based cell separation. Therefore, desired cells that express specific antigens on their cell surface are targeted with magnetic antibody-conjugated MicroBeads (Miltenyi Biotech). The cell suspension with the labeled target cells is passed over a column, which is placed in a magnetic field. The column matrix composed of ferromagnetic spheres induces a high magnetic gradient within the column, when it is placed in the magnetic field. This enables that non-labeled cells pass through while the magnetically labeled target cells remain within the column. After rinsing to wash non-labeled cells away, the column is removed out of the magnetic field and the remaining target cells are eluated by flushing the column. Positive selection was performed in these experiments, where the target cells were magnetically labeled and the flow through with the unwanted cells was discarded. Magnetic MicroBead- conjugated highly specific antibodies against CD8 (mouse CD8α MicroBeads, Miltenyi Biotech) or CD90.1 (mouse CD90.1 MicroBeads, Miltenyi) were used to purify or enrich CD8α or CD90.1 expressing T cells from lymphoid organ cell suspensions, respectively. The separation took place according to the manufacturer's protocol.

In detail, the cell suspension with the target cell population was incubated with MicroBeads of the desired specificity for 15 minutes at 4 °C, followed by adding PBS/BSA and a centrifugation step (500xg, 5 min). The cell pellet was resuspended in 2 ml PBS/BSA and the cell suspension was filtered with a 30 µm filter and applied onto an LS-column (Miltenyi Biotech) placed in the strong permanent magnetic field of the separator. The magnetic field retains MicroBead-bound cells while non-labeled cells flow through the column. After rinsing the column three times with 3 ml PBS/BSA, it was removed from the magnetic field and the retained target cells were eluated in 4 ml PBS/BSA as positively selected cells. Cells were stored on ice or 4 °C until experimental procedure was continued.

6.3 T cell transfer

Wild type OT1 T cells express a transgenic TCR specific for the ovalbumin epitope SIINFEKL in the context of H-2K^b. For T cell transfer experiments, WT OT1 cells were compared to OT1 cells that lack the transcription factor IRF4. IRF4-deficient OT1 cells were generated by crossing wild type OT1 mice with IRF4flox.E8Icre resulting in the generation of OT1.IRF4flox.E8Icre mice. Spleen and lymph node cells from donor mice were purified using a positive CD8 purification kit from Miltenyi (6.2), according to the manufacturer's instructions. Equal numbers (in all experiments, unless indicated otherwise) of donor T cells were transferred i.v. into sex-matched C57BL/6J or CD45.1 wild type mice. Always, the volume of the inoculum was 200 µl. Transferred wild type or IRF4-deficient OT1 cells were distinguished from recipient CD8+ T cells via congenic marker expression of CD90.1, CD90.2, CD45.1 and CD45.2.

6.4 Culturing and stimulation of T cells

Murine primary cells were generated, as described in Section 6.1, from lymphoid organs of mice of the desired mouse strain. *In vitro* and *ex vivo*, cells were cultured or stimulated in supplemented RPMI 1640 media (see Section 5.4.1 for details). Depending on the experimental setup, additionally to the FCS, β-ME, and antibiotics penicillin/streptomycin (P/S), different cytokines (listed in Table 5.12) or stimulating reagents (listed in Table 5.9). If FACS measurement was intended, the murine golgi-inhibitor brefeldin A (Sigma Aldrich) was added into to culture or stimulation sample and incubated for 4-6 hours at a final concentration of 10 µg/ml to enrich the amount of intracellular cytokines and prevent internalization or secretion.

6.4.1 T cell culture

T cell cultures were done with naïve CD8+ T cells. Therefore, lymphoid organ cell suspension were generated as described in Section 6.1.

After pre-enrichment of CD8 T cells via the MACS technology from Miltenyi Biotech (Section 6.2) using magnetic MicroBead-conjugated antibodies against CD8 (mouse CD8α MicroBeads, Miltenyi Biotech), cells were labeled with anti CD3, CD4, CD8, CD44 and CD62L antibodies. Naïve CD8+ T cells (CD3+ CD4- CD8+ CD44- CD62L+) were sorted using the Aria II sorter from BD. For some experiments, naïve CD8+ T cells were labeled with CFDA-SE (Molecular Probes) or additionally incubated for a certain time window with BrdU (Sigma Aldrich) to track proliferation (Section 5.10). For culture, cells were resuspended in RPMI media supplemented with FCS, β-Mercaptoethanol and antibiotics (P/S) (Section 5.4.1). Polyclonal T cell stimulation was induced by culturing the cells in a 96-well plate. The plate was coated with plate-bound 3 µg/ml αCD3 (BD Bioscience, clone 17A2) and 1 µg/ml αCD28 (BD Bioscience, clone 37.51) antibodies. Those antibodies mimic the stimulation via TCR and co-stimulatory molecules, respectively. This in turn leads to a strong T cell activation and proliferation of T cells but is independent of the TCR specificity. The 96-well U-bottom plate (Greiner) was coated with the antibodies in PBS for at least 2 hours at 37 °C and rinsed with PBS before further usage. Additionally, cells were incubated in the absence or presence of

different cytokines (as listed in Table 5.12), like murine recombinant IL2 or IL12 in their indicated concentrations (see Table 5.12). From day 2 on, cells were resuspended and transferred into bigger flat-bottom well plates (48-, 24-, 12-well plate), depending on their growth rate, and new media supplemented with cytokines was added as required. From day 3 on, all cells, independent of the initial culture conditions, were cultured in media containing IL2 (10 ng/ml) to enable viability and proliferation. At the end of a culture after 3-7 days, cells were taken out of the wells and transferred into a FACS tube by adding PBS to wash media and cytokines away. Afterwards cells were counted either by CASY or MACS Quant (Section 6.8) and restimulated (Section 6.4.2) for further analysis.

6.4.2 (Re-) stimulation of T cells

Polyclonal with PMA/Iono

Cell suspensions of the different organs were generated as described in Section 6.1. For polyclonal short-term activation or re-activation cells were resuspended in supplemented RPMI (Section 5.4.1), with the certainty that the maximum of the cell concentration with $2x10^6$ cells/ml was not exceed. Restimulation was performed at 37 °C and 5 % CO2 for 4-6 hours with 10 µg/ml PMA (Sigma Aldrich) and 1 µg/ml Ionomycin (Sigma Aldrich) in a total volume of 1 ml. Additionally, brefeldin A (10 µg/ml) was added to enrich the amount of intracellular cytokines and prevent internalization or secretion.

OVA-specific with SIINFEKL

In vitro stimulation of naive T cells or restimulation of *in vivo* primed T cells during an LM-OVA infection were performed with the native N4 (SIINFEKL) peptide or with altered peptide ligands, namely SIYNFEKL (Y3) or SIITFEKL (T4). All three class I (K^b)-restricted peptide epitopes are presented by the MHC class I molecule H-$2K^b$, but having differend TCR affinity. For restimulation of *in vivo* primed CD8+ T cells, single-cell suspensions of different organs (cell numbers can range from 1-$2x10^6$ cells/ml) were generated, as described in Section 6.1. Cells were resuspended in supplemented RPMI 1640 media and cells were incubated for 6 hours with peptide and further analyzed via flow cytometry. For stimulation experiments of transgenic CD8+ T cells expressing an OVA-specific T cell receptor (OT1), naive cells were incubated with either N4, Y3, or T4 peptide, all resulting in an activation but with different strength of the TCR engagement.

6.5 Live-dead discrimination

Different methods were used to analyze cells while discriminating dead cells and debris from viable cells.

DAPI and PI

To discriminate between viable and dead cells in non-fixed samples, DAPI (0.4 µM final) or PI (0.4 µg/ml) was given to the cells directly before measurement on the flow cytometer.

Annexin V and PI staining for apoptosis detection

Cells were resuspended at a concentration of $1x10^6$ cells/ml. After the surface staining (Section 6.7.1) was performed, cells were washed by centrifugation (500xg, 5 min) in cold Biolegend cell staining buffer (Biolegend). Next, cells were resuspended in 50 µl Annexin V Binding Buffer (Biolegend). After adding 1 µl fluorochrome conjugated Annexin V PE antibody and 2.5 µl PI solution the cells were gently vortexed and incubated for 15 minutes at RT in the dark. Afterwards, 200 µl Annexin V Binding Buffer was added and the samples were analyzed on the flow cytometer.

LD-Red

Cells to be stained were washed by centrifugation (500xg, 5 min) in PBS to remove any protein contaminations. The cell pellet was resuspended in 100 µl PBS and 2 µl of LD-Red fluorescent dye was added. After an incubation for 20 minutes at 4 °C in the dark, the cells were washed again with PBS by another centrifugation step and processed further.

6.6 Proliferation dyes and reagents

BrdU

To label cells *in vitro* with 5-bromo-2'-deoxyuridine (BrdU), a final concentration of 1 µM BrdU was added into the media to access proliferation of the CD8+ T cells during culture with a density limited to $2x10^6$ cells/ml. Cells from the same population and culture conditions without BrdU treatment were used as a negative control to determine background staining levels of the anti-BrdU antibody. Before the whole staining procedure, cells were washed in PBS and pelleted (500xg, 5 min). After 10 minutes surface staining (Section 6.7.1), cells were washed by centrifugation (500xg, 5 min) in PBS. All centrifugation steps thereafter were performed at 500xg for 10 minutes. Cells were fixed with BD Cytofix/Cytoperm solution for 20 minutes at 4 °C and washed once with 1X Perm/Wash Buffer (BD Biosciences). Thereafter, cells were incubated for 10 minutes on ice with 100 µl of Triton-X100 (0.01 % in PBS/BSA) and then washed once with 1X Perm/Wash Buffer. A re-fixation followed via an additional incubation of the cell pellet in 100 µl Cytofix/Cytoperm solution for 5 minutes at room temperature and one additional washing step with 1X Perm/Wash Buffer thereafter. Because a denaturation of the nuclear DNA into single-stranded DNA form is necessary to allow antibodies to bind to the incorporated BrdU, a DNAse treatment was performed. Therefore cells were exposured to 30 µg DNAse I (Sigma) for 1 hour at 37 °C. Next, incubation was stopped by adding 1X Perm/Wash Buffer and pelleting the cells. The cells were stained with anti-BrdU antibody for 30 minutes at 4 °C and afterwards washed by centrifugation in 1X Perm/Wash Buffer before analysis via flow cytometry.

CFSE

Cells were washed two times with PBS (490xg, 5 min) to remove protein contamination and resuspended at a density of less than $5x10^7$ cells/mL. CFDA (Molecular Probes, 5 mM in DMSO) was pre-diluted to 10 µM in PBS. The CFDA pre-dilution and the single cell suspension were mixed in equal volumes and incubated for 10 minutes at room temperature. Afterwards, cells were washed two times with PBS/BSA and resuspended

in medium to proceed further.

Cell ProliferationCell Proliferation Dye eFluor® 450
Cells were washed two times with PBS (490xg, 5 min) to remove any protein contamination and afterwards resuspended in 1 ml pre-warmed PBS. Note that the final concentration of cells should not exceed $1x10^7$ cells/mL. Cell Proliferation Dye eFluor® (10 mM in DMSO) was pre-diluted to 20 µM in PBS. The Cell Proliferation Dye eFluor V450 pre-dilution and the single cell suspension were mixed with equal volumes by vortexing and incubated for 20 minutes at RT in the dark. The labeling was stopped by adding 4-5 volumes of cold PBS/BSA and incubated on ice for 5 minutes. Afterwards, cells were washed two times with FCS supplemented media and resuspended in medium to proceed further.

6.7 Staining procedures

6.7.1 Surface staining

Expression of surface molecules was verified by ag-specific fluorescent-labeled antibody staining. Before staining with antibodies, cells were washed once with PBS to remove any protein contamination. Thereafter, cells were incubated for 15 minutes at 4 °C with the desired antibodies and afterwards washed with PBS/BSA to remove unbound antibodies. Analysis was performed using FACS LSR II machine.

6.7.2 Intracellular staining

After surface staining the cells were fixed and permeabilized with BD Fixation Permeabilization Kit. Therefore, cells were washed with PBS to remove any proteins. Afterwards, the cell pellet was resuspended in 1 ml BD Fixation Buffer and incubated for 10 minutes at room temperature, which was followed by 490xg centrifugation for 10 minutes. Supernatant was aspirated and the cell pellet was resuspended in 0.5 ml BD Permeabilization Buffer and incubated for another 10 minutes at RT. Reaction was stopped by adding PBS/BSA followed by analysis by flow cytrometry using FACS LSR II machine.

6.7.3 Tetramer staining

To analyze ag-specific CD8+ T cell responses after bacterial infection with the recombinant *Listeria monocytogenes* expressing OVA, MHC class I tetramers were used to exclusively label peptide-specific CD8+ T cells. The tetramer complexes consists of four major histocompatibility complex (MHC) molecules loaded with a specific peptide and bound to fluorescently-labeled fluorochromes. In the present experiments, the MHC class I H-2K^{b}tetramers were loaded with SIINFEKL, an ovalbumin peptide (IBA Lifescience; Cat#6-7015-005). Peptide-loaded MHC molecules were combined with Strep-Tactin PE (IBA Lifescience; Cat#6-5000-005) or Strep-Tactin APC (IBA Lifescience; Cat#6-5010-005). CD8+ T cells, which are specific for the respective peptide-loaded MHC molecule, were stained and further labeled with antibodies for cell lineage, functionality, and differentiation pattern analysis. Tetramer staining was performed prior surface and intracellular staining. For each tetramer staining reaction, 1-2x10^6 cells

were incubated with peptide-MHC tetramers bound to fluorochromes. Therefore, 0.8 µl MHC I-Strep H-2K^b molecules, containing the Strep-tag affinity tag and loaded with the Ovalbumin SIINFEKL, and 1 µl Strep-Tactin fluorochrome (PE or APC) were added to 3.7 µl PBS and incubated over night at 4 °C. Next day, this mixture was added to 1-2x10^6 cells (in 45 µl PBS) of a lymphoid organ and mixed by pipetting up and down. After an incubation of 45 minutes at 4 °C in the dark, cells were washed by adding 3-4 ml PBS. After centrifugation at 500xg for 5 minutes (4 °C), supernatant was aspirated. Thereafter, cells were resuspended in 100 µl PBS and cell surface labeling (Section 6.7.1) and intracellular staining (Section 6.7.2) were performed.

6.7.4 Complement staining

To analyze for complement deposition, splenocytes were prepared from organs like described in Section 6.1.1. Prior staining, the cell pellet was washed once with gelantine veronal buffer (GVB) [Sigma Aldrich] and centrifugated (500xg for 5 minutes, at 4 °C) and supernatant was discarded. Afterwards, the cell pellet was resuspended in GVB and incubated for 1 hour at 37 °C thereafter, cells were washed with RPMI (500xg, 5 min, 4 °C) and complement staining was performed for 45 min and additional surface staining for 15 min, both performed at 4 °C in RPMI. Cells were washed with RPMI to remove unbound antibody and analysis was performed directly using MACS Quant analyzer.

6.8 Determination of cell numbers

Counting of cells was performed using the CASY cell counter from Innovartis or the MACS Quant flow cytometer from Miltenyi Biotech. For both applications, an aliquot of the cell suspension was added into an appropriate buffer of defined volume. Absolute cell counts were determined volumetrically and were automatically calculated as events/volume for every sample. The cell number, which was determined in an aliquot, was used to calculate the absolute cell number of the original sample.

CASY

The CASY cell counter (Innovartis) was used to determine cell concentration and viability of cells in a single-cell suspension. This method is based on non-invasive electrical current exclusion and pulse area analysis, which allows quantification of cell concentration, determining the cell viability by excluding cell aggregations and debris. A cell aliquot is added into a special electrolyte solution (CASYton from Roche). This mixture is aspirated through a precision pore of defined geometry with a constant flow speed and a pulse low voltage field is applied. The electrolyte-filled measuring pore represents a defined electrical resistance where the cells displace a quantity of electrolyte corresponding to their volume. Living cells behave like an isolator as the electric current cannot go through the cellular membrane and in contrast, can go through the broken cellular membrane of dead cells, which are recorded by the size of their cell nucleus. Absolute cell number is given as viable cells per ml.

MACS Quant

The MACS Quant analyzer (Miltenyi Biotech) is a flow cytometer, which can combine multisample and multiparameter analysis. Due to volumetric measurement one can achieve simultaneous quantification of absolute target cell numbers. Because this analyzer is equipped with three lasers, two scatters and 8 fluorescent channels, a multicolor cell analysis is also possible. The absolute cell count of a sample was either based on the size, granularity, and viability of the cells or based on the expression of surface markers, which were labeled with fluorochrome coupled antibodies.

LASER	FLUORESCENT PARAMETER
405nm	2
488nm	4
635nm	2

Table 6.1: MACS Quant configuration details.

6.9 Flow cytometry and cell sorting

Flow Cytometry was used as a technique for counting, examining, and sorting of cells suspended in a stream of fluid. Light is used to illuminate the cells and a series of sensors detect the different types of light that are refracted or emitted from the different cells. Each will be assigned in its own channel. Every cell that passes through the flow cytometer is detected and classified as a distinct single event. In most applications of the flow cytometry the cell is sent to the waste after is exits the laser beam.

Flow Cytometry

In detail, a beam of a light with a single wavelength is directed onto a hydro-dynamically focused stream of fluid where cells are passed sequentially through a nozzle. At the point where the stream of the fluid passes through the light beam a series of different detectors are aimed. One detector is in line with the light beam (forward scatter or FSC) and several perpendicular to it (side scatter or SSC) and additionally a series of fluorescent detectors. Some of the laser light is scattered by the cells, which makes cell counting possible and to distinguish cell size. The extent to which light scattering occurs depends on the physical properties of the cell, meaning size and internal complexity. In detail, forward-scattered light (FSC) is proportional to cell-surface area and correlates with the cell volume or size. The side-scattered light (SSC) is proportional to cell granularity or internal complexity, i.e. shape of the nucleus or the amount and type of cytoplasmic granules. Using FSC and SSC, one can distinguish different cell subsets in a heterogeneous population. Additionally, for doublet exclusion height can be selected using FSC-H and FSC-A or by using a dump channel one can avoid false positive cells by doublet exclusion. Cells are stained with fluorochrome-conjugated antibodies that bind specific to cell surface and intracellular molecules. Different antibodies with distinct fluorochromes can be used simultaneously to distinguish separate subpopulations of cells. The laser beam excites the fluorochromes and the emitted light, which is proportional

to the antigen density, is measured via a series of detectors or by a photomultiplier tube. The acquired data by the sensors is compiled and integrated to build a picture of the sample. Each event will be plotted independently. Data are presented as one-dimensional (single parameter) histograms or two-dimensional dot plots with logarithmic axes, representing cells with fluorescent values, where each cell is shown as a dot in the plot. To define the characteristics of a subset of cells, a numerical or graphical boundary is set, namely gate. For analysis, individual cell data events are grouped into discrete populations via a set region, dependent on the similarities in light scattering and fluorescence. When this set region is used to limit the cells, which are drawn in a plot, is termed as 'gate'. Gating allows analysis of various parameters simultaneously across several different scatter-plots and histograms. In the present experiments, samples were acquired using the LSR II cytometer from BD Bioscience to perform multi-parameter detection of proteins and cellular status, such as proliferation, exhaustion or apoptosis of single cells.

FACS

Fluorescence-activated cell sorting (FACS) is a specialized type of flow cytometry. Some cytometers can not only analyze cells, they additionally can capture and collect the cells of interest out of a heterogeneous fluid mixture of cells according to their characteristics (size and fluorescence). First, the cells of interest are identified by setting a sort gate around the target cell subpopulation on the data acquisition plot. Once the population to be separated has been identified, only cells of interest are sorted out of the stream and collected into a tube dependent on their size and morphology. As the cell passes through the laser beam, the Sorter determines if this cell is a target cell according to the pre-selected sort mode. Sorting of cells is accomplished by electrical charge. Therefore, an electrical charge is applied on the cell within the fluidic drop. The charged drop is then deflected by charged electrodes and thereby sorted into different collection tubes or sent to the waste tube, which is dependent on the characteristics of the cell. In the present experiments, after magnetic bead sorting to pre-enrich the cells of interest to reduce both the number of cells that need to be sorted and the required sorting time, cell sorting was carried out on a FACS Aria Cell Sorter (BD Biosciences).

For some experiments, naive CD8+ T cells or OT1 cells either from wild type or conditional knock out mice were prepared by FACS sorting. Therefore, after pre-enrichment of CD8+ T cells via MACS technology (Section 6.2) and fluorescent surface staining (Section 6.7.1) naive CD8+ T cells were sorted CD3+ CD4- CD8+ CD44- CD62L+ with the Aria Cell Sorter. The purity was always higher than 98 %, checked as standard practice after each cell sorting. Cells were washed in cold PBS via centrifugation at 500xg for 5 min (4 °C) and resulting supernatant was discarded. Cell pellet was resuspended in the required volume and naive CD8+ T cells were transferred in 200 µl i.v. per mouse.

For the described *ex vivo* experiments, after MACS pre-enrichment, initially transferred wild type and IRF4-deficient OT1 cells were isolated via FACS Sorter according to their congenic marker expression from infected spleens of recipient mice.

6.10 Infection model - *Listeria monocytogenes*

Recombinant *Listeria monocytogenes* expressing different ovalbumin derived ligands were used to infect mice initially or one day after adoptive transfer of T cells. Mice were infected intravenously (i.v.) with 2000 CFU Listeria, expressing either the ova derived peptide N4, Y3 or T4, in PBS for primary and secondary infection. Mice were sacrificed at different time points to analyze the CD8+ T cell response in different organs after bacterial infection.

6.10.1 Listeria infection

For infection, the bacterial stock was thawed and a small amount was directly added into BHI liquid media (Section 5.4.1) and grown at 37 °C and 5 % CO_2 on a shaker. The growth was observed by measuring the optical density at 600 nm (OD_{600}) with a spectrophotometer. After an incubation time of 3-4 hours, when the exponential growth phase was achieved, bacteria were diluted as required in fresh PBS to $1x10^4$ CFU/ml. Next, mice were infected intravenously with 200 µl containing 2000 CFU of LM-OVA. To make injection into the tail vein feasible, the mice were warmed with an infrared lamp. Actual CFU were calculated following infection by plating dilutions of the inoculum on BHI agar plates, described in detail in Section 6.10.3. For quantification from bacterial titers of homogenized organs, cell suspensions were diluted 1:10 in 1 % TritonX-100 in PBS and dilutions were plated on BHI agar plates with or without C/S. After 2 days of incubation, grown colonies were counted and the initial concentration of the bacteria solution was calculated.

6.10.2 Stock preparation

To keep virulence of the Listeria stock, *in vivo* passaging is necessary as continued *in vitro* growth of the bacteria lead to a selection of less virulent organisms. For stock preparation, one C57BL/6J mouse was infected i.v. with 5000 CFU in 200 µl PBS. After 2 days of infection, the mouse was sacrificed and the spleen was harvested. After single cell preparation (6.1) of the organ, 150 µl of the cell suspension mixed 1:10 in 1 % TritonX-100 in PBS was spread out on a BHI agar plate with antibiotics (C/S) and incubated for another 2 days at 37 °C. Following, 3 colonies were picked and separately incubated in 0.5 ml BHI liquid media for 4 hours. Afterwards, 250 µl of each Listeria culture was combined into a 50 ml Falcon tube containing 30 ml BHI media. The mixed culture was expanded until an OD_{600} of 0.3 was achieved. Then, 15 ml of 50 % Glycerol (in BHI) was added, mixed well and 500 µl was aliquoted into cryovials. For long-term storage of the bacteria, Listeria were kept at -80 °C.

6.10.3 Determination of bacterial load

The concentration of the bacteria solution was verified by counting the total number of colony forming units, made by viable bacteria. Therefore, the bacteria solution to be injected was further diluted and a certain amount of this solution was spread out with a spatula on a BHI agar plate. The plate was incubated for 2 days at 37 °C in a humidified

5 % CO_2 atmosphere. Grown single colonies were counted and initial concentration of the bacteria solution was calculated.

6.11 LCMV infection

To examine whether IRF4 plays a different role for the CD8+ T cell response during viral infection compared to bacterial infection with *Listeria monocytogenes*, additionally lymphocytic choriomeningitis virus (LCMV) infections in mice were administered. LCMV infections were conducted by injecting mice i.p. with $2x10^5$ plaque forming unit (PFU) of LCMV, Armstrong strain. Therefore, the stock was diluted in an appropriate volume to generate an infection mix with $2x10^5$ PFU within 200 µl PBS. The virus stock was kindly provided by Dr. Sibel Dulanik.

6.12 Statistics

For *in vivo* experiments, each group contained 3-5 animals and the mean was calculated out of at least two independent experiments. In the graphs are shown mean values plus standard error of the mean (SEM). For *in vitro* experiments, the mean of at least two independent experiments was calculated, each consisting of 2-3 values. If two groups were analyzed, the statistical significance of the experimental results was analyzed via the paired Student's t test. Significance was defined by a variation coefficient of at least *$p<0.05$, whereas **$p<0.01$, and ***$p<0.001$ were set as highly significant. Graphs, diagrams, and statistical analysis were performed with the GraphPad Prism Software.

Part III

Results

The interferon regulatory factor 4 has been shown to play a crucial role for the differentiation and function of several cell types of the immune system, such as B cells, CD4+ T lymphocytes, and macrophages, among others. Previous studies have further evaluated that IRF4 expression correlates with T cell receptor signaling and its absence lead to abnormal immune responses upon infection [146, 153, 259]. To examine in detail the influence of IRF4 on the CD8+ T lymphocyte responses regarding activation, differentiation, and formation of a functional anti-pathogenic effector CD8+ T cell population, bacterial and viral infections were performed in a mouse model based on the Cre-Lox recombination technology.

In this study, IRF4flox.E8Icre ($IRF4KO^{CD8}$) mice and OT1.IRF4flox.E8Icre mice with a transgenic TCR were used, both mouse strains have a conditional deletion of the transcription factor IRF4 exclusively in mature CD8+ T cells, other cell types being not effected. This mouse model offers many advantages compared to the other mouse models, used in recent published studies on the role of IRF4 expression in the CD8+ T cell responses [86, 142, 162, 163, 166, 188, 262]. The present study further wanted to investigate the impact of IRF4 expression on the quality, quantity, and kinetic of the clonal expansion and its influence on the initiation of contraction of the effector CD8+ T cells upon primary infection.

Chapter 7

Special features of the IRF4flox.E8Icre mice

To determine the role of IRF4 in the CD8+ T cell development *in vivo*, a transgenic mouse strain carrying loxP-flanked alleles of IRF4 (kindly provided by U. Klein [113]) was breed. These mice were crossed to mice expressing Cre recombinase, driven by the E8Icre enhancer region and Cd8α promoter, in peripheral CD8+ T cells (kindly provided by I. Taniuchi [76]). In IRF4flox.E8Icre mice (termed as IRF4KO^{CD8} mice in this study), the Cre-mediated recombination of the loxP sites occurs in cells that normally express Cd8α, and goes along with eGFP expression in those cells being deficient for IRF4.

First, the expression of the transcription factor IRF4 in IRF4KO^{CD8} and wild type (IRF4flox mice termed as WT) mice in CD4+ and CD8+ T lymphocyte subsets (Figure 7.1 A/B) was analyzed. As expected, in IRF4KO^{CD8} mice only mature CD8+ T cells lacked IRF4 expression tested on splenocytes at day 7 after LM-OVA infection, while CD8+ T cells of WT mice expressed IRF4 up to over 60 % (Figure 7.1 C). In both, WT and IRF4KO^{CD8} mice, the CD4+ T cell compartment and the CD3 negative compartment were capable to express IRF4 after activation similarly (Figure 7.1 B/C). Therefore, in IRF4KO^{CD8} mice, only CD8+ T lymphocytes do not express IRF4 after activation, while CD4+ T lymphocytes and other cell types were not affected from the IRF4 deficiency. The simultaneous activation of eGFP expression upon Cre-mediated recombination was observed via flow cytometric analysis. The majority of peripheral CD8+ T cells of the IRF4KO^{CD8} mice was positive for eGFP expression (Figure 7.1 D). In sum, IRF4flox.E8Icre mice have a conditional deletion of IRF4 in CD8+ T cells, correlating with simultaneous eGFP expression.

To determine whether there are any initial differences between untreated wild type and IRF4KO^{CD8} mice, the size of the CD4+ and CD8+ T cell compartment was analyzed. Furthermore, an examination of the differentiation pattern of the CD8+ T cell subset in different organs of untreated 6-8 weeks old mice was performed. A normal ratio between CD4+ and CD8+ T cells was noted in IRF4KO^{CD8} mice with no differences in lymphocyte numbers and frequencies compared to age-matched wild type mice (Figure 7.2). This was true for peripheral lymphocytes in blood (Figure 7.2 C), as well as in all the other organs (thymus, spleen, and lymph nodes) tested (Figure 7.3). CD4+ and CD8+ T cell compartments were normal, with no significant differences in CD8+ T cell subset distribution. In particular, in IRF4KO^{CD8} mice the majority of CD8+ T cells were in the naïve compartment, while the effector and memory compartment were only small fractions, very similar to CD8+ T cells from WT mice (Figure 7.4 B). These results confirm that the initial generation of T lymphocytes is not altered in IRF4KO^{CD8} (IRF4flox.E8Icre) mice.

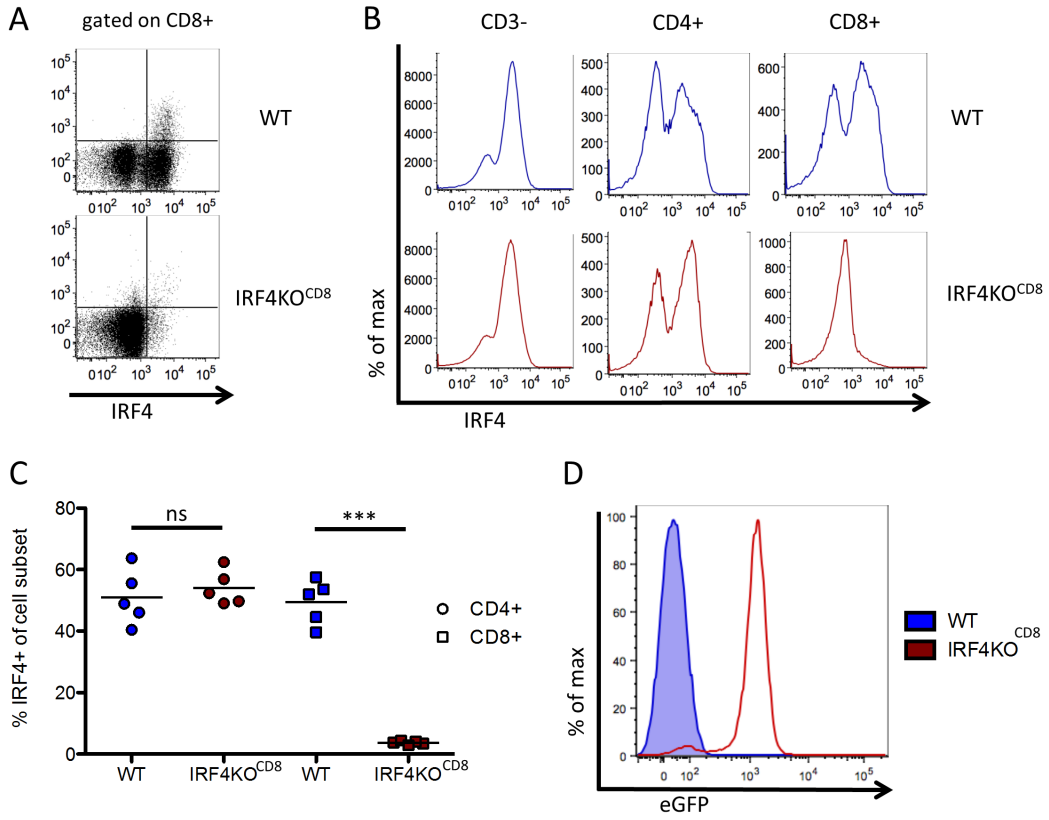

Figure 7.1: **IRF4flox.E8Icre mice have a conditional deletion of IRF4 in CD8+ T cells and simultaneously express eGFP.** Immunofluorescence analysis of IRF4 expression in splenocytes (gated on CD3+ T lymphocytes) on day 7 after LM-OVA infection in IRF4flox.E8Icre mice (termed as IRF4KO^{CD8}) and wild type mice (WT). (A) Exemplary dot plots of intracellular expression of IRF4 in splenic CD8+ T cells of IRF4KO^{CD8} and WT mice. (B) Histograms of IRF4 expression in CD4+ and CD8+ T cell subsets gated on viable splenic CD3+ T lymphocytes and in the CD3 negative compartment of the indicated mouse strain. (C) Frequency of IRF4 expressing CD4+ (circles) and CD8+ (squares) T cells of WT (blue) and IRF4KO^{CD8} (red) splenocytes. Each symbol represents an individual mouse. Small horizontal lines indicate the average. (D) Representative histogram of the eGFP expression on CD8+ T cells; blue filled line represents WT mice and empty red line represents IRF4KO^{CD8} mice. IRF4flox mice were used as WT controls. Data in graph (C) are representative of two independent experiments with similar results. Each group containing 5 mice. ns indicates statistically not significant; ***$p<0.0001$ (Student's t test).

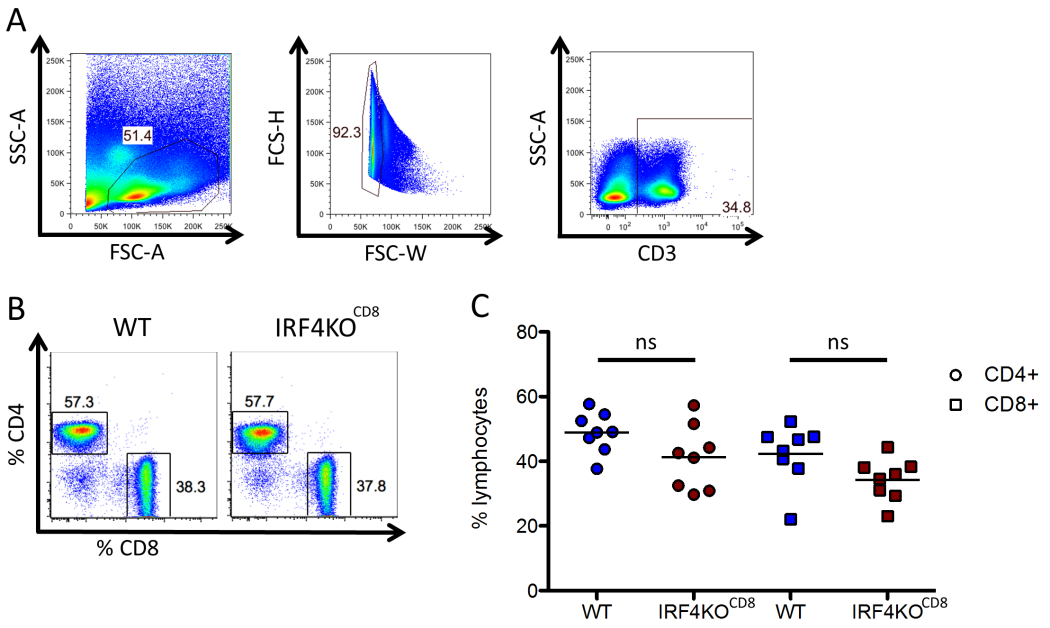

Figure 7.2: **The generation of T lymphocytes is not altered in IRF4flox.E8Icre mice.** Blood were taken from untreated 6-8 weeks old wild type (WT) and IRF4flox.E8Icre (termed as IRF4KO^{CD8}) mice. Frequencies of T cell subsets of the CD4+ and CD8+ compartment were analyzed. (A) Exemplary dot plots with the gating strategy are shown. Viable CD3 expressing T lymphocytes were further divided into CD4+ and CD8+ T cells. (B) Exemplary dot plots of the CD4+ and CD8+ T cells subsets in blood of the indicated mouse strain. (C) Frequency of CD4+ (circles) and CD8+ (squares) T cells pre-gated on CD3+ T lymphocytes in blood of 6-8 weeks old untreated mice of the indicated phenotype. Results in (C) show the mean + SEM. IRF4flox mice were used as WT controls. Data show no statistical significance (Student's t test). Data represents two independent experiments with 4 mice per strain.

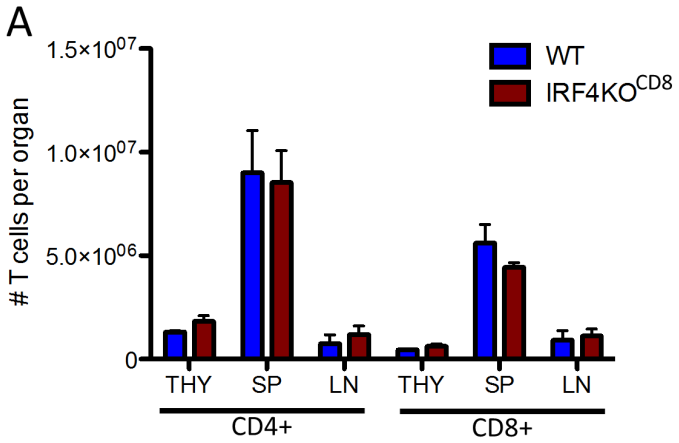

Figure 7.3: **Total numbers and organ distribution of T cell subsets are in IRF4KO^{CD8} mice similar to WT mice.** Spleen (SP), mesenteric lymph nodes (LN), and thymus (THY) were taken from untreated 6-8 weeks old wild type (WT) and IRF4flox.E8Icre (termed as IRF4KO^{CD8}) mice. Total numbers per organ of the CD4+ and CD8+ T lymphocytes were analyzed. (A) Total numbers of CD4+ and CD8+ T cells in the thymus (THY), spleen (SP), and lymph nodes (LN) of untreated 6-8 week old WT (IRF4flox mice) and IRF4KO^{CD8} mice. Data represent two independent experiments with 8-9 mice per group.

IRF4-deficient mouse models from previous publications showed a spontaneous alteration in the genotype and homeostasis of peripheral CD8+ T cells, an enlarged B cell compartment, and disease patterns (lymphadenopathy) in old (12-14 week) untreated mice [153, 162]. Therefore, this present study analyzed whether old IRF4KO^{CD8} (IRF4flox.E8Icre) mice stay healthy with age. To do so, the present analysis checked whether IRF4-deficient CD8+ T cells maintain a wild type phenotype in 12-16 weeks old IRF4KO^{CD8} mice. Furthermore, the conditional KO mice were analyzed for abnormal cell proliferation of the B cell compartment.

The frequencies of the CD4+ and CD8+ T cell compartment, as well as their differentiation pattern in different organs of untreated 12-16 weeks old IRF4KO^{CD8} mice with their aged matched wild type controls (Figure 7.4 C) were compared. A normal ratio between CD4+ and CD8+ T cells was noted in IRF4KO^{CD8} mice with no differences in lymphocyte numbers and frequencies. This was true for peripheral lymphocytes in blood (BL), as well as in spleen (SP), and mesenteric lymph nodes (LN). The CD4+ and CD8+ T cell compartment in old IRF4KO^{CD8} mice was comparable to young healthy WT mice with no significant differences in CD8+ T cell subset distribution, as shown in Figure 7.4 D. In particular, in old IRF4KO^{CD8} mice the majority of IRF4-deficient CD8+ T cells exhibited a naïve phenotype, similar to their aged matched wild type controls. As expected, the effector and memory compartment was rather small in both untreated mice strains. Additionally, present results could not detect differences in the size of the B cell compartment comparing IRF4KO^{CD8} mice with their aged matched counterparts (Figure 7.5).

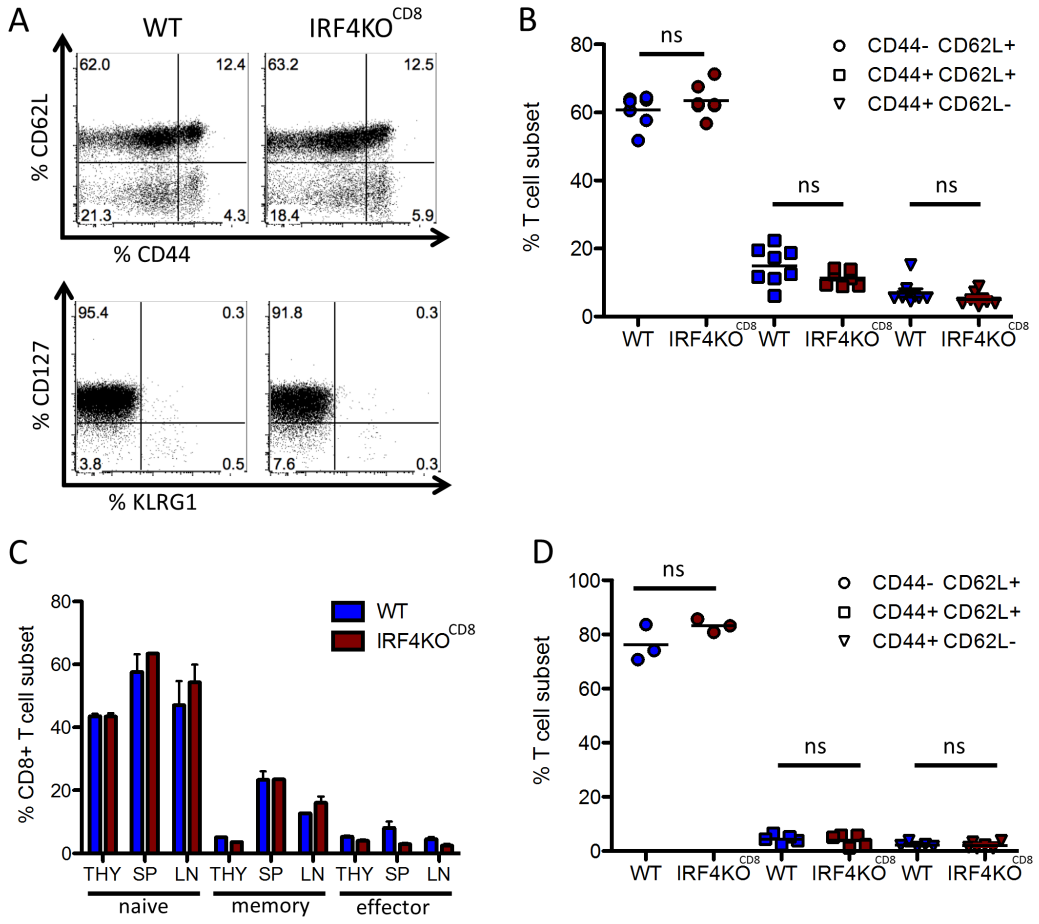

Figure 7.4: **IRF4-deficient CD8+ T cells share a wild type phenotype in untreated mice**. Spleen (SP), mesenteric lymph nodes (LN), blood (BL), and thymus (THY) were taken from untreated 6-8 weeks old and 12-16 weeks old untreated wild type (WT) and IRF4flox.E8Icre (termed as IRF4KO^{CD8}) mice. Additionally, the differentiation pattern of the CD8+ T cell subset was analyzed on the basis of their surface marker expression. (A) Exemplary dot plots of CD62L, CD44, KLRG1, and CD127 (IL7Ra) surface expression on CD8+ T cells in blood of 6-8 weeks old mice. (B) Percentage of naïve (CD44^{low} CD62L+, shown in circles), memory (CD44+ CD62L+ shown in squares) and effector (CD44+ CD62L- shown in triangles) CD8+ T cell subsets in blood of 8 weeks old WT and IRF4KO^{CD8} mice, as assed by flow cytometry. Data show no statistical significance (Student's t test). (C) Percentage of naïve (CD44^{low} CD62L+), memory (CD44+ CD62L+), and effector (CD44+ CD62L-) CD8+ T cell subsets in THY, SP, and LN of 6-8 weeks old WT and IRF4KO^{CD8} mice. (D) Percentage of naïve (CD44^{low} CD62L+), memory (CD44+ CD62L+), and effector (CD44+ CD62L-) CD8+ T cell subsets in spleen of 12-16 weeks old WT and IRF4KO^{CD8} mice. Data are representative of two independent experiments with similar results. Each symbol in (B) and (D) represents an individual mouse and small horizontal lines indicate the average. IRF4flox mice were used as WT controls. Data show no statistical significance. (Student's t test). Results in (C) show the mean + SEM.

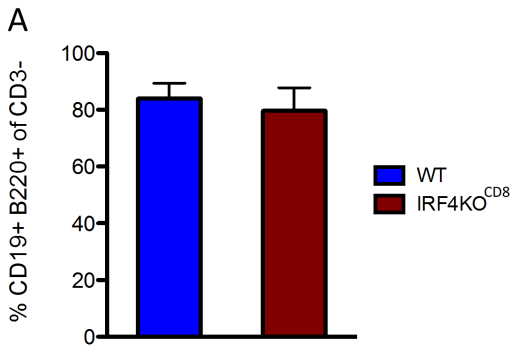

Figure 7.5: **IRF4flox.E8Icre mice show no altered B cell compartment.** Spleen (SP) were taken from untreated 12-16 weeks old wild type (WT) and IRF4flox.E8Icre (termed as IRF4KO^{CD8}) mice. The size of the B cell subset was analyzed on the basis of the CD19 and B220 cell surface expression on B cells. (A) Percentage of splenic B cells (viable CD3- CD19+ B220+) of the non-T lymphocytes of 12-16 weeks old WT and IRF4KO^{CD8} mice. Data are representative of two independent experiments with similar results. IRF4flox mice were used as WT controls. Results in (A) show the mean + SEM. There were no statistical significant differences determined (Student's t test).

In conclusion, no abnormal differentiation or cell development could be detected initially in young or old IRF4flox.E8Icre (IRF4KO^{CD8}) mice, which were used in this study. IRF4-deficient CD8+ T cells from this conditional knock out mice maintained a naive phenotype and even with ongoing age, mice stayed healthy showing no disease patterns.

Chapter 8

The importance of IRF4 in effector CD8+ T cells during infection

8.1 Induction of IRF4 expression

To examine the induction of the IRF4 expression after TCR engagement, stimulations of naïve CD8+ T cells of wild type mice with anti-CD3 and the co-stimulatory molecule anti-CD28 were performed. IRF4 was not expressed in naïve CD8+ T cells but its expression was rapidly induced following activation after TCR signaling, examined via

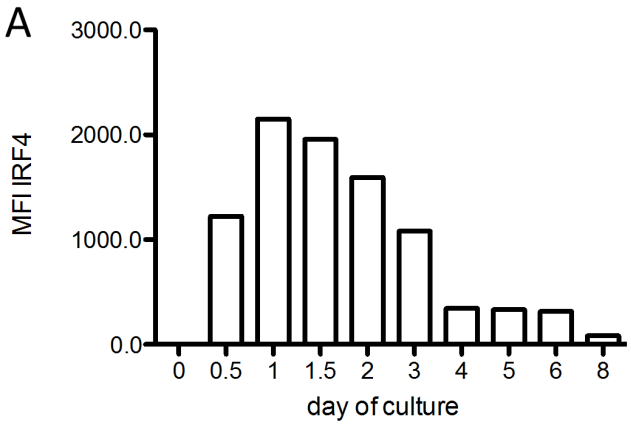

Figure 8.1: **Naïve CD8+ T cells upregulate IRF4 expression after TCR engagement.** (A) CD8+ T cells from untreated wild type mice were first naïve sorted (viable CD3+ CD4- CD44- CD62+) and *in vitro* stimulated with plate-bound aCD3/aCD28 antibody. IRF4 expression levels were determined at the indicated time points of *in vitro* cultured cells by intracellular staining via flow cytometry. Frequencies of IRF4 expression in CD8+ T cells are shown. Data are representative of two independent experiments with similar results.

intracellular staining and further flow cytometric analysis. IRF4 expression peaked between 24-36 hours after TCR stimulation and declined to lower levels for the following days (Figure 8.1).

8.2 The importance of IRF4 for the effector CD8+ T cell generation

IRF4 expression is upregulated in naive CD8+ T lymphocytes upon bacterial or viral infection after TCR-mediated activation of ag-specific cells. Therefore, this study examined whether IRF4 has a role in regulating the effector CD8+ T cell generation and thus the immunological response *in vivo*. WT (IRF4flox mice termed as WT) and IRF4KO^{CD8} (IRF4flox.E8Icre) mice were infected with a recombinant strain of *Listeria monocytogenes* expressing the ovalbumin-derived peptide SIINFEKL (N4), termed as LM-OVA or LM-OVA N4. In Figure 8.2 A, a schematic graph of the tetramer staining is shown. A tetramer staining to identify H-2K^{b}-restricted cytotoxic CD8+ T cells specific for ovalbumin (OVA) was used. Exemplary flow cytometry plots of ag-specific CD8+ T cells are shown in Figure 8.2 B. At the peak of effector response on day 7 after infection, the present analysis observed a significant reduction of SIINFEKL (SI)-specific CD8+ T cells (SI Tet+) in the spleen of IRF4KO^{CD8} mice (mean: 5,5 %) compared to WT mice (mean: 0.39 %) (Figure 8.2 C left). These differences were drastic in frequencies, as IRF4KO^{CD8} mice showed a 14-fold reduction in the percentage of SI-specific CD8+ T cells compared to WT control mice. This dramatic reduction was further

demonstrated in reduced total numbers of CD8+ T cells in IRF4KO^{CD8} mice compared to WT mice.

Additionally, WT and IRF4KO^{CD8} mice were intraperitoneal (i.p.) infected with the Armstrong strain of the lymphocytic choriomeningitis virus (LCMV). On day 8 after infection being the peak of the T cell reaction, the resulting CD8+ T cell response to the LCMV epitope GP33 (GP33 Tet+) via tetramer staining was measured. As expected, this analysis observed similar severely reduced levels of splenic ag-specific CD8+ T cells in IRF4KO^{CD8} mice (mean: 5.5 %) compared to WT control mice (mean: 1,3 %) (Figure 8.2 C right). Consistent with these results, at the peak of the CD8+ T cell response, results shown in this study found that the total number of CD8+ T cells was dramatically diminished within the spleen in IRF4KO^{CD8} mice after infection (Figure 8.2 E), where normally ag-specific CD8+ T cells should be enriched at that time point, like in wild type mice.

To determine whether the drastically decrease of ag-specific CD8+ T cells in the absence of IRF4 expression occurred already early after infection, SI-specific CD8+ T cells in WT and IRF4KO^{CD8} mice were examined via tetramer staining on day 5 after LM-OVA infection. Not surprisingly, IRF4-deficient SI-specific CD8+ T cells showed drastically reduced frequencies (mean: 0.4 %) on day 5 after infection (Figure 8.2), when normally the clonal expansion phase of CD8+ T cells led to the generation of a robust effector cell population with increasing numbers, as detected in WT mice (mean: 2.5 %).

In summary, the dramatically reduced overall quantity of ag-specific effector CD8+ T cells after bacterial and viral infection observed in IRF4KO^{CD8} mice suggests a general defect of IRF4-deficient CD8+ T cells to develop a robust anti-pathogenic CD8+ T cell response during infection. These results support the assumption that IRF4 expression plays an essential role in the generation and maintenance of ag-specific CD8+ T cells during an effector CD8+ T cell response upon primary infection.

During the primary CD8+ T cell response to acute bacterial or viral infection, naïve lymphocytes differentiate into effector CD8+ T cells. To generate a robust effector cell population, primed CD8+ T cells need to proliferate after antigen encounter to increase in numbers, not only in secondary lymphoid tissue, but also in the local sites affected by the infection. To examine the reason for the reduced magnitude of the CD8+ T cell response in the absence of IRF4 expression, this study analyzed whether their proliferative capacity was altered. Therefore, the total CD8+ T cell compartment and the OVA-K^{b}-specific CD8+ T cell population of IRF4KO^{CD8} (IRF4flox.E8Icre) and WT (IRF4flox termed as wild type) mice were analyzed. Because it was shown that Ki-67 antigen is present in all proliferating cells, we used Ki-67 as a representative proliferation associated marker [61].

Wild type (IRF4flox) and IRF4KO^{CD8} (IRF4flox.E8Icre) mice were intravenously (i.v.) infected with LM-OVA. The intracellular expression of Ki-67 within the CD8+ T cell compartment was analyzed at different time points upon bacterial infection. Seven days after Listeria infection, markedly reduced frequencies of Ki-67+ CD44+ cells among SI-specific CD8+ T cells in IRF4KO^{CD8} mice compared to WT mice were observed, analyzing the secondary lymphoid organ spleen (Figure 8.3 A) with up to 4.5 -fold reduction and liver as a target organ of Listeria infection with up to 2 -fold reduction (Figure 8.3 B).

Additionally, an acquisition of the proliferative capacity of the CD8+ T cell compartment on day 5 after Listeria infection was performed. Comparing the total CD8+

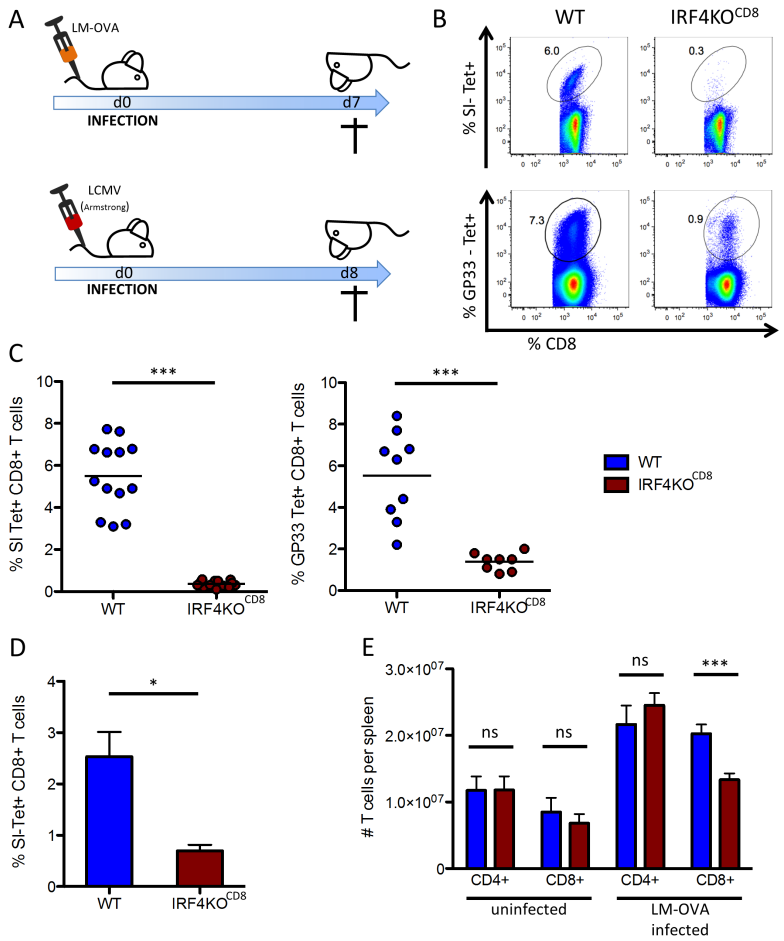

Figure 8.2: **IRF4 is required for the generation of antigen-specific CD8+ T cell after bacterial and viral infection.** (A) Schematic graph of the experimental setup. IRF4KO^{CD8} mice (IRF4flox.E8Icre mice) having IRF4-deficient CD8+ T cells or wild type (IRF4flox mice termed as WT mice) having IRF4-sufficient CD8+ T cells were infected with *Listeria monocytogenes* expressing ovalbumin (LM-OVA) or with the Armstrong strain of the lymphocytic choriomeningitis virus (LCMV). Antigen-specific CD8+ T cells were identified via tetramer staining at the peak of the CD8+ T cell response. (B) Exemplary flow cytometry plots of ag-specific CD8+ T cells. Frequency of SIINFEKL (SI)-specific CD8+ T cells on day 7 after infection with LM-OVA (upper row), or LCMV epitope GP33-specific CD8+ T cells on day 8 after LCMV infection (lower row) of the indicated mouse strain. (C) Frequencies of SI-specific CD8+ T cells after LM-OVA infection on day 7 after infection (left), and LCMV epitope GP33-specific CD8+ T cells on day 8 after LCMV infection (right) of the indicated mouse strain. (D) Frequencies of SI-specific CD8+ T cells on day 5 after LM-OVA infection are shown. (E) Total numbers of CD4+ and CD8+ T cells in spleen on day 7 after LM-OVA infection were calculated. Data are representative of two independent experiments with similar results (4-5 mice per group). Each symbol in (C) represents an individual mouse and small horizontal lines indicate the average. Data show statistical significance with ***$p<0.0001$ and *$p<0.05$ (Student's t test). Results in (D) and (E) are presented as mean + SEM.

T cell subset of both mice strains, present analysis could determine differences in the proliferative activity on day 5 after infection. The frequency of Ki-67+ CD8+ T cells was examined with around 13 % in IRF4KO^{CD8} mice, whereas in WT mice total CD8+ T cells reached a frequency of up to 20 % expressing Ki-67. Although, the mean fluorescence intensity (MFI) was similar comparing total CD8+ T cells from WT and IRF4KO^{CD8} mice, as shown in Figure 8.3 C.

Of interest, the proliferative activity, defined by Ki-67 staining, of IRF4-deficient SI-specific CD8+ T cells was found drastically reduced (mean: 18.7 %) already on 5 days after infection, compared to their WT counterparts (mean: 52.8 %) (Figure 8.3 D). This reduction of the proliferative fraction of CD8+ T cells was examined for the quantity and quality of Ki-67 expression, as IRF4-deficient SI-specific CD8+ T cells showed additionally reduced MFI values for the proliferation marker Ki-67 in IRF4KO^{CD8} mice.

Further determination of 5-bromodeoxyuridine (BrdU) incorporation within IRF4-deficient CD8+ T cells of IRF4KO^{CD8} mice and IRF4-sufficient CD8+ T cells from WT mice after LCMV infection, additionally showed drastic differences in the proliferative activity. Exemplary histograms in Figure 8.4 A show the BrdU incorporation into CD8+ T cells during the early stage of infection. In detail, the BrdU incorporation by total IRF4-deficient CD8+ T cells between day 5 and day 8 was significant lower compared to their counterparts in WT mice. More than double the CD8+ T cells in WT mice were BrdU+, compared with that by IRF4-deficient CD8+ T cells in IRF4KO^{CD8} mice. Additionally, CD8+ T cells expressing CD69, an activation marker [229], which has been shown to be rapidly expressed on mature T cells after TCR-mediated activation [189], showed the same reduced proliferative capacity. This was indicated by drastically reduced BrdU incorporation within IRF4-deficient CD8+ T cells by analyzing their proliferation between day 5 and day 8 after LCMV infection (Figure 8.4 B).

In summary, these results suggest reduced proliferation of IRF4-deficient CD8+ T cells compared to their WT counterparts at this stage of infection. Based on these results, it can be assumed that IRF4 expression is crucial for a proper proliferative capacity of CD8+ T cells after antigen encounter. These data showed that IRF4 deficiency in CD8+ T cells led to a reduced proliferative activity after an initial expansion. Thus, IRF4 expression in CD8+ T cells is required for maintained proliferation during the clonal expansion phase.

8.3 IRF4 impacts the differentiaton of effector CD8+ T cells

Besides affecting the size of the CD8+ T cell response upon primary infection, this study wanted to investigate whether the absence of IRF4 expression in CD8+ T cells also implicates in shaping the phenotypic and functional properties of CD8+ T cells. To compare the cellular phenotype of wild type and IRF4-deficient CD8+ T cell populations after bacterial infection, WT mice (IRF4flox) and IRF4KO^{CD8} mice (IRF4flox.E8Icre) were i.v. infected with LM-OVA. Splenocytes were stained for CD44 and CD62L to distinguish between naïve, effector, and memory cell populations. After antigen encounter during Listeria infection, present results observed no difference in surface expression of CD44. Wild type and IRF4-deficient CD8+ T cells expressed similar high levels of

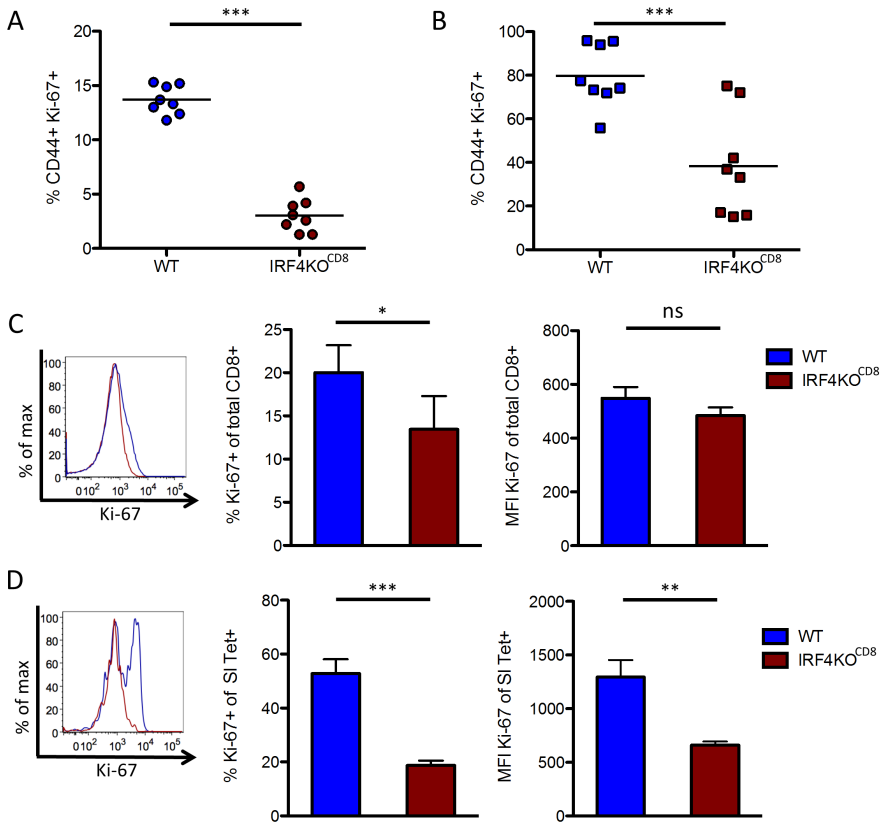

Figure 8.3: **IRF4-deficient CD8+ T cells show less proliferative capacity.** The level of intracellular Ki-67 expression was analyzed to examine the growth fraction of the total and SI-specific CD8+ T cells. Therefore, WT and IRF4KO^{CD8} mice were intravenously infected with LM-OVA and splenocytes were analyzed on day 5 or day 7 after bacterial infection. (A) Frequencies of SI-specific CD8+ T cells were identified via tetramer staining in spleens from WT (in blue) and IRF4KO^{CD8} mice (in red) on day 7 after Listeria infection, labeled for CD44 and Ki-67 marker expression. (B) Flow cytometric profile of SI-specific CD8+ T cells in liver, identified via tetramer staining, from WT (in blue) and IRF4KO^{CD8} mice (in red). Seven days after Listeria infection, tetramer+ CD8+ T cells were labeled for CD44 and Ki-67 marker expression. (C) Exemplary histogram of Ki-67 expression on total splenic CD8+ T cell population pre-gated on viable CD3+ T lymphocytes of the indicated mouse stain on day 5 prior infection (left) are shown. Frequencies of Ki-67 expressing cells (middle graph) and MFI values (right graph) were measured on day 5 after Listeria infection. (D) Exemplary histogram of the Ki-67 expression on splenic SI-specific CD8+ T cell population, pre-gated on viable CD3+ T lymphocytes of the indicated mouse stain, on day 5 prior infection (left) are displayed. Frequencies of Ki-67 expressing cells (middle graph) and mean fluorescence intensity (MFI) values (right graph) were measured after Listeria infection (d5 p.i.). IRF4-deficient CD8+ T cells are shown in red and WT CD8+ T cells are shown in blue. Data are representative of two independent experiments with similar results. Each symbol in (A) and (B) represents an individual mouse and small horizontal lines indicate the average. Data show statistical significance with ***$p<0.0001$ and *$p<0.05$ (Student's t test). Results in (C) and (D) show the mean + SEM.

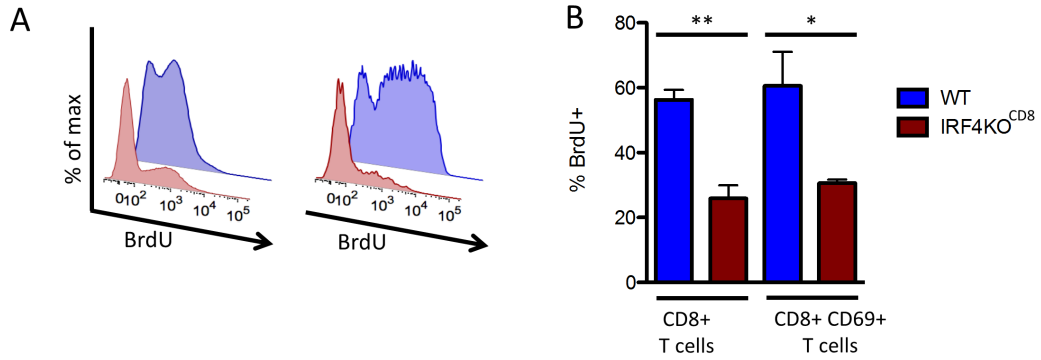

Figure 8.4: **IRF4-deficient CD8+ T cells exhibit altered rates of proliferation.** Wild type (IRF4flox mice termed as WT) and IRF4KO^{CD8} (IRF4flox.E8Icre) mice were infected with the Armstrong strain of LCMV. BrdU was given in drinking sugar water from day 5 till day 8 after infection. On day 8 at the peak of CD8+ T cell response, splenic CD8+ T cells were analyzed for BrdU incorporation. (A) Representative histogram of BrdU incorporation by total CD8+ T cells (left) and CD69+ CD8+ T cells (right) of wild type mice (shown in blue) and IRF4KO^{CD8} mice (shown in red). Data are representative of four mice per strain. (B) Graph shows the frequencies of BrdU incorporation by total CD8+ T cells and CD69+ CD8+ T cells of WT mice (shown in blue) and IRF4KO^{CD8} mice (shown in red). Graph in (B) shows the mean + SEM. Data show statistical significance with **$p<0.001$ and *$p<0.01$ (Student's t test).

CD44, as shown in Figure 8.5, indicating that an initial activation of both cell subsets occurred. Nevertheless, different to WT CD8+ T cells, which downregulated CD62L expression after antigen encounter, the majority of IRF4-deficient CD8+ T cells did not cleaved CD62L from their cell surface. Instead, IRF4-deficient CD8+ T cells maintained a high CD62L expression, as shown on day 7 after bacterial infection (Figure 8.5 A/B). Thus, the acquisition of the $CD62L^{low}$ $CD44^{high}$ effector phenotype was drastically impaired (3.7-fold decreased) in the absence of IRF4 expression in CD8+ T cells, compared to their WT counterparts (Figure 8.5 C). WT CD8+ T cells showed drastically higher frequencies (mean: 83.3 %) of $CD44^{high}$ $CD62L^{low}$ag-specific CD8+ T cells, compared to IRF4-deficient CD8+ T cells (mean: 22.2 %). Therefore, a greater proportion of IRF4-deficient CD8+ T cells acquired a T_{CM} phenotype being $CD44^{high}$ $CD62L^{high}$ (mean: 35.2 %) compared to their WT counterparts (mean: 7.8 %), leading to an over 4-fold difference.

The present study then analyzed CD8+ T cells for the expression of markers characteristically expressed on short-lived effector cells (SLEC) or memory-precursor effector cells (MPEC). The few remaining ag-specific IRF4-deficient CD8+ T cells on day 7 after Listeria infection were pre-dominantly KLRG1 negative (Figure 8.6 A/B), consistent with a memory-like phenotype, as KLRG1 is a marker of replicative senescence. This drastically reduced KLRG1 expression indicated impaired differentiation into a SLEC population. Indeed, in $IRF4KO^{CD8}$ mice, a SLEC population was almost absent (Figure 8.6 C). In contrast, the majority of WT CD8+ T cells expressed high levels of KLRG1. In WT mice, as expected on day 7 after infection, the majority of CD8+ T cells showed SLEC characterization, according to their marker expression of KLRG1 and CD127.

Furthermore, despite the increase in the MPEC percentage of up to 3-fold among the SI-specific CD8+ T cells (Figure 8.6 C) in $IRF4KO^{CD8}$ mice on day 7 after infection, the absolute numbers of MPECs in these mice were decreased (Figure 8.6 D), compared to WT controls.

These results indicated that the absence of IRF4 expression in CD8+ T cells during Listeria infection resulted in an impaired effector cell differentiation and in the absence of a proper SLEC subset. However, this phenotypic alterations in IRF4-deficient CD8+ T cell population after an initial activation, led to an enhanced development of $CD44^{high}$ $CD62L^{high}$ effector memory (T_{EM}) CD8+ T cells. In contrast, a large proportion of WT CD8+ T cells acquired a $CD44^{high}$ $CD62L^{low}$ central memory T cell (T_{CM}) phenotype, which is consistent with the generation of a robust ag-specific CD8+ T cell population. Therefore, IRF4 deficiency promotes the deformation of memory-like CD8+ T lymphocytes with detrimental impact on the generation of a proper effector T cell population after primary infection.

8.4 IRF4-deficient CD8+ T cells maintain CD62L expression

CD62L expression is required for homing of T cells to secondary lymphoid organs. Wild type effector CD8+ T cells express low levels of CD62L, as a rapid downregulation of CD62L on activated T cells is required to facilitate the migration to the sites of

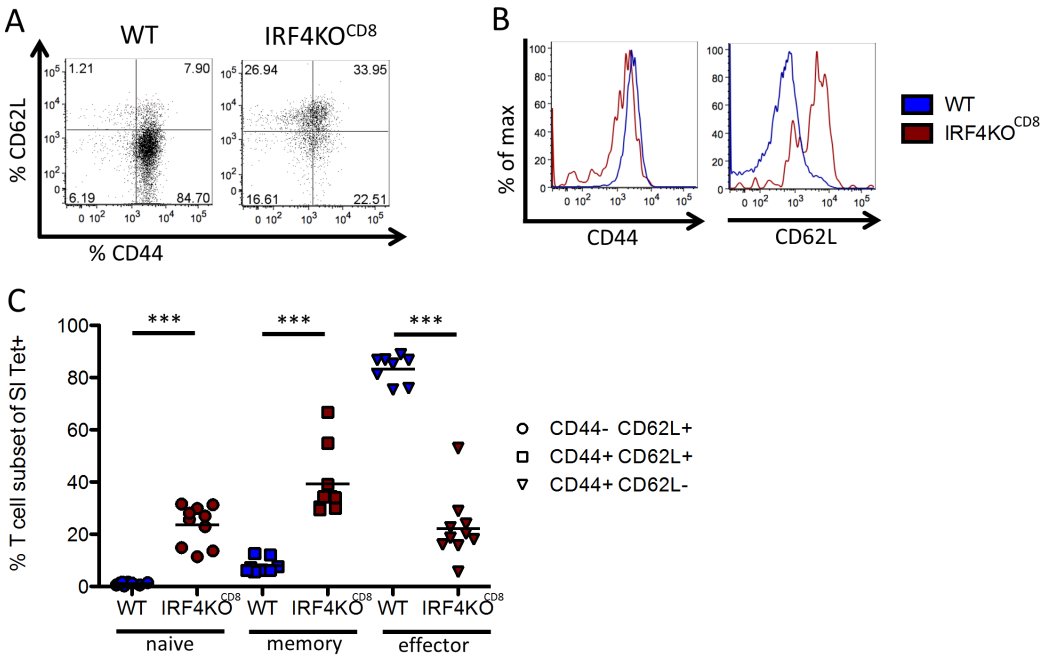

Figure 8.5: **Remaining IRF4-deficient CD8+ T cells acquire a memory-like phenotype after infection.** Double staining for the surface expression of CD44 and CD62L on SI-specific splenic CD8+ T cells was performed on day 7 after LM-OVA infection of wild type and IRF4KO^{CD8} (IRF4flox.E8Icre) mice. (A) Exemplary dot plots show CD62L versus CD44 surface expression among splenic SI-specific CD8+ T cells on day 7 after Listeria infection of the indicated mouse strain. (B) Histograms displaying CD44 and CD62L surface expression of ag-specific splenic CD8+ T cells pre-gated on viable CD3+ lymphocytes of the indicated mouse stains on day 7 after infection. (C) Percentages of naïve (CD44^{low} CD62L+, shown in circles), memory (CD44+ CD62L+ shown in squares), and effector (CD44+ CD62L- shown in triangles) CD8+ T cell subsets in splenocytes of Listeria infected WT and IRF4KO^{CD8} mice (day 7 p.i.) were measured by flow cytometry. Data are representative of two independent experiments with similar results. Each symbol in (C) represents an individual mouse and small horizontal lines indicate the average. Data show statistical significance with ***$p<0.0001$ (Student's t test).

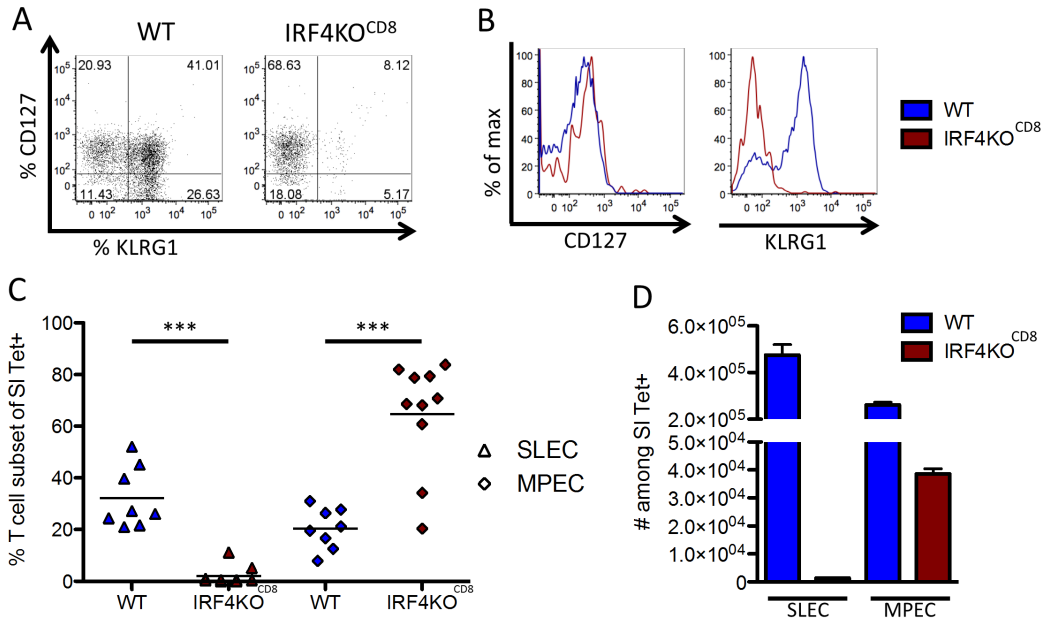

Figure 8.6: **IRF4-deficiency in CD8+ T cells inhibits SLEC formation after infection.** Double staining for the surface expression of KLRG1 and CD127 on splenic CD8+ T cells was performed on day 7 after LM-OVA infection of WT (IRF4flox) and IRF4KO^{CD8} (IRF4flox.E8Icre) mice to subdivide CD8+ T cells into SLECs and MPECs. (A) Exemplary dot plots show CD127 versus KLRG1 surface expression on splenic tetramer+ CD8+ T cells on day 7 after Listeria infection of the indicated mouse strain. (B) Histograms show CD127 and KLRG1 surface expression on tetramer+ splenic IRF4-sufficient (in blue) and IRF4-deficient (in red) CD8+ T cells pre-gated on viable CD3+ T lymphocytes. (C) Percentages of SLECs (CD127^{low} KLRG1^{high}, shown in triangles) and MPECs (CD127^{high} KLRG1^{low} shown in rectangles) in spleens of Listeria infected WT and IRF4KO^{CD8} mice (day 7 p.i.) were measured by flow cytometry. (D) Graph shows the calculated numbers of splenic SLECs and MPECs of SI-specific CD8+ T cells in WT (in blue) and IRF4KO^{CD8} (in red) mice on day 7 after infection. Data shown are pooled from 2 independently performed experiments with at least 4 mice per group. Each symbol in (C) represents an individual mouse and small horizontal lines indicate the average. Graph in (D) shows the mean + SEM. Data show statistical significance with ***$p<0.0001$ (Student's t test).

infection [199].

However, IRF4-deficient CD8+ T cells do not clear the L-selectin (CD62L) from their surface after antigen encounter, as they maintain CD62L expression, as shown in Figure 8.7 A on day 7 after Listeria infection. This is in contrast to the normal expression pattern of CD62L on wild type CD8+ T cells after activation. Therefore, this study asked whether IRF4-deficient CD8+ T cells show different homing capabilities compared to WT CD8+ T cells. To determine the effect of maintained CD62L expression on IRF4-deficient CD8+ T cell infiltration of infected tissue, IRF4KO^{CD8} and WT mice were infected with LM-OVA. CD8+ T cells in spleen, lymph nodes, and liver were monitored on day 5 post infection. Listeria-specific CD8+ T cells were identified via the expression of CD11a, an integrin shown to be upregulated upon antigen encounter via infection [190].

As expected, CD62L expression on wild type ag-specific CD8+ T cells (Figure 8.7 A) were found to be markedly reduced in secondary lymphoid organs, shown in spleen (SP) and mesenteric lymph nodes (LN), as well as in liver as a site of infection. In contrast, ag-specific IRF4-deficient CD8+ T cells were CD62L^{high} (Figure 8.7 A), in all organs tested. The effects were greater in spleen where the majority of the WT ag-specific cells downregulated CD62L, while almost all IRF4-deficient CD8+ T cells maintained CD62L expression. Listeria-specific T cells in mesenteric lymph nodes (LN) and in the target organ liver (LI) of WT mice also showed a drastic downregulation of CD62L, while IRF4-deficient CD8+ T cells did not clear the molecule from their cell surface (Figure 8.7 A). Nevertheless, the frequency of splenic Listeria-specific CD8+ T cells, identified via CD11a expression on the cell surface, did not differ in IRF4KO^{CD8} mice compared to WT mice (Figure 8.7 B). Only a slightly reduced tendency in IRF4-deficient CD8+ T cells could be detected. This observation indicated, that the accumulation of ag-specific CD8+ T cells in spleen was less affected by the IRF4 deficiency.

However, frequencies of Listeria-specific CD8+ T cells (identified as CD11a+) harvested from infected livers or the lymphatic organ LN were not similar in both mice strains. At day 5 after bacterial infection, the frequencies of CD8+ T cells responding to Listeria infection were decreased in the absence of IRF4 expression, with over 3-fold in LN and most pronounced with over 4-fold in the target organ liver (Figure 8.7 B). Nevertheless, ag-specific CD8+ T cells were located in LN and the non-lymphoid organ liver, although frequencies were drastically reduced compared to WT controls.

In summary, these data suggest that IRF4 is required for the correct tissue localization and moreover necessary for the accumulation of responding ag-specific CD8+ T cells in infected tissue. Nevertheless, activated IRF4-deficient CD8+ T cells, which maintained CD62L expression, facilitate the migration to the sites of infection, as present results detected ag-specific CD8+ T cells in the liver of infected IRF4KO^{CD8} mice, although frequencies were drastically reduced.

8.5 IRF4 expression affects the CD8+ effector T cell potential

Furthermore, this study investigated whether the phenotypic differences could be also linked to distinct functional and antibacterial protective capacities. The functionality

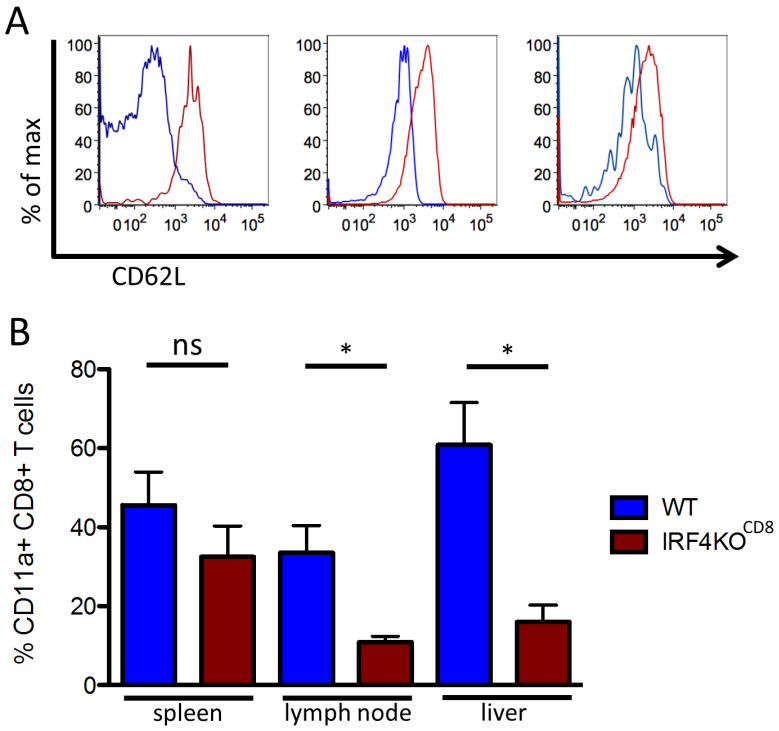

Figure 8.7: **Maintained expression of CD62L on Listeria-specific IRF4-deficient CD8+ T cells does affect the migration to the site of infection.** WT (IRF4flox) and IRF4KO^{CD8} (IRF4flox.E8Icre) mice were infected with LM-OVA. On day 5 after infection, mice were sacrificed and CD8+ T cells in spleen (SP), liver (LI), and mesenteric lymph nodes (LN) were analyzed. Cells were pre-gated on viable CD3+ CD4- CD8+ CD11a+ cells to identify ag-activated CD8+ T lymphocytes. (A) Exemplary histograms show CD62L surface expression on CD11a+ antigen-activated CD8+ T cells on IRF4-suficient (in blue) and IRF4-deficient (in red) CD8+ T cells pre-gated on viable CD3+ lymphocytes in spleen (left), liver (middle), and lymph nodes (right) on day 5 after Listeria infection. (B) Percentage of CD8+ CD11a+ T cells (pre-gated on viable CD3+ CD4- T lymphocytes) in spleen, liver, and lymph nodes on day 5 after Listeria infection of the indicated phenotype. Results in (B) show the mean + SEM. Student's t test was used for statistical analysis. *$p<0.05$; ns indicates statistically not significant.

of effector CTLs was first determined by the ability of these cells to produce cytokines, such as IFNg, TNFa, and IL2. Therefore, WT and IRF4KO^{CD8} mice were infected with LM-OVA or LCMV and sacrificed on day 7 or day 8 after infection, respectively. Listeria infected splenocytes were restimulated ag-specific with the OVA peptide SIINFEKL (SI) or polyclonal with phorbol 12-myristate 13-acetate together with Ionomycin (PMA/Iono), to determine the production of effector molecules. LCMV infected splenocytes were restimulated with GP33 immunodominant peptide. Each restimulation was performed for 6 hours in the presence of BrefA, which blocks protein segregation and causes protein enrichment of the produced cytokines. The production of IFNg, TNFa, and IL2 was determined via intracellular staining followed by flow cytometry analysis.

After primary infection, splenic ag-specific CD8+ T cells from WT mice produced high levels of IFNg (mean: 4.1 %) after restimulation with SI peptide. In contrast, acquisition of IFNg production was drastically impaired (mean: 0.2 %) in the few remaining IRF4-deficient CD8+ T cells from IRF4KO^{CD8} mice, which were located in infected spleen (Figure 8.8 A/B). This dramatic reduction in the effector cytokine production could be detected in ag-specific stimulated IRF4-deficient CD8+ T cells in the secondary lymphatic organ spleen, as well as in the non-lymphoid peripheral organ liver, being a target organ of Listeria infection (Figure 8.8 B). Importantly, the defect of the IRF4-deficient CD8+ T cells to produce IFNg was similar detectable after restimulation with the immunodominant peptide GP33 of LCMV infected splenocytes from IRF4KO^{CD8} mice (Figure 8.8 B/C). These results suggest that the phenotype of IRF4-deficient CD8+ T cells is not dependent on the infection model, rather occurs due to general intrinsic defects of the remaining ag-specific CD8+ T cells.

Wild type CD8+ T cells showed high percentages of IFNg producing cells and a high IFNg expression per cell, indicated by the intensity of the IFNg staining (MFI), while TNFa was also produced in appropriate levels (Figure 8.9 A/B). Not surprisingly, high proportion of IFNg+ wild type CD8+ T cells co-expressed TNFa and IFNg. Of interest, functional defects in the production of cytokines additionally affected the secretion of IL2 and TNFa in the absence of IRF4 expression in effector CD8+ T cells. Furthermore, the polyfunctionality was also impaired, as the frequencies of splenic IFNg+ CD8+ T cells being positive for TNFa or IL2 were dramatically decreased in IRF4-deficient CD8+ T cells (Figure 8.9 C). Of note, very low cytokine responses were also observed after non-specific polyclonal restimulation of IRF4-deficient CD8+ T cells (Figure 8.9 D).

Taken together, the ability of IRF4-deficient CD8+ T cells to respond to antigenic stimulation by cytokine production was severely impaired, in both infection models. IRF4KO^{CD8} mice had much lower frequencies of CD8+ T cells responding to infection specific antigens. Therefore, these results indicate that IRF4 is indispensable for an effective cytokine production in effector CD8+ T cell.

Wild type (IRF4flox) and IRF4KO^{CD8} (IRF4flox.E8Icre) mice were infected with *Listeria monocytogenes* and the cytotoxic capabilities of splenic CD8+ T cells on day 7 after infection were analyzed, as the presumption raised that cytotoxic capabilities are additionally severely restricted in the absence of IRF4 expression and this might result in an increased pathogen burden. This hypothesis was based on previous results represented in this present study, showing that IRF4 deficiency in CD8+ T cells resulted in a drastically decreased ag-specific effector cell population with dramatically reduced effector cytokine production.

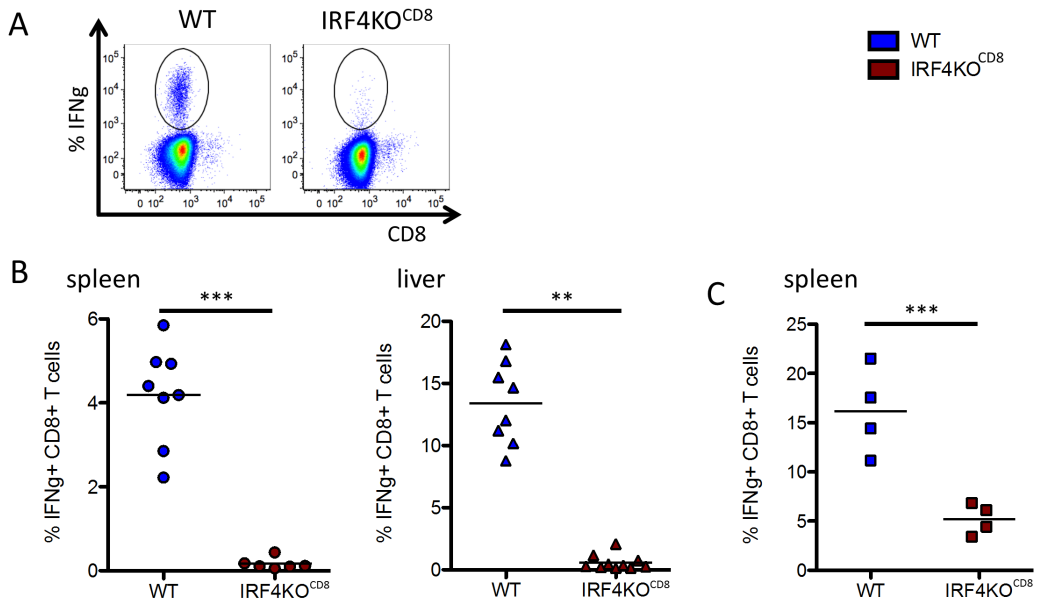

Figure 8.8: **IRF4-deficient CD8+ T cells show drastically impaired cytokine production during infection.** Dynamics of IFNg production by splenic ag-specific CD8+ T cells of IRF4KO^{CD8} (IRF4flox.E8Icre shown in red) and WT (IRF4flox shown in blue) mice after Listeria or LCMV infection. Mice were infected with LM-OVA or LCMV and sacrificed on day 7 or day 8 after infection at the peak of CD8+ T cell response, respectively. Lymphocytes were prepared from infected spleens or livers and analyzed for IFNg production by flow cytometry, after 6 hours of ag-specific *in vitro* stimulation with the indicated peptide. (A) Representative dot plots of the IFNg expression in Listeria infected splenic CD8+ T cells after 6 hours of ag-specific stimulation with SIINFEKL (SI) peptide of the indicated mouse strain are shown. (B) Frequency of IFNg expression in CD8+ T cells after SI stimulation of Listeria infected spleen (left graph, circle symbols) or liver (right graph, triangle symbols) of the indicated mouse strain. (C) Frequency of IFNg expression in splenic CD8+ T cells of WT and IRF4KO^{CD8} mice after LCMV infection are depicted. Antigen-specific *in vitro* stimulation was performed with the GP33 peptide of LCMV. Each symbol represents an individual mouse with 4-7 mice per group. Small horizontal lines indicate the average. Data are representative of at least two independent experiments with similar results. Data show statistical significance with ***$p<0.0001$ and *$p<0.05$ (Student's t test).

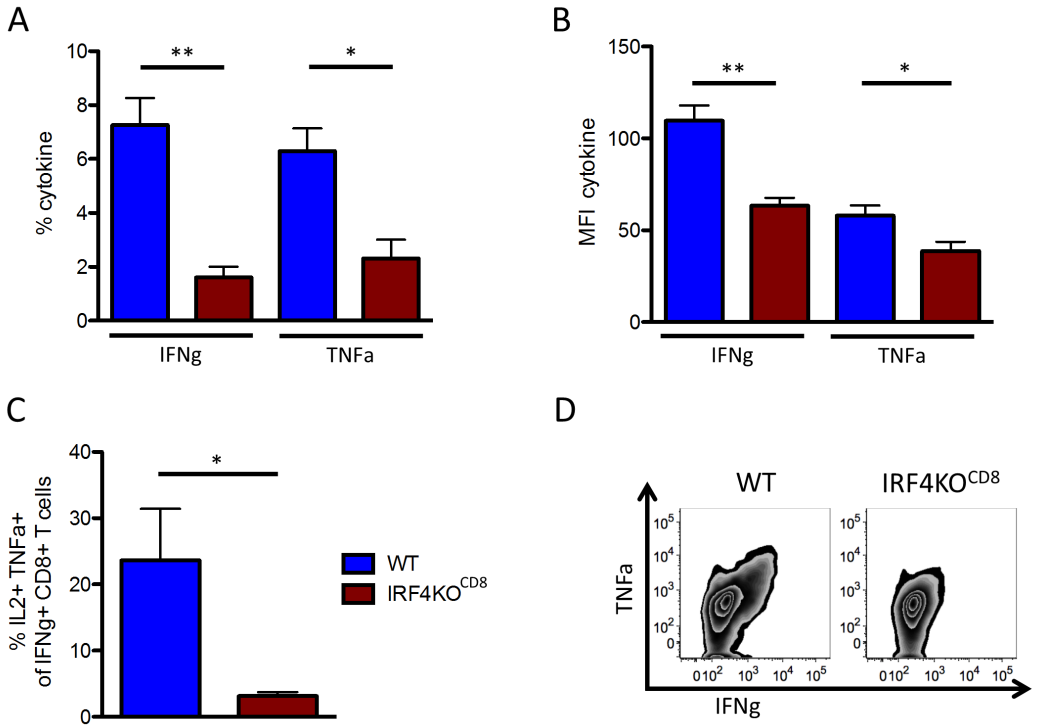

Figure 8.9: **IRF4 is indispensable for effective cytokine production and polyfunctionality.** WT (IRF4flox) and IRF4KO^{CD8} (IRF4flox.E8Icre) mice were infected with LM-OVA and sacrificed on day 7 after infection. Splenocytes were polyclonal restimulated with PMA/Iono to determine the production of effector molecules. (A) Frequencies of IFNg and TNFa expression in splenic IRF4-deficient (in red) and IRF4-sufficient (in blue) CD8+ T cells are shown. Splenocytes were harvested on day 7 after LM-OVA infection and after further 6 hours of *in vitro* stimulation with PMA/Iono, the expression of cytokines was determined via intracellular staining. (B) Mean fluorescence intensity (MFI) values of IFNg+ and TNFa+ CD8+ T cells of the indicated mouse strain are depicted. (C) Frequencies of CD8+ T cells expressing IL2, TNFa and IFNg on day 7 after Listeria infection of the indicated mouse strain. Splenocytes were 6 hours *in vitro* stimulated with SI peptide. Cytokine production was determined via intracellular staining using flow cytometry. (D) Exemplary dot plots show IFNg versus TNFa expression in splenic CD8+ T cells on day 7 after Listeria infection of the indicated mouse strain. Splenocytes were polyclonal stimulated with PMA/Iono. Results in (A), (B), and (C) show the mean + SEM. Student's t test was used for statistical analysis with *$p<0.05$ and **$p<0.005$. Data are representative of at least two independent experiments with similar results with 4-5 mice per group.

Indeed, IRF4-deficient CD8+ T cells expressed lower levels of the death receptor ligand FASL and of the degranulation marker CD107a, than their wild type counterparts. Accessorily, granzyme B expression was significantly reduced in IRF4-deficient CD8+ T cells after infection (Figure 8.10 A). These results indicated that the antibacterial protective capacities of the IRF4-deficient ag-specific CD8+ T cell subset was drastically diminished, which might lead to a less efficient clearance of the pathogen. To determine whether there are differences in the clearance capacity due to the absence of IRF4 in CD8+ T cells, the bacterial numbers in spleen on day 5 after intravenous Listeria infection in the WT and IRF4KO^{CD8} mice were examined. Colony forming units (CFU) observed in spleen were calculated. IRF4-deficiency in the CD8+ T cell compartment resulted in an increase in the bacterial burden in IRF4KO^{CD8} mice after Listeria infection, showing higher bacterial numbers per secondary lymphoid organ (Figure 8.10 B). Those findings provide evidence that IRF4 expression in the CD8+ T cell population is required to acquire cytotoxic properties to attack and destroy pathogen infected cells, as IRF4 deficiency in CD8+ T cells led to an increased bacterial burden.

8.6 IRF4 deficiency alters the transcriptional program of CD8+ T cells

The fate of the CD8+ T cell population is known to be dependent on the expression ratio between the two T-box transcription factors, namely Tbet and Eomes. Although, Tbet and Eomes show expressional overlap, it is claimed that the reciprocal expression of this master regulators correlate with the functionality and differentiation of CD8+ T cells into distinct cell subsets [91, 220]. Recent studies show that Eomes promote memory cell formation [9]. In contrast, Tbet plays a critical role for the differentiation into effector cells and contributes to the expression of effector cytokines and cytotoxic molecules [181, 220]. Additionally, Tbet is known to promote upregulation of KLRG1. Therefore, the question raised whether IRF4 deficiency results in decreased Tbet and increased Eomes expression. This presumption raised, as IRF4-deficient CD8+ T cells showed a drastic reduction in the terminal effector CD8+ T cell subset with a drastically impaired KLRG1 expression after activation (Figure 8.6).

As expected, IRF4-sufficent CD8+ T cells from day 7 infected WT mice expressed high levels of Tbet, while the percentage of CD8+ T cells expressing Eomes maintained low on day 7 after Listeria infection, as shown in Figure 8.11. This observation was consistent with recent publications determining an increase of Tbet expression after activation of naïve CD8+ T cells via TCR engagement [149]. In contrast, IRF4-deficient CD8+ T cells showed higher levels of Eomes expression (Figure 8.11), matching with the memory-like phenotype (CD44+ CD62L+ CD127+ KLRG1-) recorded on day 7 after Listeria infection. However, the percentage of Tbet expressing CD8+ T cells revealed no significant difference between both mice strains on day 7 after Listeria infection. Nevertheless, the mean fluorescence intensity (MFI) value of Tbet was significantly reduced in IRF4-deficient CD8+ T cells (Figure 8.11 B/C). Because Tbet drives terminal effector differentiation and correlates with KLRG1 expression, the unusual lack of KLRG1 expression in IRF4-deficient CD8+ T cells could be linked to the detected increased Eomes expression and diminished Tbet expression.

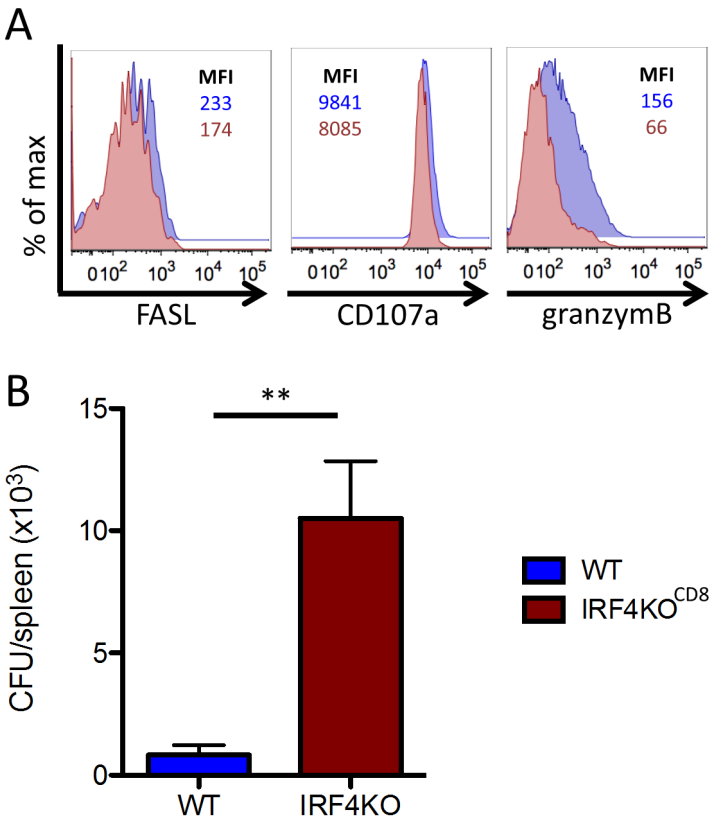

Figure 8.10: **IRF4 deficiency impairs cytotoxic CD8+ T cell functions to kill target cells.** Diminished protective cytotoxic CD8+ T cell response in the absence of IRF4 in WT (IRF4flox) and IRF4KO^{CD8} (IRF4flox.E8Icre) mice, which were infected with LM-OVA and sacrificed 5 days later. Splenocytes of infected mice were analyzed for their expression of cytotoxic markers and the bacterial load in the secondary lymphoid organ was examined. (A) Exemplary overlaying histograms of FASL, CD107a and granzymB expression in wild type (in blue) and IRF4-deficient CD8+ T cells (in red) are shown. Numbers in the histograms indicate the mean fluorescence intensity (MFI) values and percentages (%) of positive cells of the indicated marker. (B) Graph shows the numbers of bacteria in the secondary lymphoid organ spleen, determined by examining the colony forming units (CFU). Results in (B) show the mean + SEM. Statistical significance was analyzed by Student's t test with **$p<0.005$.

Examination of Tbet+ Eomes+, Tbet+ Eomes-, and Tbet- Eomes+ populations of WT and IRF4-deficient ag-specific CD8+ T cells on day 7 after Listeria infection revealed lower proportions and numbers of Tbet+ Eomes- CD8+ T cells in IRF4KO^{CD8} mice (Figure 8.12 A/B). IRF4-deficient CD8+ T cells showed higher frequencies in the Eomes+ Tbet- and Eomes+ Tbet+ proportion. In contrast, in WT mice higher frequencies of CD8+ T cells expressed Tbet alone or together with Eomes (Figure 8.12 A). Although, frequencies of Tbet- Eomes+ and Tbet+ Eomes+ CD8+ T cells were higher in IRF4KO^{CD8} mice compared to WT mice, total numbers revealed a drastic reduction of these populations (Figure 8.12 B), in agreement with overall drastically reduced numbers of ag-specific CD8+ T cells in the absence of IRF4, which were examined on day 7 after infection (Figure 8.2).

In conclusion, recent data suggest that IRF4 expression inhibited Eomes expression and positively regulated Tbet expression in WT CD8+ T cells. Represented results indicate that an abnormal transcriptional programming of IRF4-deficient CD8+ T cells might be the reason for the drastic functional impairment and successive loss of their proliferative capacity and reduced existence and survival. The untypical differentiation pattern of IRF4-deficient effector CD8+ T cells, that present results observed on day 7 after Listeria infection in IRF4KO^{CD8} mice, suggest a different underlying transcriptional profile of those few remaining ag-specific CD8+ T cells compared to their WT counterparts. This indicates that IRF4 is mandatory for the cell fate decision of CD8+ T cells after infection and important to balance the expression of the key transcription factors Tbet and Eomes.

8.7 Importance of IRF4 for CD8+ T cell memory formation and recall

Previous experiments in this study demonstrated that on day 7 after Listeria infection effector CD8+ T lymphocytes showed a memory-like phenotype (CD44+ CD62L+ CD127+ KLRG1-) in mice having IRF4 deficiency in the CD8+ T cell compartment. Thus, the question came up whether IRF4KO^{CD8} mice show an increase of ag-specific CD8+ T cells in the memory pool and if they similarly show an impaired CD8+ T cell response after secondary infection. To investigate the contribution of IRF4 expression to the formation of a robust memory CD8+ T cells subset, mice having IRF4-deficient CD8+ T cells (IRF4flox.E8Icre mice termed as IRF4KO^{CD8}) and wild type (IRF4flox) mice were infected with the Armstrong strain of lymphocytic choriomeningitis virus (LCMV). The experimental setup is shown in Figure 8.13 A.

Tetramer staining was used to examine the resulting ag-specific CD8+ T cell response to the LCMV GP33 epitope (GP33 Tet+ cells) upon acute viral infection. Splenic GP33-specific CD8+ T cells were analyzed on day 8 and day 60 after LCMV Armstrong infection, and on day 68, 8 days after antigen reencounter. Time points were chosen to analyze the effector CD8+ T cell compartment at the peak of effector response, to examine the memory formation, and to analyze the effector T cell response after secondary infection.

Not surprisingly, IRF4-deficiency changed the magnitude of the CD8+ T cell response after viral infection. Consistent with the present previous observations during primary

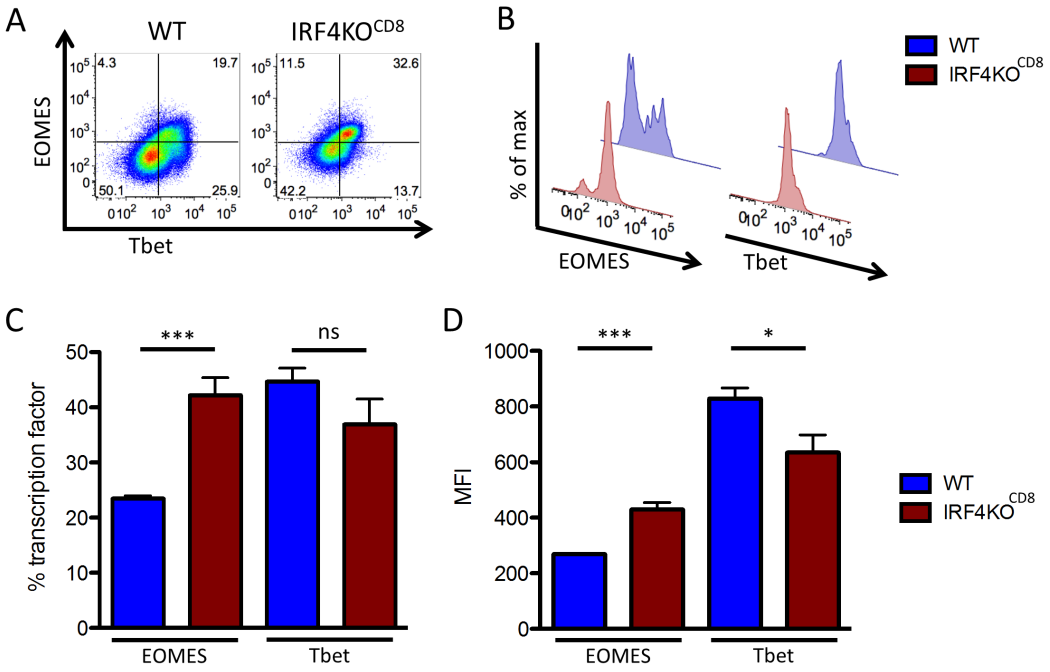

Figure 8.11: **IRF4-deficient CD8+ T cells in Listeria infected IRF4KO^{CD8} mice express high levels of Eomes.** WT (IRF4flox) and IRF4KO^{CD8} (IRF4flox.E8Icre) mice were infected with LM-OVA and on day 7 sacrificed. Splenocytes were surface stained with viability dye, anti-CD3, CD4, and CD8 antibody and intracellular stained for Eomes and Tbet expression. (A) Overlaying histograms of Eomes and Tbet expression in wild type and IRF4-deficient CD8+ T cells. (B) Histograms showing the expression of Tbet and Eomes in WT (in blue) and IRF4-deficient CD8+ T cells (in red). (C) Frequencies of splenic CD8+ T cells expressing Eomes or Tbet on day 7 after Listeria infection of the indicated mouse strain are shown. Transcription factor expression was measured via intracellular staining using flow cytometry. (D) Frequencies show the mean fluorescence intensity (MFI) values of Tbet and Eomes expression in splenic CD8+ T cells on day 7 after Listeria infection. Wild type mice are shown in blue and IRF4KO^{CD8} mice in red. Data are representative of two independent experiments with 3-6 mice per group with similar results. Result in (C) and (D) show the mean + SEM. Statistical significance was analyzed by Student's t test with *$p<0.05$, **$p<0.005$ and ***$p<0.0001$.

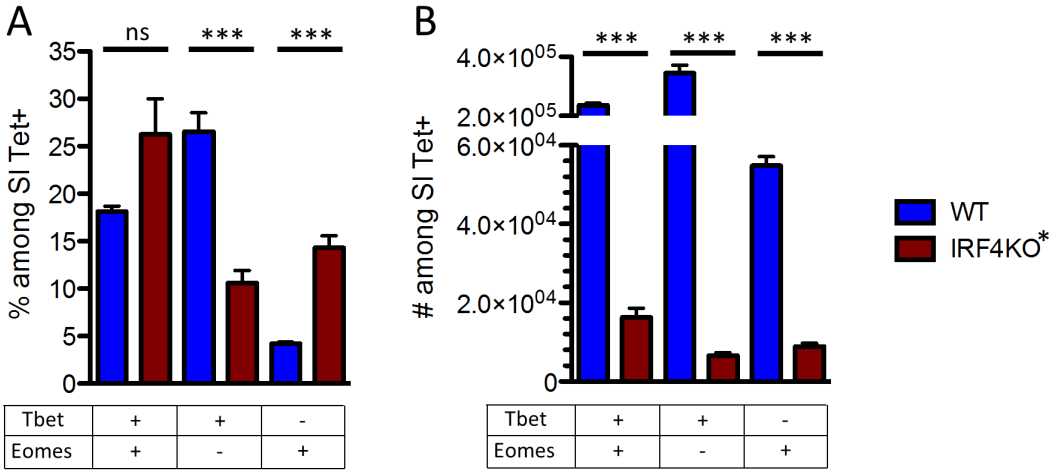

Figure 8.12: **IRF4 expression ensures the balance between Tbet and Eomes expression in CD8+ T cells.** Splenocytes from LM-OVA infected WT and IRF4KO^{CD8} mice were harvested on day 7 post infection and stained with viability dye, OVA-specific H-2K^{b}-SI tetramer, and antibodies for CD3, CD4, CD8, Tbet, and Eomes. (A) Graph shows proportions of Tbet+ Eomes+ (left), Tbet+ Eomes- (middle), and Tbet- Eomes+ (right) populations of WT (in blue) and IRF4-deficient CD8+ T cells (in red) on day 7 after LM-OVA infection. (B) Graph shows calculated numbers of Tbet+ Eomes+ (left), Tbet+ Eomes- (middle), and Tbet- Eomes+ (right) populations of WT (in blue) and IRF4-deficient CD8+ T cells (in red) on day 7 after LM-OVA infection. Data are representative for two independent experiments with 3-6 mice per group. Results in (A) and (B) show the mean + SEM. Statistical significance was analyzed by Student's t test with ***$p<0.0001$.

Listeria infection, IRF4KO^{CD8} mice showed a severely decrease in the GP33-specific CD8+ T cell population at the peak of CD8+ T cell response after primary infection (Figure 8.13 B). Interestingly, present results found similarly reduced numbers of LCMV GP33-specific CD8+ T cells on day 68, 8 days upon rechallenge with LCMV, compared to 8 days after primary infection. Comparison of the formed memory fraction of ag-specific CD8+ T cells in WT and IRF4KO^{CD8} mice on day 60 after infection showed no significant differences in frequency. LCMV GP33-specific CD8+ T cells were not reduced at this later time point (day 60 p.i.) in IRF4KO^{CD8} mice, suggesting a memory formation in WT and IRF4KO^{CD8}mice to a similar extent.

Additionally, the phenotype of ag-specific CD8+ T cells in IRF4KO^{CD8} mice was different during the acute infection phase (d8 and d68 p.i.) compared to WT mice, as shown in Figure 8.14. In detail, at the peak of T cell response on day 8 after primary LCMV infection, GP33-specific CD8+ T cells in WT mice were assigned into the effector cell compartment, being KLRG1+ CD127- CD62L- and CD44+. Similar to the primary virus infection, after secondary antigen encounter, IRF4-deficient CD8+ T cells showed an altered surface expression of CD62L and KLRG1 compared to CD8+ T cells from WT mice (Figure 8.13). A similar phenotype of IRF4-deficient CD8+ T cells was also found in IRF4KO^{CD8} mice on day 68, 8 days after rechallenge with LCMV. In contrast, IRF4-deficient CD8+ T cells showed a memory-like phenotype maintaining CD62L on their surface and expressing CD127 and CD44, but lacked KLRG1 expression. Interestingly, IRF4-deficient memory CD8+ T cells (day 60 post primary infection) were qualitative and qualitatively not different from their counterparts in WT hosts. Just minor differences could be detected, comparing WT and IRF4-deficient CD8+ T cells, as both cell subsets acquired a similar phenotype in the surface marker expression of CD44, CD62L, KLRG1, and CD127.

Taken together, these data indicate that IRF4 is necessary for a proper expansion and differentiation of effector CD8+ T cells during the onset of the immune response upon primary and secondary infection, but did not impact later (memory) T cell homeostasis or the generation of long-lived pathogen-specific CD8+ T cells.

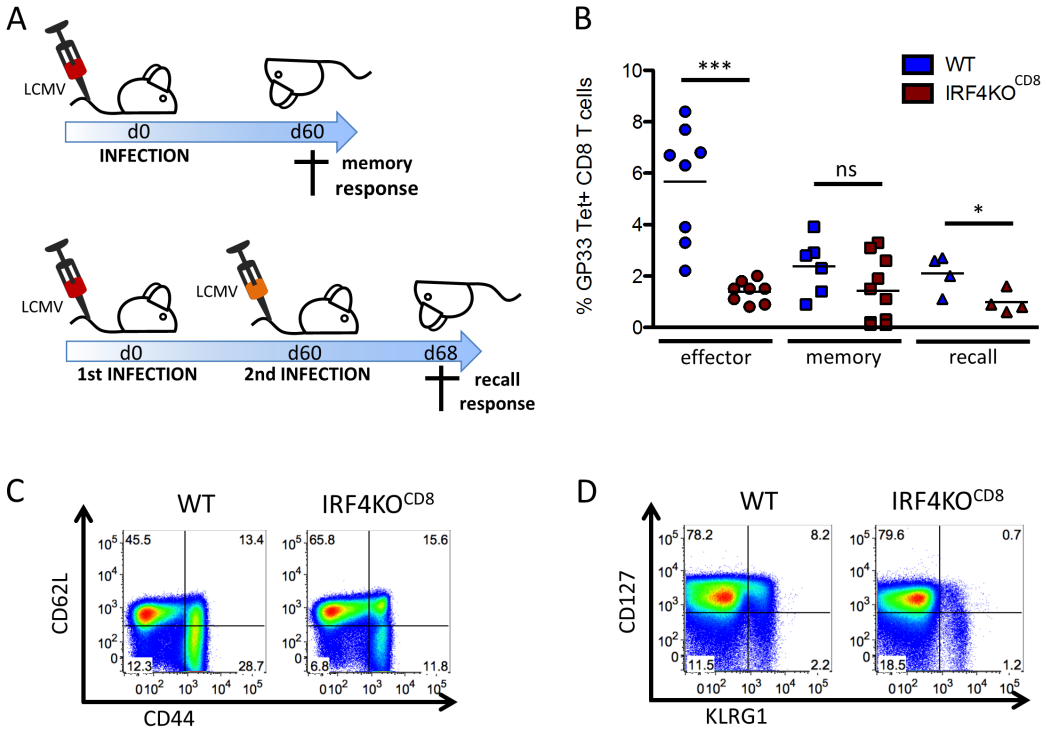

Figure 8.13: **Similar memory formation but impaired effector and effector recall CD8+ T cell response in the absence of IRF4.** (A) Schematic graph of the experimental setup. Wild type (WT) and IRF4KO^{CD8} mice were infected with lymphocytic choriomeningitis virus (LCMV) Armstrong. Splenocytes were surface stained with viability dye, anti-CD3, CD4, and CD8 antibody. Splenic GP33-specific CD8+ T cells were analyzed via tetramer staining on day 8 and day 60 after LCMV Armstrong infection, and on day 68 (8 days after second antigen reencounter). (B) Antigen-specific CD8+ T cells were determined using tetramer staining, at the peak of the effector CD8+ T cell response (day 8 p.i.), at a memory time point (day 60 p.i.), and day 68 after second antigen encounter (recall at day 60 after primary infection). (C) Exemplary flow cytometry plots of CD44 and CD62L expression on splenic CD8+ T cells, at day 60 after LCMV infection. Data are representative of two independent experiments with similar results (4-5 mice per group). Each symbol in (B) represents an individual mouse and small horizontal lines indicate the average. Data show statistical significance with ***$p<0.0001$ and *$p<0.05$ (Student's t test).

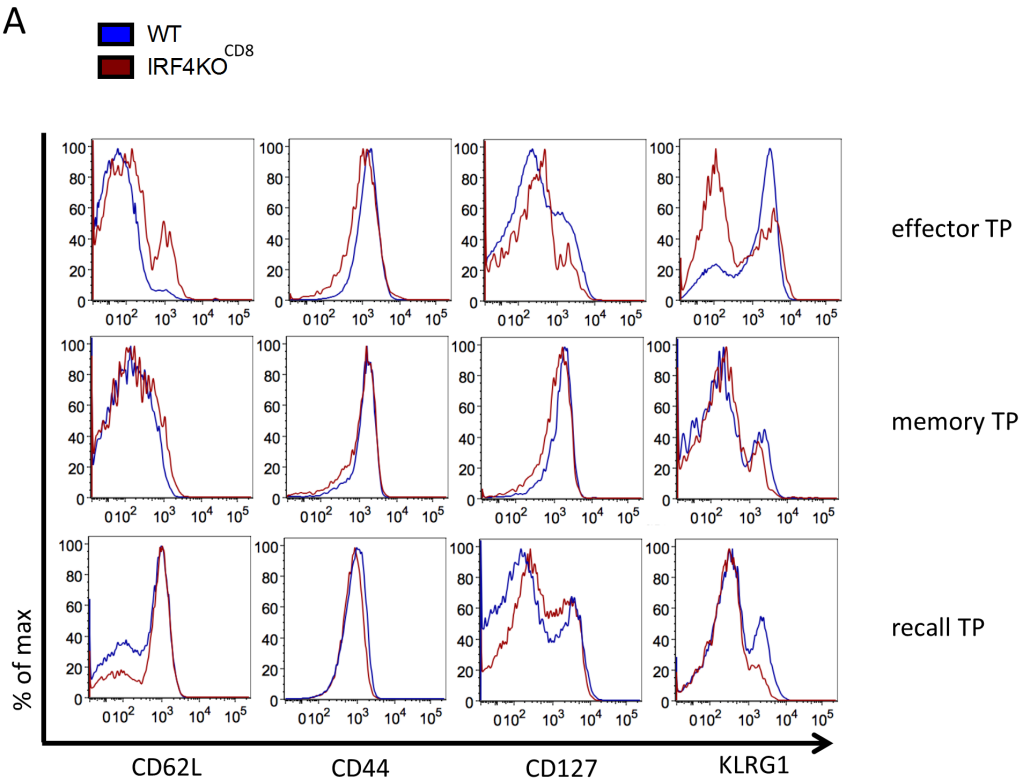

Figure 8.14: **IRF4 deficiency impacts the differentiation pattern of ag-specific CD8+ T cells after primary and secondary viral infection.** Wild type (IRF4flox termed as WT) and IRF4KO^{CD8} mice were infected with lymphocytic choriomeningitis virus (LCMV) Armstrong and analyzed on different time points (TP). Mice were sacrificed on day 8 (effector TP) or day 60 (memory TP) after primary infection. To analyze the CD8+ T cell response after antigen reencounter, secondary infection was performed 60 days after first infection and mice were sacrificed 8 days later. Splenocytes were surface stained with viability dye, anti-CD3, CD4, and CD8 antibody. GP33-specific CD8+ T cells were analyzed via tetramer staining on day 8 (effector) and day 60 (memory) after LCMV Armstrong infection, and on day 68 (recall TP being 8 days after second antigen reencounter). (A) Exemplary histograms display the surface expression of CD62L, CD44, CD127, and KLRG1 on splenic ag-specific CD8+ T cells of WT (in blue) and IRF4KO^{CD8} mice (in red) at the indicated time point. Data are representative of two independent experiments with similar results (4-5 mice per group).

Chapter 9

IRF4-deficient CD8+ T cells have an increased apoptotic potential

9.1 IRF4 deficiency leads to increased susceptibility to apoptosis

Present results in this study could observe a drastically decrease in numbers and frequency of ag-specific CD8+ T cells and less proliferative capacity in the absence of IRF4 expression already on day 5 after infection. Additionally, transfer experiments (Section 10.2) gave proof that IRF4-deficient CD8+ T cells, upon initial activation and clonal expansion, suffer from diminished proliferation capacity and are almost disappeared on day 7 after bacterial infection. Therefore, the question came up whether IRF4 deficiency leads to an increase of apoptosis and/or phagocytosis at the early clonal expansion phase and therefore to an early onset of contraction.

The decline in numbers of ag-specific CD8+ T cells during the contraction phase is controlled via several mechanisms, such as changes in the transcriptional program, exposure of eat-me molecules on the cell surface, and the expression of death inducing receptors, which all lead to the initiation of intrinsic or extrinsic apoptosis pathways. FAS-mediated cell death pathways result in activation induced cell death (AICD) and occurs via expression of death receptors on the cell surface. Phagocytosis is initiated via the exposure of find-me and eat-me signals on the target cell leading to complement activation and cell-mediated phagocytosis.

As already mentioned, apoptotic cell death can occur as a result of engagement of the death receptor FAS (known as CD95 or APO-1) on the surface of a cell prone to die. When the FAS receptor bind to its ligand, it induces extrinsic apoptosis due to signaling via an intracellular domain, the recruitment of FAS-associated death domain (FADD), and the formation of a death inducing signaling complex (DISC). These processes result in a recruitment of pro-caspases and to an activation of several caspases [29]. To determine whether IRF4-deficient CD8+ T cells are prone to cell death via the FAS-FASL mediated death pathway this study analyzed the expression of FAS on the cell surface on day 5 after Listeria infection. Wild type (IRF4flox) and IRF4KO^{CD8} (IRF4flox.E8Icre) mice were infected with Listeria and analyzed the expression of the death receptor FAS on the surface of splenic CD8+ T cells via flow cytometry. IRF4-deficient CD8+ T cells expressed significant higher levels of FAS on their surface than their wild type counterparts, as shown in Figure 9.1 A/B.

These results suggest that IRF4-deficient CD8+ T cells are more susceptible to apoptosis than their WT counterparts on day 5 after bacterial infection and that the cell

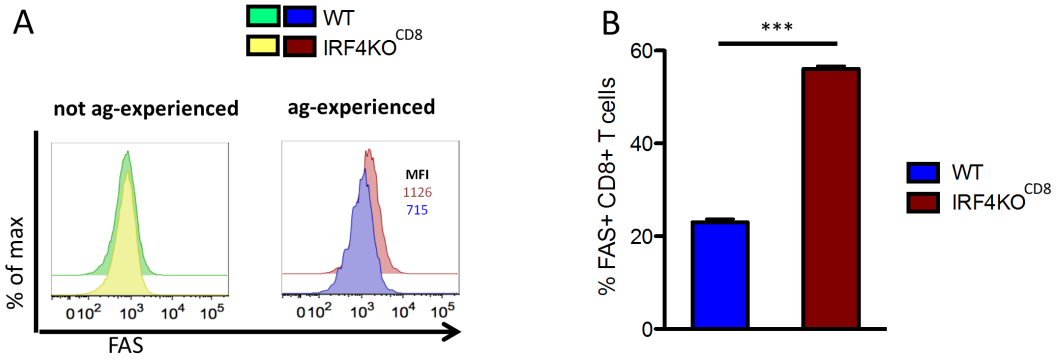

Figure 9.1: **IRF4 deficiency led to FAS-mediated apoptosis of effector CD8+ T cells**. WT (IRF4flox) and IRF4KO^{CD8} (IRF4flox.E8Icre) mice were infected with LM-OVA and on day 5 sacrificed. Splenocytes of infected mice were surface stained with viability dye, anti-CD3, CD4, and CD8 antibody. CD8+ T cells were analyzed for their expression of FAS (CD95). (A) Exemplary histogram of FAS staining on WT (indicated in blue) and IRF4-deficient CD8+ T cells (indicated in red). (B) Frequency of FAS+ CD8+T cells in the indicated mouse strain. Cells were pre-gated on viable CD3+ CD4- CD8+ T cells. Results in (B) show the mean + SEM. Data show statistical significance with ***p<0.0001 (Student's t test).

death might be mediated via the FAS-FASL pathway.

In addition, analysis of the exposure of eat-me and find-me singals on the cell surface of effector CD8+ T cells in wild type (IRF4flox) and IRF4KO^{CD8} (IRF4flox.E8Icre) mice after bacterial infection was performed. To do so, mice were infected with Listeria and the splenic CD8+ T cells were analyzed for their expression of phosphatidylserine (PS) [145], which can be detected via Annexin V staining and further flow cytometry analysis [241]. Five days after infection, IRF4-deficient CD8+ T cells exposed significantly higher levels of PS on their cell surface, indicated by Annexin V staining, than IRF4-sufficient CD8+ T cells of infected WT mice. This result in shown in Figure 9.2 and indicates that in the absence of IRF4, effector CD8+ T cells are more susceptible to phagocytosis mediated by monocytes and macrophages, or granulocytes, due to increased exposure of eat-me signals on their cell surface.

The major task of the complement system is to defend against invading microorganisms. In addition, is facilitates the elimination of early apoptotic cells due the recruitment of phagocytes. Therefore, this analysis wanted to determine whether IRF4 deficiency leads to an activation of the complement cascade to support the apoptotic process of for the premature termination of the clonal expansion phase of effector C8+ T cells. A schematic overview of the complement pathway is illustrated in Figure 1.5. The activation of the complement system can be iniciated via three different pathways, all resulting in the formation of C3 and C5 convertase, inducing the terminal lytic pathway of the complement cascade. Different regulatory mechanisms and several molecules

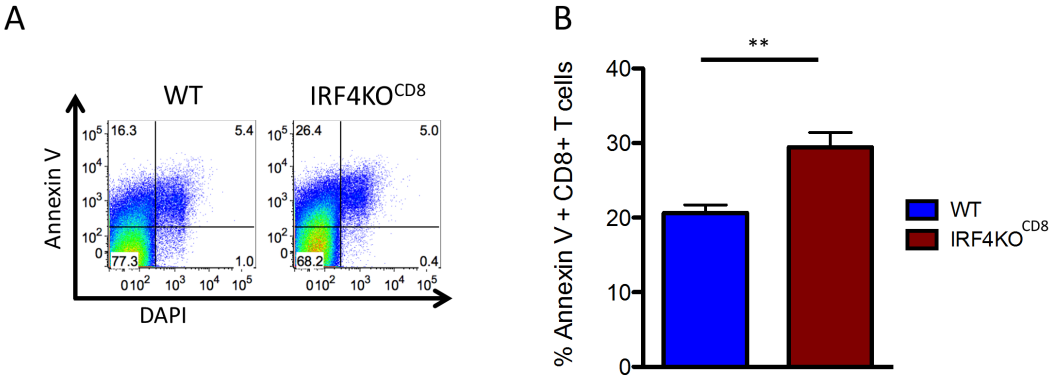

Figure 9.2: **IRF4 deficiency leads to increased phoshatidylserine (PS) exposure on CD8+ T cell surfaces.** WT (IRF4flox) and IRF4KO^{CD8} (IRF4flox.E8Icre) mice were infected with LM-OVA and on day 5 sacrificed. Splenocytes of infected mice were surface stained with viability dye, anti-CD3, CD4, and CD8 antibody. CD8+ T cells of both infected mice strains were analyzed for their exposure of phosphatidylserine (PS) on the cell surface via Annexin V staining. (A) Exemplary dot plots of Annexin V staining on the surface of WT and IRF4-deficient CD8+ T cells. Numbers in each quadrant indicate the frequency of cells being positiv or negative for the indicated marker. (B) Frequency of PS exposure on the cell surface of CD8+T cells according to their Annexin V staining. Wild type CD8+ T cells are shown in blue and IRF4-deficient CD8+ T cells in red. Cells were pre-gated on viable CD3+ CD4- CD8+ T cells. Data in (B) show the mean + SEM and are representative of two independent experiments with similar results. Data show statistical significance with **$p<0.001$ (Student's t test).

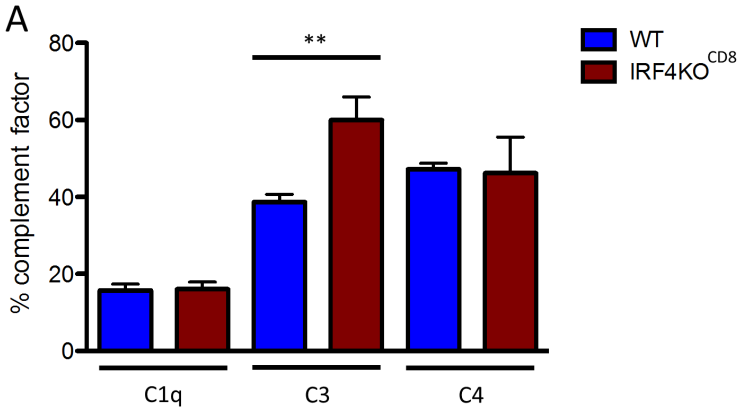

Figure 9.3: **Increased complement deposition of C3 examined on IRF4-deficient CD8+ T cells.** WT (IRF4flox) and IRF4KO^{CD8} (IRF4flox.E8Icre) mice were infected with LM-OVA. On day 5 after infection, splenic CD8+ T cells of infected mice were analyzed for complement factor deposition, such as C1q, C3 and C4. (A) Frequency of cells with deposition of the indicated complement factor in WT and IRF4-deficient CD8+ T cells. Wild type CD8+ T cells are shown in blue and IRF4-deficient CD8+ T cells in red. Cells were pre-gated on viable CD3+ CD4- CD8+ T cells. Graph shows the mean + SEM and data show statistical significance with **p<0.001 (Student's t test).

act together to induce the complement cascade triggering opsonisation and phagocytosis of the target cell.

Again, wild type (IRF4flox) and IRF4KO^{CD8} (IRF4flox.E8Icre) mice were infected with Listeria and the deposition of complement mediators on the cell surface of splenic CD8+ T cells were examined on day 5 after Listeria infection. First, the present analysis checked whether IRF4-deficiency in CD8+ T cells leads to an activation of the classical pathway of the complement system. Therefore, the C1q deposition was examinded, C1q being a subunit of the C1 component and leading to further cleavage processes and triggering of opsonization. On day 5 after infection, results could not find significant differences between both cell subsets (Figure 9.3 A). To determine the contribution of C4, its aviability on the cell surface was analyzed. Similar to C1q, present results could not detect significant differences between WT and IRF4-deficient CD8+ T cells of the complement protein C4. However, significant higher levels of C3 convertase could be detected in IRF4-deficient CD8+ T cells compared to their wild type counterparts analyzed via flow cytometry (Figure 9.3 A).

Results from flow cytometry analysis of this study give hints, that IRF4 deficiency in CD8+ T cells led to a deposition of C3 on the cell surface, which is a molecule being shared of all 3 pathways of the complement cascade. It initiates the terminal complement pathway, which induces the generation of anaphylatoxins and the assembly of the MAC.

It is very likely that CD8+ T cells cannot evade apoptotic pathways, if an engag-

ment of the death receptor FAS, an increased exposure of the eat-me signals, such as phosphatidylserine, and the deposition of complement factors occurred. All these mechanisms are indicators of early apoptotic cells, which lead to the recruitment of phagocytes and facilitate apoptotic cell recognition and uptake. This study therefore further analyzed the composition of the myeloid cell subsets in WT (IRF4flox) and IRF4KO^{CD8} (IRF4flox.E8Icre) mice in infected spleens. On day 5 after Listeria infection, frequencies of the DC and macrophage population were increase with over 2-fold in IRF4KO^{CD8} mice compared to WT mice. Furthermore, an increase of the monocyte subset could also be detected in infected spleens of IRF4KO mice on day 5 post infection. Moreover, for the granulocyte subset, an increase with over 4-fold could be detected in IRF4KO^{CD8} mice compared to their WT counterparts. These results suggest that IRF4-deficient CD8+ T cells might be more prone to cell death by phagocytes, as they showed an increase of markers, which identify apoptotic cells. Additionally, in increase recruitment of phagocytes could be detected, which facilitates the recognition and promote the clearance of the apoptotic cells.

9.2 IRF4-deficiency does not enhance the expression of inhibitory molecules

Several co-inhibitory receptors and molecules were described to be important in inhibiting T cell responses and promoting programmed cell death [14]. Therefore, quantification of inhibitory receptor expression was performed at an early time point (day 5) after primary Listeria encounter to search for an explanation for the huge impairment observed in functionality and differentiation of ag-specific CD8+ T cells. The expression of inhibitory molecules could be one reason for the drastic reduction of SI-specific CD8+ T cells detected already on day 5 after infection, when the peak of normal CD8+ T cell response is not yet achieved. To test this hypothesis, WT and IRF4KO^{CD8} mice were sacrificed on day 5 after Listeria infection and spleenocytes were processed to examine the expression of different inhibitory markers on ag-experienced CD8+ T cells. Flow cytometric analysis was performed to determine the expression of B cell lymphoma 2 (Bcl-2), 2B4 (CD244), programmed cell death 1 (PD-1), glycoprotein CD160, T cell immunoglobulin domain and mucin domain 3 (TIM3), lymphocyte activation gene 3 (LAG3), and cytotoxic T lymphocyte-associated protein 4 (CTLA4).

No difference in the expression of any of the analyzed inhibitory molecules could be detected in ag-unexperienced CD8+ T cells from WT or IRF4KO^{CD8} mice, as shown in Figure 9.5 in the upper row. Interestingly, ag-experienced IRF4-deficient CD8+ T cells and WT CD8+ T cells upregulated their expression of Tim3, 2B4, and LAG3 compared to ag-unexperienced T cells (Figure 9.5 lower row). Although, no difference could be detected between ag-experienced IRF4-deficient and IRF4-sufficient CD8+ T cells for the expression of 2B4 and LAG3 on day 5 after Listeria infection. But there was a slightly increase in the expression of Tim3 in ag-experienced IRF4-deficient CD8+ T cells compared to their WT counterparts (Figure 9.5 lower row). An increase in TIM3 expression on T cells has been shown to negatively regulate T cell activation and effector responses [95, 268]. Further analysis of the inhibitory molecules PD-1, CD160, and CTLA4 showed no increase in the expression level after ag-encounter on

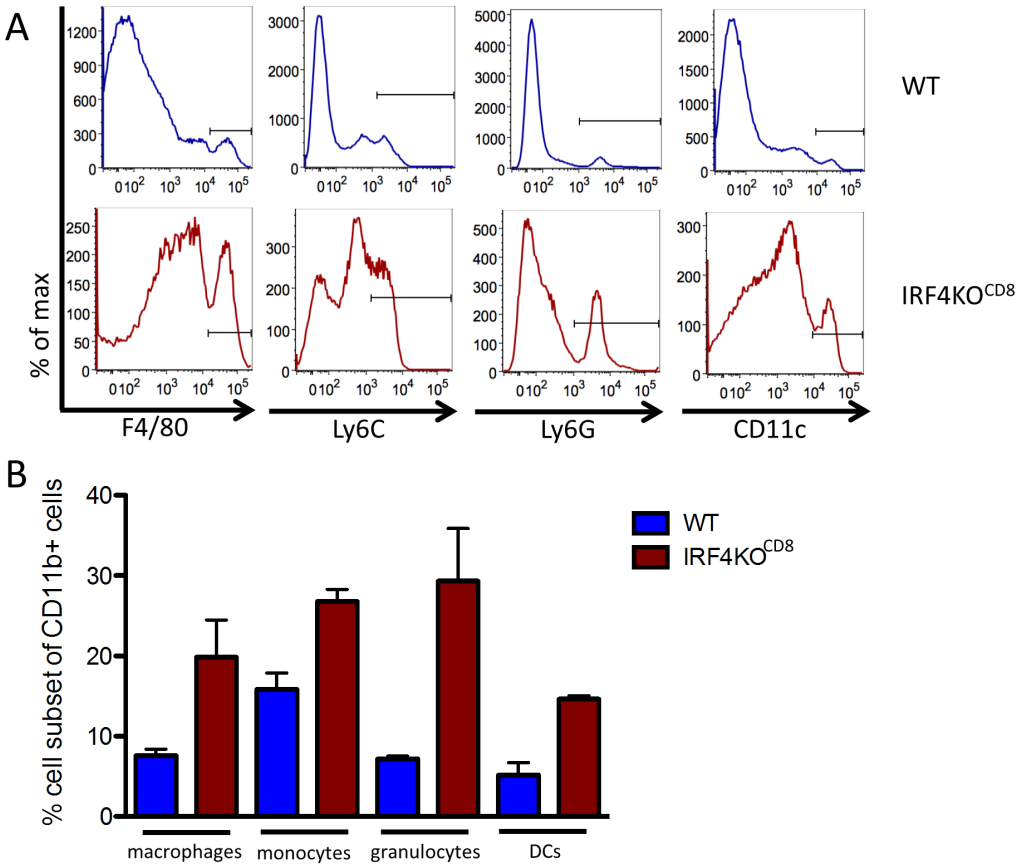

Figure 9.4: **Increased myeloid cell subsets in mice having IRF4-deficient CD8+ T cells on day 5 after infection.** WT (IRF4flox shown in blue) and IRF4KO^{CD8} (IRF4flox.E8Icre shown in red) mice were infected with LM-OVA. On day 5 after infection, spleens of infected mice were analyzed for their composition of myeloid cell subsets. First total cells were pre-gated on viable cells, additionally excluding lymhocytes (CD3+), B cells (CD19+), and natural killer cells (NK1.1+). Total myeloid cells were than identified based on their expression of CD11b and further separated into macrophages, monocytes, granulocytes and dendritic cells (DCs), dependent on their marker expression. (A) Exemplary histograms of macrophages (CD11b+ F4/80+), monocytes (CD11b+ Ly6C+), granulocytes (CD11b+ Ly6G+), and DCs (CD11b+ CD11c+). (B) Quantitative analysis of splenic macrophages (CD11b+ F4/80+), monocytes (CD11b+ Ly6C+), granulocytes (CD11b+ Ly6G+), and DCs (CD11b+ CD11c+). Data show 3 mice per group and graph shows the mean + SEM.

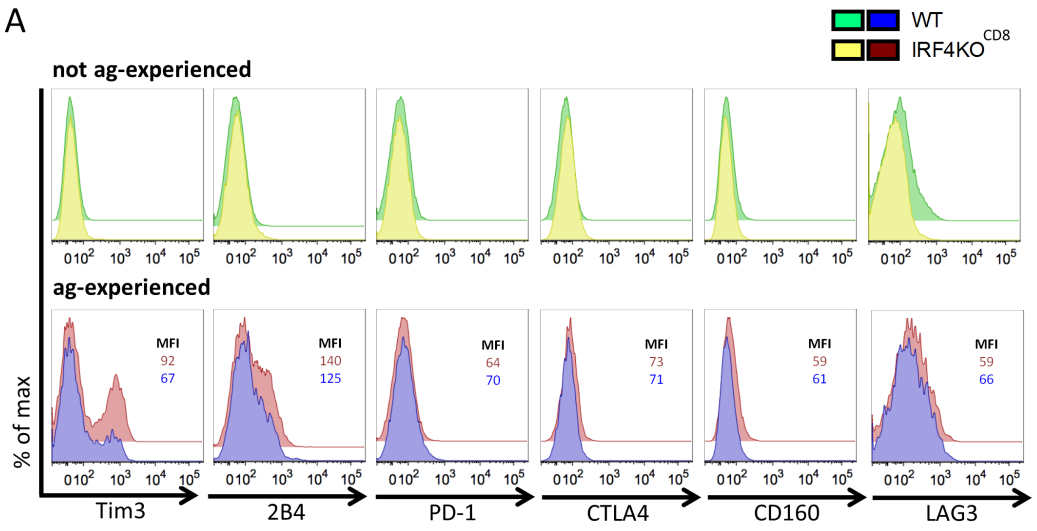

Figure 9.5: **No alteration in the expression of exhaustion markers in IRF4-deficient CD8+ T cells.** WT (IRF4flox) and IRF4KO (IRF4flox.E8Icre) mice were infected with LM-OVA and on day 5 sacrificed. Splenic CD8+ T cells of infected mice were analyzed for their expression of several inhibitory receptors and molecules, including B-cell lymphoma 2 (Bcl-2), 2B4 (CD244), programmed cell death 1 (PD-1), glycoprotein CD160, T-cell immunoglobulin domain and mucin domain 3 (Tim3), lymphocyte-activation gene 3 (LAG3), and cytotoxic T-lymphocyte-associated Protein 4 (CTLA4). (A) Exemplary overlaying histograms of Bcl-2, 2B4, PD-1, CD160, Tim3, LAG3 and CTLA4. Numbers in each histogram indicate the mean fluorescence intensity (MFI) values for the indicated marker. Antigen-experienced wild type (in blue) and IRF4-deficient CD8+ T cells (in red) were pre-gated for viable CD3+ CD4- CD8+ T cells. Not ag-experienced IRF4-deficient CD8+ T cells are shown in yellow and WT CD8+ T cells in green.

the CD8+ T cell subset of IRF4KO^{CD8} or WT mice compared to their control cells (not ag-experienced), neither any differences between both CD8+ T cell subsets from infected WT and IRF4KO^{CD8} mice. Taken together, IRF4-deficiency did not result in an increased expression of pro-apoptotic molecules on CD8+ T cells. These results suggest that the huge impairment in the quality and quantity of ag-speccific CD8+ T cells already early during the effector phase of the T cell response against invading pathogens is not due to enhanced exhaustion.

Chapter 10

IRF4 expression levels dictate the onset of CD8+ T cell contraction

10.1 Regulation of the IRF4 expression

To determine whether the levels and maintenance of IRF4 expression were affected by the strength of the TCR signaling, naïve OT1 TCR-transgenic CD8+ T cells were stimulated with three different affinity peptides, T4, Y3, and N4, leading to a weak, intermediate, or strong TCR stimulation, respectively. IRF4 expression levels were examined by intracellular staining. The stimulation with all three peptides induced IRF4 expression in OT1 cells and increased to similar MFI values after 24 hours of stimulation (Figure 10.1). Nevertheless, activation with the high-affinity OT1 TCR ligand peptide N4 maintained the IRF4 expression level high for several days, while OT1 T cells stimulated with the intermediate and low-affinity peptides (Y3 and T4) showed an affinity-dependent decline in the IRF4 expression already after 48 hours after stimulation. Nevertheless, also the expression of IRF4 via strong TCR signaling was only transient.

10.2 Strong TCR signaling and normal environment could not rescue IRF4-deficient CD8+ T cells

Represented results of this study show (in Chapter 8) that mice with IRF4-deficient CD8+ T cells generate drastic lower numbers of ag-specific effector cells after bacterial and viral infection compared to that of control mice. Therefore, the present analysis wanted to investigate whether strong TCR signals combined with a wild type environment might rescue the IRF4-deficient phenotype.

To test this, an adoptively transfer experimental setup based on OT1 TCR transgenic CD8+ T cells was performed, with CD8+ T cells expressing an H-2K^{b} OVA-specific T cell antigen receptor. Bacterial infections were performed with a recombinant *Listeria monocytogenes* strain expressing the high TCR affinity ovalbumin derived SIINFEKL epitope (N4). Thus, on day -1, purified naïve WT and IRF4-deficient OT1 cells, both cell subsets having a transgenic TCR for ovalbumin, were mixed in equal proportions and adoptively transferred i.v. into naïve wild type CD45.1 recipient mice that were infected with OVA expressing Listeria (LM-OVA) 24 hours later, illustrated in Figure 10.2 A. Of interest, transferred OT1 cells could be distinguished from endogenous CD8+ T cells via the congenic marker expression of CD45.1 and CD45.2 on T cells. Wild type OT1 cells being CD45.1- CD45.2+ CD90.1+ could be easily distinguish from

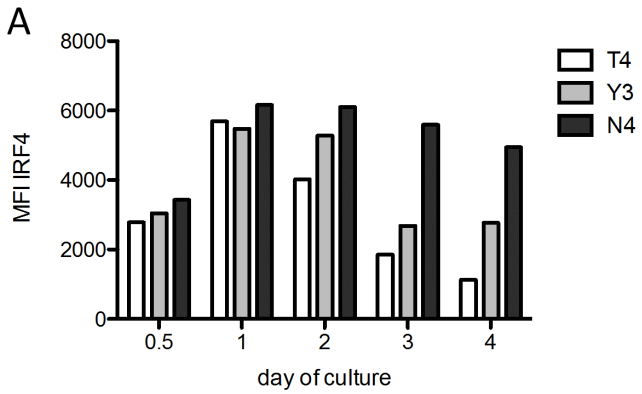

Figure 10.1: **Changes in the kinetic of the IRF4 expression is TCR strength-depend.** Ovalbumin-specific TCR-transgenic CD8+ T cells from untreated OT1 mice were naïve sorted (viable CD3+ CD4- CD44- CD62+) and invitro stimulated with SIINFEKL derived altered peptide ligands of Ovalbumin that vary in their potency to activate OT1 cells. (N4, Y3, and T4). IRF4 expression levels were determined at the indicated time points of invitro cultured from N4 (high affinity), Y3 (intermediate affinity), and T4 (low affinity) stimulated cells by intracellular staining via flow cytometry. (A) Frequencies of IRF4 expression in CD8+ T cells are shown. Data are representative of two independent experiments with similar results.

IRF4-deficient OT1 cells being CD45.1- CD45.2+ but CD90.1 negative.

The expansion of both transferred cell populations, each congenically different marked, was equal till day 3 after Listeria infection, as the ratio between both cell subsets maintained 1:1 (Figure 10.2 C), as initially transferred (Figure 10.2 B). Of note, from day 4 on, the proportion of IRF4-deficient OT1 cells in spleen was dramatically declined to almost not detectable levels on day 7 after infection. Present results speculated, that this drastic observed discrepancy might be due to different homing capacities, as IRF4-deficient CD8+ T cells did not clear the L-selectin molecule CD62L from their cell surface. But despite their maintained CD62L expression, IRF4-deficient CD8+ T cells were not found enriched in secondary lymphoid organs, like spleen and lymph nodes, and were detected in drastically lower numbers in the same organs as WT CD8+ T cells being $CD62L^{low}$. These results give the evidence that strong TCR signaling combined with a normal environment can not rescue IRF4-deficient CD8+ T cells. The results of this study suggest that IRF4-deficient CD8+ T cells have intrinsic defects, which could not be rescued via strong TCR signaling activation or wild type environment.

10.3 IRF4 deficiency impacts the kinetic of T cell expansion

Results, obtained in this study and also by other investigators [27, 86, 142, 162, 262], could show that IRF4 expression is induced in naïve CD8+ T cells after TCR ligand interaction (Section 8.1). Additionally, its expression kinetic and magnitude in CD8+ T cells is tightly linked to the strength of the TCR activation signal. Measurements performed in this study to analyze the IRF4 expression kinetic after stimulation with different affinity epitopes of ovalbumin (N4, Y3, T4) in transgenic CD8+ T cells (expressing an H-$2K^b$ OVA-specific TCR), are in agreement with recently published similar findings [163]. Therefore, this study wanted to examine whether IRF4 deficiency mimics low TCR signaling and therefore leads to a false translation of the strong TCR signaling, which actually induced the activation of the naïve CD8+ T cell. This has led us to ask if IRF4-deficient CD8+ T cells in the end just suffer the same fate as wild type CD8+ T cells, which has been activated via weak TCR ligand interaction. As it has been shown that low affinity activated CD8+ T cells display an earlier termination of the expansion phase [264]. Furthermore, Zehn and colloquies [264, 265] have demonstrated that those low affinity T cells go through fewer cell divisions or even disappear, and acquire reduced effector potential, as they acquire a more memory-like phenotype (KLRG1-) and being $CD62L^{high}$, a characteristic of central-memory T cells.

To test this hypothesis, naïve wild type OT1 and IRF4-deficient ($IRF4KO^{CD8}$) OT1 TCR transgenic CD8+ T cells were adoptively co-transferred into CD45.1 wild type recipient mice. One day later, recipient mice were i.v. infected with a recombinant *Listeria monocytogenes* strain expressing OVA protein, either containing the low affinity epitope SIITFEKL (T4) or the high affinity epitope SIINFEKL (N4). The low affinity peptide T4 leads to weak TCR engagement and the high affinity peptide N4 to strong TCR engagement. Of interest, transferred OT1 cells could be distinguished from endogenous CD8+ T cells via the congenic marker expression of CD45.1 and CD45.2 on T cells. Wild type OT1 cells being CD45.1- CD45.2+ CD90.1+ could be easily distinguish from IRF4-deficient OT1 cells being CD45.1- CD45.2+ without CD90.1 expres-

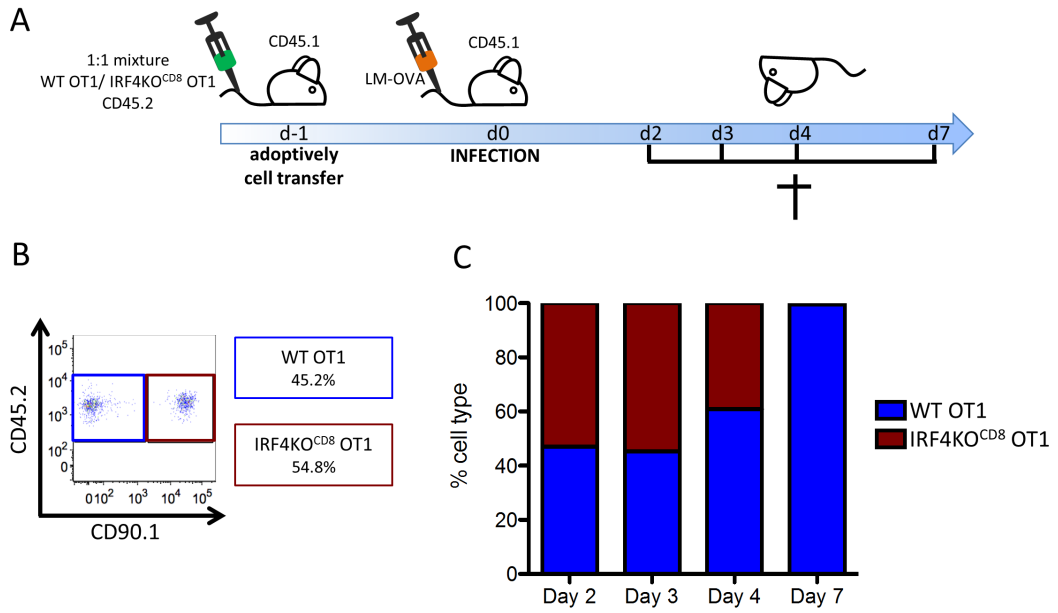

Figure 10.2: **Strong TCR signaling and normal environment could not rescue IRF4-deficient effector CD8+ T cells.** (A) Scheme of the experimental setup of the cell transfer experiment. On day -1, WT (CD45.2+ CD90.1+) and IRF4-deficient (CD45.2+ CD90.1-) OT1 cells were adoptively transferred with equally numbers into wild type CD45.1 recipient mice. One day later, recipient mice were infected with LM-OVA N4 and transferred cell subsets were analyzed on day 2, 3, 4 and 7 after infection. (B) Exemplary plot of the WT and IRF4-deficient OT1 mixture for the cell transfer. (C) The graph depicts the ratio of transferred WT (shown in blue) and IRF4-deficient CD8+ T cells (shown in red) in spleen on day 2, 3, 4, and 7 after infection. Transferred and endogenous CD8+ T cells were distinguished from each other via their congenic marker expression.

sion (Figure 10.3 A). On day 5 after infection, mice were sacrificed and the proportions of transferred WT OT1 and IRF4-deficient OT1 TCR transgenic CD8+ T cells from spleen of recipient mice were analyzed. Not surprisingly, in recipient mice, which have been infected with LM-OVA expressing the high affinity TCR epitope N4 (SIINFEKL), the majority of transferred OT1 cells consists of WT OT1 cells (Figure 10.3 A upper row). In contrast, IRF4-deficient OT1 cells were greatly outnumbered, as they represented just one quarter of the transferred cell population (Figure 10.3 A, lower row). These results are in agreement with the present results in Section 10.2 of this study showing that IRF4-deficient OT1 cells initially proliferate after LM-OVA N4 infection but already drastic decline in numbers from day 4 on after infection. Of great interest, in recipient mice, which have been infected with LM-OVA expressing the low affinity TCR epitope T4 (SIITFEKL), both transferred cell populations expanded equally, as the ratio between both cell subsets maintained 1:1, as initially transferred (Figure 10.3 A, lower row).

As already indicated by the approximately 1:4 ratio of transferred WT OT1 cells to IRF4-deficient OT1 cells from spleen of recipient mice, which have been infected with LM-OVA N4, determination of the total numbers of transferred OT1 cells per 10.000 endogenous CD8+ T cells revealed drastically reduced numbers of IRF4-deficient OT1 cells compared to WT OT1 cells with up to 5-fold differences (Figure 10.3 B). This result suggests that IRF4-deficient OT1 cells could not translate the strong activating TCR signal into an appropriate developmental and transcriptional program, as the WT OT1 cells did, which formed a proper population after strong TCR engagement.

Additionally, analysis of the total numbers of transferred OT1 cells from spleen of recipient mice was performed, which have been infected with the LM-OVA T4, inducing an activation via weak TCR signaling. On day 5 after transfer, very similar numbers of WT and IRF4-deficient OT1 cells per 10.000 endogenous CD8+ T cells were detected in spleens of recipient mice (Figure 10.3 B). This was not surprising, as this equal distribution was already indicated by the maintained 1:1 ratio of the transferred OT1 cells from spleen of recipient mice, which were observed after LM-OVA T4 infection.

Of great interest, determination of the total numbers of transferred OT1 cells populations per 10.000 endogenous CD8+ T cells revealed very similar numbers comparing the numbers of IRF4-deficient OT1 cells from recipient mice, which have been infected with LM-OVA N4, and WT or IRF4-deficient OT1 cells from recipient mice, which have been infected with LM-OVA T4. These results suggest that the differentiation and expansion of the IRF4-deficient OT1 cells were similar to WT OT1 cells, which have been activated via low TCR engagement. Therefore, these results strongly suggest that IRF4-deficiency mimics weak TCR signaling, independent of the actually signaling strength, leading to a developmental and transcriptional program very similar to the one being initiated in WT CD8+ T cells, which have been activated via weak TCR signaling.

Present analysis further examined whether both transferred cell populations show the same increased susceptibility to death when the activation was induced via weak TCR engagement. As in fact, weak TCR signaling activation in wild type T cells has been shown to result in an earlier termination of the clonal expansion and an earlier onset of contraction [264]. This study therefore suggest that IRF4 deficiency translates any TCR signal into a weak TCR activation signal, which in turn triggers the premature onset of contraction due to initiation of death and phagocytosis of those cells. In line

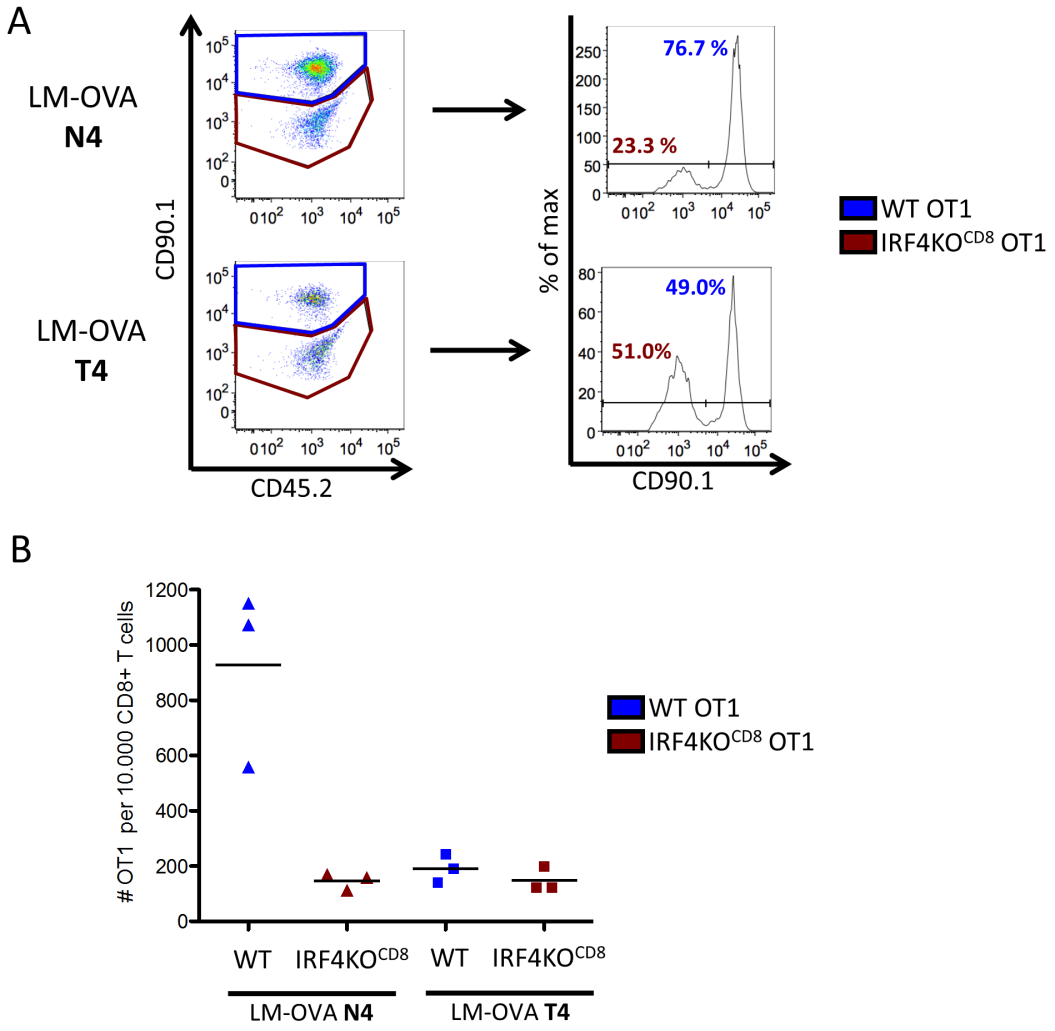

Figure 10.3: **IRF4 deficiency impacts the CD8+ T cell fate decision.** Wild type OT1 and IRF4-deficient OT1 TCR transgenic CD8+ T cells were adoptively co-transferred into CD45.1 wild type recipient mice. One day later, recipient mice were i.v. infected with a recombinant *Listeria monocytogenes* strain expressing OVA protein, either containing the low affinity epitope SIITFEKL (T4) or the high affinity epitope SIINFEKL (N4). On day 5 after infection, mice were sacrificed and the proportions of transferred WT OT1 and IRF4-deficient OT1 TCR transgenic CD8+ T cells from spleens of recipient mice were analyzed. Cells were distinguished, from each other and endogenous CD8+ T cells, via their congenic marker expression. (A) Exemplary plots (left) show CD90.1 and CD45.2 staining of transferred WT OT1 (shown in blue) and IRF4-deficient OT1 cells (shown in red). Histograms display the ratio of transferred OT1 cells and numbers indicate the frequencies of WT OT1 (shown in blue) and IRF4-deficient OT1 cells (shown in red). (B) Total cell numbers of transferred WT and IRF4-deficient OT1 cells per 10.000 endogenous CD8+ T cells. Each symbol in (B) represents an individual mouse and small horizontal lines indicate the average.

with this hypothesis, presented previous data of this study already have been shown that IRF4-deficient CD8+ T cells suffer from several apoptotic inducing pathways, leading to programmed cell death or clearance via phagocytosis, on day 5 after infection of IRF4KO^{CD8} mice. Thus, the present study analyzed the surface expression of the anti-apoptotic molecule Bcl-2, the death receptor expression of FAS, and the exposure of phosphatidylserine on the cell surface, which act as an eat-me signal for phagocytic cells, on both transferred cell populations.

Indeed, as shown in Figure 10.3 A, WT OT1 cells, which have been activated via strong TCR engagement (N4) expressed high levels of Bcl-2 on their cell surface (line in dark blue). In contrast, IRF4-deficient OT1 cells (shown in orange), as well as WT OT1 cells (shown in light blue), which have been activated via weak TCR ligand interaction by T4, similarly expressed much lower levels of the Bcl-2 molecule, which has been shown to prevent cells to undergo cell death [80, 144]. Additionally, the expose of phosphatidylserine (PS) on the cell surface of both transferred cell populations was analyzed. Surprisingly, WT OT1 cells (shown as light blue line) and IRF4-deficient OT1 cells (shown in orange), which have been activated by low affinity peptide T4, exposed similarly high levels of PS on their cell surface, as determined by the Annexin V staining on day 5 after LM-OVA T4 infection (Figure 10.3 B). Analysis of the frequency of Annexin V positiv WT OT1 (shown in blue) and IRF4-deficient (shown in red) OT1 cells, which have been activated via low TCR signaling, showed similar frequencies of CD8+ T cells, which showed a increased PS exposure on their cell surface, as indicated via Annexin V staining (Figure 10.3 C). This indicates that both cell types are highly endangered by recognition and uptake by phagocytes. In contrast, WT OT1 cells, which have been primed via the high affinity epitope N4 exposed almost none PS on their surface, as shown by the low Annexin V staining in Figure 10.3 A (as dark blue line).

Furthermore, measurements of the FAS expression levels on the cell surface of WT OT1 and IRF4-deficient OT1 cells were performed, which have been primed via low affinity epitope T4 (Figure 10.3 D). Interestingly, both cell subsets activated via weak TCR engagement, displayed very high death receptor expression (Figure 10.3 E), which led to higher susceptibility to programmed cell death, mediated via caspase activation.

In sum, these results give evidence that IRF4 deficiency mimics low affinity and weak TCR engagement, which in turn leads to a premature termination of the expansion phase and a drastically decrease of the effector cell subset. Furthermore, these results show that IRF4 deficiency initiates, independent of the strength of the TCR ligand interaction, an early contraction of the effector CD8+ T cell population, similar to the fate that occurs to weak TCR signaling activated wild type CD8+ T cells. Interestingly, present results could show that IRF4-deficient CD8+ T cells, similar to weak TCR signaling activated wild type CD8+ T cells, are efficiently eliminated via the activation of multiple death inducing pathways.

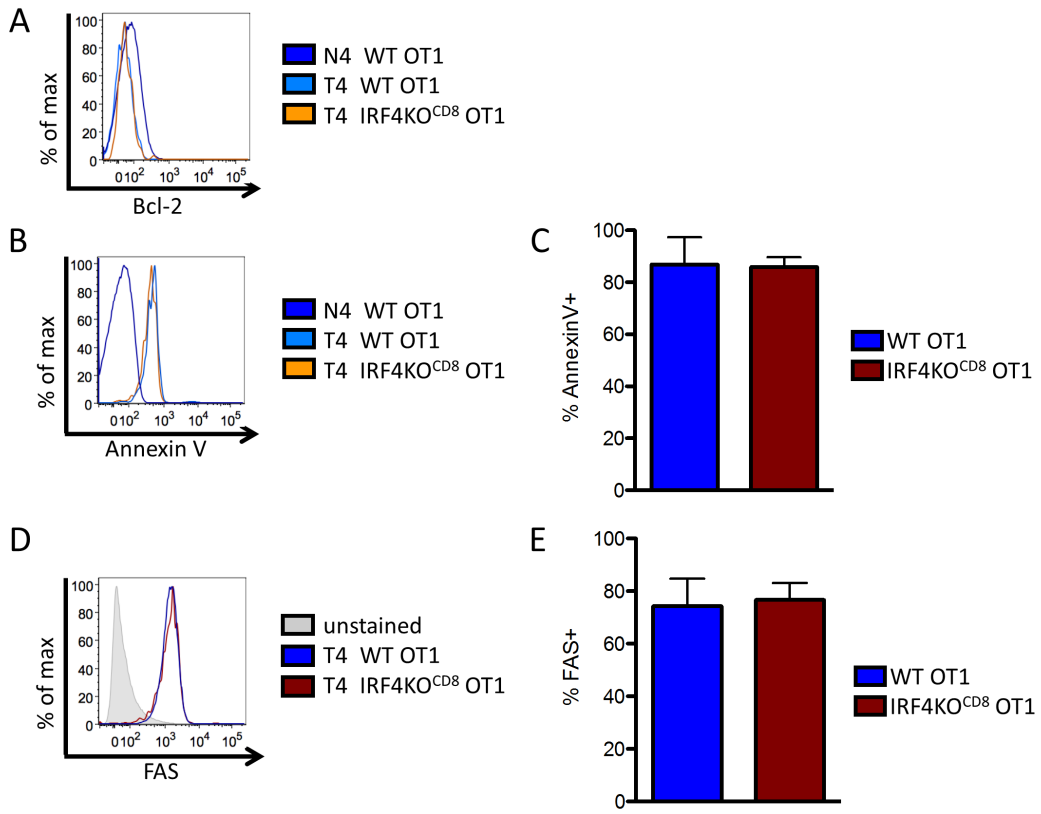

Figure 10.4: **IRF4 deficiency mimics weak TCR activation signaling.** Wild type OT1 and IRF4-deficient OT1 TCR transgenic CD8+ T cells were adoptively co-transferred into CD45.1 wild type recipient mice. One day later, recipient mice were i.v. infected with a recombinant *Listeria monocytogenes* strain expressing OVA protein, either containing the low affinity epitope SIITFEKL (T4) or the high affinity epitope SIINFEKL (N4). On day 5 after infection, mice were sacrificed and the proportions of transferred WT OT1 and IRF4-deficient OT1 TCR transgenic CD8+ T cells from spleens of recipient mice were further analyzed. Cells were distinguished, from each other and endogenous CD8+ T cells, via their congenic marker expression. Transferred cell polulations were analyzed for their Bcl-2 and FAS expression, and for their exposure of phosphatidylserine (PS) via Annexin V staining. (A) Exemplary overlaying histogram of the Bcl-2 expression on transferred OT1 cells of the indicated cell subset. (B) Exemplary overlaying histogram of Annexin V staining on the cell surface of transferred OT1 cells of the indicated cell subset, representing PS exposure on the cell surface. (C) Frequency of PS exposure on OT1 cells of the indicated cell subset, according to their Annexin V staining. (D) Exemplary overlaying histogram of the FAS expression on transferrred OT1 cells of the indicated cell subset. (E) Frequency of FAS expression on OT1 cells of the indicated cell subset. Cell subsets in (A), (B), and (D) represent LM-OVA N4 activated WT OT1 cells in dark blue, LM-OVA T4 activated WT OT1 cells in light blue and LM-OVA N4 IRF4-deficient OT1 cells in orange. Cell subsets in (C) and (E) represent LM-OVA N4 activated WT OT1 cells in red and IRF4-deficient OT1 cells in blue. Graph show the mean + SEM.

Chapter 11

Cytokines impact the IRF4-deficient CD8+ T cell phenotype

11.1 The influence of interleukins on IRF4-deficient CD8+ T cells

It is well known, environmental factors, such as cytokines and chemokines, are important for CD8+ T cell proliferation and differentiation. Furthermore, cytokines like IL2 and IL12 have an impact on the differentiation and longevity of CD8+ T cells [253, 257]. Several publication have shown the influence of IL7 and IL15 to maintain T cell homeostasis [64, 238]. Recent results of this studies showed, IRF4 deficiency led to diminished expansion and to reduced viability of effector CD8+ T cells, starting around day 4 after primary bacteria encounter (Figure 10.2). As IRF4-deficient CD8+ T cells could not be rescued *in vivo*, neither via strong TCR signaling activation nor due to a wild type environment (Section 10.2), the question raised whether *ex vivo* cytokine supply could support IRF4-deficient CD8+ T cells to overcome their proliferation problems and the increased susceptibility to cell death.

To determine whether IRF4-deficient CD8+ T cells can be rescued when such environmental factors are available, an *ex vivo* culture of *in vivo* primed OT1 cells were performed. Cells were treated with different cytokines (listed in Table 5.12). Purified naïve WT and IRF4-deficient OT1 cells (Section 6.9), both cell subsets having a transgenic TCR for ovalbumin, were mixed in equal proportions and adoptively transferred i.v. into naïve wild type CD45.1 recipient mice one day prior infection. Recipient mice were infected with a recombinant *Listeria monocytogenes* strain expressing ovalbumin derived SIINFEKL epitope N4 (illustrated in Figure 10.2 A). On day 4 after LM-OVA infection, both transferred OT1 cell subsets were re-isolated, according to their congenic marker expression, from infected spleens of recipient mice, and further cultivated under different cytokine conditions.

In detail, transferred OT1 cells (CD45.2+) could be distinguished from endogenous CD8+ T cells (CD45.1+) via the congenic marker expression of CD45.1 and CD45.2 on T cells. Wild type OT1 cells being CD45.1- CD45.2+ CD90.1+ could be easily distinguish from IRF4-deficient OT1 cells being CD45.1- CD45.2+ but CD90.1 negative. To monitor cell proliferation, cells were prior labeled with Proliferation Dye V450 (Section 5.10). From the start of the culture, the dye was equally distributed between the daugther cells, as with each further cell division a successive halving the fluorescent dye occurred. Cells were cultured in supplemented RPMI medium with either IL2 (20U), IL7, IL12, or IL15.

As shown in Figure 11.1 the division profile between wild type and IRF4-deficient OT1 cells altered between different cytokine conditions, on day 3 of *ex vivo* culture. Almost in all treatments, wild type OT1 cells compared to IRF4-deficient CD8+ T cells showed a higher overall proliferation rate, being highest with IL2 treatment and lowest with IL12, indicated by the reduction of the proliferation dye. Further analysis of the frequency of cell clones, which showed high proliferation (indicated with orange) additionally observed highest frequencies of WT and IRF4-deficient CD8+ T cells with IL2 treatment. Although, treatment with IL12 showed highest frequencies for intermediate proliferating clones. Nonetheless, IL12 treatment induced the lowest proliferation of both cell subsets, as the comparison of the frequencies of not proliferating cells was highest with IL12 treatment.

Similar to WT OT1 cells, IRF4-deficient OT1 cells showed the highest proliferative capacity when the medium was supplemented with IL2 and the lowest proliferation capacity with IL12 treatment. However, IRF4-deficient OT1 cells proliferated more than WT when treated with IL15. Nevertheless, the highest increase in the proliferative capacity after 3 days of *ex vivo* cultivation could be observed in both cell types with IL2 supplemented medium. These results indicate that the proliferative capacity of *in vivo* primed IRF4-deficient CD8+ T cells can be influenced by cytokine treatment, while IL2 had the highest impact on the proliferative capacity and survival.

Previous results in this study indicated a drastically increase in the proliferative capacity of *in vivo* primed IRF4-deficient OT1 cells when they were further *ex vivo* cultivated with IL2, as shown in Chapter 11. Therefore, this study wanted to investigate whether high IL2 concentration leads in turn to a further increase in the proliferative capacity of IRF4-deficient CD8+ T cells and may rescue the IRF4-deficient phenotype. To determine whether the enhancement of the proliferative capacity is IL2 concentration dependent, a similar experiment was performed, as described previously in Chapter 11. On day 4 after LM-OVA infection, transferred WT and IRF4-deficient OT1 cells were re-isolated to perform an *ex vivo* culture under different IL2 concentrations, ranging from 0 - 50U. As shown in Figure 11.2 A, the proliferation rate of WT OT1 cells could be increased due to *ex vivo* IL2 treatment of the cells in a concentration dependent manner. Of interest, the proliferative capacity of IRF4-deficient OT1 cells increased similarly IL2 concentration dependent but not with the same intensity. Although IRF4-deficient OT1 cells proliferated much better in the presents of high IL2 concentrations, they could not reach the same proliferative capacity like WT OT1 cells (Figure 11.2 B). These results show that *ex vivo* treatment with high IL2 concentrations can partially rescue the diminished proliferative capacity of IRF4-deficient CD8+ T cells. Furthermore, they imply a special role for soluble factors like IL2 that promote T cell survival and proliferation.

As mentioned earlier in Chapter 7, IRF4 deletion in matured CD8+ T cells leads to the expression of eGFP after CRE-mediated recombination. Naive IRF4-deficient CD8+ T cells from IRF4flox.E8Icre (IRF4KO^{CD8}) and OT1.IRF4flox.E8Icre (OT1.IRF4KO^{CD8}) mice were always FACS sorted according to their surface marker expression (CD3+ CD4- CD8+ CD44- CD62L+) and their eGFP expression. Of interest, results could observe that under certain circumstances, some of the eGFP+ IRF4-deficient OT1 cells loose their eGFP expression under stressful conditions, such as bacterial encounter during infection or low cytokine supply (Figure 11.2 C/D). The examined successively disap-

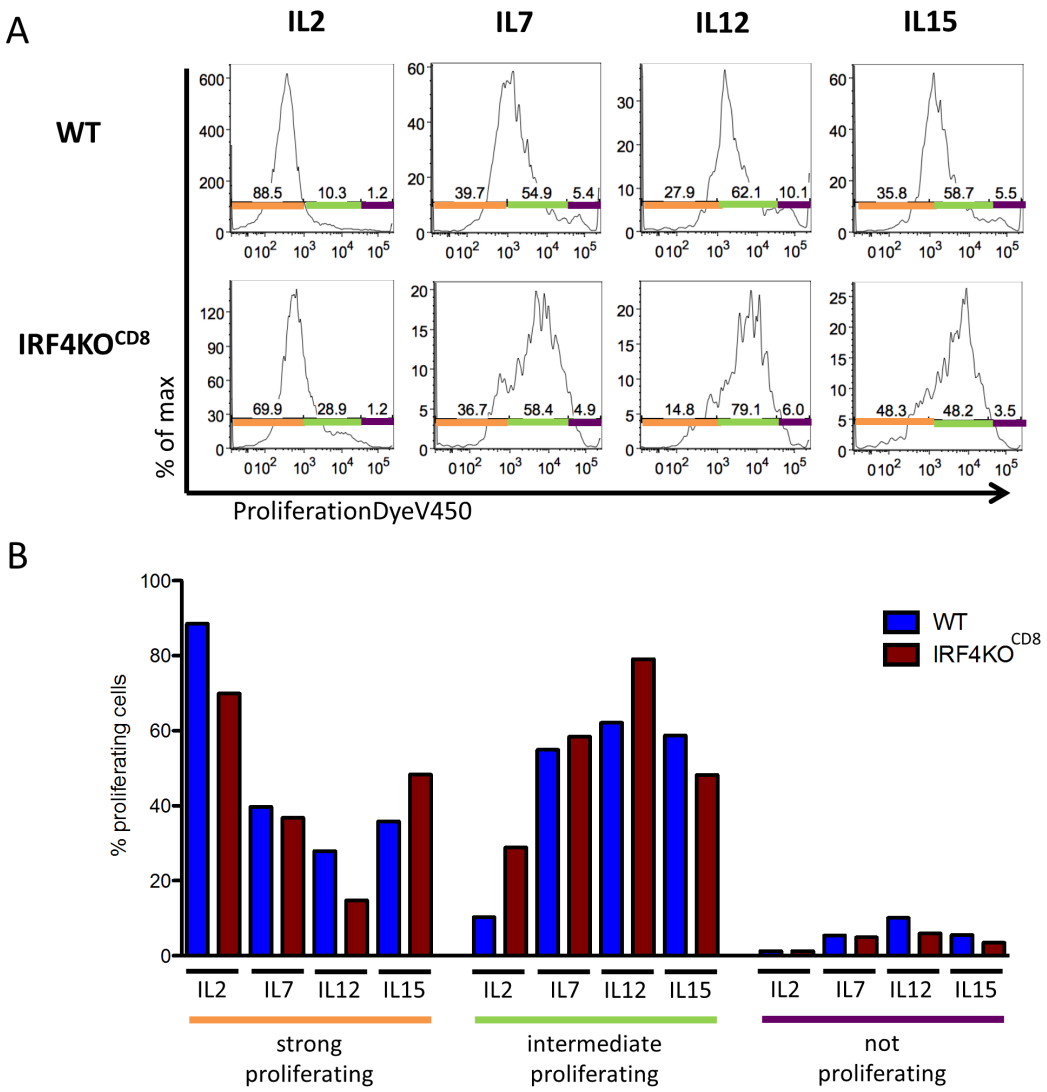

Figure 11.1: ***Ex vivo* cytokine treatment influences the proliferation of *in vivo* primed IRF4-deficient CD8+ T cells.** Wild type (CD45.2+ CD90.1+) and IRF4-deficient (CD45.2+ CD90.1-) OT1 cells were adoptively transferred with equal numbers into wild type CD45.1 recipient mice. One day later, recipient mice were infected with LM-OVA and transferred OT1 cell subsets were re-isolated on day 4 after Listeria infection. Purified OT1 cells were further *ex vivo* cultured with different cytokines, such as IL2, IL7, IL12, and IL15. (A) Exemplary histograms of the proliferation dye dilution due to cell divisions on the cell surface of either WT (upper row) or IRF4-deficient (lower row) OT1 cells. Cells in the histrograms are divided into 3 groups, namely strong proliferating cells (indicated with orange), intermediate proliferating cells (indicated with green), and not proliferating cells (indicated in violet). (B) The graph depicts the percentage of the 3 different groups depending on their proliferation rate of cells, identified by reduced proliferation dye labeling, which were treated with the indicated cytokine. WT OT1 cells are shown in blue and IRF4-deficient CD8+ T cells in red.

pearance of the eGFP expression correlated with the proliferative behavior of the cells. Results observed an upregulation of eGFP expression in proliferating cells. When further cultivation without IL2 supplementation occurred, in vivo primed IRF4-deficient OT1 cells proliferated very poorly and almost all showed no eGFP expression anymore after 3 days of *ex vivo* culture. In contrast, treatment with low or intermediated IL2 concentrations led to a separation into eGFP expressing and non-expression cells (Figure 11.2 C). The ratio of eGFP+ and eGFP- cells was strongly influenced by the IL2 concentration, as higher IL2 concentrations resulted in higher frequencies of eGFP expressing IRF4-deficient OT1 cells (Figure 11.2 D).

Present results observed that *ex vivo* cultured IRF4-deficient OT1 T cells can be partially rescued via treatment with high IL2 concentrations but nevertheless cytokine treatment was not able to completely overcome the intrinsic problems of IRF4-deficient effector CD8+ T cells.

Interestingly, during the CD8+ T cell expansion phase IRF4-deficient CD8+ T cells showed decreased expression of the IL-2Rβ (CD122) compared to their WT counterparts. This is shown in Figure 11.3. That might be a reason why IRF4-deficient CD8+ T cells can just partially be rescued by addition of IL2, because IL2 signaling is diminished due to less receptor expression on the cell surface of ag-specific CD8+ T cells in the absence of IRF4.

11.2 The impact of IL2 treatment during *in vitro* priming for the IRF4-deficient CD8+ T cells

Although, recent data claimed that IRF4-deficient CD8+ T cells could not be rescued by addition of high amounts of IL2 (*in vitro*) [188], presented results of this study observed that *ex vivo* cultured IRF4-deficient CD8+ T cells, could be partially rescued via treatment with high amounts of recombinant IL2. Several publications demonstrated that, in general, IL2 signaling promotes the generation of effector cells and longevity. Therefore the question raised whether the IRF4-deficient phenotype of CD8+ T cells, which was detected early during immune response during the premature clonal expansion phase, could be altered or even rescued due to a priming of those cells in the presents of high IL2 amounts. Adoptive transfer experiments of *in vitro* primed OT1 cells were performed to test this hypothesis. A scheme of the experimental setup is shown in Figure 11.4.

Naive sorted (viable, CD3+ CD4- CD8+ CD44- CD62L+) WT and IRF4-deficient (eGFP+) OT1 cells, isolated from spleen and lymph nodes from untreated mice, were *in vitro* primed with anti-CD3 and the co-stimulatory molecule anti-CD28. To monitor cell proliferation, cells were prior labeled with ProliferationDyeV450 (Section 5.10). From the start of the culture, the dye was equally distributed between the daugther cells, as with each further cell division a successive halving the fluorescent dye occurred. Cells were cultured separately in supplemented RPMI medium with additional IL2 supply in different concentrations (1U, 10U, and 50U).

After *in vitro* culture for 4 days, WT and IRF4-deficient OT1 cells were first analyzed for their proliferation rate (Figure 11.5 A). WT OT1 cells and IRF4-deficient OT1 cells proliferated nicely with 10U and 50U IL2 supplement, as indicated by the dilution of the

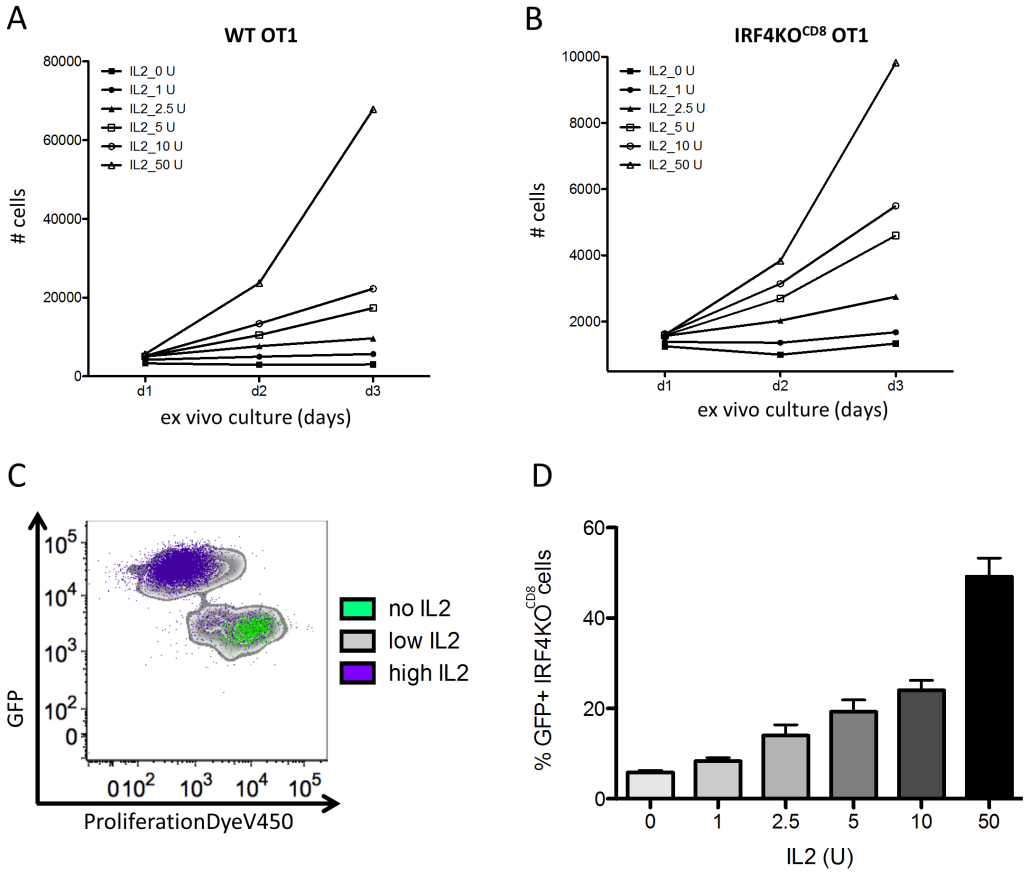

Figure 11.2: ***Ex vivo* IL2 treatment alters the proliferation capacity of CD8+ T cells concentration dependent.** Wild type (CD45.2+ CD90.1+) and IRF4-deficient (CD45.2+ CD90.1-) OT1 cells were adoptively transferred with equal numbers into wild type CD45.1 recipient mice. One day later, recipient mice were infected with LM-OVA and transferred OT1 cell subsets were re-isolated on day 4 after Listeria infection. Purified OT1 cells were further *ex vivo* cultured with different IL2 concentrations (ranging from 0 - 50U). (A) Graph shows the numbers of WT OT1 cells cultivated with different IL2 concentrations on day 1, 2, and 3 after *ex vivo* culture. (B) Graph shows the numbers of IRF4-deficient OT1 cells cultivated with different IL2 concentrations on day 1, 2, and 3 after *ex vivo* culture .
(C) Exemplary dot plot of IRF4-deficient OT1 cells *ex vivo* cultivated for 3 days with different IL2 concentrations. No IL2 supply is shown in green, while the administration of 2.5U IL2 is shown in gray and 50U in violet. (D) Graph show the percentage of IRF4-deficient OT1 cells expressing eGFP dependent on the IL2 concentration, which was supplied.

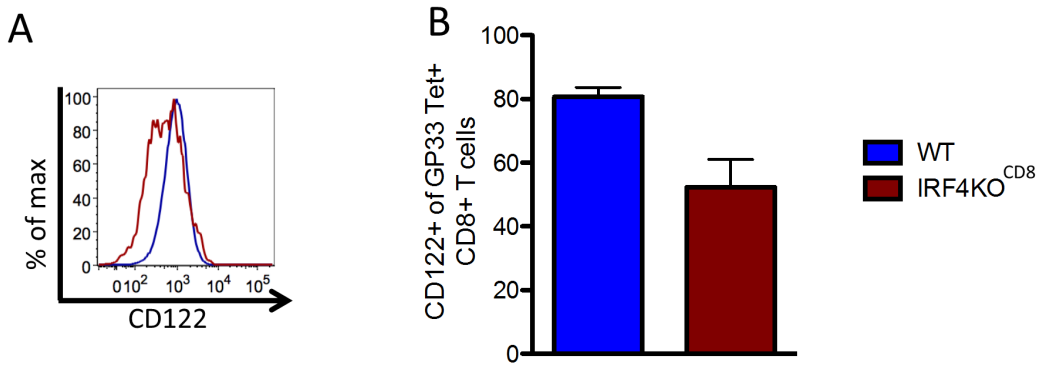

Figure 11.3: **IRF4 deficiency alters the expression of CD122 on ag-specific CD8+ T cells.** Wild type (WT) and IRF4KO^{CD8} mice were infected with lymphocytic choriomeningitis virus (LCMV) Armstrong. Splenocytes were surface stained with viability dye, anti-CD3, CD4, and CD8 antibody. Splenic GP33-specific CD8+ T cells were analyzed via tetramer staining on day 8 after LCMV Armstrong infection. (A) Exemplary overlaying histogram of the CD122 expression on splenic GP33-specific WT and IRF4-deficient CD8+ T cells. (B) Graph shows the percentages of CD122 expressing GP33-specific CD8+ T cells of the indicated mouse strain. Graph in (B) shows the mean + SEM. WT CD8+ T cells are indicated in blue and IRF4-deficient CD8+ T cells are indicated in red. Data are representative of two independent experiments with similar results (4-5 mice per group). Data show statistical significance with *p<0.05 (Student's t test).

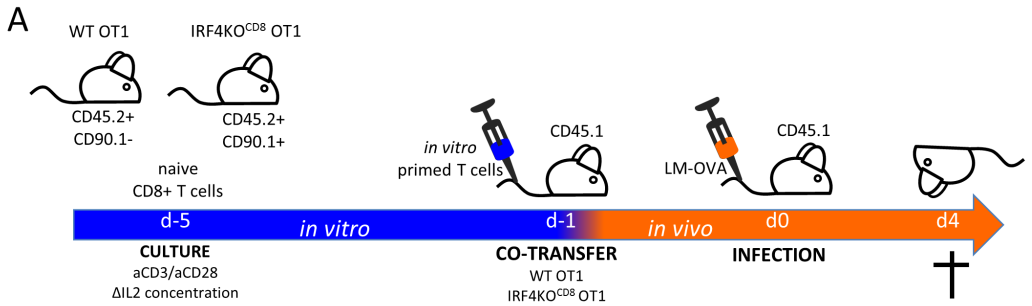

Figure 11.4: **Scheme of a co-transfer experiment of *in vitro* primed OT1 cells.** Naive sorted (viable, CD3+ CD4- CD8+ CD44- CD62L+) WT and IRF4-deficient (eGFP+) OT1 cells isolated from spleen and lymph nodes from untreated mice were *in vitro* primed with anti-CD3/anti-CD28 with different amounts of IL2. On day 4 after culture, WT (CD45.2+ CD90.1-) and IRF4-deficient (CD45.2+ CD90.1+) OT1 cells primed under the same condition were equally mixed and adoptively co-transferred into WT (CD45.1+) recipient mice, which was subsequently infected with LM-OVA. On day 4 after infection, mice were sacrificed and organs were analyzed for their proportions of transferred OT1 cells.

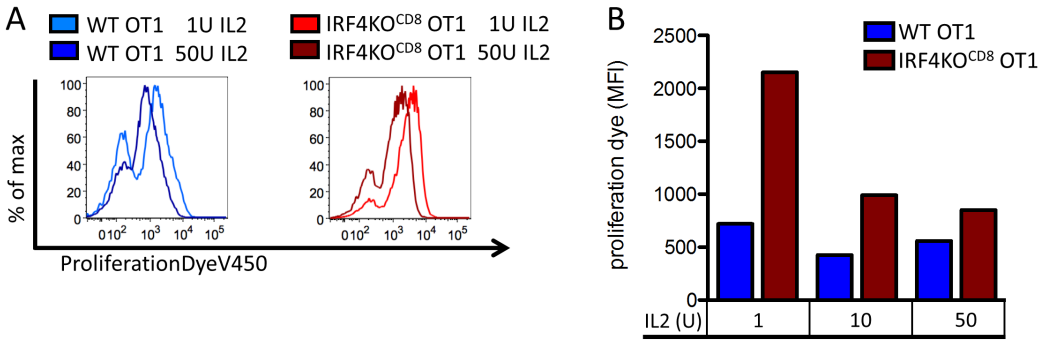

Figure 11.5: **Increased proliferation rate of IRF4-deficient CD8+ T cells by addition of high amounts of IL2.** Naive sorted (viable CD3- CD4- CD8+ CD44- CD62L+) wild type and IRF4-deficient (additionally GFP+) OT1 cells were stimulated with aCD3/aCD28 in medium, which was supplemented with different IL2 concentrations. Before cell culture, cells were stained with Proliferation DyeV450 to monitor cell division. (A) Exemplary histograms of the proliferation dye dilution due to cell divisions on the cell surface of either WT (shown in blue) or IRF4-deficient (shown in red) OT1 cells cultured for 4 days with different IL2 amounts as indicated. (B) Graph depicts the mean fluorescence intensity (MFI) values of the proliferation dye of WT and IRF4-deficient OT1 cells cultured for 4 days with different IL2 amounts as indicated.

proliferation dye. As expected, the proliferation rate of both cell subsets was strongly IL2 concentration dependent, as high amounts of IL2 increased the proliferative capacity and low IL2 concentration led to diminished expansion (Figure 11.5 B). This impaired proliferation capacity was drastic in IRF4-deficient CD8+ T cells, which proliferated very poorly under this condition. An addition of high amounts of IL2 (50U) led to a similar proliferation rate of IRF4-deficient OT1 cells and their WT counterparts, almost showing the same dilution of the proliferation dye after 4 days of *in vitro* culture.

Harvested cells were washed and both OT1 cell populations, which were primed with the same amount of IL2 were equally mixed Figure 11.6 A/B. Afterwards, this congenically marked WT (CD45.2+ CD90.1-) and IRF4-deficient (CD45.2+ CD90.1+) OT1 cell mixtures were co-transferred into WT (CD45.1+) recipient mice, which was subsequently infected with LM-OVA. After antoher 4 days, infected mice were harvested and spleen, lymph nodes, blood and liver were analyzed for the proportions of transferred OT1 cells.

Substantially greater proportions of WT OT1 cells relative to the proportion of IRF4-deficient OT1 cells were observed in spleen, lymph nodes, blood, and liver, as shown in Figure 11.7 A-D. This trend was observed in all organs tested and for all IL2 priming conditions. The priming with different IL2 amounts did not led to an increased proportion of WT OT1 cells in spleen and lymph nodes. However, analysis of the WT proportion in blood and liver revealed significantly increased proportion of WT OT1 cells, which were primed with 50U IL2 compared to low IL2 (1U) addition. This was also observed

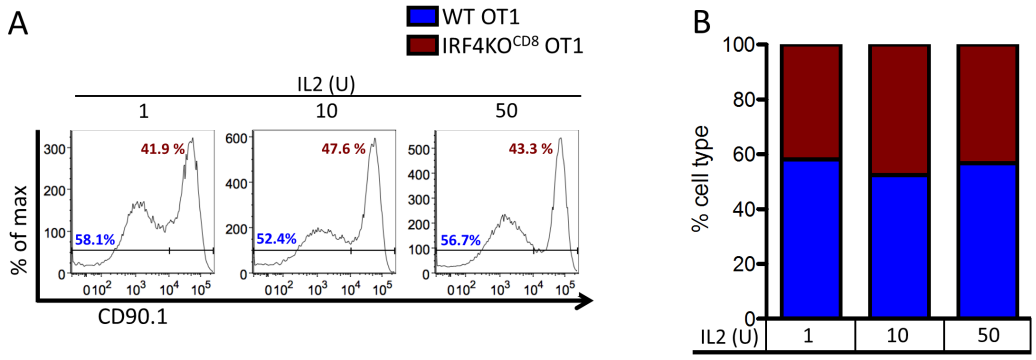

Figure 11.6: **Co-transfer of equally distributed IRF4-deficient and WT OT1 cells after *in vitro* priming with IL2.** WT and IRF4-deficient OT1 cells were mixed in a 1:1 ratio after *in vitro* priming with different IL2 amounts. Before adoptive transfer of congenically marked OT1 cells was performed, the ration of mixed cells was analyzed. (A) Exemplary histograms show the ratio of each mixture of WT and IRF4-deficient OT1 cells, which was adoptively transferred into WT mice. (B) Graph shows the frequencies of WT and IRF4-deficient OT1 T cells, of the mixture which was primed under the indicated condition.

for IRF4-deficient OT1 cells, were cells which were primed with high amounts of IL2 (50U) showed a significantly increase in proportion located in blood and liver of infected recipient mice, compared to low IL2 (1U) primed cells.

Analysis of the differentiation pattern of WT and IRF4-deficient OT1 cells in the spleen of infected recipient mice observed a similar expression of CD44, independent on the initial priming condition, as shown in Figure 11.8. This suggests that both cell proportions of each condition showed an similar activation status. Interestingly, also in this experimental setup, IRF4-deficient CD8+ T cells maintained CD62L expression in all three conditions analyzed. In contrast, WT OT1 cells cleared the L-selectin from their cell surface after activation as expected.

Nonetheless, these results show that addition of high amounts of IL2 during the priming phase of IRF4-deficient OT1 cells could not rescue ag-specific effector cells during the early cause of Listeria infection. Overall, these findings indicate a defect in the ability to clonal expand to the same extend like the WT OT1 proportion. This suggests that high amounts of IL2 supply during the priming phase and activation of IRF4-deficient CD8+ T cells is less important, compared to later time points during the expansion phase of effector CD8+ T cells. This assumption was made based on the data of this study, which showed that *ex vivo* addition of high amounts of IL2 could partially rescue the ag-specific CD8+ T cells with IRF4 deficiency and could significantly increase their proliferative capacity.

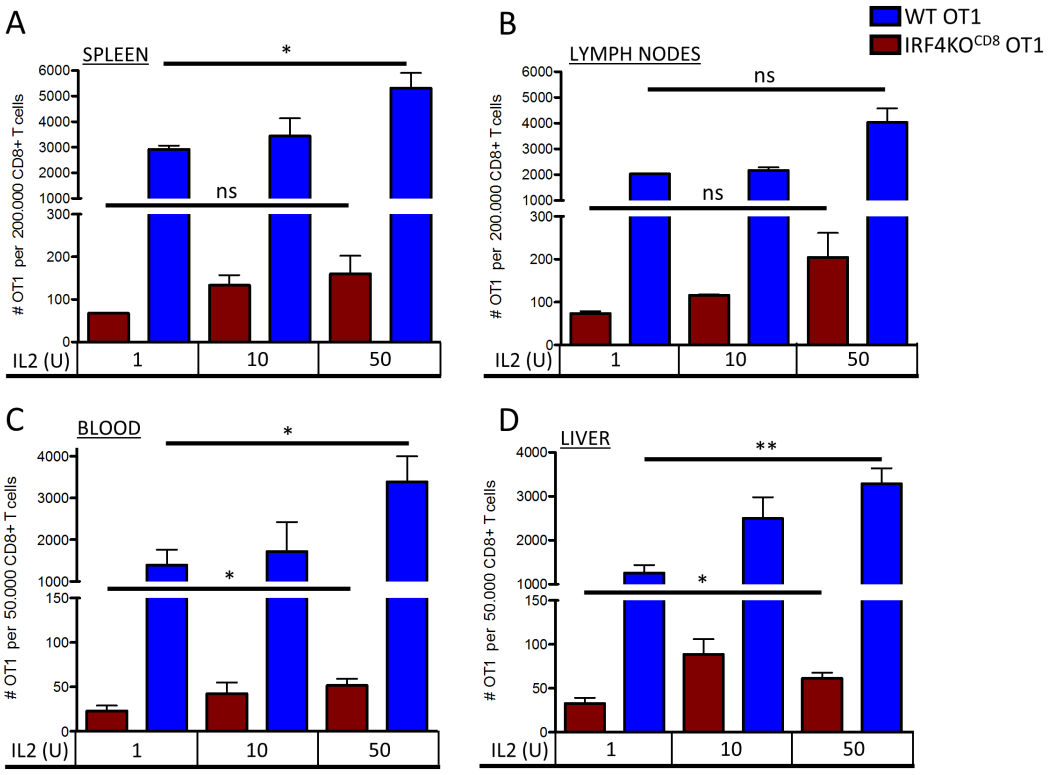

Figure 11.7: **Proportions of *in vitro* primed WT and IRF4-deficient OT1 cells in infected recipient mice.** The proportions of *in vitro* primed WT (CD45.2+ CD90.1-) and IRF4-deficient (CD45.2+ CD90.1) OT1 cells after adoptively co-transfer into WT (CD45.1+) mice, which were subsequently infected with LM-OVA, were analyzed. Transferred OT1 cell proportions in spleen (A), lymph nodes (B), blood (C), and liver (D) are shown in the graphs. WT OT1 cells are shown in blue and IRF4-deficient OT1 cells in red. Cells were primed with aCD3/aCD28 and different amounts of IL2 (1U, 10U, and 50U). Data show the mean + SEM and statistical signifcance with **p<0.001 and *p<0.05 (Student's t test).

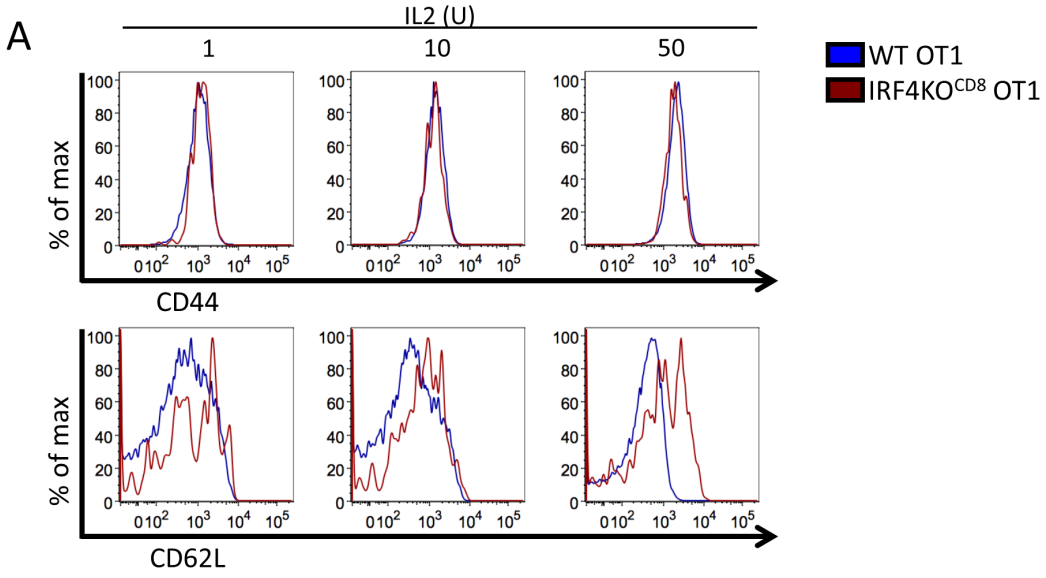

Figure 11.8: ***In vitro* primed IRF4-deficient OT1 cells maintain CD62L expression in infected recipient mice.** The proportion of WT (CD45.2+ CD90.1-) and IRF4-deficient (CD45.2+ CD90.1) OT1 cells, which were adoptively co-transferred into WT (CD45.1+) mice, which were subsequently infected with LM-VA, were analyzed for their differentiation pattern. The expression of CD44 and CD62L was examined via surface staining on WT and IRF4-deficient OT1 cells from spleen of infected recipient mice. (A) Exemplary histograms show the CD44 expression on WT (in blue) and IRF4-deficient (in red) OT1 cells on day 4 after Listeria infection of recipient mice, which were primed with different IL2 amounts, as indicated.

Part IV

Discussion

Chapter 12

Special features of the IRF4flox.E8Icre mice

12.1 IRF4 expression is exclusively absent in mature CD8+ T cells

Previous studies have already pointed out the essential role of IRF4 for a proper CD8+ T cell response against infection [86, 142, 162, 163, 166, 188, 262]. Several of these experiments have been done using a transgenic mouse model based on the Cre-Lox recombination technology [1, 83, 84, 218]. The advantage of this gene knockout system by its self is that the gene of interest is selectively inactivated in a cell specific manner. The majority of investigators of the above mentioned publications showed the essential role of IRF4 in CD8+ T cell responses due to infection in IRF4flox mice [113] mated with CD4cre mice. In this transgenic mouse model, the Cre protein expression causes a recombination under the control of the Cd4 regulatory elements [130]. The Cd4 promoter therefore drives the Cre expression. Thus, when the Cd4 promoter becomes active, the Cre protein expression causes the loxP sites to recombine and excise the LoxP-flanked IRF4 locus (known as floxed), hence progressively removing the IRF4 protein expression in all $\alpha\beta$ T cells [162]. The fact remains, that mature CD4+ and CD8+ single positive T cells arise from double positive (DP) CD4+ CD8+ T lymphocytes [63]. Therefore, transgenic IRF4flox.CD4cre mice lack IRF4 expression in both, the CD4+ and CD8+ T cell compartment, as the IRF4 deletion is initiated at the DP stage in the thymus. It has already been published that the lack of IRF4 in CD4+ T cells has led to dysfunctionality in several CD4+ T cell subsets, which also affects the regulatory

T cells [267] and Th1/Th2 helper populations [85, 138], among other CD4+ T cell subsets [21, 215].

Several studies have pointed out the requirement of CD4+ T cell help for the initiation and persistence of the CD8+ T cell response [266]. Moreover, it has been shown that CD4+ T cells are required for a proper primary and secondary CD8+ T cell response [165], as well as for clonal expansion and survival of CTL [13]. Defects in CD4+ T cell help can directly entail phenotypic and functional alterations of CD8+ T cells, as CD4+ T cells secrete cytokines and chemokines that activate and recruit other cells of the immune system and therefore might be critically involved in controlling pathogen levels and hence antigen load. On the basis of the above mentioned facts, experimental results regarding the role of IRF4 for the CD8+ T cell response in IRF4flox.CD4cre mice might be distorted due to the fact, that IRF4 expression is additionally absent in the CD4+ T cell compartment leading to results, which might be partially or completely modified due to the loss of a proper CD4+ T cell help and not only due to the lack of IRF4 expression in CD8+ T cells.

Moreover it has been reported, that in untreated mice peripheral CD8+ T cells in IRF4flox.CD4cre mice spontaneously convert into a memory-like phenotype and polyclonal activation of peripheral T cells occurs due to impaired Treg function [162]. Some other investigators [142, 162] used bone marrow chimera models to determine the role of IRF4 in CD8+ T cell responses. The source for the generation of these mix bone marrow chimera mice were performed with IRF4-deficient mice created by Mittrücker and colloquies [153]. In detail, in this mice the Exon 2 and 3 of the IRF4 gene is replaced by a resistance gene, leading to the absence of the IRF4 protein in all developing cell types in those mice. Importantly, there are several hints pointing out that IRF4 deficiency in all cell types and from the beginning of the onset of cell development causes several disadvantages, which are discussed below.

It has been published that IRF4 is already critical for the T lymphoid-primed progenitor cell fate to prevent conversion of these progenitors into myeloid cells at the pre-thymic stage and for their homing to the thymus [246]. Furthermore, Nayar and colleagues [162] demonstrated a transiently upregulation of IRF4 during the maturation of CD4+CD8+ double positive into single positive CD4+ or CD8+ T cells in the thymus. Hence, showing that IRF4 expression probably plays a critical role already in intrathymic T cell development. However, they claim a normal thymic development of IRF4-deficient T cells. Furthermore, in intermediate CD4+ $CD8^{low}$ cells and CD4 single positive thymocytes it has been recently shown that IRF4 represses Runx3 transcription [27, 115], which is known to promote CD8 lineage commitment [258].

This present study examined the role of IRF4 in the CD8+ T cell development and functionality during anti-pathogenic responses. In contrast to previous published data, a conditional IRF4flox.E8Icre mice (termed as $IRF4KO^{CD8}$ mice) or OT1.IRF4flox.E8Icre mice (IRF4flox.E8Icre mice bred to transgenic OT1 mice termed as $OT1.IRF4KO^{CD8}$), were used in all experimental setups in this study. The big advantage, IRF4flox.E8Icre mice and OT1.IRF4flox.E8Icre mice, both have a conditional deletion of IRF4 exclusively in mature peripheral CD8+ T lymphocytes. The deletion of the IRF4 expression being exclusively absent in mature CD8+ T cells was confirmed, going along with simultaneous expression of eGFP in cells deficient for IRF4 (Figure 7.1). Other immune cells, such as non-lymphocytes (CD3- cells) and especially CD4+ T cells, being not affected from

the IRF4 gene excision, as it was often the case in the recent published studies.

Before experiments started, the presence of any initial differences between WT and IRF4KO^{CD8} mice and the occurrence of any disease patterns in older mice were determined. Analysis of untreated mice confirmed that there are no initial differences in numbers and frequencies of CD4+ and CD8+ T lymphocyte subsets, comparing numbers and frequencies of T cells in IRF4KO^{CD8} and WT mice (Figure 7.2). Additionally, IRF4KO^{CD8} mice showed a normal phenotypic characterization of lymphocytes and cell subsets were equally distributed upon all organs tested (Figure 7.3). Moreover, IRF4KO^{CD8} mice showed no alteration in the B cell compartment (Figure 7.5). Furthermore, mice showed no alterations in cell homeostasis and none disease pattern, such as an enlarged spleen, also not with advanced age. As already mentioned, the mouse model that has been used in this study allows normal homing of the T lymphoid progenitor cells to the thymus, as well as a normal thymic development, and maturation of all T lymphocytes. Neither the CD4+ nor CD8+ T cell development is affected by the deletion of the IRF4 protein, as in IRF4flox.E8Icre mice the excision of the IRF4 gene exclusively occurs in mature CD8+ T lymphocytes.

12.2 Untreated young and old IRF4flox.E8Icre mice appeared phenotypically normal

Untreated IRF4KO mice, created by Mittrücker and colleagues [153], developed severe lymhadenopathy, pointing out general defects in cell homeostasis. Up to 10-15 weeks of age, total IRF4 knock out mice showed an enlarged spleen. This occurred due to a drastic expansion of the CD4+ and CD8+ T lymphocytes, as well as the B cell compartment. These results suggest that, with ongoing age, those mice stay not healthy and are therefore not similar to their wild type counterparts. This further implies that CD8+ T cells generated in IRF4 total knockout mice might be initially altered in their epigenetic programming, as they changed their differentiation and homeostasis without environmental influences, such as infection or inflammation. Therefore, the initial stage of the IRF4-deficient and sufficient CD8+ T cells is not equal. IRF4-deficient CD8+ T cells created by Mittrücker and colleagues [153] seem to be already directed into a memory cell fate, which might have a further influence on the ongoing cell development and differentiation during a primary infection. In addition, in the study published by Nayar and colleagues [162] it has been claimed that the deletion of IRF4 in all $\alpha\beta$ T cells, using mice with a conditional allele of IRF4, which was crossed to CD4cre transgenic mice, resulted in an impaired peripheral tolerance besides the spontaneous conversion into a memory-like phenotype of the majority of all CD8+ T cells. Further, impaired Treg functionality resulted in polyclonal activation of peripheral T cells [267].

In contrast, untreated IRF4flox.E8Icre mice (here termed as IRF4KO^{CD8} mice), which were used in this study maintained a naïve stage similar to their WT counterparts (Chapter 7), also with advanced age. Furthermore, they did not spontaneously converted into a memory-like phenotype (Figure 7.4) or showed any disease patterns. Indeed, also with ongoing age, IRF4-deficient CD8+ T cells from IRF4flox.E8Icre (IRF4KO^{CD8}) mice maintained the same phenotypic characterization and numbers of lymphocytes, as their age matched wild type counterparts. These results strongly suggest that there are no

alterations in the initial epigenetic programming of the CD8+ T cells in IRF4KO^{CD8} mice.

Chapter 13

IRF4 deficiency leads to impaired CD8+ T cell responses to infection

13.1 IRF4 expression is induced after TCR engagement

Different to the majority of the members of the IRF family of transcription factors, IRF4 expression cannot be induced via IFN signaling. Instead, IRF4 expression is rapidly upregulated after TCR activation, as already published by several studies [48, 146, 153]. As expected, recent results could show that TCR stimulation with anti-CD3 antibody and the co-stimulatory molecule anti-CD28 led to a robust expression of IRF4 in naïve murine CD8+ T cells (Section 8.1). *In vitro*, the expression level of IRF4 in the murine infection model used in this study peaked between 24 and 36 hours after TCR engagement in wild type CD8+ T lymphocytes and subsequent declined in the following days. Thus, the induction of IRF4 expression transmits the TCR activation signal as IRF4 act as downstream regulator of the p-MHC-TCR ligation.

13.2 IRF4 is required for the effector CD8+ T cell generation after infection

In this study the role of IRF4 in CD8+ T cells in host defenses was determined against the intracellular bacterial pathogen *Listeria monocytogenes* or against viral infection caused by LCMV. At the peak of CD8+ T cell response, the total numbers and frequencies of splenic IRF4-deficient CD8+ T cells and ag-specific CD8+ T cells after bacterial and viral infection in IRF4KO^{CD8} mice were drastically decreased compared to WT mice (Figure 8.2). These results go in line with previous published data by various groups [142, 163, 188, 262] similarly demonstrating a drastic reduction in numbers and frequencies of ag-specific CD8+ T cells after bacterial and viral infection. Here, it has been additionally shown that the discrepancy in the number and frequency of OVA-specific CD8+ T cells and the altered proliferative activity, in the absence of IRF4 expression in peripheral CD8+ T cells, could already be detected on day 5 after LM-OVA infection in IRF4KO^{CD8} mice. Of note, as in this study shown, this difference in the

CD8+ T cell response upon infection was not due to different initial numbers of naïve CD8+ T cells recruited to the immune response in WT and IRF4KO^{CD8} mice (Figure 7.2). Therefore, the severely reduced overall quantity of ag-specific effector CD8+ T cells after infection in the absence of IRF4 expression in peripheral CD8+ T lymphocytes in IRF4KO^{CD8} mice correlated with a general reduction of the CD8+ T cell compartment after primary response to infection (Figure 8.2). These results point out that the lack of the transcription factor IRF4 resulted in an altered effector CD8+ T cell generation. Thus, IRF4 is critical for the generation of ag -specific CD8+ T lymphocytes during primary infection.

During the cause of an infection, naïve CD8+ T cells become activated and undergo clonal expansion to generate high numbers of functional cytotoxic CD8+ T cells with distinct effector functions to eliminate invading pathogens. To examine lymphocyte proliferation, Ki-67 was used as a marker of proliferating cells, as KI-67 is expressed during several phases of the cell cycle but not at the G0 phase [61].

Not surprisingly, the fraction of proliferating CD8+ T lymphocytes, as measured by the percentage of cells expressing the marker Ki-67, was rather big in wild type (IRF4flox) mice after Listeria infection (Figure 8.3). However, present data showed that WT and IRF4KO^{CD8} (IRF4flox.E8Icre) mice had a distinct cell turnover of total (1.5-fold difference) and ag-specific (more than 2.5-fold difference) CD8+ T cells during the clonal expansion phase on day 5 after bacterial infection (Figure 8.3). Although, Ki-67 expression occurred in total CD8+ T cells to a similar extend, as indicated by similar MFI values. By having a closer look on SI-specific CD8+ T cells on day 5 after bacterial infection, a drastic reduction could be examined comparing frequencies and MFI values of the Ki-67 expression on IRF4-deficient CD8+ T cells with their WT counterparts. Thus indicating that in the absence of IRF4 expression, less ag-specific CD8+ T cells express Ki-67, a marker selectively expressed in dividing cells [205], and additionally to a reduced extend.

Ki-67+ CD8+ T cells were enriched in the activated CD44 expressing proportion of IRF4-sufficient CD8+ T cells in spleen and liver on day 7 after Listeria infection, whereas less IRF4-deficient CD8+ T cells expressed Ki-67 (Figure 8.3). Data revealed a 4.5-fold reduction in spleen and a 2-fold reduction in liver of Ki-67 expression on CD44+ CD8+ T cells. Overall, these data suggest a lower proliferative activity of total and ag-specific CD8+ T cells in the absence of IRF4 expression at this stage of infection. This proliferative defect was reflected in the lower numbers and decreased frequencies of ag-specific CD8+ T cells, found in IRF4KO^{CD8} mice on day 5 and day 7 after Listeria infection (Section 8.2).

Analysis of BrdU incorporation by total IRF4-deficient CD8+ T cells between day 5 and day 8 was found to be signicantly lower compared to their counterparts in WT mice. More than double the total CD8+ T cells in WT mice were BrdU+, compared with that by IRF4-deficient CD8+ T cells in IRF4KO^{CD8} mice (Figure 8.4). This was also examined in the absence of IRF4 expression for the recent activated CD8+ T cell compartment indicated by CD69 upregulation, which showed a similar drastic reduction in the BrdU incorporation. These results suggest reduced proliferation of IRF4-deficient CD8+ T cells compared to their WT counterparts at this early stage of infection. Thus, IRF4 deficiency in CD8+ T cells led to reduced proliferative capacity after an initial expansion. In summary, although an activation and effector CD8+ T cell response can

be induced in the absence of IRF4 expression, it became clear that sustained clonal expansion of CTLs is crucial IRF4 dependent.

13.3 Remaining IRF4-deficient CD8+ T cells acquire a memory-like phenotype after infection

In WT mice, the majority of ag-specific CD8+ T cells evoked by an infection show an effector phenotype ($CD44^{high}$ $CD62L^{low}$) after activation, as CD44 is rapidely upregulated and L-selectin (CD62L) is cleared from the cell surface after antigen encounter. In the infection mouse model, which was used in this study, both cell types showed a similarly increase in the CD44 expression, indicating an antigen encounter with an initial activation of IRF4-deficient CD8+ T cells in the onset of infection. Nevertheless, IRF4-deficient CD8+ T cells showed drastic phenotypic alterations after Listeria infection compared to WT CD8+ T cells (Section 8.3). It is well known that after infection, a heterogeneous pool of effector CD8+ T cells is formed, composed of SLECs and MPECs, identified via their surface expression of KLRG1 and CD127 [101].

In this study as shown in Section 8.3, examination of these populations showed drastic differences between WT (IRF4flox) and $IRF4KO^{CD8}$ (IRF4flox.E8Icre) mice on day 7 after infection. The majority of ag-specific CD8+ T cells in WT mice downregulated CD62L and upregulated KLRG1, which is consistent with an effector phenotype. In contrast, the few remaining IRF4-deficient CD8+ T cells failed to acquire a $CD62L^{low}$ $KLRG1^{high}$ effector phenotype, as they maintained CD62L expression and could only properly induce KLRG1 expression after activation (Figure 8.6). This clearly demonstrated that this cell population showed a memory-like phenotype and could be mainly characterized as MPEC ($KLRG1^{low}$ $CD127^{high}$) subset. Furthermore, despite the increase in the percentage of the MPEC population in $IRF4KO^{CD8}$ mice, the absolute numbers of MPECs and SLECs were drastically decreased compared to WT mice. Thus, these results suggest that the few remaining IRF4-deficient CD8+ T cells analyzed on day 7 after Listeria infection phenotypically resembled effector memory cells (T_{EM}). In contrast, the CD8+ T cells in WT mice acquired a $CD44^{high}$ $CD62L^{low}$ central memory (T_{CM}) phenotype (Figure 8.5).

Taken together, these data showed that IRF4 signaling is involved in the regulation of the differentiation pattern of CD8+ T cells. Furthermore, IRF4-deficient CD8+ T cells fail to further undergo a gradual differentiation process into a robust effector CD8+ T cell population in an appropriate number and frequency, although an initial activation occurred. These results are in agreement with previous reports showing that IRF4-deficient CD8+ T cells fail to downregulate CD62L and upregulate KLRG1 after antigen encounter after influenza and LCMV infection [142, 163, 188, 261]. In sum, IRF4 deficiency leads to phenotypic alterations of the effector CD8+ T cell population favoring memory cell formation.

Ordinarily, after activation via antigen encounter during infection, CD8+ T cells show a rapid down regulation of the lymph node homing receptor molecule CD62L, as it is required to facilitate the migration away from secondary lymphoid organs to the sites of infection. However, IRF4-deficient CD8+ T cells did not clear CD62L from their cell surface after activation, as IRF4-sufficient CD8+ T cells did (Section 8.4).

To determine the effect of maintained CD62L expression, IRFKO^{CD8} and WT control mice were infected with LM-OVA. On day 5 after infection, the frequencies of IRF4-deficient and IRF4-sufficient CD8+ T cells among the CD11a expressing subset were determined (Figure 8.7). In the present analysis, CD11a was used as a marker to distinguish ag-activated CD8+ T effector cells from naïve cells, as CD11a has been shown that its expression is induced on T lymphocytes after antigen encounter but not due to inflammatory changes [190]. At day 5 after Listeria infection, no significant differences were detected in the distribution of splenic ag-activated CD8+ T cells comparing WT with IRF4KO^{CD8} mice (Figure 8.7). This result suggest that the migration and accumulation of antigen-specific CD8+ T cells in the spleen is less dependent on the downregulation of CD62L and therefore less affected by IRF4-deficiency.

Of interest, ag-activated CD8+ T cells were found in both organs, lymph nodes and liver, of infected IRF4KO^{CD8} mice. Although, the frequencies of CD11a+ CD8+ T cells were significantly reduced in the absence of IRF4 in mesenteric lymph nodes and the target organ liver compared to day 5 infected WT mice (Figure 8.7). Results show over 3 to 4-fold reduction of ag-specific CD8+ T cells in the absence of IRF4 expression.

In sum, these results strengthen the presumption that the inability to downregulate CD62L does not prevent the migration of the ag-specific CD8+ T cells to the sites of infection, such as Listeria infected liver, although frequencies were dramatically reduced in this non-lymphoid peripheral tissue. These results suggest that the reduced frequencies of IRF4-deficient Listeria-specific CD8+ T cells are due to a drastic overall reduction of ag-specific CD8+ T cells in the absence of IRF4 and not due to a defect in the infiltration or accumulation in the infected tissue.

13.4 IRF4 is indispensable for cytotoxic effector CD8+ T cell responses

To evaluate the functional activity of IRF4-deficient CD8+ T cells according to their phenotype, in this study the cytokine secretion was measured on day 7 after Listeria infection. The production of IFNg, IL2, and TNFa were measured, as they play a major role for the protective immune response to pathogens [108, 176].

Present results in Section 8.5 observed drastic differences between WT and IRF4-deficient CD8+ T cells, as the few remaining IRF4-deficient CD8+ T cells on day 7 after infection were critically impaired in their cytokine production. Of note, the capacity to produce effector molecules separately and simultaneously was strongly impaired in IRF4-deficient CD8+ T cells. Frequencies of IFNg single producers and IFNg/TNFa and IFNg/IL2 double producers among the IRF4-deficient CD8+ T cell population were dramatically reduced, indicating a defect in single and simultaneous production of effector molecules and therefore a confined functionality. Together, these results indicated that the magnitude and the polyfunctionality of CD8+ T cell responses to viral and bacterial antigens were much lower when IRF4 expression was absent in the CD8+ T cell subset. In conclusion, IRF4 is essential for the generation of effector CD8+ T cells and their acquisition of cytokine production, as IRF4 deficiency led to drastic defects in the capability to produce effector cytokines during bacterial and viral infection. These results are consistent with recent published studies demonstrating a strong impaiment

in effector CD8+ T cell cytokine production in the absence of IRF4 after bacterial [188] and viral infection, such as LCMV and influenza [142, 262]. Therefore, IRF4-deficient CD8+ T cells showed a big disadvantage, as they lacked the ability to produce large amounts of effector cytokines, which are important to alert other cells of the immune system, to control infection *in vivo*, and to clear efficient the invading pathogens. The decrease in the production of cytokines and cytotoxic molecules reported in this study (Section 8.5), represents an important indicator that the lack of IRF4 expression in CD8+ T cells selectively modulates the effector program of CD8+ T cells. This in turn, is likely to be accompanied by additional changes in the gene expression program, which negatively impacts the protective capacity of those cells.

Because there was a drastically impaired functional characteristics and a transition into a memory-like phenotype of the few remaining IRF4-deficient CD8+ T cells after Listeria infection detected, this finding expected a reduction in the cytolytic activity in the absence of IRF4. Ordinarily, after initial antigen encounter, naïve cells first need to become activated and clonal expand, while they differentiate into effector CTLs. Naïve CD8+ T cells are incapable of immediate of killing infected cells, therefore this feature need to be acquired. Besides the expression of several effector cytokines, they additionally acquire very high levels of cytotoxic activity. Several studies have shown that cytotoxic effector CD8+ T cells kill their target cells by programming them to undergo apoptosis [31]. Therefore, CD8+ T cells can express high levels of FASL (CD95L) molecules [208]. In target cells, which express the death receptor FAS on their cell surface, the FAS-FASL interaction leads to an activation of a death domain, which in turn triggers a caspase-dependent apoptosis pathway [248].

In this regard, the determination of the cytotoxic functionality of effector CD8+ T cells was performed (Section 8.5). First, flow cytometric analysis of FASL expression in CD8+ T cells of IRF4KO^{CD8} mice on day 5 after Listeria infection was examined. Not surprisingly, present results observed differences in the killing ability of CD8+ T cells, as splenic CD8+ T cells from IRF4KO^{CD8} mice expressed lower levels of FASL compared to wild type CD8+ T cells, on day 5 after Listeria infection (Figure 8.10 A). Thus, the induction of the FAS receptor induced apoptosis pathway in target cells was impaired in IRF4-deficient CD8+ T cells.

Despite this receptor binding induced apoptosis, effector CD8+ T cells store cytotoxic molecules like granzymes and perforin in their lytic granules. These molecules can be released to induce cell death of infected cells or directly act on cytosolic pathogens [136, 213]. Cytotoxic proteins, like granzymes and perforin, need to cooperate to trigger apoptosis in target cells, as released serine proteases cannot enter the membrane. First, perforin needs to lyse the target cells by creating pores in the membrane to allow granzymes to enter the cell to induce fragmentation of cellular DNA. This process results in caspase-dependent and -independent death pathways. This study therefore additionally analyzed the expression of granzym B on both effector CD8+ T cell types and observed critically decreased granzyme B expression in IRF4-deficient CD8+ T cells compared to their WT counterparts (Figure 8.10 A).

In addition, recent studies have shown that cytotoxic CD8+ T cells express lysosome-associated membrane protein CD107a (LAMP-1) [2]. The expression of this molecule correlates with the cytotoxic cell-mediated lysis of target cells. In CD8+ T cells, CD107a is used as a marker for cell degranulation and has been proposed to be involved in

protecting the cellular membrane from attack by lytic enzymes in the granules [56]. Its surface expression is shown to correlate with the cytotoxic cell-mediated lysis of target cells [2]. Furthermore, it has been shown to be needed to deliver granzymes and perforin to the target cells [119, 183]. Reduced expression levels of CD107a in CD8+ T cells from IRF4KO^{CD8} (IRF4flox.E8Icre) mice were observed, which were 5 days prior analysis intravenously infected with Listeria (Figure 8.10 A).

These results indicate that IRF4-deficient CD8+ T cells were impaired in their killing ability of infected target cells via FAS-FASL engagement and granzym B mediated cell death induction. Both death pathways influencing the kinetic of the pathogen clearance. Taken together, these results show that the absence of IRF4 expression in CD8+ T cells during infection led to profound developmental and functional defects in effector CD8+ T cells. The ability to exert full effector capacity was drastically diminished in the absence of IRF4 expression in CD8+ T cells (Chapter 8). Moreover, the dramatically impaired effector cytokine production and declined cytotoxic capacity of IRF4-deficient CD8+ T cells, as well as the drastically reduced numbers of ag-specific CD8+ T cells, correlated with an increase of the bacterial burden in IRF4KO^{CD8} mice after Listeria infection compared to wild type mice (Figure 8.10 B).

This is in agreement with previous reports also showing that IRF4 is critical for bacterial clearance after *Listeria monocytogenes* infection [188] but also indispensable for to protective CD8+ T cell response against viral infection, as demonstrated in an influenza infection model [262] and LCMV infection model [142]. Taken together, IRF4 is crucial for a protective CD8+ T cell response upon bacterial and viral infection.

13.5 IRF4 affects the trancriptional program of CD8+ T cells

T box transcription factor expressed in T lymphocytes (Tbet) and its counter player eomesodermin (Eomes) represent a pair of transcription factors, which are crucial for the determination of the CD8+ T lymphocyte phenotype, cell fate, and function [91]. In this study, results indicated that IRF4-deficient CD8+ T cells have defects in their effector gene expression, as they showed lower amounts of Tbet expression (Section 8.6). However, differences in frequencies of Tbet+ cells did not reach statistical significance, although a tendency was indicated with reduced Tbet expression in IRF4-deficient CD8+ T cells on day 7 after infection. This result suggests that Tbet expression might be less influenced by IRF4 than other transcription factors influencing the effector cell fate. Nevertheless, the minor reduction of Tbet was already reflected in a drastic impairment of effector function and a severely impaired protective capacity, as well as drastically reduced KLRG1 expression, measured at the peak of CD8+ T cell response after bacterial and viral infection (Section 8.5). These findings are in agreement with recent published data showing that Tbet deficiency led to profound absence of a proper SLEC (KLRG1^{high} CD127^{low}) population after infection [96], strongly urge the effector CD8+ T cells toward the MPEC pathway. Moreover, it has been shown that Tbet deficiency or reduced expression levels correlated with T cell dysfunctionality [106]. Thus, these published results additionally go in line with the finding that IRF4-deficient CD8+ T cells maintained CD62L expression and failed to express KLRG1, as well as they displayed

drastic diminished effector functionality (Section 8.5).

Interestingly, the lack of IRF4 expression in CD8+ T cells led to an increased Eomes expression, which resulted in a downregulation of the cytotoxic programming (Figure 8.10) and an acquisition of a memory-like phenotype, instead of a terminal effector cell type. Therefore, these data provide further evidence that IRF4 expression links TCR activation to molecular and transcritional mechanisms. This is in agreement with a recent report [162], which had demonstrated that IRF4 suppresses Eomes expression after TCR signaling via IL2 inducible T cell kinase (ITK) and the mammalien target of rapamycin (mTor), and thus regulates CD8+ T cell differentiation after T cell activation. Furthermore, a recent report has suggested that the upregulation of Eomes in CD8+ T cells is necessary to promote longevity and homeostatic proliferation of memory T cells [91]. Taken together, these and the presented data in this study suggest that IRF4 expression influences the cell fate of CD8+ T cells. This is consistent with a previous published report, additionally demonstrating that IRF4 is esssential for the expression of several transcription factors being important for the effector cell development [100], such as Blimp-1, Id2, and RunX [188]. Furthermore, it has been shown that IRF4 expression represses Bim and cyclin-dependent kinase (CDK) inhibitors to control survival of effector CD8+ T cells [262]. In addition, IRF4 acts as interaction partner for several other transcription factors, such as BATF [121], being important for T cell differentiation and functional development. Moreover, a recent study has demonstrated that IRF4, together with its binding partner BATF, bind directly to the Tbet and Eomes loci in effector CD8+ T cells, indicating a direct regulatory role of these key transcription factors.

Consitent with recent publications [162, 188], the results shown in this study suggest that the absence of IRF4 expression enforces a formation of CD8+ T cell MPEC population to the expense of a functional effector CD8+ T cell population. In summary, IRF4-deficiency led to dysfunctional programming of the effector CD8+ T cells subset, which is reflected by dramatic changes in a broad set of distinct pathways, an altered expression of effector genes, and lineage determining transcription factors, such as Eomes and Tbet.

13.6 The role of IRF4 in CD8+ T cell memory formation and effector recall response

After the peak of CD8+ T cell response, when the pathogens have been cleared, the majority of effector CD8+ T cells undergo contraction to convert into a small but stable pool of memory cells. Those memory cells are than able, upon antigen reencounter, to form rapidly a robust and efficient effector population. IRF4-deficiency had a drastic impact on the generation of the SLEC compartment (Section 8.3), as it was almost absent in IRF4 deficient CD8+ T cells after primary bacterial and viral infection. Therefore, the question came up whether IRF4-deficient CD8+ T cells, which displayed a MPEC (CD127+ KLRG1-) and central memory (CD127+ CD62L+) phenotype in the effector phase (day 7 p.i.), would have a better memory formation. Additionally, the CD8+ T cell response upon secondary infection was determined to analyze the impact of IRF4 expression in the recall response.

Consistent with the represented observations during primary bacterial infection, which were made in this study, IRF4-deficiency in CD8+ T cells resulted in a more than 4-fold reduction of the antiviral CD8+ T cell response at the peak of primary LCMV infection (Section 8.7). This was pointed out by a lower frequency of the GP33-specific CD8+ T cell population, being severely reduced in IRF4KO^{CD8} mice compared to WT control mice on day 8 after primary LCMV infection. These data suggest that IRF4 deficiency impacts the effector CD8+ T cell formation independent of the type of infection.

Interestingly, IRF4-deficiency in CD8+ T cells had no impact in the memory formation or T cell homeostasis. Both mice strains, WT and IRF4KO^{CD8} mice, showed a similar memory formation on day 60 after primary LCMV infection with no significant difference in the frequencies of LCMV GP33-specific CD8+ T cells on day 60 post infection. However, similar to the here presented observations regarding the frequency of effector CD8+ T cells during primary infection, the IRF4-deficient CD8+ T cell population during secondary infection was similar affected by the absence of IRF4 expression. In detail, IRF4-deficiency resulted in a more than 2-fold reduction of the GP33-specific CD8+ T cells on day 8 after antigen reencounter.

This study (Section 8.1) and also others could show that IRF4 expression is induced after TCR engagement in a transient manner. The expression of this transcription factor peaks after induction but than declines in the following days after activation. Although, IRF4 expression kinetic is dependent on the strength of the activating TCR signal (Section 8.1), IRF4 expression decreases after some time. This could be an explanation why IRF4 expression did not impact the T cell homeostasis of memory CD8+ T cells, as it is not expressed during this state of the immune response. But in contrast, IRF4 deficiency did impact the effector and effector recall response. These findings suggest that the expression of IRF4 not only contribute to the optimal differentiation and functionality of CD8+ T cells in primary infected hosts. Furthermore, it is also critical for a proper phenotypic and functional maturation of CD8+ T cells upon secondary antigen encounter.

Chapter 14

IRF4-deficient CD8+ T cells have an increased apoptotic potential

14.1 IRF4 deficiency leads to increased susceptibility to apoptosis

This present study analyzed whether IRF4-deficient CD8+ T cells are more susceptible to death and phagocytosis, as they go earlier into contraction phase than their wild type counterparts. As it is well known that multiple death pathways driving contraction, different cell-death inducing processes were analyzed.

First, several receptors and molecules being involved in different apoptotic pathways were determined. Apoptotic cell death requires the expression of molecules that positively regulate several death pathways. This process requires, among others, the expression of death receptors, such as FAS. FAS expression initiates the FAS-mediated death pathway due to its binding on its ligand, namly FASL. Additionally, when the signaling cascade is triggered, it leads to the activation of key death-inducing enzymes, termed caspases, which in turn lead to protein cleavage and cell death [4]. To determine whether IRF4-deficient CD8+ T cells are eliminated via the FAS-mediated death pathway, the expression of FAS on day 5 after Listeria infection was examined. Results in this study have observed that IRF4 deficiency in CD8+ T cells led to an upregulation of the FAS receptor expression, which might be the reason for the initiation of programmed cell death in these cells.

Recent publications claim that high frequent expression of FAS on T cells occurs during contraction phase, offering an additional ability to control the proliferation and perform contraction of the effector CD8+ T cell subset via the FAS-FASL death pathway [161]. These results are in agreement with the present previous data, where reduced levels of ag-specific CD8+ T cells and less proliferative capacity already on day 4 after bacterial infection (Section 10.2) in IRF4KO^{CD8} mice could be examined. In contrast, their wild type counterparts kept on proliferation and showed a functional effector phenotype.

In sum, IRF4-deficient CD8+ T cells expressed significantly higher levels of the death mediator FAS on their cell surface, which may result in a higher susceptibility to programmed cell death, mediated via caspase activation. Consistent with that finding, Man et al. [142] and Yao et al. [262] published data showing that more IRF4-deficient CD8+ T cells than WT CD8+ T cells expressed the active form of caspase 3, strongly indicating an activation of the caspase cascade, which have been shown to result in programmed cell death. The here presented results provide additionally evidence for

the importance of IRF4 expression to inhibit the expression of the FAS receptor and in turn surpressing caspase activation. Therefore, this study claim that IRF4 deficiency led to an early onset of contraction phase, as its absence induced programmed cell death already on day 5 after infection, much earlier than in WT CD8+ T cells, although mice were infected with Listeria leading to strong TCR signaling.

Further analysis whether IRF4-deficient CD8+ T cells expose eat-me signals, such as phosphatidylserine (PS) to a higher extend than IRF4-sufficient CD8+ T cells on their surface, which facilitate their recognition and uptake by phagocytes, was performed. In fact, present results detected increased exposure of PS on IRF4-deficient CD8+ T cells, indicated by increased Annexin V levels. PS is an anionic phospholipid, which is normally confined to the inner leaflet of the plasma membrane of the intact cell [145]. The loss of the plasma membrane symmetry results in the increased exposure of PS on the cell surface and thus, leads to the recognition by phagocytes via their membrane receptors, which are involved in the elimination process of early apoptotic cells. This suggest that IRF4 expression in CD8+ T cells is important to protect effector CD8+ T cells from phagocytosis mediated by macrophages, monocytes, DCs, and granulocytes.

Second, analysis of the possibility whether IRF4 deficiency in CD8+ T cells might also leads to an activation of the complement system was performed. Its activation has been shown to contribute to the elimination of effector CD8+ T cells early during clonal expansion. Ordinarily, cells express surface proteins or recruit complement inhibitors, which interfere with complement effector functions and delay or even block the complement cascade. The absence of a single protein might already result in incomplete local protection. Changes in the expression of several complement regulatory proteins, indicate that those cells are more susceptible to death. The downregulation of protective molecules and the increase of eat-me signal exposure allow cell death to accur, due to the initiation of the complement cascade [269].

The deposition of complement mediators, such as C1q, C4, and C3, was determined to analyze whether IRF4-deficiency results in an initiation of the complement cascade during the clonal expansion phase (day 5 p.i.) of effector CD8+ T cells. Present results could not detect increased C1q or C4 deposition on IRF4-deficient CD8+ T cell surfaces via flow cytometry analysis on day 5 after Listeria infection. Interestingly, the present analysis observed an activation of the complement pathway due to an significantly increase of C3 convertase aviability on IRF4-deficient CD8+ T cells.

Furthermore, an increase in the recruitment of phagocytes into infected spleens could be detected in IRF4KO^{CD8} mice on day 5 post infection. Macrophages, granulocytes, DCs, and monocytes were more then 2-fold enriched in infected spleens of IRF4KO^{CD8} mice compared to WT mice. The reason for this might be the increased display of early apoptotic markers on the cell surface of IRF4-deficient CD8+ T cells due to an early induction of contraction. Furthermore, the induction of the complement pathway, which was indicated by increased C3 deposition on IRF4-deficient CD8+ T cells, promotes opsonization and phagocytosis. Although, most tissues contain resident phagocytotic cells, such as macrophages, it is not unusual that a recruitment of additional phagocytes ooccurs to the sites where the load of apoptotic cells is high. Those phagocytes express a large number of membrane-bound receptors which facilitate the recognition and clearance of cells undergoing apoptosis.

However, there are reports documenting discrepant results for the apoptosis induc-

tion in IRF4-deficient CD8+ T cells, claiming that there is no increased apoptosis in the absence of IRF4 expression in CD8+ T cells [188]. In contrast, results shown in this study suggest that IRF4 act as a potent inhibitor of several apoptotic pathways, protecting effector CD8+ T cells from a premature termination of the expansion phase and therefore from an early onset of contraction. Of interest, in contrast to the publication from Raczkowski et al. [188] but in agreement with the results obtained in this study, recent reports could demonstrate that the absence of IRF4 expression in CD8+ T cells led to enhanced programmed cell death, as evidenced by increased Annexin V staining and enhanced percentages of active caspase 3+ CD8+ T cells [142, 262]. Taken together, IRF4 expression is critical for the survival of effector CD8+ T cells.

In summary, IRF4 deficiency in CD8+ T cells resulted in an altered apoptotic state of effector CD8+ T cells already in the middle of the expansion phase. Results of this study suggest that enhanced cell death and phagocytosis were the cause for the collapse during proliferative CD8+ T cell response and the disappearance of the ag-specific CD8+ T cells.

14.2 IRF4-deficiency does not enhance the expression of inhibitory molecules

To investigate the influence of regulatory molecules and receptors, the expression of several molecules being associated with impaired T cell function, reduced proliferation, and diminished effector function were analyzed. The CD8+ T cell compartment in the spleen of WT and IRF4KO^{CD8} mice were analyzed 5 days after Listeria infection for their expression of Tim3, 2B4, PD-1, CTL4 (known as CD152), CD160, and LAG3. No difference in the expression of any of those markers could be detected in ag-unexperienced CD8+ T cells comparing IRF4KO^{CD8} with WT mice. This suggest that IRF4 deficiency does not impact the expression of inhibitory markers on CD8+ T cells in untreated IRF4KO^{CD8} mice.

Comparison of the Tim3, 2B4, and LAG3 expression levels revealed an increase in ag-experienced IRF4-defcient CD8+ T cells and WT CD8+ T cells compared to their ag-unexperienced control cells. Although, no difference could be detected between ag-experienced IRF4-defcient and IRF4-suffcient CD8+ T cells for the expression of 2B4 and LAG3 on day 5 after Listeria infection. An overall upregulation of 2B4 (known as CD244), as detected in ag-experienced WT and IRF4-deficient CD8+ T cells, has been shown to be required for optimal activation and proliferation of T cells upon binding to its ligand CD48 [104, 214]. Recent publication examine the role of the lymphocyte-activation gene 3 (LAG3) to negatively regulate T cell expansion and memory cell formation [256]. Cytotoxic T-lymphocyte-associated protein 4 (CTLA4) is one of the receptors that profoundly have been shown to inhibit immune activation after binding to different B7 family members [107, 131]. However, WT and IRF4-deficient CD8+ T cells showed similar LAG3 and CTLA4 expression levels after infection.

Interestingly, compared to their WT counterparts, a slightly increase was observed in the expression of Tim3 in ag-experienced IRF4-deficient CD8+ T cells. Most published data regarding TIM3 expression have been shown that TIM3 expression negatively regulates effector responses and diminishes cytokine secretion or even induces cell death

through its interaction with Galectin-9 [95, 268]. These findings go in line with presented previous findings in this study, which suggest that IRF4-deficiency resulted in impaired cytotoxicity and cytokine production (Chapter 8), an induction of pro-apoptotic pathways, and the initiation of phagocytosis (Section 9.1) already during the clonal expansion phase on day 5 after bacterial infection.

Recent studies have implicated that CD160 expression led to reduced proliferative capacity and functional T cell impairment [242]. Programmed death 1 (PD-1, CD279) molecule has been shown to inhibit T cell activation, the responses to infection, and regulating T cell exhaustion [10, 42, 109]. Furthermore, other studies claim that PD-1/PD-L engagement antagonizes TCR signaling, leading to decreased cytokine secretion and protein synthesis, as well as diminished proliferative capacity [55]. However, analysis of the expression levels of CD160 and PD-1 could not detected any differences between ag-experienced IRF4-deficient CD8+ T cells in comparison to their WT counterparts. Additionally, there was no altered expression of CTLA4 detected on ag-experienced CD8+ T cells, nor in the absence neither in the presence of IRF4 expression in CD8+ T cells on day 5 after infection.

In summary, IRF4-deficiency did not altered the expression of immune-inhibitory factors, which have been implicated in T cell dysfunction and have been put into the context of apoptotic processes. Therefore, these results suggest that the drastically impaired quality and quantity of the effector CD8+ T cell response in the absence of IRF4 expression was not due to increased expression of inhibitory molecules and exhaustion markers. In line with the findings in this study, a previous publication [188] claimed that reduced numbers of antigen-specific IRF4-deficient CD8+ T cells are not due to increased expression of exhaustion markers.

However, although previous reports showed increased susceptibility to programmed cell death [142, 262], overexpression of Bcl-2 in the absence of IRF4 could not rescue the impaired phenotype of IRF4-deficient effector CD8+ T cells [142]. This further supports the hypothesis that the cause of the diminished cell survival and disappearance of IRF4-deficient CD8+ T cells most likely occurs as a consequence of multiple effects, which alters the proliferative behavior and activates different apoptosic pathways, one complementing another to efficiently eliminate those cells.

Chapter 15

IRF4 expression levels dictate the onset of CD8+ T cell contraction

15.1 IRF4 expression kinetic is TCR strength dependent

This study (Figure 10.1) and also recent publications [142, 162, 262] could show that IRF4 expression levels are dependent on the TCR signaling strength, whereas high and low affinity peptides are sufficient to initial induce IRF4 expression. Here, results showed that stimulation of OT1 cells with low affinity ovalbumin (OVA)-derived peptides (T3, Y4) induced IRF4 expression, very similar to the high affinity peptide N4 (SIINFEKL). But of interest, after low affinity peptide stimulation, IRF4 expression levels declined successive, while high affinity peptide stimulation led to a robust and sustained IRF4 expression over the next following days. Thus, a varying strength of the TCR activation led to a similar induction of IRF4 expression after 24 hour but in turn resulted in a different kinetic profile of the IRF4 expression.

Consistent with recent published data, results of this study show that IRF4 expression levels can be directly linked to the strength of the TCR signaling, as interaction with peptides having a different affinity lead to different maintenance of high IRF4 expression levels. Strong TCR engagement resulted in a prolonged expression of IRF4 in CD8+ T cells and induced greater and prolonged expansion after activation. These results strongly indicated that differences in TCR affinity of the CD8+ T cells in the heterogeneous population of effector T cells lead to varying levels of IRF4, which in turn might trigger a different transcriptional program of the effector CD8+ T cell population, compared to high TCR signaling activation, which induces high and sustained IRF4 expression levels.

There is an extensive evidence that CD8+ T cells differentiate and develop into a robust effector cell subset dependent on the strength of the TCR signal [44, 112], which critically determines the quality and quantitiy of T cell expansion and functionality. The concept of TCR signaling shaping the outcome of effector cell population has been described earlier [264] and has profoundly expanded with the finding that enhanced IRF4 expression is required for the generation and maintenance of functional effector CD8+ T cell population. Overall, these findings let suggest that IRF4 plays a very important role in translating the TCR signaling strength and therefore might act as key regulator of effector CD8+ T cell development.

15.2 Strong TCR signaling and normal environment could not rescue IRF4-deficient CD8+ T cells

Results shown in this study observed that the initial proliferation and maintenance of IRF4-deficient OT1 cells was similar to WT OT1 cells, as the ratio of WT and IRF4-deficient transferred T cells remained equally till day 3 after infection (Section 10.2). These result supposed, that the initial activation and proliferation was similar after primary antigen encounter in the beginning of the infection. This data indicates that IRF4 expression is not required for the early activation of CD8+ T cells upon infection. Of interest, IRF4-deficient CD8+ T cells, although they initially increased in cell numbers relative to that of wild type cells, were not able to further increase or maintain their proliferative capacity and effector functionality from day 3 on after LM-OVA infection (Figure 10.2). As shown in this study, further survival and proliferation of effector CD8+ T cells from day 3 on after infection was critically depend on IRF4 expression. This resulted in a nearly disappearance of this cell subset on day 7 after infection. Therefore, IRF4 is crutial for effector CD8+ T cells to maintain and further proliferate after activation. Additionally, these results demonstrate that IRF4-deficient CD8+ T cells suffer from a cell intrinsic defect, which could not be revoked by a wild type environment. This is in agreement with recent published data [188] showing that the proliferative defect could not be rescued, as IRF4 is crucial for the differentiation of CD8+ T cells into a terminal effector cell population.

However, the reduction of ag-specific CD8+ T cells was not due to a different homing behavior leading to altered tissue distribution, as present analysis observed similarly very low levels in spleen and all other organs tested (Figure 7.3). The proportion of ag-specific CD8+ T cells in spleen of IRF4-deficient and sufficient OT1 cells became significantly different during the cause of infection, suggesting that the levels of proliferation or/and the survival capacity of ag-specific cells were not equivalent in both cell subsets. This was further indicated by the reduced BrdU incorporation in IRF4-deficient CD8+ T cells compared to their WT counterparts between day 5 and day 8 after LCMV infection (Figure 8.4). Moreover, also an day 7 after Listeria infection, IRF4-deficient CD8+ T cells showed less Ki-67 expression (Figure 8.3), indicating less proliferative capacity at this state of infection.

In conclusion, these results demonstrate that IRF4 is crucial for maintained proliferation, sustained effector differentiation, and normal T cell homeostasis of effector cells during the expansion phase after primary response to infection. Neither strong TCR engagement nor the environment of a wild type mouse could prevent the disappearance of IRF4-deficient effector CD8+ T cells, pointing out drastic intrinsic defects of IRF4-deficient ag-specific CD8+ T cells. Thus, optimal sustained expansion and continued proliferation, both critically required IRF4.

15.3 IRF4 deficiency mimics weak TCR signaling activation

Notably, the affinity and strength of the TCR engagement critically influences the phenotype and functionality of CD8+ T cells, with strong TCR stimulation favoring effector cell differentiation at the expense of memory CD8+ T cell differentiation. Additionally,

it has been published that although weak TCR engagement results in initial activation and proliferation of low affinity T cells, only strong TCR ligation led to a sustained T cell expansion and a highly functional cytotoxic effector cell population [264]. Thus, weak TCR engagement results in a premature termination of the clonal expansion and an early onset of contraction as a result of clonal competition. IRF4 expression is upregulated after peptide-MHC-TCR ligation. Furthermore, the kinetic of its expression level is dependent on the activating TCR signaling strength, as high affinity peptides leading to strong TCR engagement resulting in a sustained IRF4 expression. Thus, IRF4 translates the TCR signaling strength of the activating signal and transmits it into a proper differential program.

In this study, results have shown that IRF4 deficiency, independent of the strength of the TCR engagement, led to an impaired effector CD8+ T cell response, in respect to frequencies of ag-specific cells (Section 8.2), their ability to produce effector cytokines and cytotoxic molecules (Section 8.5), as well as to an altered differentiation pattern (Section 8.3). Although, weak and strong TCR signaling were sufficient to induce initial activation and proliferation, IRF4 deficiency led to the absence of a sustained T cell expansion and disappearance of the highly functional effector cell population. Therefore this study hypothesized that IRF4 deficiency mimics low TCR signaling and thus leads to a false translation of the strong TCR signaling, which actually induced the activation of the naïve CD8+ T cell. This in turn leads to an initiation of a developmental program triggering a T cell fate, which is similar to low affinity activated CD8+ T cells.

To elucidate a potential role for IRF4 in CD8+ T cell antigen-driven differentiation, proliferation, and its impact on the termination of the expansion phase, dependent on the strength of the TCR engagement, a TCR transgenic system was used. Naïve wild type OT1 and IRF4-deficient OT1 TCR transgenic CD8+ T cells were adoptively co-transferred into CD45.1 wild type recipient mice. One day later, recipient mice were i.v. infected with a recombinant *Listeria monocytogenes* strain expressing OVA protein, either containing the low affinity epitope SIITFEKL (T4) or the high affinity epitope SIINFEKL (N4). The ratio and total numbers of transferred WT and IRF4-deficient OT1 cells from spleen of infected recipient mice were determined. Further analysis of the exposure of PS on the cell surface, and the expression of Bcl-2 and FAS on each OT1 cell population was performed.

Present results could show that on day 5 after LM-OVA N4 infection, IRF4-sufficient CD8+ T cells formed a robust effector cell population after strong N4-MHC-TCR ligation (Figure 10.3). This goes in line with high affinity CD8+ T cells being selectively expanded during infections, indicating their importance in anti-pathogenic immune responses [264, 265]. Of interest, IRF4-deficient CD8+ T cells could not proper translate the strong N4-MHC-TCR interaction into an appropriate differentiation program, which leads normally to an enhanced proliferation and cytotoxic effector T cell formation. Instead, the lack of IRF4 expression upon T4-MCH-TCR activation mimicked an activation via a weak TCR signal, which favors ordinarily memory cell formation and the onset of contraction. Therefore, the signals which were transmitted in the absence of IRF4 were much weaker than those in WT OT1 cells.

Interestingly, IRF4-deficient OT1 and WT OT1 CD8+ T cells displayed the same proliferative capacity after weak T4-MHC-TCR ligation, as their proportion sustained equal as originally transferred (Figure 10.3). Moreover, it has been shown in this study

that under these conditions, WT and IRF4-deficient OT1 cells showed a similarly increased susceptibility to death and phagocytosis (Section 9.1). In this regard, CD8+ T cells cannot evade apoptotic pathways, if an engagement of death receptors or cytokine derivation or inhibition of cytokine signaling occurs [43, 118, 144]. These results are in agreement with previous published data [262] showing that consistent with their IRF4 expression, WT CD8+ T cells stimulated with weak TCR activation signals show enhanced cell death and diminished cell proliferation capacity after activation. Furthermore, present results in this study expand previous knowledge and confirm that low affinity activated CD8+ T cells and IRF4-deficient CD8+ T cells limited their own expansion via ligation of cell surface molecules and the exposure of pro-apoptotic molecules (Section 10.3). Both cell subsets exposed high levels of PS on their surface (Figure 10.3), which promote the clearance of the target cell, as it facilitates recognition by engulfment receptors on the surface of phagocytes [72]. Furthermore, both CD8+ T cell subsets expressed high levels of the death receptor FAS (Figure 10.3), efficiently implement the FAS-mediated activation-induced cell death (AICD) [99]. This observation revealed that both cell types suffer similar from AICD at an early state of infection, which might be one mechanism of the premature termination of the immune resonse of low affinity T cell clones.

Moreover, after weak TCR activation, both CD8+ T cell subsets showed a decrease in their Bcl-2 expression compared to WT CD8+ T cells, which were activated via LM-OVA N4. It has been shown that a reduction in the Bcl-2 expression leads to reduced CD8+ T cell responses and less protection of the activated cell against death [6].

In this regard, IRF4-deficiency mimicking low TCR engagement, or true weak peptide-MHC-TCR ligation by itself, resulted in a premature termination of clonal expansion and an early onset of contraction, due to the activation of several death inducing pathways. IRF4-deficient CD8+ T cells represented a terminally differentiated population, which was destined for clearance by apoptosis indicating that less functional subpopulations of T cells being selectively depleted from the system.

In summary, the absence of IRF4, which mimicked weak TCR stimulation, although a strong TCR engagement has occurred, led to an initially activation and expansion but resulted in a hasted termination of the expansion and an inaccurate differentiation of CD8+ T cells with defective effector function. IRF4 is a key regulator of CD8+ T cell fate choices and its expression levels are related to a particular transcriptional program, dictating the activation and differentiation status of the T cells and determines the fate choice. Thus, these observations imply that IRF4 deficient CD8+ T cells were not capable of translating strong TCR signal activation into a proper intrinsic molecular program and that the rate of T cell apoptosis in IRF4-deficient CD8+ T cells occurred concurrently during the phase of clonal expansion, even after strong TCR engagement.

Chapter 16

The influence of cytokines on *in vivo* primed IRF4-deficient CD8+ T cells

16.1 The influence of interleukins on IRF4-deficient CD8+ T cells

Present results of this study showed that IRF4 deficiency led to drastically diminished expansion and to reduced viability of effector CD8+ T cells, starting around day 4 after primary bacteria encounter. As IRF4-deficient CD8+ T cells could not be rescued *in vivo,* neither via strong TCR signal activation nor due to a normal environment (Section 10.2), the question raised whether *ex vivo* cytokine supply could support IRF4-deficient CD8+ T cells to overcome their proliferation problems and the increased susceptibility to cell death.

Several recent publications pointed out the important influence of soluble factors like cytokines, acting in an autocrine and paracrine manner on T cell proliferation, differentation, and homeostasis [7, 97, 203, 221]. Furthermore, recent studies indicate an influence of several cytokines like IL2 on distinct transcriptional programs [184]. Therefore, the impact of cytokine treatment, such as IL2, IL7, IL12, and IL15 on the proliferative behavior in *ex vivo* cultures of *in vivo* primed WT and IRF4-deficient CD8+ T cells after infection were analyzed.

Therefore, re-isolated OT1 cells (experimental setup as illustrated in Figure 10.2) were labeled with Proliferation Dye V450 to quantify the number of cell divisions, prior starting the culture. On day 3 of culture, independent of the cytokine which was supplemented, almost in all conditions WT OT1 cells proliferated much better than IRF4-deficient OT1 cells with the exception of IL15 treatment. Furthermore, similar to WT OT1 cells, IRF4-deficient OT1 cells showed the highest division rate when the medium was supplemented with IL2 and the lowest proliferation capacity with IL12 supply. Present results provide the evidence that extrinsic provision of IL2 impacts the proliferation of *in vivo* primed IRF4-deficient OT1 cells. This result is contrary to a recent published study claiming that IL2 administration has no impact on the survival and proliferative capacity of IRF4-deficient CD8+ T cells [188]. Therefore, although the cytokine milieu influences the proliferative potential and transcription factor profile of CD8+ T cells, the intrinsic defects of IRF4-deficient CD8+ T cells could not be completely overcome.

In contrast, in agreement with previous studies, claiming that even during contraction phase IL2 supply can increase the survival of effector CD8+ T cells [16], this study could show that high IL2 supply protected the majority of the IRF4-deficient *in vivo*

primed T cells from cell death (Figure 11.2). Moreover, an interesting observation was that *ex vivo* administration of high IL2 concentrations could partially restore the proliferation and could rescue the majority (up to 70 %) of IRF4-deficient T cells from cell death, although not to the same extend like in WT T cells (up to 90 %). Furthermore, the addition of IL2 into the culture of *in vivo* primed IRF4-deficient CD8+ T cells antagonized T cell contraction, as it promoted proliferation, albeit not to a full rescue. This goes in line with recent published data demonstrating that the expression of the pro-survival molecule Bcl-2 is induced via IL2 signaling [239]. This suggest that treatment with recombinant IL2 increases the survival of ag-specifc IRF4-deficient CD8+ T cells during the premature contraction phase. These findings suggest that the fate to undergo apoptosis is not fully imprinted during T cell priming, as IL2 signals achieved from the environment could partially rescue the IRF4-deficient *in vivo* primed CD8+ T cells due to improvement of their proliferation capacity. Results in this study could show rescue of IRF4-deficient ag-specific CD8+ T cells with high amounts of IL2 (although just partially) whether other studies claim no rescue could be detected via high addition of IL2 [188]. This discrepancy could arise from differential priming conditions of CD8+ T cells between CD8+ T cells which were primed in vitro with aCD3/aCD28 and invitro primed T cells in response to infection.

IL2 signaling via its receptor IL-2Rβ (CD122) has been shown to be crucial for the generation of effector cells [253]. Analysis of the CD122 expression on GP33-specific CD8+ T cells in WT and IRF4KO^{CD8} mice observed a significantly reduced expression in the absence of IRF4 (Figure 11.3). This suggests that IL2 signaling is diminished due to a drastic reduction of the IL2 receptor expression on the cell surface of ag-specific CD8+ T cells in the absence of IRF4. This finding might be a reason why IRF4-deficient CD8+ T cells can just partially be rescued by addition of high amounts of IL2, as its influence is limited by its receptor expression on the cell surface of the T cells.

16.2 IL2 treatment during *in vitro* priming could not rescue the IRF4-deficient phenotype after infection

Cytokines, such as IL2, have been shown to influence the generation of CD8+ T cells [253]. IL2 is a very potent cytokine, which promotes effects on lymphocyte cell survival and proliferation. Present results in this study demonstrated that IRF4-deficient CD8+ T cells could *ex vivo* partially rescued via addition of high amounts of IL2. Therefore, the question raised whether the IRF4-defcient phenotype of CD8+ T cells, which was detected early during immune response during the premature clonal expansion phase, could be altered or even rescued due to a priming of these cells in the presents of high IL2 amounts.

Adoptive transfer experiments of in vitro primed OT1 cells were performed, as illustrated in Figure 11.4. First, the proliferation rate (Figure 11.5) was examined 4 days after *in vitro* culture. WT and IRF4-deficient OT1 cells showed a high poliferative capacity under high IL2 supplementation (50U). The proliferation of both cell subsets was highly IL2-concentration dependend, as high amounts of IL2 increased the proliferative capacity and low IL2 concentration led to diminished expansion. This impaired proliferation capacity was drastic in IRF4-defcient CD8+ T cells, which proliferated very

poorly under this condition.

Both congenically marked OT1 cell populations, which were primed with the same amount of IL2 were equally mixed (Figure 11.6) and adoptively transferred into WT (CD45.1) mice. Recipient mice were infected and on day 5, the proportion of WT and IRF4-deficient OT1 cells were found drastical different (Figure 11.7). WT OT1 cells formed a proper effector generation, which was detected in spleen, lymph nodes, blood, and liver of infected recipient mice. Substantially smaller proportions of IRF4-deficient OT1 cells compared to WT proportions were found in all organs tested. This trend was observed for all IL2 priming conditions and suggests that the addition of high amounts of IL2 during the priming phase has no impact on the proliferative capacity, the survival, and effector T cell fate of in vivo challenged ag-specific IRF4-deficient CD8+ T cells.

Although, IRF4-deficient OT1 cells, which were primed with high IL2 amounts, showed initially similar proliferation rates compared to their WT counterparts, the defect in the ability of IRF4-deficient CD8+ T cells to expand was drastically diminished in the following *in vivo* conditions (Figure 11.7). The priming of IRF4-deficient CD8+ T cells in the presence of high amounts of IL2 initially increased the proliferative capacity during *in vitro* culture but cells could not sustained their proliferation and survival capacity, as the initial transfer ratio from 1:1 could not be maintained. Analysis of the differentiation pattern of both cell proportions in spleen of infected WT recipient mice observed maintained CD62L expression on CD8+ T cells in the absence of IRF4, while WT CD8+ T cells cleared the molecule from their surface (Figure 11.8). Ordinary, the CD62L expression is down regulated after activation, as this is required for a proper migration of T cells to the sites of inflammation and infection. However, $CD62L^{high}$ IRF4-deficient CD8+ T cells were found in all organs tested, although proportions were very small, compared to their WT counterparts.

Overall, these results indicate that addition of high amounts of IL2 can not rescue ag-specific CD8+ T cells in the absence of IRF4, when it is administered during the priming phase. In contrast, findings in this study showed that addition of IL2 during the clonal expansion phase could improve the proliferative capacity and survival of ag-specific IRF4-deficient CD8+ T cells. This suggest that differrences in the effect of IL2 treatment arise from differences in the time points of IL2 administration. Based on the results of this study, it seems that IL2 is not so important during the clonal expansion phase of ag-specific IRF4-deficient CD8+ T cells but showed an impact on the survival and proliferation rate during early immune response upon infection. It might be, that an administration of IL2 in infected $IRF4KO^{CD8}$mice during the clonal expansion phase, lead to an increased survival, proliferation and increased effector response of IRF4-deficient ag-specifc CD8+ T cells. This has to be further analyzed.

Part V

Concluding remarks

The transcription factor IRF4 is critically required for several cell types of the immune system, such as B cells and several T lymphocyte subsets [21, 87, 138, 153, 215, 230]. During the cause of this study, a wealth of data have been additional subsequently published in the last 2 years [86, 142, 162, 163, 166, 188, 262], indicating an extreme important role of IRF4 for a proper CD8+ T cell expansion, effector cell development, functionality, protective capacity, and energy metabolism. Nonetheless, it still has remained unclear how IRF4 impacts the fate decision and continuance of effector CD8+ T cells. In this study, to examine in detail the impact of IRF4 on the expansion and initiation of T cell contraction, a mouse model was used where the IRF4 gene is exclusively excised in mature peripheral CD8+ T cells (IRF4flox.E8Icre mice) and murine listeriosis was mainly used as an infection system.

In line with recent published data, also this study could show that IRF4 deficient CD8+ T cells fail to mount a protective T cell response upon bacterial and viral infection, as IRF4 deficiency strongly impaired the effector cytokine production, cytotoxic functionality, led to an altered differentiation pattern, and a drastic reduction of ag-specific CD8+ T cells. This drastically diminished protective CD8+ T cell response could be observed upon bacterial and viral infection, finally not only due to dramatically diminished numbers and frequencies of pathogen-specific effector CD8+ T cells. Of note, remaining IRF4-deficient CD8+ T cells exhibited a memory-like phenotype compared with WT T cells. CD8+ T cells from IRF4KO^{CD8} mice showed a CD44+ CD62L+ KLRG1- CD127+ expression pattern, indicating a loss of short-lived effector cell formation during CD8+ T cell response against invading pathogens. Although, IRF4 expression was not required for initial activation and expansion of ag-specific CD8+ T cells, it was essential for a sustained clonal expansion and for a proper and maintained formation of a protective effector cell population. Therefore, IRF4 expression can be directly put in relationship with the magnitude and quality of effector CD8+ T cell responses, being essential for their development and critical for their cytotoxic function. In summary, in the absence of IRF4, distinct functional properties and transcriptional changes were assigned compared to WT CD8+ T cells, with respect to cytokine and cytotoxic molecule secretion, proliferative potential and transcription factor expression, as well as metabolic alterations.

The naïve T cell repertoire is diverse and this heterogeneous population contains

T cells that can respond to a foreign antigen with a broad range of low and high affinities. There is a strong evidence that the TCR signaling strength determines the nature of the CD8+ T cell response and the T cell fate. The quality and kinetic of the CD8+ T cell response is fundamentally depended on the overall strength, including affinity and duration, of the peptide-MHC-TCR ligation. Although, weak and strong TCR signaling are sufficient to induce initial activation and proliferation, only strong TCR engagement is sufficient for a prolonged expansion and formation of a terminal effector cell population [264]. Strong or high TCR stimulation affects the metabolic programming, as extensive proliferation during the clonal expansion phase requires high energy supply, which can be optimal obtained via high glycolytic activity. Weak TCR signals diminish the magnitude of clonal expansion and accelerate the onset of contraction, as they favor the development of memory cells at the expense of effector cells. The depletion of low affinity T cells at the early stage of infection may occur to allow for maximal expansion of high affinity clones, which supposed to be the best responders and therefore mainly participate in the control of infection. Moreover, high affinity TCR stimulation rescues effector cells from early apoptosis by strong antigenic stimulation and further activate to proliferate and differentiate into high functional effector T cells, which mount a protective immune response.

The transcription factor IRF4 is upregulated after TCR engagement. Its expression level and kinetic is strongly dependent on the strength of the TCR activation signal, as strong signaling led to high and sustained IRF4 expression. In turn, graded IRF4 expression levels translate variations in the strength of the TCR signaling into an appropriate transcriptional and differential program. Thus, these results strongly indicate that IRF4 act as a key player, determining the fate of activated CD8+ T cells by influencing the kinetic of clonal expansion and defining the onset of contraction, as result of clonal competition. Therefore the question raised, based on the fact that graded levels of IRF4 directly translate the strength of the TCR ligand interaction, whether the absence of IRF4 mimics weak peptide-MHC-TCR interaction, even when a strong activation with a high affinity peptide took place. Finally, resulting in a premature termination of clonal expansion and on early onset of contraction.

Indeed, this study further expand the understanding of the role of IRF4 in TCR affinity dependent regulation of clonal expansion and CD8+ T cell contraction. The present results give evidence that the absence of IRF4 expression in CD8+ T cells altered the apoptotic state of effector CD8+ T cells early during primary infection. A hasted termination and premature contraction was initiated by the FAS-mediated death pathway. Furthermore, present analysis demonstrated that IRF4-deficient CD8+ T cells exposed molecules on their cell surface, which facilitate their recognition and uptake by phagocytes. Of note, an increase in the recruitment of phagocytes could be detected in the spleen of mice with IRF4-deficient CD8+ T cells early during primary infection, which might led to an increased recognition, uptake, and clearance of IRF4-deficient CD8+ T cells, which are prone to undergo cell death already early after initiation of the protective immune response, as the absence of IRF4 initiates a premature contraction phase.

Moreover, present protein analysis revealed an increase of molecules correlating with complement activation and the promotion of complement component binding. Additionally, a decrease in the expression of the anti-apoptotic molecule Bcl-2 could be examined in CD8+ T cells when IRF4 expression was absent or WT CD8+ T cells were activated

via weak TCR signal. The frequency of dying CD8+ T cells in the absence of IRF4 were similar in the second lymphoid organ spleen, as well as in infected liver tissue analyzed from IRF4KO^{CD8} mice. Data strongly indicate that this early contraction of IRF4-deficient CD8+ T cells is a systemic process. The increased susceptibility to death and phagocytosis, initiated due to the premature contraction phase of IRF4-deficient CD8+ T cells, correlated with their progressive loss of function, their altered differentiation pattern, and examined changes in their energy metabolism.

Taken together, due to the lack of IRF4 expression in CD8+ T cells, independent of the TCR signaling strength, IRF4-deficient effector CD8+ T cells were unable to mount productive effector cell response, although they were activated via a strong TCR engagement, which leads ordinarily to a robust and protective effector CD8+ T cell response. Instead, present results extent previous published data, by demonstrating that IRF4-deficient CD8+ T cells fated to die already early upon bacterial or viral infection, independent of the activating TCR signaling strength. Their premature contraction was mediated via several pathways resulting in apoptosis or phagocytosis. The results in this study further support the hypothesis that the cause of diminished cell survival and the almost complete disappearance of IRF4-deficient CD8+ T cells occurred most likely as a consequence of multiple effects, which altered the proliferative capacity and activated different death inducing pathways, one complementing another to efficiently eliminate those cells.

Thus, strong TCR ligand activation does not result in the initiation of the appropriate transcriptional differentiation program in the absence of IRF4. This result provides new evidence that IRF4 deficiency mimics weak peptide-MHC-TCR interaction, resulting in a premature termination of clonal expansion and an early onset of contraction. In sum, these results demonstrate that IRF4 is essential to promote a heterogeneous effector CD8+ T cell population. As this transcription factor promotes the competition between high and low affinity T cell clones, favoring the expansion of high-affinity T cell clones by influencing the transcriptional and metabolic program to maintain survival, functionality, and proliferation. Of interest, WT CD8+ T cells displayed after weak affinity TCR activation, consistent with their tailed IRF4 expression after weak TCR engagement, the same diminished proliferative capacity, as IRF4-deficient CD8+ T cells. Furthermore, weak TCR activation of WT CD8+ T cells with low affinity peptides resulted in an increased susceptibility to death and phagocytosis, very similar to the fate of IRF4-deficient CD8+ T cells.

In summary, these observations are well in line with previous published data and further support the presumption that graded IRF4 expression levels translate the variety in TCR signaling activation and initiates the transmission into a proper differentiation program. Results of this study reveal a previously unappreciated role of IRF4 for the kinetic of the CD8+ T cell response upon infection in effector CD8+ T cells. IRF4 is essential in CD8+ T cell responses, as its expression leads to an inhibition of the FAS-mediated death pathway, decreased exposure of eat me signals on the cell surface, and blocks complement activation and pro-inflammatory signaling, all processes leading to programmed cell death or elimination of these cells by phagocytes. Nevertheless, defects in the clonal expansion and the premature contraction are the consequence of multiple effects, including metabolic and transcriptional chances, altered proliferation behavior, and activation of death and phagocytosis inducing pathways.

Bibliography

[1] K. Abremski, R. Hoess, and N. Sternberg. Studies on the properties of p1 site-specific recombination: evidence for topologically unlinked products following recombination. *Cell*, 32(4):1301–1311, 1983. Cited on page 115.

[2] E. Aktas, U. C. Kucuksezer, S. Bilgic, G. Erten, and G. Deniz. Relationship between cd107a expression and cytotoxic activity. *Cellular immunology*, 254(2): 149–154, 2009. Cited on page 122 and 123.

[3] M. L. Albert, B. Sauter, and N. Bhardwaj. Dendritic cells acquire antigen from apoptotic cells and induce class I-restricted CTLs. *Nature*, 392(6671):86–89, 1998. Cited on page 18.

[4] M. R. Alderson, T. W. Tough, T. Davis-Smith, S. Braddy, B. Falk, K. A. Schooley, R. G. Goodwin, C. Smith, F. Ramsdell, and D. H. Lynch. Fas ligand mediates activation-induced cell death in human t lymphocytes. *The Journal of experimental medicine*, 181(1):71–77, 1995. Cited on page 126.

[5] C. Angelin-Duclos, G. Cattoretti, K.-I. Lin, and K. Calame. Commitment of b lymphocytes to a plasma cell fate is associated with blimp-1 expression in vivo. *The Journal of Immunology*, 165(10):5462–5471, 2000. Cited on page 36.

[6] B. Antonsson and J.-C. Martinou. The bcl-2 protein family. *Experimental cell research*, 256(1):50–57, 2000. Cited on page 133.

[7] V. P. Badovinac, a. R. Tvinnereim, and J. T. Harty. Regulation of antigen-specific CD8+ T cell homeostasis by perforin and interferon-gamma. *Science (New York, N.Y.)*, 290(5495):1354–1358, 2000. Cited on page 22 and 134.

[8] K. Bahl, A. Hüebner, R. J. Davis, and R. M. Welsh. Analysis of apoptosis of memory t cells and dendritic cells during the early stages of viral infection or exposure to toll-like receptor agonists. *Journal of virology*, 84(10):4866–4877, 2010. Cited on page 25.

[9] A. Banerjee, S. M. Gordon, A. M. Intlekofer, M. A. Paley, E. C. Mooney, T. Lindsten, E. J. Wherry, and S. L. Reiner. Cutting edge: The transcription factor eomesodermin enables cd8+ t cells to compete for the memory cell niche. *The Journal of Immunology*, 185(9):4988–4992, 2010. Cited on page 82.

[10] D. L. Barber, E. J. Wherry, D. Masopust, B. Zhu, J. P. Allison, A. H. Sharpe, G. J. Freeman, and R. Ahmed. Restoring function in exhausted cd8 t cells during chronic viral infection. *nature*, 439(7077):682–687, 2006. Cited on page 129.

[11] M. Barry and R. C. Bleackley. Cytotoxic T lymphocytes: all roads lead to death. *Nature reviews. Immunology*, 2(6):401–409, 2002. Cited on page 21.

[12] C. K. Baumgartner, H. Yagita, and L. P. Malherbe. A tcr affinity threshold regulates memory cd4 t cell differentiation following vaccination. *The Journal of immunology*, 189(5):2309–2317, 2012. Cited on page 20.

[13] M. J. Bevan. Helping the cd8+ t-cell response. *Nature Reviews Immunology*, 4(8):

595–602, 2004. Cited on page 116.

[14] S. D. Blackburn, H. Shin, W. N. Haining, T. Zou, C. J. Workman, A. Polley, M. R. Betts, G. J. Freeman, D. A. Vignali, and E. J. Wherry. Coregulation of cd8+ t cell exhaustion by multiple inhibitory receptors during chronic viral infection. *Nature immunology*, 10(1):29–37, 2009. Cited on page 94.

[15] J. N. Blattman, R. Antia, D. J. D. Sourdive, X. Wang, S. M. Kaech, K. Murali-Krishna, J. D. Altman, and R. Ahmed. Estimating the precursor frequency of naive antigen-specific CD8 T cells. *The Journal of experimental medicine*, 195(5): 657–664, 2002. Cited on page 23.

[16] J. N. Blattman, J. M. Grayson, E. J. Wherry, S. M. Kaech, K. A. Smith, and R. Ahmed. Therapeutic use of il-2 to enhance antiviral t-cell responses in vivo. *Nature medicine*, 9(5):540–547, 2003. Cited on page 134.

[17] N. Bollig, A. Brüstle, K. Kellner, W. Ackermann, E. Abass, H. Raifer, B. Camara, C. Brendel, G. Giel, E. Bothur, et al. Transcription factor irf4 determines germinal center formation through follicular t-helper cell differentiation. *Proceedings of the National Academy of Sciences*, 109(22):8664–8669, 2012. Cited on page 36.

[18] M. Bonazzi, M. Lecuit, and P. Cossart. Listeria monocytogenes internalin and e-cadherin: from structure to pathogenesis. *Cellular microbiology*, 11(5):693–702, 2009. Cited on page 30.

[19] A. L. Brass, E. Kehrli, C. F. Eisenbeis, U. Storb, and H. Singh. Pip, a lymphoid-restricted irf, contains a regulatory domain that is important for autoinhibition and ternary complex formation with the ets factor pu. 1. *Genes & development*, 10(18):2335–2347, 1996. Cited on page 34.

[20] S. Brown, I. Heinisch, E. Ross, K. Shaw, C. D. Buckley, and J. Savill. Apoptosis disables cd31-mediated cell detachment from phagocytes promoting binding and engulfment. *Nature*, 418(6894):200–203, 2002. Cited on page 25.

[21] A. Brüstle, S. Heink, M. Huber, C. Rosenplänter, C. Stadelmann, P. Yu, E. Arpaia, T. W. Mak, T. Kamradt, and M. Lohoff. The development of inflammatory th-17 cells requires interferon-regulatory factor 4. *Nature immunology*, 8(9):958–966, 2007. Cited on page 36, 37, 116, and 137.

[22] N. a. Buchmeier and R. D. Schreiber. Requirement of endogenous interferon-gamma production for resolution of Listeria monocytogenes infection. *Proceedings of the National Academy of Sciences of the United States of America*, 82(21):7404–7408, 1985. Cited on page 32.

[23] D. H. Busch and E. G. Pamer. MHC class I/peptide stability: implications for immunodominance, in vitro proliferation, and diversity of responding CTL. *Journal of immunology (Baltimore, Md. : 1950)*, 160(9):4441–4448, 1998. Cited on page 30.

[24] D. H. Busch and E. G. Pamer. T lymphocyte dynamics during Listeria monocytogenes infection. *Immunology letters*, 65(1-2):93–98, 1999. Cited on page 20.

[25] D. H. Busch, I. M. Pilip, S. Vijh, and E. G. Pamer. Coordinate regulation of complex T-cell populations responding to bacterial infection. *Immunity*, 8:353–362, 1998. Cited on page 23.

[26] J. L. Cannons, S. G. Tangye, and P. L. Schwartzberg. Slam family receptors and sap adaptors in immunity. *Annual review of immunology*, 29:665–705, 2011. Cited on page 25.

[27] Y. Cao, H. Li, Y. Sun, X. Chen, H. Liu, X. Gao, and X. Liu. Interferon regulatory factor 4 regulates thymocyte differentiation by repressing Runx3 expression. *European Journal of Immunology*, 40(11):3198–3209, 2010. Cited on page 36, 99, and 116.

[28] B. M. Carreno and M. Collins. The b7 family of ligands and its receptors: new pathways for costimulation and inhibition of immune responses. *Annual review of immunology*, 20(1):29–53, 2002. Cited on page 25.

[29] P. E. Carrington, C. Sandu, Y. Wei, J. M. Hill, G. Morisawa, T. Huang, E. Gavathiotis, Y. Wei, and M. H. Werner. The structure of fadd and its mode of interaction with procaspase-8. *Molecular cell*, 22(5):599–610, 2006. Cited on page 90.

[30] M. C. Carroll. The complement system in regulation of adaptive immunity. *Nature immunology*, 5(10):981–986, 2004. Cited on page 27.

[31] L. Chavez-Galan, M. Arenas-Del Angel, E. Zenteno, R. Chavez, and R. Lascurain. Cell death mechanisms induced by cytotoxic lymphocytes. *Cellular & molecular immunology*, 6(1):15–25, 2009. Cited on page 122.

[32] B. J. W. Conlan and R. J. North. Neutrophils Are Essential for Early. 179 (January), 1994. Cited on page 32.

[33] J. Conlan. Early pathogenesis of listeria monocytogenes infection in the mouse spleen. *Journal of medical microbiology*, 44(4):295–302, 1996. Cited on page 32.

[34] P. Cossart and C. Kocks. The actin-based motility of the facultative intracellular pathogen Listeria monocytogenes. *Molecular Microbiology*, 13(3):395–402, 1994. Cited on page 30.

[35] E. Cretney, A. Xin, W. Shi, M. Minnich, F. Masson, M. Miasari, G. T. Belz, G. K. Smyth, M. Busslinger, S. L. Nutt, et al. The transcription factors blimp-1 and irf4 jointly control the differentiation and function of effector regulatory t cells. *Nature immunology*, 12(4):304–311, 2011. Cited on page 36.

[36] J. M. Curtsinger, C. S. Schmidt, a. Mondino, D. C. Lins, R. M. Kedl, M. K. Jenkins, and M. F. Mescher. Inflammatory cytokines provide a third signal for activation of naive CD4+ and CD8+ T cells. *Journal of immunology (Baltimore, Md. : 1950)*, 162(6):3256–3262, 1999. Cited on page 20.

[37] J. M. Curtsinger, C. M. Johnson, and M. F. Mescher. CD8 T cell clonal expansion and development of effector function require prolonged exposure to antigen, costimulation, and signal 3 cytokine. *Journal of immunology (Baltimore, Md. : 1950)*, 171(10):5165–5171, 2003. Cited on page 20.

[38] J. M. Curtsinger, J. O. Valenzuela, P. Agarwal, D. Lins, and M. F. Mescher. Type I IFNs provide a third signal to CD8 T cells to stimulate clonal expansion and differentiation. *Journal of immunology (Baltimore, Md. : 1950)*, 174(8):4465–4469, 2005. Cited on page 22.

[39] P. E. Czabotar, G. Lessene, A. Strasser, and J. M. Adams. Control of apoptosis by the bcl-2 protein family: implications for physiology and therapy. *Nature reviews*

Molecular cell biology, 15(1):49–63, 2014. Cited on page 25.

[40] J. Darnell, I. M. Kerr, and G. R. Stark. Jak-stat pathways and transcriptional activation in response to ifns and other extracellular signaling proteins. *Science*, 264(5164):1415–1421, 1994. Cited on page 34.

[41] M. P. Davenport, D. A. Price, and A. J. McMichael. The t cell repertoire in infection and vaccination: implications for control of persistent viruses. *Current opinion in immunology*, 19(3):294–300, 2007. Cited on page 20.

[42] C. L. Day, D. E. Kaufmann, P. Kiepiela, J. A. Brown, E. S. Moodley, S. Reddy, E. W. Mackey, J. D. Miller, A. J. Leslie, C. DePierres, et al. Pd-1 expression on hiv-specific t cells is associated with t-cell exhaustion and disease progression. *nature*, 443(7109):350–354, 2006. Cited on page 129.

[43] L. M. D'Cruz, M. P. Rubinstein, and A. W. Goldrath. Surviving the crash: transitioning from effector to memory cd8+ t cell. In *Seminars in immunology*, volume 21, pages 92–98. Elsevier, 2009. Cited on page 25 and 133.

[44] A. E. Denton, R. Wesselingh, S. Gras, C. Guillonneau, M. R. Olson, J. D. Mintern, W. Zeng, D. C. Jackson, J. Rossjohn, P. D. Hodgkin, et al. Affinity thresholds for naive cd8+ ctl activation by peptides and engineered influenza a viruses. *The Journal of Immunology*, 187(11):5733–5744, 2011. Cited on page 130.

[45] J. Dietrich, a. Neisig, X. Hou, a. M. Wegener, M. Gajhede, and C. Geisler. Role of CD3 gamma in T cell receptor assembly. *The Journal of cell biology*, 132(3): 299–310, 1996. Cited on page 18.

[46] O. Disson, G. Nikitas, S. Grayo, O. Dussurget, P. Cossart, and M. Lecuit. Modeling human listeriosis in natural and genetically engineered animals. *Nature protocols*, 4(6):799–810, 2009. Cited on page 30.

[47] P. L. Dunn and R. J. North. Early gamma interferon production by natural killer cells is important in defense against murine listeriosis. *Infection and Immunity*, 59(9):2892–2900, 1991. Cited on page 32.

[48] C. F. Eisenbeis, H. Singh, and U. Storb. Pip, a novel irf family member, is a lymphoid-specific, pu. 1-dependent transcriptional activator. *Genes & Development*, 9(11):1377–1387, 1995. Cited on page 34 and 118.

[49] M. R. Elliott, F. B. Chekeni, P. C. Trampont, E. R. Lazarowski, A. Kadl, S. F. Walk, D. Park, R. I. Woodson, M. Ostankovich, P. Sharma, et al. Nucleotides released by apoptotic cells act as a find-me signal to promote phagocytic clearance. *Nature*, 461(7261):282–286, 2009. Cited on page 25.

[50] K. Elward and P. Gasque. "eat me" and "don't eat me" signals govern the innate immune response and tissue repair in the cns: emphasis on the critical role of the complement system. *Molecular immunology*, 40(2):85–94, 2003. Cited on page 25.

[51] K. Elward, M. Griffiths, M. Mizuno, C. L. Harris, J. W. Neal, B. P. Morgan, and P. Gasque. Cd46 plays a key role in tailoring innate immune recognition of apoptotic and necrotic cells. *Journal of Biological Chemistry*, 280(43):36342–36354, 2005. Cited on page 25.

[52] J. A. Ember and T. E. Hugli. Complement factors and their receptors. *Immunopharmacology*, 38(1):3–15, 1997. Cited on page 27.

[53] C. L. Ewen, K. P. Kane, and R. C. Bleackley. A quarter century of granzymes. *Cell Death and Differentiation*, 19(1):28–35, 2012. Cited on page 20.

[54] G. Fousteri, A. Dave, A. Juedes, T. Juntti, B. Morin, L. Togher, D. L. Farber, and M. von Herrath. Increased memory conversion of naive cd8 t cells activated during late phases of acute virus infection due to decreased cumulative antigen exposure. *PloS one*, 6(1):e14502, 2011. Cited on page 20.

[55] L. M. Francisco, P. T. Sage, and A. H. Sharpe. The pd-1 pathway in tolerance and autoimmunity. *Immunological reviews*, 236(1):219–242, 2010. Cited on page 129.

[56] M. Fukuda et al. Lysosomal membrane glycoproteins. structure, biosynthesis, and intracellular trafficking. *J Biol Chem*, 266(32):21327–21330, 1991. Cited on page 123.

[57] C. Gaboriaud, N. M. Thielens, L. A. Gregory, V. Rossi, J. C. Fontecilla-Camps, and G. J. Arlaud. Structure and activation of the c1 complex of complement: unraveling the puzzle. *Trends in immunology*, 25(7):368–373, 2004. Cited on page 27.

[58] L. Galluzzi, I. Vitale, J. Abrams, E. Alnemri, E. Baehrecke, M. Blagosklonny, T. Dawson, V. Dawson, W. El-Deiry, S. Fulda, et al. Molecular definitions of cell death subroutines: recommendations of the nomenclature committee on cell death 2012. *Cell Death & Differentiation*, 19(1):107–120, 2012. Cited on page 24.

[59] S. J. Gardai, K. A. McPhillips, S. C. Frasch, W. J. Janssen, A. Starefeldt, J. E. Murphy-Ullrich, D. L. Bratton, P.-A. Oldenborg, M. Michalak, and P. M. Henson. Cell-surface calreticulin initiates clearance of viable or apoptotic cells through trans-activation of lrp on the phagocyte. *Cell*, 123(2):321–334, 2005. Cited on page 25.

[60] M. M. Gedde, D. E. Higgins, L. G. Tilney, and D. a. Portnoy. Role of listeriolysin O in cell-to-cell spread of Listeria monocytogenes. *Infection and Immunity*, 68(2): 999–1003, 2000. Cited on page 30.

[61] J. Gerdes, H. Lemke, H. Baisch, H.-H. Wacker, U. Schwab, and H. Stein. Cell cycle analysis of a cell proliferation-associated human nuclear antigen defined by the monoclonal antibody ki-67. *The Journal of Immunology*, 133(4):1710–1715, 1984. Cited on page 69 and 119.

[62] R. N. Germain. MHC-dependent antigen processing and peptide presentation: Providing ligans for T lymphocyte activation. *Cell*, 76:287–299, 1994. Cited on page 18.

[63] R. N. Germain. T-cell development and the cd4–cd8 lineage decision. *Nature Reviews Immunology*, 2(5):309–322, 2002. Cited on page 19 and 115.

[64] J. G. Giri, D. M. Anderson, S. Kumaki, L. S. Park, K. H. Grabstein, and D. Cosman. IL-15, a novel T cell growth factor that shares activities and receptor components with IL-2. *Journal of leukocyte biology*, 57(5):763–766, 1995. Cited on page 22 and 105.

[65] E. Glasmacher, S. Agrawal, A. B. Chang, T. L. Murphy, W. Zeng, B. Vander Lugt, A. A. Khan, M. Ciofani, C. J. Spooner, S. Rutz, et al. A genomic regulatory element that directs assembly and function of immune-specific ap-1–irf complexes.

Science, 338(6109):975–980, 2012. Cited on page 35.

[66] A. C. Goldberg and L. V. Rizzo. Mhc structure and function–antigen presentation. part 1. *Einstein (São Paulo)*, 13(1):153–156, 2015. Cited on page 20.

[67] A. W. Goldrath and M. J. Bevan. Selecting and maintaining a diverse T-cell repertoire. *Nature*, 402(6759):255–262, 1999. Cited on page 18.

[68] A. W. Goldrath, P. V. Sivakumar, M. Glaccum, M. K. Kennedy, M. J. Bevan, C. Benoist, D. Mathis, and E. a. Butz. Cytokine requirements for acute and Basal homeostatic proliferation of naive and memory CD8+ T cells. *The Journal of experimental medicine*, 195(12):1515–1522, 2002. Cited on page 22.

[69] P. L. Goossens and G. Milon. Induction of protective CD8+ T lymphocytes by an attenuated Listeria monocytogenes actA mutant. *International immunology*, 4 (12):1413–1418, 1992. Cited on page 30.

[70] C. D. Gregory. Cd14-dependent clearance of apoptotic cells: relevance to the immune system. *Current opinion in immunology*, 12(1):27–34, 2000. Cited on page 25.

[71] M. Hamon, H. Bierne, and P. Cossart. Listeria monocytogenes: a multifaceted model. *Nature reviews. Microbiology*, 4(6):423–434, 2006. Cited on page 29.

[72] R. Hanayama, M. Tanaka, K. Miwa, A. Shinohara, A. Iwamatsu, and S. Nagata. Identification of a factor that links apoptotic cells to phagocytes. *Nature*, 417 (6885):182–187, 2002. Cited on page 25 and 133.

[73] H. Harada, T. Fujita, M. Miyamoto, Y. Kimura, M. Maruyama, A. Furia, T. Miyata, and T. Taniguchi. Structurally similar but functionally distinct factors, irf-1 and irf-2, bind to the same regulatory elements of ifn and ifn-inducible genes. *Cell*, 58(4):729–739, 1989. Cited on page 34.

[74] M. Harboe and T. E. Mollnes. The alternative complement pathway revisited. *Journal of cellular and molecular medicine*, 12(4):1074–1084, 2008. Cited on page 27.

[75] J. T. Harty and M. J. Bevan. Responses of CD8(+) T cells to intracellular bacteria. *Current opinion in immunology*, 11(1):89–93, 1999. Cited on page 21.

[76] H. Hassan, S. Sakaguchi, M. Tenno, A. Kopf, N. Boucheron, A. C. Carpenter, T. Egawa, I. Taniuchi, and W. Ellmeier. Cd8 enhancer e8i and runx factors regulate cd8α expression in activated cd8+ t cells. *Proceedings of the National Academy of Sciences*, 108(45):18330–18335, 2011. Cited on page 62.

[77] E. a. Havell. Evidence that tumor necrosis factor has an important role in antibacterial resistance. *Journal of immunology (Baltimore, Md. : 1950)*, 143(9): 2894–2899, 1989. Cited on page 32.

[78] W. R. Heath and J. F. Miller. Expression of two alpha chains on the surface of T cells in T cell receptor transgenic mice. *The Journal of experimental medicine*, 178(5):1807–1811, 1993. Cited on page 48.

[79] J. W. Heusel, J. W. Heusel, R. L. Wesselschmidt, R. L. Wesselschmidt, S. Shresta, S. Shresta, J. H. Russell, J. H. Russell, T. J. Ley, and T. J. Ley. Cytotoxic lymphocytes require granzyme B for the rapid induction of DNA fragmentation

and apoptosis in allogenic target cells. *Cell*, 76(1980):989–1000, 1994. Cited on page 21.

[80] D. A. Hildeman, Y. Zhu, T. C. Mitchell, J. Kappler, and P. Marrack. Molecular mechanisms of activated t cell death in vivo. *Current opinion in immunology*, 14 (3):354–359, 2002. Cited on page 103.

[81] R. Hingorani, B. Bi, T. Dao, Y. Bae, A. Matsuzawa, and I. N. Crispe. Cd95/fas signaling in t lymphocytes induces the cell cycle control protein p21cip-1/waf-1, which promotes apoptosis. *The Journal of Immunology*, 164(8):4032–4036, 2000. Cited on page 27.

[82] A. Hochreiter-Hufford and K. S. Ravichandran. Clearing the dead: apoptotic cell sensing, recognition, engulfment, and digestion. *Cold Spring Harbor perspectives in biology*, 5(1):a008748, 2013. Cited on page 26.

[83] R. H. Hoess and K. Abremski. Interaction of the bacteriophage p1 recombinase cre with the recombining site loxp. *Proceedings of the National Academy of Sciences*, 81(4):1026–1029, 1984. Cited on page 115.

[84] R. H. Hoess, A. Wierzbicki, and K. Abremski. The role of the loxp spacer region in pi site-specific recombination. *Nucleic acids research*, 14(5):2287–2300, 1986. Cited on page 115.

[85] K. Honma, D. Kimura, N. Tominaga, M. Miyakoda, T. Matsuyama, and K. Yui. Interferon regulatory factor 4 differentially regulates the production of th2 cytokines in naive vs. effector/memory cd4+ t cells. *Proceedings of the National Academy of Sciences*, 105(41):15890–15895, 2008. Cited on page 116.

[86] M. Huber and M. Lohoff. Irf4 provides rations for cytotoxic cd8+ t cell soldiers. *Immunity*, 39(5):797–799, 2013. Cited on page 36, 61, 99, 115, and 137.

[87] M. Huber, A. Brüstle, K. Reinhard, A. Guralnik, G. Walter, A. Mahiny, E. von Löw, and M. Lohoff. Irf4 is essential for il-21-mediated induction, amplification, and stabilization of the th17 phenotype. *Proceedings of the National Academy of Sciences*, 105(52):20846–20851, 2008. Cited on page 36 and 137.

[88] H. Ichii, A. Sakamoto, M. Hatano, S. Okada, H. Toyama, S. Taki, M. Arima, Y. Kuroda, and T. Tokuhisa. Role for Bcl-6 in the generation and maintenance of memory CD8+ T cells. *Nature immunology*, 3(6):558–563, 2002. Cited on page 23.

[89] G. Iezzi, K. Karjalainen, and A. Lanzavecchia. The duration of antigenic stimulation determines the fate of naive and effector T cells. *Immunity*, 8(1):89–95, 1998. Cited on page 20 and 24.

[90] S. Iida, P. H. Rao, M. Butler, P. Corradini, M. Boccadoro, B. Klein, R. Chaganti, and R. Dalla-Favera. Deregulation of mum1/irf4 by chromosomal translocation in multiple myeloma. *Nature genetics*, 17(2):226–230, 1997. Cited on page 35.

[91] A. M. Intlekofer, N. Takemoto, E. J. Wherry, S. a. Longworth, J. T. Northrup, V. R. Palanivel, A. C. Mullen, C. R. Gasink, S. M. Kaech, J. D. Miller, L. Gapin, K. Ryan, A. P. Russ, T. Lindsten, J. S. Orange, A. W. Goldrath, R. Ahmed, and S. L. Reiner. Effector and memory CD8+ T cell fate coupled by T-bet and eomesodermin. *Nature immunology*, 6(12):1236–1244, 2005. Cited on page 23, 82, 123, and 124.

[92] N. Itoh and S. Nagata. A novel protein domain required for apoptosis. mutational analysis of human fas antigen. *Journal of Biological Chemistry*, 268(15):10932–10937, 1993. Cited on page 26.

[93] S. C. Jameson and D. Masopust. Diversity in T Cell Memory: An Embarrassment of Riches. *Immunity*, 31(6):859–871, 2009. Cited on page 23.

[94] M. L. Janas, P. Groves, N. Kienzle, and A. Kelso. IL-2 regulates perforin and granzyme gene expression in CD8+ T cells independently of its effects on survival and proliferation. *Journal of immunology (Baltimore, Md. : 1950)*, 175(12):8003–8010, 2005. Cited on page 22.

[95] R. B. Jones, L. C. Ndhlovu, J. D. Barbour, P. M. Sheth, A. R. Jha, B. R. Long, J. C. Wong, M. Satkunarajah, M. Schweneker, J. M. Chapman, et al. Tim-3 expression defines a novel population of dysfunctional t cells with highly elevated frequencies in progressive hiv-1 infection. *The Journal of experimental medicine*, 205(12):2763–2779, 2008. Cited on page 94 and 129.

[96] N. S. Joshi, W. Cui, A. Chandele, H. K. Lee, D. R. Urso, J. Hagman, L. Gapin, and S. M. Kaech. Inflammation Directs Memory Precursor and Short-Lived Effector CD8+ T Cell Fates via the Graded Expression of T-bet Transcription Factor. *Immunity*, 27(2):281–295, 2007. Cited on page 123.

[97] N. S. Joshi, W. Cui, A. Chandele, H. K. Lee, D. R. Urso, J. Hagman, L. Gapin, and S. M. Kaech. Inflammation directs memory precursor and short-lived effector cd8+ t cell fates via the graded expression of t-bet transcription factor. *Immunity*, 27(2):281–295, 2007. Cited on page 22, 23, 25, and 134.

[98] M. Józsi. *Anti-complement autoantibodies in membranoproliferative glomerulonephritis and dense deposit disease*. INTECH Open Access Publisher, 2011. Cited on page 28.

[99] S.-T. Ju, D. J. Panka, H. Cui, R. Ettinger, M. Ei-Khatib, D. H. Sherr, B. Z. Stanger, and A. Marshak-Rothstein. Fas (cd95)/fasl interactions required for programmed cell death after t-cell activation. *Nature*, 373(6513):444–448, 1995. Cited on page 133.

[100] S. M. Kaech and W. Cui. Transcriptional control of effector and memory cd8+ t cell differentiation. *Nature Reviews Immunology*, 12(11):749–761, 2012. Cited on page 20, 23, and 124.

[101] S. M. Kaech, J. T. Tan, E. J. Wherry, B. T. Konieczny, C. D. Surh, and R. Ahmed. Selective expression of the interleukin 7 receptor identifies effector CD8 T cells that give rise to long-lived memory cells. *Nature immunology*, 4(12):1191–1198, 2003. Cited on page 22 and 120.

[102] D. Kägi, B. Ledermann, K. Bürki, H. Hengartner, and R. M. Zinkernagel. Cd8+ t cell-mediated protection against an intracellular bacterium by perforin-dependent cytotoxicity. *European journal of immunology*, 24(12):3068–3072, 1994. Cited on page 20.

[103] A. Kallies, A. Xin, G. T. Belz, and S. L. Nutt. Blimp-1 Transcription Factor Is Required for the Differentiation of Effector CD8+ T Cells and Memory Responses. *Immunity*, 31(2):283–295, 2009. Cited on page 23.

[104] T. Kambayashi, E. Assarsson, B. J. Chambers, and H.-G. Ljunggren. Cutting edge: regulation of cd8+ t cell proliferation by 2b4/cd48 interactions. *The Journal of Immunology*, 167(12):6706–6710, 2001. Cited on page 128.

[105] Y. Kanno, B.-Z. Levi, T. Tamura, and K. Ozato. Immune cell-specific amplification of interferon signaling by the irf-4/8-pu. 1 complex. *Journal of interferon & cytokine research*, 25(12):770–779, 2005. Cited on page 35.

[106] C. Kao, K. J. Oestreich, M. A. Paley, A. Crawford, J. M. Angelosanto, M.-A. A. Ali, A. M. Intlekofer, J. M. Boss, S. L. Reiner, A. S. Weinmann, et al. Transcription factor t-bet represses expression of the inhibitory receptor pd-1 and sustains virus-specific cd8+ t cell responses during chronic infection. *Nature immunology*, 12(7): 663–671, 2011. Cited on page 123.

[107] D. E. Kaufmann, D. G. Kavanagh, F. Pereyra, J. J. Zaunders, E. W. Mackey, T. Miura, S. Palmer, M. Brockman, A. Rathod, A. Piechocka-Trocha, et al. Upregulation of ctla-4 by hiv-specific cd4+ t cells correlates with disease progression and defines a reversible immune dysfunction. *Nature immunology*, 8(11):1246–1254, 2007. Cited on page 128.

[108] S. H. Kaufmann and G. Kaplan. Immunity to intracellular bacteria [editorial]. *Research in Immunology*, 147(8-9):487–489, 1996. Cited on page 29, 32, and 121.

[109] M. E. Keir, M. J. Butte, G. J. Freeman, and A. H. Sharpe. Pd-1 and its ligands in tolerance and immunity. *Annu. Rev. Immunol.*, 26:677–704, 2008. Cited on page 129.

[110] J. M. Kelly, S. J. Sterry, S. Cose, S. J. Turner, J. Fecondo, S. Rodda, P. J. Fink, and F. R. Carbone. Identification of conserved T cell receptor CDR3 residues contacting known exposed peptide side chains from a major histocompatibility complex class I-bound determinant. *European journal of immunology*, 23(12): 3318–3326, 1993. Cited on page 48.

[111] S. J. Keppler, K. Theil, S. Vucikuja, and P. Aichele. Effector T-cell differentiation during viral and bacterial infections: Role of direct IL-12 signals for cell fate decision of CD8+ T cells. *European Journal of Immunology*, 39(7):1774–1783, 2009. Cited on page 22.

[112] C. G. King, S. Koehli, B. Hausmann, M. Schmaler, D. Zehn, and E. Palmer. T Cell Affinity Regulates Asymmetric Division, Effector Cell Differentiation, and Tissue Pathology. *Immunity*, 37(4):709–720, 2012. Cited on page 20 and 130.

[113] U. Klein, S. Casola, G. Cattoretti, Q. Shen, M. Lia, T. Mo, T. Ludwig, K. Rajewsky, and R. Dalla-Favera. Transcription factor IRF4 controls plasma cell differentiation and class-switch recombination. *Nature immunology*, 7(7):773–782, 2006. Cited on page 36, 37, 48, 62, and 115.

[114] A. Klos, E. Wende, K. J. Wareham, and P. N. Monk. International union of basic and clinical pharmacology. lxxxvii. complement peptide c5a, c4a, and c3a receptors. *Pharmacological reviews*, 65(1):500–543, 2013. Cited on page 27.

[115] K. Kohu, T. Sato, S.-i. Ohno, K. Hayashi, R. Uchino, N. Abe, M. Nakazato, N. Yoshida, T. Kikuchi, Y. Iwakura, et al. Overexpression of the runx3 transcription factor increases the proportion of mature thymocytes of the cd8 single-positive

lineage. *The Journal of Immunology*, 174(5):2627–2636, 2005. Cited on page 116.

[116] G. a. Kolumam, S. Thomas, L. J. Thompson, J. Sprent, and K. Murali-Krishna. Type I interferons act directly on CD8 T cells to allow clonal expansion and memory formation in response to viral infection. *The Journal of experimental medicine*, 202(5):637–650, 2005. Cited on page 22.

[117] X. Kong, A. Banks, T. Liu, L. Kazak, R. R. Rao, P. Cohen, X. Wang, S. Yu, J. C. Lo, Y.-H. Tseng, et al. Irf4 is a key thermogenic transcriptional partner of pgc-1α. *Cell*, 158(1):69–83, 2014. Cited on page 35.

[118] P. H. Krammer, R. Arnold, and I. N. Lavrik. Life and death in peripheral t cells. *Nature Reviews Immunology*, 7(7):532–542, 2007. Cited on page 25 and 133.

[119] K. Krzewski, A. Gil-Krzewska, V. Nguyen, G. Peruzzi, and J. E. Coligan. Lamp1/cd107a is required for efficient perforin delivery to lytic granules and nk-cell cytotoxicity. *Blood*, 121(23):4672–4683, 2013. Cited on page 123.

[120] M. S. Kuhns, M. M. Davis, and K. C. Garcia. Deconstructing the form and function of the TCR/CD3 complex. *Immunity*, 24(2):133–139, 2006. Cited on page 18.

[121] M. Kurachi, R. A. Barnitz, N. Yosef, P. M. Odorizzi, M. a. DiIorio, M. E. Lemieux, K. Yates, J. Godec, M. G. Klatt, A. Regev, E. J. Wherry, and W. N. Haining. The transcription factor BATF operates as an essential differentiation checkpoint in early effector CD8+ T cells. *Nature immunology*, 15(4):373–83, 2014. Cited on page 124.

[122] H. Kwon, D. Thierry-Mieg, J. Thierry-Mieg, H.-P. Kim, J. Oh, C. Tunyaplin, S. Carotta, C. E. Donovan, M. L. Goldman, P. Tailor, et al. Analysis of interleukin-21-induced prdm1 gene regulation reveals functional cooperation of stat3 and irf4 transcription factors. *Immunity*, 31(6):941–952, 2009. Cited on page 35.

[123] N. Labrecque, L. S. Whitfield, R. Obst, C. Waltzinger, C. Benoist, and D. Mathis. How much TCR does a T cell need? *Immunity*, 15(1):71–82, 2001. Cited on page 20.

[124] C. H. Ladel, I. E. Flesch, J. Arnoldi, and S. H. Kaufmann. Studies with MHC-deficient knock-out mice reveal impact of both MHC I- and MHC II-dependent T cell responses on Listeria monocytogenes infection. *Journal of immunology (Baltimore, Md. : 1950)*, 153(7):3116–3122, 1994. Cited on page 32.

[125] a. Lalvani, R. Brookes, S. Hambleton, W. J. Britton, a. V. Hill, and a. J. McMichael. Rapid effector function in CD8+ memory T cells. *The Journal of experimental medicine*, 186(6):859–865, 1997. Cited on page 24.

[126] M. Lam, G. Dubyak, L. Chen, G. Nunez, R. L. Miesfeld, and C. W. Distelhorst. Evidence that bcl-2 represses apoptosis by regulating endoplasmic reticulum-associated ca2+ fluxes. *Proceedings of the National Academy of Sciences*, 91(14): 6569–6573, 1994. Cited on page 25.

[127] J. F. Lau, J.-P. Parisien, and C. M. Horvath. Interferon regulatory factor subcellular localization is determined by a bipartite nuclear localization signal in the dna-binding domain and interaction with cytoplasmic retention factors. *Proceedings of the National Academy of Sciences*, 97(13):7278–7283, 2000. Cited on page 35.

[128] A. Le Monnier, N. Autret, O. F. Join-Lambert, F. Jaubert, A. Charbit, P. Berche, and S. Kayal. ActA is required for crossing of the fetoplacental barrier by Listeria monocytogenes. *Infection and Immunity*, 75(2):950–957, 2007. Cited on page 29.

[129] M. Lecuit, S. Vandormael-Pournin, J. Lefort, M. Huerre, P. Gounon, C. Dupuy, C. Babinet, and P. Cossart. A transgenic model for listeriosis: role of internalin in crossing the intestinal barrier. *Science (New York, N.Y.)*, 292(5522):1722–1725, 2001. Cited on page 30.

[130] P. P. Lee, D. R. Fitzpatrick, C. Beard, H. K. Jessup, S. Lehar, K. W. Makar, M. Pérez-Melgosa, M. T. Sweetser, M. S. Schlissel, S. Nguyen, et al. A critical role for dnmt1 and dna methylation in t cell development, function, and survival. *Immunity*, 15(5):763–774, 2001. Cited on page 115.

[131] P. J. Leibson. The regulation of lymphocyte activation by inhibitory receptors. *Current opinion in immunology*, 16(3):328–336, 2004. Cited on page 128.

[132] G. Lemke and C. V. Rothlin. Immunobiology of the tam receptors. *Nature Reviews Immunology*, 8(5):327–336, 2008. Cited on page 26.

[133] W. J. Leonard, E. W. Shores, and P. E. Love. Role of the common cytokine receptor gamma chain in cytokine signaling and lymphoid development. *Immunological reviews*, 148(148):97–114, 1995. Cited on page 22.

[134] K. Li, K. J. Anderson, Q. Peng, A. Noble, B. Lu, A. P. Kelly, N. Wang, S. H. Sacks, and W. Zhou. Cyclic amp plays a critical role in c3a-receptor–mediated regulation of dendritic cells in antigen uptake and t-cell stimulation. *Blood*, 112 (13):5084–5094, 2008. Cited on page 29.

[135] P. Li, R. Spolski, W. Liao, L. Wang, T. L. Murphy, K. M. Murphy, and W. J. Leonard. Batf-jun is critical for irf4-mediated transcription in t cells. *Nature*, 490 (7421):543–546, 2012. Cited on page 35.

[136] C.-C. Liu, C. M. Walsh, and J. D.-E. Young. Perforin: structure and function. *Immunology today*, 16(4):194–201, 1995. Cited on page 122.

[137] M. Lohoff and T. W. Mak. Roles of interferon-regulatory factors in T-helper-cell differentiation. *Nature reviews. Immunology*, 5(2):125–135, 2005. Cited on page 35.

[138] M. Lohoff, H.-W. Mittrücker, S. Prechtl, S. Bischof, F. Sommer, S. Kock, D. a. Ferrick, G. S. Duncan, A. Gessner, and T. W. Mak. Dysregulated T helper cell differentiation in the absence of interferon regulatory factor 4. *Proceedings of the National Academy of Sciences of the United States of America*, 99(18):11808–11812, 2002. Cited on page 36, 116, and 137.

[139] M. Lohoff, H.-W. Mittrücker, S. Prechtl, S. Bischof, F. Sommer, S. Kock, D. A. Ferrick, G. S. Duncan, A. Gessner, and T. W. Mak. Dysregulated t helper cell differentiation in the absence of interferon regulatory factor 4. *Proceedings of the National Academy of Sciences*, 99(18):11808–11812, 2002. Cited on page 37.

[140] N. J. MacIver, R. D. Michalek, and J. C. Rathmell. Metabolic regulation of t lymphocytes. *Annual review of immunology*, 31:259, 2013. Cited on page 23.

[141] Y. Maekawa, Y. Minato, C. Ishifune, T. Kurihara, A. Kitamura, H. Kojima, H. Yagita, M. Sakata-Yanagimoto, T. Saito, I. Taniuchi, S. Chiba, S. Sone, and

K. Yasutomo. Notch2 integrates signaling by the transcription factors RBP-J and CREB1 to promote T cell cytotoxicity. *Nature immunology*, 9(10):1140–1147, 2008. Cited on page 48.

[142] K. Man, M. Miasari, W. Shi, A. Xin, D. C. Henstridge, S. Preston, M. Pellegrini, G. T. Belz, G. K. Smyth, M. a. Febbraio, S. L. Nutt, and A. Kallies. The transcription factor IRF4 is essential for TCR affinity-mediated metabolic programming and clonal expansion of T cells. *Nature immunology*, 14(11):1155–65, 2013. Cited on page 36, 61, 99, 115, 116, 118, 120, 122, 123, 126, 128, 129, 130, and 137.

[143] S. Marecki, M. L. Atchison, and M. J. Fenton. Differential expression and distinct functions of ifn regulatory factor 4 and ifn consensus sequence binding protein in macrophages. *The Journal of Immunology*, 163(5):2713–2722, 1999. Cited on page 35.

[144] P. Marrack and J. Kappler. Control of t cell viability. *Annu. Rev. Immunol.*, 22: 765–787, 2004. Cited on page 25, 103, and 133.

[145] S. Martin, C. Reutelingsperger, A. J. McGahon, J. A. Rader, R. Van Schie, D. M. LaFace, and D. R. Green. Early redistribution of plasma membrane phosphatidylserine is a general feature of apoptosis regardless of the initiating stimulus: inhibition by overexpression of bcl-2 and abl. *The Journal of experimental medicine*, 182(5):1545–1556, 1995. Cited on page 25, 91, and 127.

[146] T. Matsuyama, A. Grossman, H.-W. Mittrücker, D. P. Siderovski, F. Kiefer, T. Kawakami, C. D. Richardson, T. Taniguchi, S. K. Yoshinaga, and T. W. Mak. Molecular cloning of lsirf, a lymphoid-specific member of the interferon regulatory factor family that binds the interferon-stimulated response element (isre). *Nucleic acids research*, 23(12):2127–2136, 1995. Cited on page 34, 61, and 118.

[147] a. J. McAdam, a. N. Schweitzer, and a. H. Sharpe. The role of B7 co-stimulation in activation and differentiation of CD4+ and CD8+ T cells. *Immunological reviews*, 165:231–247, 1998. Cited on page 20.

[148] K. K. McKinstry, T. M. Strutt, and S. L. Swain. Regulation of cd4+ t-cell contraction during pathogen challenge. *Immunological reviews*, 236(1):110–124, 2010. Cited on page 25.

[149] L. M. McLane, P. P. Banerjee, G. L. Cosma, G. Makedonas, E. J. Wherry, J. S. Orange, and M. R. Betts. Differential localization of t-bet and eomes in cd8 t cell memory populations. *The Journal of Immunology*, 190(7):3207–3215, 2013. Cited on page 82.

[150] D. Meraro, S. Hashmueli, B. Koren, A. Azriel, A. Oumard, S. Kirchhoff, H. Hauser, S. Nagulapalli, M. L. Atchison, and B.-Z. Levi. Protein-protein and dna-protein interactions affect the activity of lymphoid-specific ifn regulatory factors. *The Journal of Immunology*, 163(12):6468–6478, 1999. Cited on page 34.

[151] M. F. Mescher, J. M. Curtsinger, P. Agarwal, K. a. Casey, M. Gerner, C. D. Hammerbeck, F. Popescu, and Z. Xiao. Signals required for programming effector and memory development by CD8+ T cells. *Immunological Reviews*, 211:81–92, 2006. Cited on page 20.

[152] M. Miksa, D. Amin, R. Wu, W. Dong, T. S. Ravikumar, and P. Wang. Fractalkine-induced mfg-e8 leads to enhanced apoptotic cell clearance by macrophages. *Molecular Medicine*, 13(11-12):553, 2007. Cited on page 25.

[153] H.-W. Mittrücker, T. Matsuyama, A. Grossman, T. M. Kündig, J. Potter, A. Shahinian, A. Wakeham, B. Patterson, P. S. Ohashi, and T. W. Mak. Requirement for the transcription factor lsirf/irf4 for mature b and t lymphocyte function. *Science*, 275(5299):540–543, 1997. Cited on page 35, 36, 61, 65, 116, 117, 118, and 137.

[154] M. Miyamoto, T. Fujita, Y. Kimura, M. Maruyama, H. Harada, Y. Sudo, T. Miyata, and T. Taniguchi. Regulated expression of a gene encoding a nuclear factor, irf-1, that specifically binds to ifn-β gene regulatory elements. *Cell*, 54(6):903–913, 1988. Cited on page 34.

[155] T. E. Mollnes, W.-C. Song, and J. D. Lambris. Complement in inflammatory tissue damage and disease. *Trends in immunology*, 23(2):61–64, 2002. Cited on page 27.

[156] B. P. Morgan. The complement system: an overview. In *Complement methods and protocols*, pages 1–13. Springer, 2000. Cited on page 27.

[157] a. Müllbacher. The long-term maintenance of cytotoxic T cell memory does not require persistence of antigen. *The Journal of experimental medicine*, 179(1):317–321, 1994. Cited on page 24.

[158] T. L. Murphy, R. Tussiwand, and K. M. Murphy. Specificity through cooperation: Batf-irf interactions control immune-regulatory networks. *Nature Reviews Immunology*, 13(7):499–509, 2013. Cited on page 35.

[159] E. Murray, R. Webb, and M. Swann. A disease of Rabbits characterised by a large mononuclear Leucocytosis, caused by a hitherto undescribed bacillus Bacterium monocytogenes. *The Journal of Pathology and Bacteriology*, 29(4):407–39, 1926. Cited on page 29.

[160] K. P. Murray, S. Mathure, R. Kaul, S. Khan, L. F. Carson, L. B. Twiggs, M. G. Martens, and A. Kaul. Expression of complement regulatory proteins—cd 35, cd 46, cd 55, and cd 59—in benign and malignant endometrial tissue. *Gynecologic oncology*, 76(2):176–182, 2000. Cited on page 28.

[161] S. Nagata and P. Golstein. The Fas death factor. *Science (New York, N.Y.)*, 267 (5203):1449–1456, 1995. Cited on page 26 and 126.

[162] R. Nayar, M. Enos, A. Prince, H. Shin, S. Hemmers, J.-k. Jiang, and U. Klein. TCR signaling via Tec kinase ITK and interferon T-cell differentiation. *PNAS*, 109(41):16420–16421, 2012. Cited on page 61, 65, 99, 115, 116, 117, 124, 130, and 137.

[163] R. Nayar, E. Schutten, B. Bautista, K. Daniels, A. L. Prince, M. Enos, M. a. Brehm, S. L. Swain, R. M. Welsh, and L. J. Berg. Graded levels of IRF4 regulate CD8+ T cell differentiation and expansion, but not attrition, in response to acute virus infection. *Journal of immunology (Baltimore, Md. : 1950)*, 192(12):5881–93, 2014. Cited on page 36, 61, 99, 115, 118, 120, and 137.

[164] H. Negishi, Y. Ohba, H. Yanai, A. Takaoka, K. Honma, K. Yui, T. Matsuyama,

T. Taniguchi, and K. Honda. Negative regulation of toll-like-receptor signaling by irf-4. *Proceedings of the National Academy of Sciences of the United States of America*, 102(44):15989–15994, 2005. Cited on page 36.

[165] P. Novy, M. Quigley, X. Huang, and Y. Yang. Cd4 t cells are required for cd8 t cell survival during both primary and memory recall responses. *The Journal of Immunology*, 179(12):8243–8251, 2007. Cited on page 116.

[166] H. N. Nowyhed, T. R. Huynh, A. Blatchley, R. Wu, G. D. Thomas, and C. C. Hedrick. The nuclear receptor nr4a1 controls cd8 t cell development through transcriptional suppression of runx3. *Scientific reports*, 5, 2015. Cited on page 61, 115, and 137.

[167] S. L. Nutt and D. M. Tarlinton. Germinal center b and follicular helper t cells: siblings, cousins or just good friends [quest]. *Nature immunology*, 12(6):472–477, 2011. Cited on page 36.

[168] A. Nyfeldt. Etiologie de la mononucleose infectieuse. *CR Soc. Biol*, 101:590–591, 1929. Cited on page 29.

[169] J. J. Obar, E. R. Jellison, B. S. Sheridan, D. a. Blair, Q.-M. Pham, J. M. Zickovich, and L. Lefrançois. Pathogen-induced inflammatory environment controls effector and memory CD8+ T cell differentiation. *Journal of Immunology*, 187(10):4967–4978, 2011. Cited on page 22.

[170] L. O'Connor, A. Strasser, L. A. O'Reilly, G. Hausmann, J. M. Adams, S. Cory, and D. C. Huang. Bim: a novel member of the bcl-2 family that promotes apoptosis. *The EMBO journal*, 17(2):384–395, 1998. Cited on page 25.

[171] P. M. Odorizzi and E. J. Wherry. Inhibitory receptors on lymphocytes: insights from infections. *The Journal of Immunology*, 188(7):2957–2965, 2012. Cited on page 25.

[172] C. A. Ogden, R. Kowalewski, Y. Peng, V. Montenegro, and K. B. Elkon. Igm is required for efficient complement mediated phagocytosis of apoptotic cells in vivo. *Autoimmunity*, 38(4):259–264, 2005. Cited on page 26.

[173] N. Ohkura and S. Sakaguchi. Maturation of effector regulatory t cells. *Nature immunology*, 12(4):283–284, 2011. Cited on page 36.

[174] E. Pamer and P. Cresswell. Mechanisms of MHC class I–restricted antigen processing. *Annual review of immunology*, 16:323–358, 1998. Cited on page 20.

[175] E. G. Pamer. Direct sequence identification and kinetic analysis of an mhc class i-restricted listeria monocytogenes ctl epitope. *The Journal of Immunology*, 152 (2):686–694, 1994. Cited on page 30.

[176] E. G. Pamer. Immune responses to listeria monocytogenes. *Nature Reviews Immunology*, 4(10):812–823, 2004. Cited on page 31, 33, and 121.

[177] E. G. Pamer, J. T. Harty, and M. J. Bevan. Precise prediction of a dominant class i mhc-restricted epitope of listeria monocytogenes. *Nature*, 353(6347):852, 1991. Cited on page 30.

[178] E. G. Pamer, a. J. Sijts, M. S. Villanueva, D. H. Busch, and S. Vijh. MHC class I antigen processing of Listeria monocytogenes proteins: implications for

dominant and subdominant CTL responses. *Immunological reviews*, 158:129–136, 1997. Cited on page 32.

[179] M. Pangburn and H. Müller-Eberhard. Relation of putative thioester bond in c3 to activation of the alternative pathway and the binding of c3b to biological targets of complement. *The Journal of experimental medicine*, 152(4):1102–1114, 1980. Cited on page 27.

[180] T. Patel, G. J. Gores, and S. H. Kaufmann. The role of proteases during apoptosis. *The FASEB journal : official publication of the Federation of American Societies for Experimental Biology*, 10(5):587–597, 1996. Cited on page 21.

[181] E. L. Pearce, A. C. Mullen, G. a. Martins, C. M. Krawczyk, A. S. Hutchins, V. P. Zediak, M. Banica, C. B. DiCioccio, D. a. Gross, C.-A. Mao, H. Shen, N. Cereb, S. Y. Yang, T. Lindsten, J. Rossant, C. a. Hunter, and S. L. Reiner. Control of effector CD8+ T cell function by the transcription factor Eomesodermin. *Science (New York, N.Y.)*, 302(5647):1041–1043, 2003. Cited on page 23 and 82.

[182] C. Peter, S. Wesselborg, and K. Lauber. Molecular suicide notes: last call from apoptosing cells. *Journal of molecular cell biology*, 2(2):78–80, 2010. Cited on page 25.

[183] P. J. Peters, J. Borst, V. Oorschot, M. Fukuda, O. Krähenbühl, J. Tschopp, J. W. Slot, and H. J. Geuze. Cytotoxic t lymphocyte granules are secretory lysosomes, containing both perforin and granzymes. *The Journal of experimental medicine*, 173(5):1099–1109, 1991. Cited on page 123.

[184] M. E. Pipkin, J. A. Sacks, F. Cruz-Guilloty, M. G. Lichtenheld, M. J. Bevan, and A. Rao. Interleukin-2 and inflammation induce distinct transcriptional programs that promote the differentiation of effector cytolytic t cells. *Immunity*, 32(1):79–90, 2010. Cited on page 134.

[185] J. Pongubala, S. Nagulapalli, M. Klemsz, S. McKercher, R. Maki, and M. Atchison. Pu. 1 recruits a second nuclear factor to a site important for immunoglobulin kappa 3'enhancer activity. *Molecular and Cellular Biology*, 12(1):368–378, 1992. Cited on page 34 and 35.

[186] D. Portnoy, T. Chakraborty, W. Goebel, and P. Cossart. Molecular Determinants of Listeria Pathogenesis. *Infection and Immunity*, 60(4):1263–1267, 1992. Cited on page 30.

[187] M. Prlic, G. Hernandez-Hoyos, and M. J. Bevan. Duration of the initial TCR stimulus controls the magnitude but not functionality of the CD8+ T cell response. *The Journal of experimental medicine*, 203(9):2135–2143, 2006. Cited on page 20.

[188] F. Raczkowski, J. Ritter, K. Heesch, V. Schumacher, A. Guralnik, L. Höcker, H. Raifer, M. Klein, T. Bopp, H. Harb, et al. The transcription factor interferon regulatory factor 4 is required for the generation of protective effector cd8+ t cells. *Proceedings of the National Academy of Sciences*, 110(37):15019–15024, 2013. Cited on page 61, 108, 115, 118, 120, 122, 123, 124, 128, 129, 131, 134, 135, and 137.

[189] K. Radulovic, V. Rossini, C. Manta, K. Holzmann, H. A. Kestler, and J. H. Niess. The early activation marker cd69 regulates the expression of chemokines and cd4

t cell accumulation in intestine. 2013. Cited on page 71.

[190] D. Rai, N.-L. L. Pham, J. T. Harty, and V. P. Badovinac. Tracking the total cd8 t cell response to infection reveals substantial discordance in magnitude and kinetics between inbred and outbred hosts. *The Journal of Immunology*, 183(12): 7672–7681, 2009. Cited on page 77 and 121.

[191] K. S. Ravichandran. "recruitment signals" from apoptotic cells: invitation to a quiet meal. *Cell*, 113(7):817–820, 2003. Cited on page 25.

[192] K. S. Ravichandran. Find-me and eat-me signals in apoptotic cell clearance: progress and conundrums. *The Journal of experimental medicine*, 207(9):1807–1817, 2010. Cited on page 25.

[193] K. S. Ravichandran. Beginnings of a good apoptotic meal: the find-me and eat-me signaling pathways. *Immunity*, 35(4):445–455, 2011. Cited on page 25 and 26.

[194] J. C. Renauld, a. Vink, and J. Van Snick. Accessory signals in murine cytolytic T cell responses. Dual requirement for IL-1 and IL-6. *Journal of immunology (Baltimore, Md. : 1950)*, 143(6):1894–1898, 1989. Cited on page 20.

[195] J. Rengarajan, K. A. Mowen, K. D. McBride, E. D. Smith, H. Singh, and L. H. Glimcher. Interferon regulatory factor 4 (irf4) interacts with nfatc2 to modulate interleukin 4 gene expression. *The Journal of experimental medicine*, 195(8):1003–1012, 2002. Cited on page 35.

[196] D. Ricklin, G. Hajishengallis, K. Yang, and J. D. Lambris. Complement: a key system for immune surveillance and homeostasis. *Nature immunology*, 11(9):785–797, 2010. Cited on page 27.

[197] E. Robey and B. J. Fowlkes. Selective events in T cell development. *Annual review of immunology*, 12:675–705, 1994. Cited on page 18.

[198] R. Roozendaal and M. C. Carroll. Complement receptors cd21 and cd35 in humoral immunity. *Immunological reviews*, 219(1):157–166, 2007. Cited on page 29.

[199] F. Sallusto, D. Lenig, R. Förster, M. Lipp, and A. Lanzavecchia. Two subsets of memory t lymphocytes with distinct homing potentials and effector functions. *Nature*, 401(6754):708–712, 1999. Cited on page 23 and 77.

[200] S. Sarkar, V. Kalia, W. N. Haining, B. T. Konieczny, S. Subramaniam, and R. Ahmed. Functional and genomic profiling of effector CD8 T cell subsets with distinct memory fates. *The Journal of experimental medicine*, 205(3):625–640, 2008. Cited on page 22 and 36.

[201] T. Satoh, O. Takeuchi, A. Vandenbon, K. Yasuda, Y. Tanaka, Y. Kumagai, T. Miyake, K. Matsushita, T. Okazaki, T. Saitoh, et al. The jmjd3-irf4 axis regulates m2 macrophage polarization and host responses against helminth infection. *Nature immunology*, 11(10):936–944, 2010. Cited on page 36 and 37.

[202] M. S. Schlissel. Regulating antigen-receptor gene assembly. *Nature reviews. Immunology*, 3(11):890–899, 2003. Cited on page 18.

[203] K. S. Schluns, W. C. Kieper, S. C. Jameson, and L. Lefrançois. Interleukin-7 mediates the homeostasis of naïve and memory CD8 T cells in vivo. *Nature immunology*, 1(5):426–432, 2000. Cited on page 22 and 134.

[204] C. S. Schmidt and M. F. Mescher. Peptide antigen priming of naive, but not memory, CD8 T cells requires a third signal that can be provided by IL-12. *Journal of immunology (Baltimore, Md. : 1950)*, 168(11):5521–5529, 2002. Cited on page 20.

[205] R. Schwarting, J. Gerdes, J. Niehus, L. Jaeschke, and H. Stein. Determination of the growth fraction in cell suspensions by flow cytometry using the monoclonal antibody ki-67. *Journal of immunological methods*, 90(1):65–70, 1986. Cited on page 119.

[206] R. Sciammas, A. Shaffer, J. H. Schatz, H. Zhao, L. M. Staudt, and H. Singh. Graded expression of interferon regulatory factor-4 coordinates isotype switching with plasma cell differentiation. *Immunity*, 25(2):225–236, 2006. Cited on page 36.

[207] L. Shi, S. Mai, S. Israels, K. Browne, J. a. Trapani, and a. H. Greenberg. Granzyme B (GraB) autonomously crosses the cell membrane and perforin initiates apoptosis and GraB nuclear localization. *The Journal of experimental medicine*, 185(5):855–866, 1997. Cited on page 21.

[208] S. Shresta, C. T. Pham, D. A. Thomas, T. A. Graubert, and T. J. Ley. How do cytotoxic lymphocytes kill their targets? *Current opinion in immunology*, 10(5): 581–587, 1998. Cited on page 21 and 122.

[209] V. Shukla and R. Lu. Irf4 and irf8: governing the virtues of b lymphocytes. *Frontiers in biology*, 9(4):269–282, 2014. Cited on page 35.

[210] A. Sjöberg, L. Trouw, and A. Blom. Complement activation and inhibition: a delicate balance. *Trends in immunology*, 30(2):83–90, 2009. Cited on page 27.

[211] G. a. Smith and D. a. Portnoy. How the Listeria monocytogenes ActA protein converts actin polymerization into a motile force. *Trends in Microbiology*, 5(7): 272–276, 1997. Cited on page 30.

[212] G. a. Smith, H. Marquis, S. Jones, N. C. Johnston, D. a. Portnoy, and H. Goldfine. The two distinct phospholipases C of Listeria monocytogenes have overlapping roles in escape from a vacuole and cell-to-cell spread. *Infection and Immunity*, 63 (11):4231–4237, 1995. Cited on page 30.

[213] M. J. Smyth, J. M. Kelly, V. R. Sutton, J. E. Davis, K. A. Browne, T. J. Sayers, and J. A. Trapani. Unlocking the secrets of cytotoxic granule proteins. *Journal of leukocyte biology*, 70(1):18–29, 2001. Cited on page 122.

[214] D. E. Speiser, M. Colonna, M. Ayyoub, M. Cella, M. J. Pittet, P. Batard, D. Valmori, P. Guillaume, D. Liénard, J.-C. Cerottini, et al. The activatory receptor 2b4 is expressed in vivo by human cd8+ effector $\alpha\beta$ t cells. *The Journal of Immunology*, 167(11):6165–6170, 2001. Cited on page 128.

[215] V. Staudt, E. Bothur, M. Klein, K. Lingnau, S. Reuter, N. Grebe, B. Gerlitzki, M. Hoffmann, A. Ulges, C. Taube, N. Dehzad, M. Becker, M. Stassen, A. Steinborn, M. Lohoff, H. Schild, E. Schmitt, and T. Bopp. Interferon-Regulatory Factor 4 Is Essential for the Developmental Program of T Helper 9 Cells. *Immunity*, 33 (2):192–202, 2010. Cited on page 36, 116, and 137.

[216] V. Staudt, E. Bothur, M. Klein, K. Lingnau, S. Reuter, N. Grebe, B. Gerlitzki, M. Hoffmann, A. Ulges, C. Taube, et al. Interferon-regulatory factor 4 is essential for the developmental program of t helper 9 cells. *Immunity*, 33(2):192–202, 2010.

Cited on page 37.

[217] C. Stemberger, K. M. Huster, M. Koffler, F. Anderl, M. Schiemann, H. Wagner, and D. H. Busch. A Single Naive CD8+ T Cell Precursor Can Develop into Diverse Effector and Memory Subsets. *Immunity*, 27(6):985–997, 2007. Cited on page 22.

[218] N. Sternberg and D. Hamilton. Bacteriophage p1 site-specific recombination: I. recombination between loxp sites. *Journal of molecular biology*, 150(4):467–486, 1981. Cited on page 115.

[219] L. M. Stuart, K. Takahashi, L. Shi, J. Savill, and R. A. B. Ezekowitz. Mannose-binding lectin-deficient mice display defective apoptotic cell clearance but no autoimmune phenotype. *The Journal of Immunology*, 174(6):3220–3226, 2005. Cited on page 27.

[220] B. M. Sullivan, A. Juedes, S. J. Szabo, M. von Herrath, and L. H. Glimcher. Antigen-driven effector cd8 t cell function regulated by t-bet. *Proceedings of the National Academy of Sciences*, 100(26):15818–15823, 2003. Cited on page 82.

[221] C. D. Surh and J. Sprent. Regulation of mature T cell homeostasis. *Seminars in Immunology*, 17(3):183–191, 2005. Cited on page 22 and 134.

[222] S. Suzuki, K. Honma, T. Matsuyama, K. Suzuki, K. Toriyama, I. Akitoyo, K. Yamamoto, T. Suematsu, M. Nakamura, K. Yui, et al. Critical roles of interferon regulatory factor 4 in cd11bhighcd8α–dendritic cell development. *Proceedings of the National Academy of Sciences of the United States of America*, 101(24):8981–8986, 2004. Cited on page 36 and 37.

[223] K. Takahashi, W. E. Ip, I. C. Michelow, and R. A. B. Ezekowitz. The mannose-binding lectin: a prototypic pattern recognition molecule. *Current opinion in immunology*, 18(1):16–23, 2006. Cited on page 27.

[224] K. Takeda and S. Akira. TLR signaling pathways. *Seminars in Immunology*, 16 (1):3–9, 2004. Cited on page 32.

[225] T. Tamura, P. Tailor, K. Yamaoka, H. J. Kong, H. Tsujimura, J. J. O'Shea, H. Singh, and K. Ozato. Ifn regulatory factor-4 and-8 govern dendritic cell subset development and their functional diversity. *The Journal of Immunology*, 174(5): 2573–2581, 2005. Cited on page 36 and 37.

[226] T. Tamura, H. Yanai, D. Savitsky, and T. Taniguchi. The irf family transcription factors in immunity and oncogenesis. *Annu. Rev. Immunol.*, 26:535–584, 2008. Cited on page 34.

[227] N. Tanaka, T. Kawakami, and T. Taniguchi. Recognition dna sequences of interferon regulatory factor 1 (irf-1) and irf-2, regulators of cell growth and the interferon system. *Molecular and cellular biology*, 13(8):4531–4538, 1993. Cited on page 34.

[228] C. Tanchot, F. a. Lemonnier, B. Pérarnau, a. a. Freitas, and B. Rocha. Differential requirements for survival and proliferation of CD8 naïve or memory T cells. *Science (New York, N.Y.)*, 276(5321):2057–2062, 1997. Cited on page 24.

[229] R. Testi, J. H. Phillips, and L. L. Lanier. T cell activation via leu-23 (cd69). *The Journal of Immunology*, 143(4):1123–1128, 1989. Cited on page 71.

[230] N. Tominaga, K. Ohkusu-Tsukada, H. Udono, R. Abe, T. Matsuyama, and K. Yui. Development of th1 and not th2 immune responses in mice lacking ifn-regulatory factor-4. *International immunology*, 15(1):1–10, 2003. Cited on page 36 and 137.

[231] J. a. Trapani and M. J. Smyth. Functional significance of the perforin/granzyme cell death pathway. *Nature reviews. Immunology*, 2(10):735–747, 2002. Cited on page 20 and 21.

[232] L. A. Truman, C. A. Ford, M. Pasikowska, J. D. Pound, S. J. Wilkinson, I. E. Dumitriu, L. Melville, L. A. Melrose, C. A. Ogden, R. Nibbs, et al. Cx3cl1/fractalkine is released from apoptotic lymphocytes to stimulate macrophage chemotaxis. *Blood*, 112(13):5026–5036, 2008. Cited on page 25.

[233] S. J. Turner, S. C. Jameson, and F. R. Carbone. Functional mapping of the orientation for tcr recognition of an h2-kb-restricted ovalbumin peptide suggests that the beta-chain subunit can dominate the determination of peptide side chain specificity. *The Journal of Immunology*, 159(5):2312–2317, 1997. Cited on page 30.

[234] E. R. Unanue. Studies in listeriosis show the strong symbiosis between the innate cellular system and the T-cell response. *Immunological Reviews*, 158:11–25, 1997. Cited on page 32.

[235] D. Usharauli and T. Kamala. Brief antigenic stimulation generates effector cd8 t cells with low cytotoxic activity and high il-2 production. *The Journal of Immunology*, 180(7):4507–4513, 2008. Cited on page 20.

[236] M. Van Lookeren Campagne, C. Wiesmann, and E. J. Brown. Macrophage complement receptors and pathogen clearance. *Cellular microbiology*, 9(9):2095–2102, 2007. Cited on page 29.

[237] L. Van Parijs and a. K. Abbas. Role of Fas-mediated cell death in the regulation of immune responses. [Review] [70 refs]. *Curr.Opin.Immunol.*, 8(3):355–361, 1996. Cited on page 26.

[238] a. Vella, T. K. Teague, J. Ihle, J. Kappler, and P. Marrack. Interleukin 4 (IL-4) or IL-7 prevents the death of resting T cells: stat6 is probably not required for the effect of IL-4. *The Journal of experimental medicine*, 186(2):325–330, 1997. Cited on page 22 and 105.

[239] A. T. Vella, S. Dow, T. A. Potter, J. Kappler, and P. Marrack. Cytokine-induced survival of activated t cells in vitro and in vivo. *Proceedings of the National Academy of Sciences*, 95(7):3810–3815, 1998. Cited on page 135.

[240] D. Vercammen, G. Brouckaert, G. Denecker, M. Van de Craen, W. Declercq, W. Fiers, and P. Vandenabeele. Dual signaling of the fas receptor: initiation of both apoptotic and necrotic cell death pathways. *The Journal of experimental medicine*, 188(5):919–930, 1998. Cited on page 27.

[241] I. Vermes, C. Haanen, H. Steffens-Nakken, and C. Reutellingsperger. A novel assay for apoptosis flow cytometric detection of phosphatidylserine expression on early apoptotic cells using fluorescein labelled annexin v. *Journal of immunological methods*, 184(1):39–51, 1995. Cited on page 91.

[242] S. Viganò, R. Banga, F. Bellanger, C. Pellaton, A. Farina, D. Comte, A. Harari, and M. Perreau. Cd160-associated cd8 t-cell functional impairment is independent

of pd-1 expression. 2014. Cited on page 129.

[243] H. von Boehmer and H. J. Fehling. Structure and function of the pre-T cell receptor. *Annual review of immunology*, 15:433–452, 1997. Cited on page 18.

[244] I. Voskoboinik, J. C. Whisstock, and J. a. Trapani. Perforin and granzymes: function, dysfunction and human pathology. *Nature Reviews Immunology*, 15(6): 388–400, 2015. Cited on page 20.

[245] R. Wallis, D. A. Mitchell, R. Schmid, W. J. Schwaeble, and A. H. Keeble. Paths reunited: Initiation of the classical and lectin pathways of complement activation. *Immunobiology*, 215(1):1–11, 2010. Cited on page 27.

[246] S. Wang, Q. He, D. Ma, Y. Xue, and F. Liu. Irf4 regulates the choice between t lymphoid-primed progenitor and myeloid lineage fates during embryogenesis. *Developmental cell*, 34(6):621–631, 2015. Cited on page 116.

[247] X. Z. Wang, S. E. Stepp, M. A. Brehm, H. D. Chen, L. K. Selin, and R. M. Welsh. Virus-specific cd8 t cells in peripheral tissues are more resistant to apoptosis than those in lymphoid organs. *Immunity*, 18(5):631–642, 2003. Cited on page 25.

[248] P. Waring and A. Müllbacher. Cell death induced by the fas/fas ligand pathway and its role in pathology. *Immunology and cell biology*, 77(4):312–317, 1999. Cited on page 122.

[249] A. Weigert, S. Cremer, M. V. Schmidt, A. von Knethen, C. Angioni, G. Geisslinger, and B. Brüne. Cleavage of sphingosine kinase 2 by caspase-1 provokes its release from apoptotic cells. *Blood*, 115(17):3531–3540, 2010. Cited on page 25.

[250] E. J. Wherry, S.-J. Ha, S. M. Kaech, W. N. Haining, S. Sarkar, V. Kalia, S. Subramaniam, J. N. Blattman, D. L. Barber, and R. Ahmed. Molecular signature of cd8+ t cell exhaustion during chronic viral infection. *Immunity*, 27(4):670–684, 2007. Cited on page 25.

[251] J. K. Whitmire, J. T. Tan, and J. L. Whitton. Interferon-gamma acts directly on CD8+ T cells to increase their abundance during virus infection. *The Journal of experimental medicine*, 201(7):1053–1059, 2005. Cited on page 22.

[252] M. A. Williams and M. J. Bevan. Effector and memory ctl differentiation. *Annu. Rev. Immunol.*, 25:171–192, 2007. Cited on page 24.

[253] M. a. Williams, A. J. Tyznik, and M. J. Bevan. Interleukin-2 signals during priming are required for secondary expansion of CD8+ memory T cells. *Nature*, 441(7095):890–893, 2006. Cited on page 22, 105, and 135.

[254] P. Wong and E. G. Pamer. CD8 T cell responses to infectious pathogens. *Annual review of immunology*, 21(2):29–70, 2003. Cited on page 20.

[255] T. M. Woodruff, K. S. Nandakumar, and F. Tedesco. Inhibiting the c5–c5a receptor axis. *Molecular immunology*, 48(14):1631–1642, 2011. Cited on page 29.

[256] C. J. Workman, L. S. Cauley, I.-J. Kim, M. A. Blackman, D. L. Woodland, and D. A. Vignali. Lymphocyte activation gene-3 (cd223) regulates the size of the expanding t cell population following antigen activation in vivo. *The Journal of Immunology*, 172(9):5450–5455, 2004. Cited on page 128.

[257] Z. Xiao, K. a. Casey, S. C. Jameson, J. M. Curtsinger, and M. F. Mescher. Pro-

gramming for CD8 T cell memory development requires IL-12 or type I IFN. *Journal of immunology (Baltimore, Md. : 1950)*, 182(5):2786–2794, 2009. Cited on page 22 and 105.

[258] Y. Xiong and R. Bosselut. Cd4-cd8 differentiation in the thymus: connecting circuits and building memories. *Current opinion in immunology*, 24(2):139–145, 2012. Cited on page 116.

[259] W.-D. Xu, H.-F. Pan, D.-Q. Ye, and Y. Xu. Targeting irf4 in autoimmune diseases. *Autoimmunity reviews*, 11(12):918–924, 2012. Cited on page 61.

[260] T. Yamagata, J. Nishida, S. Tanaka, R. Sakai, K. Mitani, M. Yoshida, T. Taniguchi, Y. Yazaki, and H. Hirai. A novel interferon regulatory factor family transcription factor, icsat/pip/lsirf, that negatively regulates the activity of interferon-regulated genes. *Molecular and cellular biology*, 16(4):1283–1294, 1996. Cited on page 35.

[261] S. Yao, B. F. Buzo, D. Pham, L. Jiang, E. J. Taparowsky, M. H. Kaplan, and J. Sun. Interferon regulatory factor 4 sustains CD8+ T cell expansion and effector differentiation. *Immunity*, 39(5):833–845, 2013. Cited on page 120.

[262] S. Yao, B. F. Buzo, D. Pham, L. Jiang, E. J. Taparowsky, M. H. Kaplan, and J. Sun. Interferon regulatory factor 4 sustains cd8+ t cell expansion and effector differentiation. *Immunity*, 39(5):833–845, 2013. Cited on page 36, 61, 99, 115, 118, 122, 123, 124, 126, 128, 129, 130, 133, and 137.

[263] Y. Yin, C. Zhang, H. Dong, Z. Niu, Z. Pan, J. Huang, and X. Jiao. Protective immunity induced by a LLO-deficient Listeria monocytogenes. *Microbiology and Immunology*, 54(4):175–183, 2010. Cited on page 30.

[264] D. Zehn, S. Y. Lee, and M. J. Bevan. Complete but curtailed T-cell response to very low-affinity antigen. *Nature*, 458(7235):211–214, 2009. Cited on page 20, 48, 99, 101, 130, 132, and 138.

[265] D. Zehn, S. Roepke, K. Weakly, M. J. Bevan, and M. Prlic. Inflammation and tcr signal strength determine the breadth of the t cell response in a bim-dependent manner. *The Journal of Immunology*, 192(1):200–205, 2014. Cited on page 99 and 132.

[266] S. Zhang, H. Zhang, and J. Zhao. The role of cd4 t cell help for cd8 ctl activation. *Biochemical and biophysical research communications*, 384(4):405–408, 2009. Cited on page 116.

[267] Y. Zheng, A. Chaudhry, A. Kas, P. DeRoos, J. M. Kim, T.-T. Chu, L. Corcoran, P. Treuting, U. Klein, and A. Y. Rudensky. Regulatory T-cell suppressor program co-opts transcription factor IRF4 to control T(H)2 responses. *Nature*, 458(7236): 351–356, 2009. Cited on page 37, 116, and 117.

[268] C. Zhu, A. C. Anderson, A. Schubart, H. Xiong, J. Imitola, S. J. Khoury, X. X. Zheng, T. B. Strom, and V. K. Kuchroo. The tim-3 ligand galectin-9 negatively regulates t helper type 1 immunity. *Nature immunology*, 6(12):1245–1252, 2005. Cited on page 94 and 129.

[269] P. F. Zipfel and C. Skerka. Complement regulators and inhibitory proteins. *Nature Reviews Immunology*, 9(10):729–740, 2009. Cited on page 127.